External Review Draft

NIOSH Current Intelligence Bulletin:

Health Effects of Occupational Exposure to Silver Nanomaterials

DEPARTMENT OF HEALTH AND HUMAN SERVICES
Centers for Disease Control and Prevention
National Institute for Occupational Safety and Health

Disclaimer

Mention of any company or product does not constitute endorsement by the National Institute for Occupational Safety and Health (NIOSH). In addition, citations to websites external to NIOSH do not constitute NIOSH endorsement of the sponsoring organizations or their programs or products. Furthermore, NIOSH is not responsible for the content of these websites. All Web addresses referenced in this document were accessible as of the publication date.

Ordering Information

To receive documents or other information about occupational safety and health topics, contact NIOSH at

Telephone: **1–800–CDC–INFO** (1–800–232–4636)
TTY: 1–888–232–6348
E-mail: cdcinfo@cdc.gov

or visit the NIOSH website at **www.cdc.gov/niosh**.

For a monthly update on news at NIOSH, subscribe to *NIOSH eNews* by visiting **www.cdc.gov/niosh/eNews**.

Suggested Citation

NIOSH [2015]. External Review Draft - Current Intelligence Bulletin: Health Effects of Occupational Exposure to Silver Nanomaterials. By Zumwalde RD, Kuempel ED, Holdsworth G. Cincinnati, OH: U.S. Department of Health and Human Services, Centers for Disease Control and Prevention, National Institute for Occupational Safety and Health.

Date: December 18, 2015

On the Cover: Image to be provided.

Abstract

Engineered silver nanomaterials are used in a growing number of consumer and medical products. The National Institute for Occupational Safety and Health (NIOSH) assessed the scientific literature to investigate whether workers exposed to silver nanomaterials are at increased risk of adverse health effects and whether sufficient data are available to develop recommended exposure limit (REL) that is specific to particle size. No studies were found that reported adverse health effects in workers exposed to silver nanomaterials. The few studies that investigated health effects in workers with long-term exposures to silver dust and fume reported argyria, which is bluish-gray pigmentation to the skin and mucous membranes, and argyrosis, which is bluish-gray pigmentation to the eyes. No studies were found that specifically evaluated the role of silver particle size or solubility on modifying the health effects in humans or in chronic studies in animals.

NIOSH reviewed the published studies on silver nanomaterials in experimental animals or cells and used the two published subchronic inhalation studies in rats to evaluate the potential occupational health risk of silver nanomaterials. These studies reported lung and liver effects, including early-stage lung inflammation and liver bile duct hyperplasia, associated with exposure to 15-20 nanometer diameter silver nanoparticles. NIOSH used a published physiologically-based pharmacokinetic (PBPK) model to estimate the working lifetime exposures to silver nanoparticles that would not be expected to result in adverse lung or liver effects. These estimates ranged from 0.19 to 195 micrograms per cubic meter ($\mu g/m^3$) (8-hour time-weighted average airborne concentration), and depended on assumptions about the particle size, biologically-relevant tissue dose (soluble or total silver), rat effect level estimate, and PBPK model parameters. In addition, NIOSH evaluated published data involving humans exposed to silver of unknown particle size who had developed argyria. NIOSH estimated that exposures to 47 to 253 $\mu g/m^3$ of silver nanoparticles over a 45-year working lifetime would result in an amount of silver in the skin equivalent to the minimum amount observed in humans with argyria.

The current NIOSH REL for silver metal dust and soluble compounds is 10 µg/m^3 as an 8-hour time-weighted average airborne concentration (total mass sample). This limit was developed to protect against argyria and argyrosis. REL estimates for silver nanoparticles based on the animal data were both above and below the current NIOSH REL. Uncertainties in these estimates include the quantification of the silver tissue doses, the clinical significance of the rat lung and liver effects, the role of particle size and solubility on the observed effects, and the selection of uncertainty factors. Although the experimental animal and cellular studies are useful for showing potential risks from exposure to silver nanomaterials, NIOSH considers the currently available data to be too limited to develop a REL for silver that is specific to particle size. NIOSH recommends that effective risk management control practices be implemented so that worker exposures to silver nanomaterials do not exceed the NIOSH REL of 10 µg/m^3 (8-hour time-weighted average) for silver metal dust, fume, and soluble compounds, measured as a total airborne mass concentration. NIOSH recommends additional prudent measures including conducting workplace exposure and hazard assessments and medical surveillance of workers potentially exposed to silver nanomaterials.

Executive Summary

Background

Nanotechnology is an enabling technology involving structures generally defined as having one, two, or three external dimensions in the nanoscale size range of approximately 1 to 100 nanometers (nm) [ISO/TS 2008]. Manufacturing substances at the nanoscale results in specific physical-chemical characteristics that may differ from those of the bulk substances or particles of larger size [Wijnhoven et al. 2009]. These unique or enhanced characteristics of engineered nanomaterials have led to their increasing manufacture and use in many promising applications. One example of these substances is silver nanomaterials, which have been used for decades in applications as diverse as jewelry, utensils, photography, monetary currency, and antibacterials [Wijnhoven et al. 2009; Nowack et al. 2011]. Because of their physical-chemical properties at the nanoscale, silver nanomaterials are used in an increasing number of medical and consumer products, such as electronics or coating in textiles. The United States produced an estimated 20 tons of silver nanomaterials in 2010 [Hendren et al. 2011], and an estimated 450–542 tons were produced worldwide in 2014 [Future Markets 2014]. Studies in animals and cells have shown that the fate and biologic activity of silver is affected by its physical-chemical properties, such as solubility and surface properties [Johnston et al. 2010; Foldbjerg et al. 2011; Beer et al. 2012], particle size [Park et al. 2011c; Kim et al. 2012; Gliga et al. 2014; Braakhuis et al. 2014], and particle shape [Stoehr et al. 2011].

The current Occupational Safety and Health Administration (OSHA) permissible exposure limit (PEL) and the National Institute for Occupational Safety and Health (NIOSH) recommended exposure limit (REL) are both 10 micrograms per cubic meter ($\mu g/m^3$) as an 8-hour time-weighted average (TWA) concentration (total mass sample) for silver (metal dust and soluble compounds, as Ag) [NIOSH 2007]. The NIOSH REL for silver was adopted from the OSHA PEL [OSHA 1988]. The PEL and REL are based on preventing workers from developing argyria, which is bluish-gray pigmentation to the

skin and mucous membranes, and argyrosis, which is bluish-gray pigmentation to the eyes (see Terminology/Glossary section and Section 6.1 Human Health Basis for the NIOSH REL). The term “fume” is not currently included in the NIOSH REL definition for silver, but exposures to silver fumes have been reported in workers. For clarification, NIOSH will add the term “fume” to the NIOSH REL for silver (i.e., metal dust, fume, and soluble compounds, as Ag). Because fumes are often composed of nanometer-size particles, the NIOSH REL implicitly includes nanoparticles of silver generated during silver soldering/brazing and other high-temperature silver processes (e.g., Miller et al. [2010]). However, the REL has not been evaluated specifically for silver nanomaterials. Recent studies in rats exposed by subchronic inhalation to silver nanoparticles of 15–20 nm in diameter showed exposure-related lung and liver effects. The no observed adverse effect level (NOAEL) and other effect levels from subchronic (13-week) inhalation studies in rats were evaluated in this Current Intelligence Bulletin and used as a point of departure to estimate equivalent exposures in workers that would not be expected to be associated with adverse effects. The estimated human-equivalent tissue concentrations were estimated and compared with silver tissue concentrations measured in humans [ICRP 1960; Brune 1980].

Workers can be exposed to silver throughout its lifecycle, including ore extraction, melting/refining, product fabrication, use, disposal, and recycling. Published information on workers’ exposure to silver is limited, but it indicates that when good risk management practices, such as engineering controls, are not followed, workplace airborne concentrations can exceed the current OSHA permissible exposure level (PEL) and the NIOSH REL of 10 µg/m^3, 8-hour TWA concentration (total mass sample). In the literature, workplace exposures to silver have been reported to occur during brazing and soldering operations (≤ 6.0 µg/m^3 TWA) [NIOSH 1973, 1981,1998]; during manufacturing of silver nitrate and silver oxide (39–378 µg/m^3 TWA) [Rosenman et al. 1979, 1987]; during smelting and refining of silver (1–100 µg/m^3 TWA) [DiVincenzo et al. 1985]; and during reclamation of silver from photographic film (5–240 µg/m^3 TWA) [Pifer et al. 1989; Williams and Gardner 1995; NIOSH 2000]. Although these reports provide little information on airborne-particle characteristics, such as size or shape, it is

likely that the fumes generated while melting silver or during brazing and soldering contained silver nanoparticles and/or agglomerates of silver nanoparticles. In a few studies, exposures to silver nanoparticles have been measured and characterized [Park et al. 2009; Lee et al. 2011a, b; Lee et al. 2012; Miller et al. 2010]. Worker exposures to airborne concentrations of silver nanoparticles were reported to range from 0.02 to 2.43 μg/m^3 TWA during their production [Lee et al. 2011a, b; Lee et al. 2012], whereas airborne concentrations were found to range from 13 to 94 μg/m^3 TWA at a precious metal processing facility where melting and electro refining of silver occurred [Miller et al. 2010].

Summary of Adverse Health Effects

Human studies

Published reports of workers occupationally exposed to silver are limited, but they indicate that long-term exposure to silver can cause localized (in dermal and mucous membranes) and generalized (systemic) argyria [ATSDR 1990; Drake and Hazelwood 2005; Wijnhoven et al. 2009; Johnston et al. 2010; Lansdown 2012]. Ocular argyrosis has been observed in workers exposed to either soluble or insoluble silver, but no deficits in visual performance could be attributed to the silver deposits [Rosenman et al. 1979; Pifer et al. 1989]. Although argyria appears to occur more frequently in workers exposed to soluble silver compounds—probably because of a higher content of free silver ions—the observed effects reported in these studies could not always be fully apportioned to the solubility potential of the silver compound.

A few studies have investigated worker health effects other than argyria. A study of 27 silver reclamation workers reported no adverse clinical effects in pulmonary function, chest x-ray, and liver or kidney function tests compared with referent workers [Pifer et al. 1989]. The silver dust exposures were primarily to insoluble silver compounds during the processes of smelting, refining, and incineration. The mean exposure concentration was 110 μg/m^3 TWA, and the duration was a mean of 20 years [Pifer et al. 1989]. Other studies have reported some cases of abnormal kidney function, including significantly

increased mean levels of urinary enzyme N-acetyl-B-D glucosaminidase (NAG), which were correlated with blood silver concentration and age [Rosenman et al. 1987] and reduced creatinine clearance [Rosenman et al. 1979] in silver workers compared with unexposed workers. However, the silver-exposed workers also had concurrent exposures to known nephrotoxins such as cadmium and solvents. Rosenman et al. [1987] also observed upper respiratory irritation, such as sneezing, stuffy or runny nose, and chest tightness, in 15 of 27 workers (56%). Acute silver poisoning has been reported in a young worker due to a single "massive" exposure to silver vapors during the melting of silver ingots for 4 hours in a closed room without ventilation [Forycki et al. 1983].

Animal studies

The most comprehensive data set on the potential toxicity of silver nanoparticles comes from experimental animal studies. In vivo studies of rats exposed to silver nanoparticles by subchronic inhalation exposure provide evidence of (1) the uptake of silver ions or nanoparticles in the blood and subsequent distribution to all major organs and tissues; (2) perturbation of lung function and induction of inflammatory responses [Sung et al. 2008, 2009; Song et al. 2013]; and (3) histopathologic changes in the kidney and especially in the liver, in which bile duct hyperplasia was identified [Sung et al. 2009]. Although the biological interactions with inhaled silver nanoparticles are not fully understood, the possible mechanisms include dissolution and release of soluble silver species, and particle transformation through sulfidation (binding with sulfur) or opsonization (binding with protein), which can stabilize the silver [Liu et al. 2011; Loeschner et al. 2011; Bachler et al. 2013]. Silver nanoparticles are considered to have a greater potential for dissolution and release of ions than microscale particles due to the increased surface area per unit mass of nanoparticles [Wijnhoven et al. 2009].

Evidence from animal studies indicates that following deposition of silver in the lungs, silver can be transported via blood to the liver and other organs [Sung et al. 2008, 2009] and that soluble silver can clear from the lungs in a manner similar to that of elemental silver nanoparticles, suggesting that both entities can be readily absorbed via the lungs

and be systemically distributed [Takenaka et al. 2001]. Following exposure to silver nanoparticles, significant increases in the amount of silver have been observed in major organs and tissues, including the lungs, liver, spleen, kidneys, olfactory bulb, brain, and blood in both male and female rats [Ji et al. 2007b; Kim et al. 2008; Sung et al. 2009; Kim et al. 2010a; Lankveld et al. 2010; Lee et al. 2013c]. In addition, the distribution of silver in the kidneys appears to be rat gender-specific, as higher silver tissue concentrations were observed in female rats in 28-day and 12- or 13-week inhalation studies [Sung et al. 2009; Kim et al. 2011; Song et al. 2013; Dong et al. 2013], and in a 13-week oral study [Kim et al. 2010a]. Because the kidneys are the target organ for several hormones, it has been suggested that these gender differences are associated with metabolism and hormonal regulation. No adverse effects were reported to be associated with the higher retained silver kidney doses in female rats.

A common feature of the systemic toxicological effects of silver nanoparticles, irrespective of exposure route, is the reported histopathologic effects on the liver in both Sprague-Dawley and F344 rats [Sung et al. 2009; Kim et al. 2010a]. Rats exposed at the highest doses in both studies developed bile duct hyperplasia and signs of hepatic necrosis. In the 90-day oral study [Kim et al. 2010a], these effects were accompanied by changes in clinical chemistry parameters that indicated perturbations in liver metabolism, including increases in serum cholesterol concentration and alkaline phosphatase (AP) activity. In a 13-week (90-day) inhalation study by Sung et al. [2008, 2009], these systemic effects were accompanied by lung function deficits (decreased tidal volume, minute volume, and peak inspiration flow), the development of inflammation responses, and alveolar accumulation of macrophages in male and female rats [Sung et al. 2008]. In a subsequent 12-week inhalation study by the same group [Song et al. 2013], lung function decreases and lung inflammation were observed in male rats, which persisted in the high-dose group at 12 weeks after cessation of exposure. In female rats, in contrast to the results in the first study [Sung et al. 2008], no consistent decrease in lung function was observed in the second study, and the lung inflammation gradually resolved after cessation of exposure [Song et al. 2013].

In vivo studies comparing effects of exposure to different particle sizes of silver (micro- and nano-diameter) are limited, but one short-term exposure study in rats showed an acute pulmonary inflammation response to 15 nm diameter silver nanoparticles, but not to 410 nm diameter silver particles, 24 hours after the end of a 4-day (6 hours/day) inhalation exposure to approximately 170 µg/m^3. However, the effects resolved by 7 days post-exposure [Braakhuis et al. 2014]. For rats inhaling silver nanoparticles, the internal mass dose was 3.5 times higher and the particle number dose was 66,000 times higher than in rats inhaling the larger silver particles. Silver nanoparticles were observed inside lung cells at 24 hours post-exposure, and the average particle size was reduced to <5 nm, indicating that dissolution had occurred. The higher toxicity of the silver nanoparticles in rats was attributed to both the higher lung dose (as particle number or surface area) and a higher release rate of silver ions [Braakhuis et al. 2014]. In an acute (5-hour) inhalation study in rats exposed to spray products containing silver (ionic or nanoparticles), the ionic silver spray was more bioactive than the silver nanoparticle spray by causing mild cardiovascular and lung effects that resolved by 7-day post-exposure [Roberts et al. 2013].

Cellular studies

In contrast to the limited information on the toxicological and human health impacts of silver nanoparticle exposure in vivo, a considerable number of research studies have addressed the impacts of silver nanoparticles in cellular systems. These studies provide inferential evidence of the capacity of silver nanoparticles to bring about cellular changes of potential toxicological consequence, including (1) development of oxidative stress and induction of apoptosis, and (2) DNA damage/genotoxicity. A number of in vitro studies with mammalian cells have also examined the comparative toxicity of elemental silver nanoparticles and ionic silver. The results of these studies indicate that the mammalian cytotoxic response to elemental silver nanoparticles may be influenced by the physical-chemical properties of the particles, and that the response is similar to that observed with ionic silver, especially to silver nanoparticles with small diameters (approximately <30 nm) [Park et al. 2011c; Kim et al. 2012; Gliga et al. 2012, 2014]. Key

findings from in vitro studies of exposure to either silver nanoparticles or ionic silver include increased levels of reactive oxygen species [Hussain et al. 2005a; Carlson et al. 2008; Foldbjerg et al. 2009; Kim et al. 2009c], induction of oxidative stress management genes [Kim et al. 2009c; Miura and Shinohara 2009], and increased percentage of apoptotic cells [Hsin et al. 2008; Foldbjerg et al. 2009; Miura and Sinohara 2009]. Results of some cellular assay studies indicate that ionic silver can be more potent than silver nanoparticles in causing apoptosis [Foldbjerg et al. 2009] and reducing cell viability [Carlson et al. 2008; Greulich et al. 2009; Kim et al. 2009c; Miura and Shinohara 2009], whereas results of other studies provide evidence of a correlation between the increase in intracellular reactive oxygen species and particle size. In one study, significant reactive oxygen species generation was detected only from the 15 nm diameter silver nanoparticles—not the 30 or 55 nm diameter silver nanoparticles [Carlson et al. 2008]. DNA damage and high levels of apoptosis and necrosis were associated with exposure to both silver nanoparticles and ionic silver [Foldbjerg et al. 2009, 2011]. Exposure to silver nanoparticles has also been found to generate more reactive oxygen species than silver ions, suggesting that the reactive oxygen species production is due to specific characteristics of silver nanoparticles and not only ion release [Liu et al. 2010b]. Although dissolution of silver nanoparticles accounts for at least a degree of the toxicity observed with silver nanoparticle exposure, the effects cannot be fully apportioned to the measured dissolved fraction of silver. Although certain silver nanoparticles may have low solubility in certain media and conditions, their contact with biologic receptors may cause a release of ions that could be sustained over a long period.

Non-spherical silver particles

Based on results of in vitro [Stoehr et al. 2011] and in vivo [Schinwald et al. 2012; Kenyon et al. 2013] studies with silver nanowires, inhalation exposure to silver nanowires may pose a greater health risk than exposure to silver nanoparticles because of their high aspect ratios and potential for reduced clearance from the lungs. Stoehr et al. [2011] found silver nanowires (1.5 to 25 micrometers, µm, in length; 100 to 160 nm in

diameter) to be more toxic to alveolar epithelial A549 cells than silver nanoparticles (30 nm in diameter) or micron-scale silver particles (<45 µm in diameter) at concentrations expressed as either mass or surface area. Although no effects on A549 cells were observed with silver nanoparticles and micron-scale silver particles at the doses used, silver nanowires induced a strong cytotoxicity, loss in cell viability, and early calcium influx that appeared to be independent of the length of the silver nanowires. No studies of silver nanowire exposures in workers were found.

Recommended Exposure Limit (REL) for Silver Nanomaterials

Human evidence

The current NIOSH REL for silver (metal dust and soluble compounds, as Ag) of 10 µg/m^3, as an 8-hour TWA concentration, using total airborne mass sampling, was adopted from the OSHA PEL [NIOSH 2007; OSHA 1988]. The OSHA PEL was derived from biomonitoring data in workers and estimates of the body burden. The PEL was derived from the estimated equivalent airborne concentration of silver over 20 years that was below, by a factor of five, the lowest dose associated with argyria. It should be noted that the factor of five would be approximately two over a 45-year working lifetime. Airborne particle size was not reported or evaluated as a specific factor in the basis for the OSHA PEL or NIOSH REL. More recent studies have reported worker exposures to silver nanoparticles [Miller et al. 2010; Lee et al. 2011a, b]. NIOSH is not aware of any studies or reports to date of adverse health effects in workers exposed to silver nanoparticles. Human data on the lowest skin tissue doses of silver associated with argyria were used in a physiologically-based pharmacokinetic (PBPK) model to estimate the equivalent 45-year working lifetime exposure concentrations (as discussed below in “PBPK modeling approach, Argyria” and in Section 6.5.2.1).

Animal evidence

Two subchronic (13-week) inhalation studies in rats (reported in three papers: Sung et al. [2008, 2009]; Song et al. [2013]) show dose-response relationships between inhaled silver nanoparticles and early stage adverse lung and liver (bile duct) effects. These data in rats were used to estimate the working lifetime exposure concentrations of silver nanoparticles associated with a no or low risk of adverse effects. Two risk assessment methods were used to derive these estimates: (1) a standard uncertainty factor approach applied to the rat NOAEL or other effect level estimates (Section 6.5.3.1), and (2) the use of a published PBPK model [Bachler et al. 2013] to estimate human-equivalent tissue doses (Section 6.5.3.2). In addition, an acute inhalation study in rats exposed to ionic Ag or silver nanoparticle spray [Roberts et al. 2013] was used to estimate the human-equivalent single day, 8-hour TWA exposure concentration associated with the rat acute NOAEL.

Human-equivalent exposure estimates

Acute exposure

A single-day (5-hour) inhalation study in rats exposed to silver colloidal nanoparticle sprays reported no significant adverse health effects [Roberts et al. 2013], which provides data to estimate an acute NOAEL. The human-equivalent single 8-hour airborne concentration to the NOAEL in rats is based on the estimated equivalent deposited lung dose to that measured in rats. The human-equivalent single 8-hour NOAEL estimates are 60 to 700 times greater than the NIOSH REL of 10 µg/m^3 (Section 6.5.1.1). This finding suggests that the current NIOSH REL is sufficiently protective for acute inhalation exposure to these silver colloidal nanoparticles; however, this study does not provide information on possible effects from repeated exposures. The ionic silver was observed to be more bioactive than the silver nanoparticle and resulted in mild cardiovascular and lung effects following acute exposure [Roberts et al. 2013].

Subchronic/chronic exposures

Uncertainty factor approach

Occupational exposure limits (OELs) of 0.6–1.7 µg/m^3 were estimated based on the use of an uncertainty factor of 60 that was applied to the NOAELs of 49, 117, or 133 µg/m^3 reported in the rat subchronic studies [Sung et al. 2008, 2009; Song et al. 2013] (Section 6.5.3.1) (Table 6-1). OEL estimates of 18–51 µg/m^3 were derived when using an uncertainty factor of 2 (implicit in deriving the current REL for the prevention of argyria in workers, after accounting for a 45-year working lifetime) (Section 6.1) (Table 6-1).

PBPK modeling approach

Early-stage lung or liver effects: A PBPK model for silver nanoparticle was recently developed by Bachler et al. [2013] using rat silver nanoparticle kinetics data, extrapolated to humans, and validated using some biomonitoring data on silver workers (Section A.2). The PBPK model was used to estimate the human-equivalent silver nanoparticle tissue doses to the rat effect level estimates from the subchronic inhalation studies, using the measured tissue doses of Ag in rat lung and liver tissues at the end of the 13-week exposure [Sung et al. 2008, 2009; Song et al. 2013]. These tissue doses were associated with the NOAELs or $BMDL_{10}$ estimates from the rat subchronic inhalation studies. The NOAEL is defined as the highest dose in an experiment that is not associated with a significant increase in any adverse effect. The $BMDL_{10}$ is the 95% lower confidence limit estimate of the benchmark dose associated with a benchmark response (BMR). The BMR is a 10% added risk of chronic alveolar inflammation of minimal severity or bile duct hyperplasia in rats based on histopathological examination.

The estimates of the 45-year working lifetime airborne concentration of silver nanoparticles associated with the NOAELs as lung or liver tissue burdens depended on the assumed nanoparticle size and form (total Ag or soluble/active fraction). Working lifetime exposure concentrations of 9.7 or 61 µg/m^3 for 15 nm silver nanoparticles, or 31

or 195 µg/m^3 for 100 nm silver nanoparticles, were estimated to result in estimated equivalent lung tissue doses of soluble/active Ag as those at the rat NOAELs in the two studies [Song et al. 2013; Sung et al. 2009, respectively]. These NOAELs are based on the highest dose that was not associated with chronic alveolar inflammation in female rats (Table 6-2). Working lifetime airborne concentrations of 6.2 or 11 µg/m^3 for 15 nm silver nanoparticles, or 20 or 37 µg/m^3 for 100 nm silver nanoparticles, were derived based on the $BMDL_{10}$ estimate associated with a 10% increase over background in the proportion of animals having minimal or higher severity of bile duct hyperplasia (Table 6-2). Much lower working lifetime exposure concentrations (0.19 to 3.8 µg/m^3) were estimated for 15 or 100 nm silver nanoparticles when assuming total silver nanoparticle mass tissue dose as the biologically effective dose metric for these same response endpoints (Table A-12). These working lifetime exposure estimates do not include uncertainty factors.

The OEL estimates derived from the rat subchronic inhalation data depended on the silver nanoparticle dose metric (exposure concentration or tissue dose of soluble/active or total silver nanoparticle) and the uncertainty factor applied to the human-equivalent doses. Based on the PBPK model, the OEL estimates were 0.10–1.0 µg/m^3 for 15 nm silver nanoparticles, or 0.33–3.2 µg/m^3 for 100 nm silver nanoparticles, assuming a soluble/active silver nanoparticle dose metric and an uncertainty factor of 60 (Section 6.5.3.1) (Table 6-2). These estimates were 3.1–30 µg/m^3 for 15 nm silver nanoparticles or 10–98 µg/m^3 for 100 nm silver nanoparticles, when using an uncertainty factor of 2, which was implicit in deriving the current REL, after accounting for a 45-year working lifetime (Section 6.1) (Table 6-2).

Argyria: Working lifetime (45-year) exposure concentrations of 47 µg/m^3 (8-hour TWA) of ionic silver, 78 µg/m^3 (8-hour TWA) of 15 nm diameter silver nanoparticles, or 253 µg/m^3 (8-hour TWA) of 100 nm diameter silver nanoparticles were estimated to result in a skin tissue dose of silver associated with argyria in humans. This was 3.2 µg silver per gram of tissue, which was the lowest measured concentration reported, as discussed in Bachler et al. [2013] (Section 6.5.2.1). These PBPK model-based

estimates suggest an approximately a 5- to 25-fold margin of exposure between the current NIOSH REL of 10 µg/m^3 and the lowest reported human dose associated with argyria.

These exposure concentration estimates associated with argyria (47 - 253 µg/m^3) are similar to, or higher than, the estimated human-equivalent exposure concentrations associated with the NOAEL or $BMDL_{10}$ estimates for early-stage lung or liver effects in rat subchronic studies (i.e., 0.19 - 195 µg/m^3, depending on assumptions on the particle size and form). Assuming equivalent dose-response relationships for these effects in humans and rats, these findings suggest that early-stage lung and liver effects might be expected to occur in workers who had developed argyria. However, no lung and liver effects have been reported in individuals with argyria in the few studies in workers that included clinical tests of lung and liver function (Section 3). NIOSH is not aware of any cases of lung or liver effects in workers exposed at the NIOSH REL, although data are limited on the particle size of exposures to silver in the workplace.

Sources of uncertainty in the rat-based OEL estimates

Several limitations of the animal subchronic inhalation studies result in uncertainty in deriving these human-equivalent concentration and OEL estimates (Table 6-2). These limitations include the following:

1. The small number of animals per exposure group, and especially the 4 or 5 rats per group in Song et al. [2013].
2. The large variability in the measured tissue doses in the rats exposed to similar airborne concentrations of silver nanoparticles at the NOAELs in the two studies. The lung tissue dose was 672 nanograms per gram (ng/g) in female rats exposed to 117 µg/m^3 in Song et al. [2013], while the lung tissue dose was 4,421 ng/g in female rats exposed to 133 µg/m^3 in Sung et al. [2008, 2009].
3. The large variability in lung responses across studies within gender. An example of this variability is that female rats were reported to have lung function deficits and

decreased minute volume and peak inspiration flow at the lowest exposure concentration of 49 µg/m^3 in Sung et al. [2008], while no lung function deficits were observed in female rats at the highest exposure concentration of 381 µg/m^3 in Song et al. [2013]. Liver tissue findings were reported in only one of the two subchronic studies [Song et al. 2009]. This large variability in results from these subchronic studies, which were conducted by the same laboratory using the same silver nanoparticle generation method, contributes to the uncertainty about the dose that would be associated with possible adverse lung or liver effects to inhaled silver nanoparticles in rats, and consequently in the estimated human-equivalent exposure concentrations.

Another source of uncertainty in using the rat data to derive an OEL is whether the observed rat lung and liver effects have potential health significance to humans. It is not known if the observed effects in the rat studies are clinically significant for workers due to uncertainties that include the following:

1. The quantification of the silver tissue concentrations in the rat subchronic inhalation studies with silver nanoparticles and in the human autopsy studies that measured tissue concentrations of various metals in the general population.
2. The similar liver tissue concentrations of silver found in the rat studies with silver nanoparticles at the no or low effect level to those reported in the human general population. The rat effect level estimates for silver liver tissue concentrations were 6–14 ng/g, and the reported human silver liver tissue concentrations were 17 ng/g in the general population [ICRP 1960] or 32 ng/g in unexposed workers [Brune 1980] (Section A.2.5.2.3).
3. The high variability in the estimated human-equivalent working lifetime exposure concentrations (0.19 – 195 µg/m^3) to the rat no or low effect levels for early stage lung and liver effects. This variability translates to high uncertainty in the REL estimates (0.1 – 98 µg/m^3). These estimates depend on the rat effect levels, modeling assumptions, and uncertainty factors used.

4. Whether the rat low-dose lung or liver effects persist or have predictive value to humans exposed for up to a 45-year working lifetime. The physico-chemical properties of the silver nanoparticle and the biological mechanisms that caused these effects are also not clearly known, and there is uncertainty whether the key causal factor is the silver ions and/or silver particles.

Conclusions

NIOSH has determined that workers would be unlikely to develop argyria if airborne concentrations of silver nanoparticles are maintained below the current NIOSH REL of 10 µg/m^3, 8-hour TWA, for soluble and insoluble silver dust and fume. To date, NIOSH is not aware of any studies reporting adverse lung or liver effects in workers exposed to silver nanoparticles. In the absence of human dose-response data, the best available evidence on the potential adverse health effects of silver nanoparticles is from the subchronic inhalation studies in rats, which reported early-stage adverse effects in the lungs and liver [Sung et al. 2008, 2009; Song et al. 2013].

The effects of argyria reported in humans exposed to silver differ from the lung and liver effects observed in the rat studies. The role of silver ions versus nanoparticles in causing lung and liver effects in animals is not known, nor is the role of particle size; and no studies of microscale silver were available for comparison. A critical question is whether workers exposed to an airborne concentration of nanoscale silver particles at 10 µg/m^3, 8-hour TWA, would have a different risk than workers exposed to 10 µg/m^3 of microscale silver particles. One of the key complexities in hazard and risk assessment of silver particles, including nanoparticles, is uncertainty about the dissolution of various types and sizes of silver particles or silver compounds in the body and the extent to which possible adverse effects may be due to the ionic versus particulate forms of silver.

After evaluating the available human and animal evidence, NIOSH has determined that the current evidence is insufficient to support developing a REL for silver that is specific

to particle size. NIOSH recommends that effective risk management control practices be implemented so that worker exposures to silver nanomaterials do not exceed the NIOSH REL of 10 µg/m^3 (8-hour time-weighted average) for silver metal dust, fume, and soluble compounds, measured as a total airborne mass concentration. NIOSH based these conclusions on the following evidence:

1. Some information on worker exposures to silver nanoparticles was inherently included in deriving the current REL. This includes fume from high temperature silver processes that contained microscale and nanoscale particles.
2. The lung and liver effects observed in the rat subchronic inhalation studies were of uncertain clinical significance at the doses extrapolated to humans, and the estimates of the tissue dose effect levels were highly variable and included silver tissue concentrations in the range of background silver liver tissue concentrations found in the general population.
3. The range of estimated worker-equivalent exposure concentrations of silver nanoparticles associated with the rat-based effect levels (NOAELs) includes the NIOSH REL of 10 µg/m^3.

Uncertainties in evaluating the health risks to nanoscale silver may be reduced as new information becomes available from ongoing research studies, such as the National Institute of Environmental Health Sciences nanoGo consortium research [Schug et al. 2013]. As new data become available, NIOSH will assess the results and determine whether additional recommendations are warranted.

Recommendations

Although NIOSH is not aware of any reports of adverse lung and liver effects in workers exposed to silver nanoparticles, the results from the animal subchronic inhalation exposure to silver nanoparticles indicate the need to take precautionary measures and minimize worker exposure to silver nanomaterials until research can fully explain the physical-chemical properties of these nanomaterials that define their potential toxicity. In

light of current scientific evidence from experimental animal studies concerning the hazard potential of silver nanomaterials, steps should be taken to implement an occupational health surveillance program that includes elements of hazard (that is, toxicity and exposure assessment) and medical screening and surveillance. NIOSH recommends that employers and workers take the following steps to minimize potential health risks associated with exposure to silver, including exposure to silver nanomaterials, such as silver nanoparticles and silver nanowires. A complete listing of recommendations is given in Section 7.

1. Recommendations for employers

- Use available information to do periodic assessments of potential hazards related to silver nanomaterial exposures. Make appropriate changes, such as risk management strategies to minimize exposures, to protect worker health. At a minimum, the requirements of the OSHA Hazard Communication Standard [CFR 1910.1200(h)] and the Hazardous Waste Operation and Emergency Response Standard [29 CFR 1910.120] should be followed.

- Identify and characterize processes and job tasks where workers may be exposed to silver.

- Do a comprehensive exposure assessment, including exposures to other potential hazards, as part of an overall hazard and exposure assessment.

- Substitute a nonhazardous or less hazardous material for silver nanomaterials. When substitution is not possible, use engineering controls as the primary method to minimize worker exposure to silver nanomaterials, such as silver nanoparticles and silver nanowires.

- Establish criteria and procedures to select, install, and evaluate the performance of engineering controls to ensure proper operating conditions. Make sure workers are trained on how to check and use exposure controls.

- Routinely evaluate airborne exposures to ensure that control measures are working properly and that worker exposures to silver, including silver nanomaterials, are being maintained below the NIOSH REL of 10 µg/m^3 as an 8-hour TWA concentration (total airborne mass sample).

- Because silver nanoparticles can enter the body through the skin (specifically, abraded and lacerated skin), measures should be taken to reduce dermal exposure by using protective clothing and gloves. Clothing and gloves made of nonwoven material have been shown to be most resistant to penetration by particles, including nanoscale particles (see section 7.5 dermal protection). Workers should be trained on proper personal protective equipment (PPE), including when the PPE must be used.

- Educate workers on the sources and job tasks that may expose them to silver nanomaterials (such as silver nanoparticles and silver nanowires), and train them how to use exposure control measures, apply good work practices, and wear PPE to minimize exposure.

- Provide facilities for hand washing to reduce inadvertent oral and dermal exposure and encourage workers to make use of these facilities before eating, smoking, or leaving the worksite.

- Provide facilities for showering and changing clothes, with separate facilities for storage of non-work clothing, to prevent the inadvertent cross-contamination of non-work areas (including take-home contamination).

- Develop contingency procedures to address inadvertent spills, which can result in high or unpredictable exposures to workers. To mitigate these exposures, develop procedures to facilitate efficient clean-up/disposal and to ensure that workers are adequately protected during the clean-up response. Higher levels of personal protective equipment, pre-training of workers, and management

supervision of the clean-up may be required to ensure that the response is carried out safely and responsibly.

- When providing respirators for worker protection, follow the OSHA respiratory protection standard [29 CFR 1910.134], requiring that a respiratory protection program be established with the following elements:
    - Medical evaluation of workers' ability to perform the work while wearing a respirator.
    - Regular training of personnel.
    - Periodic workplace exposure monitoring.
    - Respirator fit testing.
    - Respirator maintenance, inspection, cleaning, and storage.
- When developing labels and Safety Data Sheets [OSHA 2012], consider using the information on potential health risks and recommended risk management practices contained in this Current Intelligence Bulletin.
- Implement a medical screening and surveillance program for workers at risk of silver exposure (as described in Section 7.7). The program should include the following:
    - Participation by all workers involved in tasks qualitatively assessed to have a higher likelihood of exposure to silver (such as soldering, brazing, or melting silver or handling silver powders). This should also include workers exposed to concentrations of silver, including silver nanomaterials, in excess of the REL, which is airborne silver

concentrations above 10 µg/m^3, as an 8-hour TWA concentration (total airborne mass sample).

- Oversight by a qualified health-care professional who is informed and knowledgeable about potential workplace exposures, routes of exposure, and health effects related to silver.

- An initial baseline examination of each participating worker, including an occupational and medical history that emphasizes previous sources of silver exposure, physical examination for signs of early argyria, and additional tests at the discretion of the overseeing medical professional.

- Periodic reexaminations at set intervals, along with reexaminations when work tasks or processes significantly change, if accidental exposure occurs, if signs of argyria or other malady manifest, or as the overseeing medical professional deems necessary.

- Written documentation of all examinations, and communication of silver-exposure related findings and recommendations to the employer. For confidentiality reasons, only information pertaining to a worker's ability to work with silver should be communicated.

- Communication to workers regarding workplace silver-exposure, including the nature, risks, and routes of exposure, instructions for reporting symptoms, and information about the medical screening program.

- Periodic evaluation of aggregated data from the medical surveillance program to identify worker health patterns that may be linked to work activities and practices that require additional primary prevention efforts, and to ensure the program is effective and consistent with current knowledge regarding occupational exposure to silver, including

nanomaterials. Confidentiality should be maintained in accordance with applicable regulation and guidelines.

2. Recommendations for workers

- Ask your supervisor for training on how to protect yourself from possible hazards of your job, which include working around silver.

- Know and use the tools or equipment to keep silver nanomaterials away from you. Know what you should do on the job to keep nanomaterials out of the air and to keep them off your skin.

- Understand when and how to wear a respirator and other personal protective equipment, such as gloves and clothing, that your employer might give you.

- Avoid handling silver nanomaterials in powder form.

- Store silver nanomaterials in tightly sealed containers whenever possible. Do this for both silver nanomaterials that are suspended in liquids or in a powder form. Handling these materials in open containers is generally not an acceptable work practice.

- Clean work areas at least at the end of each work shift, using a HEPA-filtered vacuum cleaner or by wet-wiping. Do not clean work areas by dry sweeping or using air hoses.

- Do not store, eat food, or drink beverages in workplaces where silver is handled.

- Shower and change into clean clothes at the end of each workday. This will help keep you from accidently contaminating other areas, including your home.

Contents

Abbreviations and Definitions

AB	Alamar Blue
ACGIH	American Conference of Governmental Industrial Hygienists
Ag	silver
Ag^+	ionic silver
AgCl	silver chloride
Ag_2CO_3	silver carbonate
Ag/Cu	silver copper
$AgNO_3$	silver nitrate
Ag_2O	silver oxide
Ag_3PO_4	silver phosphate
Ag_2S	silver sulfide
Ag_2SO_4	silver sulfate
AgNP	silver nanoparticle
AgNW	silver nanowire
AIC	Akaike information criterion
Al_20_3	aluminum oxide
ALT	alanine aminotransferase
AMG	auto-metallography
AP	alkaline phosphatase
ATSDR	Agency for Toxic Substances and Disease Registry
BAL	broncho alveolar fluid
BMC	benchmark concentration (maximum likelihood estimate)
BMCL	95% lower confidence limit estimate of BMC
$BMCL_{10}$	95% lower confidence limit estimate of the exposure concentration associated with a 10% increase over background in the proportion of animals with an adverse response
BMD	benchmark dose (maximum likelihood estimate)
BMDL	95% lower confidence limit estimate of BMD
$BMDL_{10}$	95% lower confidence limit estimate of the dose (e.g., measured in tissues) associated with a 10% increase over background in the proportion of animals with an adverse response

BMR	benchmark response, i.e., an increase in an adverse response that is associated with a BMD, typically in the low dose and response region of the data (e.g., 10% excess risk level).
BW	body weight
°C	degrees Celsius
$C_6H_5Ag_3O_7$	silver citrate
CIB	Current Intelligence Bulletin
CKAP4	cytoskeleton-associated protein 4
cm	centimeter
cm^2	centimeter squared
CMC	carboxymethyl cellulose
CPC	condensation particle counter
DCF	dichlorofluorescein
DNA	deoxyribonucleic acid
EC_{50}	median effective concentration
ECHA	EU European Chemicals Agency
EDS	energy dispersive X-ray spectroscopy
EPA	U.S. Environmental Protection Agency
ESP	electrostatic precipitator
EU	European Union
°F	degrees Fahrenheit
FAAS	Fame atomic absorption spectrometry
FITC	fluorescein isothiocyanate
FMPS	fast mobility particle sizer
FSH	follicle stimulation hormone
g	gram
GD	gestation day
GJIC	gap-junction intercellular communication
GM	geometric mean
GP	glutathione peroxidase
GSD	geometric standard deviation
GSH	glutathione
HEC	human equivalent concentration

HED	human equivalent dose
HEPA	high-efficiency particulate air
hMSC	human mesenchymal stem cell
hr	hour
HT	hydroxytryptamine
IC_{50}	median inhibitory concentration
ICP-MS	inductively coupled plasma-mass spectroscopy
Ig	immunoglobulin
INEL	indicative no-effect level
ISO	International Organization for Standardization
JNK	c-Jun NH_2-terminal kinase
kg	kilogram
L	liter
L/min	liters per minute
LC_{50}	concentration resulting in a mortality of 50%
LCL	lower confidence limit
LD_{50}	median lethal dose
LDH	lactate dehydrogenase
LEV	local exhaust ventilation
LFA	long amosite fibers
LH	luteinizing hormone
lpm	liters per minute
LOAEL	lowest observed adverse effect level, i.e., the lowest dose in an experimental animal study that is associated with a significant increase in one or more adverse effects
MAD	mean aerodynamic diameter
MALDI-TOFMS	matrix-assisted laser desorption/ionization–time-of-flight mass spectrometry
MEF	mouse embryonic fibroblasts
MES	mouse embryonic stem
mg/L	milligram per liter
mg/m^3	milligram per cubic meter
min	minute

ml	milliliter
MMAD	mass median aerodynamic diameter
MN	marrow micronucleus
MNPCE	micronucliated polychromatic erythrocytes
MPPD	multiple-path particle dosimetry
MOA	mode of action
MOE	margin of exposure
MPPD	multiple-path particle dosimetry
mRNA	messenger ribonucleic acid
MWM	Morris water maze
NA	not applicable
$NaBH_4$	sodium borohydride
NAC	N-acetyl cysteine
NAG	N-acetyl-B-D glucosaminidase
ND	nondetectable
ng/cm^2	nanograms per square centimeter
ng/g	nanograms per gram
NIEHS	National Institute of Environmental Health Sciences
NIOSH	National Institute for Occupational Safety and Health
NIST	National Institute of Standards and Technology
nm	nanometer
nm^2/cm^3	square nanometer per cubic centimeter
NOAEL	no observed adverse effect level, i.e., the highest dose in an experimental animal study that is not associated with a significant increase in any adverse effect
NTRC	Nanotechnology Research Center
OEB	occupational exposure band
OECD	Organisation for Economic Cooperation and Development
OEL	occupational exposure limit
OSHA	Occupational Safety and Health Administration
PBPK	physiologically-based pharmacokinetic model
PBS	phosphate buffered saline
PBZ	personal breathing zone

PCR	polymerase chain reaction
PI	propidium iodide
PKC	protein kinase C
POD	point of departure; an effect level, e.g., in rodents, which is extrapolated to humans in the estimation of an equivalent dose and exposure limits
PPE	personal protective equipment
PSM	process safety management
PtD	prevention through design
PVP	polyvinylpyrrolidone
PVR	poliovirus receptor
RBC	red blood cell
RCC	relative cell count
REL	recommended exposure limit
RNA	ribonucleic acid
ROS	reactive oxygen species
RT-PCR	reverse transcription polymerase chain reaction
SD	standard deviation
SEGs	similarly exposed groups
SEM	scanning electron microscope
SFA	short amosite fibers
SLC7A13	solute carrier family 7, member 13
SOD	superoxide dismutase
SOP	standard operating procedures
SPECT	single-photon emission computerized tomography
SPMS	scanning mobility particle sizer
STEM	scanning transmission electron microscopy
TEM	transmission electron microscope
TGF-β	transforming growth factor-beta
THF	tetrahydrofuran
TiO_2	titanium dioxide
TLV®	threshold limit value
TWA	time-weighted average
UF	uncertainty factor

µg	microgram
µg/dL	microgram per deciliter
µg/g	microgram per gram
µg/kg	microgram per kilogram
µg/L	microgram per liter
µg/m^3	microgram per cubic meter
µg/mL	microgram per milliliter
µL	microliter
µm	micrometer
U/L	units per liter
UCL	upper confidence limit
WBC	white blood cell
WHO	World Health Organization
wk	week
wt	weight
yr	year
%	percent

Terminology/Glossary

A number of terms used in the field of nanotechnology have specialized meanings, and definitions of certain terms have important biologic, legal, regulatory, and policy implications. Experimental animal and in vitro studies cited in this report frequently describe exposures to 'silver,' 'nanosilver,' 'nanoscale silver,' 'silver nanoparticles (AgNPs),' or 'silver nanowires (AgNWs)' without always providing complete information on particle dimension, species, and other physical-chemical properties. The absence of such information, especially from some in vitro studies, limits the ability to compare the toxicological outcomes reported in the in vitro studies with the exposure concentrations and doses that brought about AgNP-related effects observed in the in vivo studies.

Nanomaterials: The International Organization for Standardization (ISO) has developed nomenclature and terminology for nanomaterials [ISO/TS 2008]. According to ISO 27687:2008, a *nano-object* is material with one, two, or three external dimensions in the size range of approximately 1–100 nanometers (nm). Subcategories of a nano-object are (1) *nanoplate,* a nano-object with one external dimension at the nanoscale (1–100 nm); (2) *nanofiber,* a nano-object with two external dimensions at the nanoscale (a nanotube is defined as a *hollow nanofiber*, and a nanorod is defined as a *solid nanofiber*); and (3) *nanoparticle,* a nano-object with all three external dimensions at the nanoscale. Nano-objects are commonly incorporated in a larger matrix or substrate called a *nanomaterial.* The term 'silver nanomaterial' used by NIOSH in this Current Intelligence Bulletin includes engineered AgNPs and AgNWs.

Silver nanoparticles (AgNPs): This document focuses primarily on exposure to engineered AgNPs. Synthesis of AgNPs are typically conducted using either modifications of the Lee-Meisel or Creighton methods in which different silver salts and reducing agents are used, or through high-temperature reduction in porous solid matrices, vapor-phase condensation of a metal onto a solid support, laser ablation of a metal target into a suspending liquid, photo-reduction of silver ions, chemical vaporization, dry powder dispersion, and electrolysis of a silver salt solution. Most of the

in vitro and in vivo studies described in this document do not report the source of exposure to AgNPs. Some studies of workers employed in industries using silver were likely exposed to AgNPs generated as a fume during the melting and electro-refining of silver or during brazing/soldering operations.

Aggregate and **agglomerate:** In many circumstances, primary AgNPs can aggregate or agglomerate into secondary particles with dimensions greater than 100 nm. These two terms have specific meanings [ISO 2006]: an *aggregate* is a heterogeneous group of nanoparticles held together by relatively strong forces (for example, covalent bonds), and thus are not easily broken apart. An *agglomerate* is a group of nanoparticles held together by relatively weak forces, including van der Walls forces, electrostatic forces, and surface tension. Aggregates and agglomerates of silver particles can occur in work environments where engineered AgNPs are synthesized and handled (such as during removal from the reactor or handling of "free" powder forms of AgNPs) and where fumes are generated during the melting of silver and silver alloys and during silver brazing/soldering. The extent to which AgNPs occurred as an aggregate or agglomerate in the cited studies with workers and in the in vitro and in vivo studies was often not described by the authors. Whether the constituent primary particles remained agglomerated or aggregated during the entire study period is also unknown.

Colloid: The term 'colloid' used in the cited studies refers to an assemblage of AgNPs suspended within a given medium that are smaller than microscale (less than 10^{-6} m). For example, Wijnhoven et al. [2009] refers to colloidal silver as comprising silver particles primarily in the range of 250–400 nm, thereby distinguishing nanoscale silver from colloidal silver.

Argyria: Argyria is frequently described as a gray-blue discoloration of the skin, mucous membranes, and/or internal organs as a result of exposure to silver. Argyria may occur in an area of repeated or abrasive dermal contact with silver or silver compounds, or it may occur more extensively over widespread areas of skin after long-term oral or inhalation exposure. Localized argyria can occur in the eyes (argyrosis), where gray-

blue patches of pigmentation are formed without evidence of tissue reaction. Generalized argyria is recognized by the widespread pigmentation of the skin due to the deposition of silver complexes and to a silver-induced increase in melanin [Hathaway and Proctor 2004].

Acknowledgments

This Current Intelligence Bulletin (CIB) was developed by the scientists and staff of the National Institute for Occupational Safety and Health (NIOSH), Education and Information Division (EID), Nanotechnology Research Center (NTRC), with contributions by external collaborators. Paul Schulte is the Director of EID and Co-Manager of the NTRC; Charles Geraci is the NIOSH Associate Director for Nanotechnology and Co-Manager of the NTRC; and Laura Hodson is the Coordinator of the NTRC. This document was authored by Ralph Zumwalde and Eileen Kuempel, EID/NTRC, and by George Holdsworth, Oak Ridge Institute for Science and Education (ORISE), who provided an initial hazard review of the toxicology studies. The data analyses were performed by Eileen Kuempel and Nathan Drew, EID/NTRC, and by Gerald Bachler, Institute for Chemical and Bioengineering, Zurich, Switzerland, who provided the PBPK modeling estimates used in the risk assessment. We would like to acknowledge John A. Decker, Senior Scientist in the NIOSH Office of the Director for his scientific and policy reviews of this document.

A special acknowledgment goes to the following NIOSH NTRC researchers who provided scientific and technical input during the internal review of this document:

Ann Hubbs, Jenny Roberts, and Bean Chen [Health Effects Laboratory Division]
Aleksandr Stefaniak [Division of Respiratory Disease Studies]
Kevin H. Dunn [Division of Applied Research and Technology]
Douglas Trout and Matthew Dahm [Division of Surveillance, Hazard Evaluation, and Field Studies]
Lee Portnoff and Pengfei Gao [National Personal Protective Technology Laboratory]
David Dankovic, Randall Smith, Kathleen MacMahon, and Gary Roth [EID]

We gratefully acknowledge Seleen Collins, Ellen Galloway, and John Lechliter, EID, for their editorial assistance on this document.

Peer Reviewers (to be added)

Public Review (to be added)

Introduction

This Current Intelligence Bulletin (CIB) presents an assessment of the potential health risks to workers occupationally exposed to silver, with emphasis on workers' exposure to silver nanomaterials. The CIB presents (1) workplace exposure data for silver; (2) information on the absorption, systematic distribution, metabolism, and excretion of silver; (3) an assessment of toxicological data from experimental animal studies; (4) an analysis of in vitro and mechanistic studies; (5) an assessment of the health risk to workers exposed to silver and silver nanomaterials; and (6) a recommended exposure limit (REL) for silver and silver nanomaterials. Recommendations for additional research are also provided.

1.1 Background

Silver (Ag) is a rare, naturally occurring element. It is often found as a mineral ore deposit—in association with copper, lead-zinc, and gold—from which it is extracted [USGS 2014]. In 2012, the United States produced approximately 1,050 metric tons of silver. Chemically, silver is the most reactive of the noble metals, but it does not oxidize readily; rather, it tarnishes by combining at ordinary temperatures with sulfur (H_2S). Silver is slightly harder than gold and is very ductile and malleable. Silver can form many different inorganic and organic complexes, and its most stable oxidation states are elemental (+0) and monovalent silver ion (Ag^{+}), although other cationic states (Ag^{+2}, Ag^{+3}) exist as well [USGS 2014]. The most abundant silver compounds are silver sulfide (Ag_2S), silver nitrate ($AgNO_3$), and silver chloride (AgCl).

Elemental silver has been commercially available for decades and used in applications as diverse as coins and medals, electrical components and electronics, jewelry and silverware, dental alloy, explosives, and biocides [Wijnhoven et al. 2009; Nowack et al. 2011; USGS 2014]. For centuries the antimicrobial potential of silver (medicinal silver colloids) for healing wounds and preserving materials [Nowack et al. 2011] has been

recognized, and within the last century silver has been used in antimicrobial tonics, in bandages for wound care, and in the processing of radiographic and photographic materials [Quadros and Marr 2010; Hendren et al. 2011]. The industrial demand for silver has declined for photographic applications, jewelry, electronic applications, and coins, but it has increased for brazing alloys and solders, as a replacement metal for platinum in automobile catalytic converters, and as a catalyst in numerous chemical reactions [USGS 2014].

Within the past decade, the demand has increased for production of silver nanomaterials to create different nanostructures such as spheres and wires [Wijnhoven et al. 2009]. These nanostructures of silver are typically commercialized as powders, flakes, grains, and ingots and are sold in suspensions (such as in water, alcohol, or surfactant), colloidal preparations, and dry powders [Future Markets, 2013]. These various silver compounds have different physical-chemical properties, such as solubility and surface charge, which all may affect their fate and biologic activity. Silver nanomaterials are increasingly being used in consumer and medical products, mainly to take advantage of their high antimicrobial activity. The consumer products and applications include coatings, paints, conductive inks, soaps and laundry detergents, refrigerator and laundry machine components, cooking utensils, medical instruments (dressings, catheters, pacemakers), drug delivery devices, water purifiers, textiles, antibacterial sprays, personal care products (toothpaste, shampoo, cosmetics), air filters, and humidifiers [Quadros and Marr 2010]. Additionally, different nano-forms of silver can be used in the field of electronics (e.g., transparent conducting films, transparent electrodes for flexible devices, flexible thin-film tandem solar cells) [Reidy et al. 2013]. These applications exploit their conductivity and electrical properties rather than antimicrobial properties. The Woodrow Wilson International Center for Scholars "Project on Emerging Nanotechnologies" (http://www.nanotechproject.org/) lists over 100 consumer products containing silver nanomaterials. It was estimated that 20 tons of silver nanomaterials were produced in the United States in 2010 [Hendren et al. 2011], and an estimated worldwide production of 450–542 tons/yr was projected for 2014 [Future Markets 2013]. As new products utilizing silver nanomaterials are produced and

applications expanded, the potential for worker and consumer exposure to airborne silver nanomaterials (such as AgNPs) is expected to escalate throughout the materials' life cycle (that is, their synthesis, use, disposal, and recycling).

Numerous methods have been used to synthesize silver nanomaterials, which can be arbitrarily divided into traditional and nontraditional categories [Evanoff and Chumanov 2005; Chen and Schluesener 2008; Quadros and Marr 2010]. Traditional methods include solution-phase synthesis techniques that are based on various modifications of the Lee-Meisel or Creighton methods, in which different silver salts and reducing agents are used. The most common traditional method for the synthesis of AgNPs is the reduction of $AgNO_3$ with $NaBH_4$. The nontraditional methods include silver particle synthesis through high-temperature reduction in porous solid matrices, vapor-phase condensation of a metal onto a solid support, laser ablation of a metal target into a suspending liquid, photo-reduction of silver ions, chemical vaporization, dry powder dispersion, and electrolysis of a silver salt solution. Although each method has certain advantages and disadvantages, the selection of a method typically depends on the nature of the nanomaterial application. After synthesis, AgNPs can be coated with oxides or coated/embedded into organic polymeric matrices such as poly-(dimethylsiloxane), poly-(4-vinylpyridine), polystyrene, polymethacrylate, and Teflon. These coatings are used to tailor the surface chemical properties of the AgNP to particular applications and to protect them from chemically aggressive environments.

The metallic forms of silver nanomaterials are not soluble in water but can form stable suspensions in which the nanoscale silver slowly dissolves into silver ions [U.S. EPA 2012]. Nanoscale silver may also include other insoluble particulate forms, such as silver carbonate (Ag_2CO_3), silver citrate ($C_6H_5Ag_3O_7$), silver phosphate ($AgPO_4$), silver oxide (Ag_2O), silver sulfate (Ag_2SO_4), and silver sulfide (Ag_2S). However, the metallic salts of silver including nitrate ($AgNO_3$) and silver chloride (AgCl) are soluble in water [WHO 2005]. The highly insoluble forms of silver typically have a low dissolution rate for releasing silver ions, whereas the completely soluble forms of silver (such as $AgNO_3$) have a high ion dissolution release potential in water. Factors that can affect the

dissolution of AgNPs in water include size [Ma et al. 2012], surface coatings [Zook et al. 2011; Li et al. 2012; Tejamaya et al. 2012], pH [Elzey and Grassain 2010;], and the solution concentration of sulfur or sodium chloride [Kent and Vikesland 2012]. Also, as the particle size of silver decreases, the potential for releasing silver ions via dissolution increases because of rising surface availability per mass of silver [Wijnhoven et al. 2009].

Although the overall amount of animal toxicological information is small and the studies have been of comparatively short duration, the knowledge base includes these findings: (1) AgNPs in the body by various routes of exposure can be absorbed and become transported to target tissues; (2) lung inflammation and lung function decrements have been observed at certain exposure concentrations of AgNPs following subchronic inhalation in rats, suggesting the potential for chronic adverse health effects; and (3) the liver and (to a lesser extent) the kidney represent the primary target organs for systemic accumulation of silver and adverse effects associated with exposure to AgNPs. The studies also indicate that the higher surface volume ratio of AgNPs, compared with larger respirable-size silver particles, is a cause of concern because it makes AgNPs potentially more reactive than larger silver particles and makes it more difficult to predict how they will interact with biological systems (Table 1-1).

Table 1-1. Differences between ionic, nanoparticulate, and bulk silver.

Ions	Nanoparticles	Bulk (microscale) particles
• Smaller particle size and higher total surface area of nanoparticles (per unit mass) increase ionization rate • Highly reactive precipitates • Easily get inside cells • Form complexes with inorganic and organic compounds	• Larger particle surface area (per unit mass) increases dissolution and ionization rates • Highly reactive • Oxidative potential • Ability for uptake via active processes • Binding of biomolecules • As size decreases, ability to get inside cells increases	• Smaller particle surface area (per unit mass) results in slower dissolution and ionization rates • Lower acute oxidative capacity • Lower uptake by cells • Limited binding of biomolecules

Adapted from Reidy et al. [2013].

1.2 Bases for Current Occupational Exposure Limits

The accumulation of silver over time (body burden) has been shown to result in a health condition known as argyria. This condition, a pathologic consequence of prolonged silver exposure, has been described as a blue-grey discoloration of the skin and mucous membranes (argyria) or as a localized condition of the eyes (argyrosis) [Harker and Hunter 1935; Hill and Pillsbury 1939]. Exposure to the soluble forms of silver has frequently been associated with the development of argyria [ATSDR 1990; Drake and

Hazelwood 2005; Wijnhoven et al. 2009; Johnston et al. 2010; Lansdown AB 2012]. Generalized occupational argyria in exposed workers can occur as a result of the absorption of silver through the lungs, the digestive tract, or wounds in the skin.

The prevention of argyria is the basis for the current occupational exposure limits (OELs) in the United States and other countries. The Occupational Safety and Health Administration (OSHA) permissible exposure limit (PEL) and the National Institute for Occupational Safety and Health (NIOSH) recommended exposure limit (REL) are 10 µg/m^3 (total dust) for silver (metal dust and soluble compounds) as an 8-hr time-weighted average (TWA) concentration [OSHA 1988, 2014; NIOSH 2007]. The American Conference of Governmental Industrial Hygienists (ACGIH) threshold limit values (TLVs®) [ACGIH 2001] and the German MAK Commission MAK values are also 10 µg/m^3 for soluble silver but are higher, at 100 µg/m^3, for insoluble silver compounds (Table 1-2). The evidence basis and derivation of the NIOSH REL are discussed further in Section 6.

Table 1-2. Current OELs for silver in the United States and other countries

Authority	Particle Size	Form	OEL (µg/m^3)	Reference
OSHA PEL*	Metal dust and soluble compounds, as Ag; total mass fraction	Soluble or insoluble	10	NIOSH [2007]
NIOSH REL	Metal dust and soluble compounds, as Ag; total mass fraction	Soluble or insoluble	10	NIOSH [2007]
ACGIH TLV	Metal dust and fume; inhalable fraction	Soluble	10	ACGIH [2001]
		Insoluble	100	
MAK†	Inhalable fraction	Silver salts (as Ag)	10	DFG [2013]
		Silver (Ag)	100	

*Current regulatory limit in the United States. †Maximum Workplace Concentration (Germany).

There is a growing body of toxicological evidence indicating that exposure to some forms and particle sizes of silver may pose a more severe health risk to workers than other forms and sizes. The literature search strategy for this document is described in Appendix D. Recent experimental animal studies with rats (for up to 3 months) exposed to AgNP concentrations of approximately 100 µg/m^3 (10 times the current OSHA PEL and NIOSH REL) showed mild adverse lung effects, including pulmonary inflammation and lung function deficits that persisted after the end of exposure. Bile duct hyperplasia has also been observed in rats after the inhalation of relatively low-mass concentrations of silver and AgNPs (Appendix F, Table F-5). It is not known how universal these adverse effects are, that is, whether they occur in animals exposed to all forms and particle sizes of silver. Most importantly, it is not known whether similar adverse health effects occur in humans following exposure to AgNPs. The extent to which workers are exposed to silver in the workplace, including exposure to silver nanomaterials, is also unclear because of limited published exposure data.

2 Occupational Exposures to Silver

Worker exposure to silver can occur throughout the life cycle of the metal (ore extraction, melting/refining, product fabrication, use, disposal, recycling) [Maynard and Kuempel 2005]. Inhalation and dermal contact with silver are considered to be the main exposure routes [ATSDR 1990; Wijnhoven et al. 2009]. Published information on worker exposure to silver is limited to studies that found airborne silver exposures during brazing and soldering operations [NIOSH 1973, 1981, 1998]; fabrication of silver jewelry [NIOSH 1992; Armitage et al. 1996]; recovery of silver from photographic fixer solutions [Williams and Gardner 1995; NIOSH 2000]; production of silver oxide and silver nitrate [Rosenman et al. 1979, 1987; Moss et al. 1979]; refinement of silver [Williams and Gardner 1995]; reclamation of silver [Pifer et al. 1989; Armitage et al. 1996]; and handling of insoluble silver compounds [DiVincenzo et al. 1985; Wobling et al. 1988]. The reports of these studies lack information on the physical-chemical characteristics (such as particle size or species) of the aerosol to which workers were exposed, although it's likely that aerosols/fumes generated during brazing/soldering [NIOSH 1973, 1981, 1998], the melting of silver alloys [NIOSH 1992], the refinement of silver [Williams and Gardner 1995], and the recovery of silver from photographic fixer solutions [Williams and Gardner 1995; NIOSH 2000] contained some nanometer-size silver particles and/or agglomerates of silver particles. In several workplace studies, airborne exposure to AgNPs was measured during the synthesis of engineered AgNPs [Park et al. 2009; Lee et al. 2011a, b; Lee et al. 2012] and during the electro-refining of silver [Miller et al. 2010]. Workplace findings on the potential for dermal absorption of silver during handling of colloidal suspension (gel form) and liquid AgNPs also have been reported [Ling et al. 2012]. Table 2-1 summarizes reported workplace exposures to silver.

NIOSH has reported on several workplace studies in which workers were found to be exposed to silver and other airborne contaminants during brazing/soldering and milling operations performed at an air conditioning equipment company [NIOSH 1973], a metal

fabrication facility [NIOSH 1981], and a manufacturer of construction equipment [1998]. Workers were found to be exposed to airborne silver concentrations that ranged from nondetectable (ND) to 6 μg/m^3 during brazing and soldering operations while assembling air conditioning equipment [NIOSH 1973] in which the use of exposure controls was minimal. At the other two manufacturing facilities, workers performing brazing and soldering were exposed to airborne silver concentrations that were below the OSHA PEL and NIOSH REL of 10 μg/m^3 [NIOSH 1981] or ranged from ND to 0.015 μg/m^3 [NIOSH 1998]. In both facilities, controls were used to minimize worker exposure. NIOSH also reported on a survey at a manufacturer of silver jewelry [NIOSH 1992], in which workers were potentially exposed to silver, copper, lead, and cadmium fume as well as to carbon monoxide and nitrogen dioxide. Exposure to silver was detected during the metal casting operation, in which 100 ounces of an Ag/Cu alloy were melted with an air-acetylene and oxy–natural gas torch. The operation took approximately 84 minutes, and the airborne silver concentration to which the worker was exposed during this time was 54 μg/m^3. Local exhaust ventilation (LEV) was used during the casting operation. The highest airborne silver concentrations were found at a precious metal recycling facility [NIOSH 2000] during the recovery of silver from photographic fixer solutions. Silver was recovered by the "metallic replacement method," in which steel wool and fiberglass were used within a recovery cartridge to extract the dissolved silver ions from the fixer solution. The cartridges were then placed into silicon carbide or clay graphite crucibles and heated at a temperature of 2200–2300^{o}F to separate silver from the impurities. A personal sample collected on a worker during the silver recovery process revealed an airborne TWA silver concentration of 140 μg/m^3. Area airborne samples collected over the full work shift at this facility revealed silver concentrations that ranged from 9 to 190 μg/m^3.

Airborne exposure to engineered AgNPs has been documented during their synthesis in a liquid-phase production process [Park et al. 2009]. The airborne release of AgNPs was evaluated at the reactor (wet chemical method), dryer, and grinding processes with use of a scanning mobility particle sizer (SMPS), to determine the size and particle number concentration, and with an electrostatic precipitator (ESP) to collect samples for

particle characterization by transmission electron microscopy (TEM). Exposure measurements of AgNPs taken at the opening of the reactor showed the release of particles with diameters of 50–60 nm, which agglomerated into 100-nm particles shortly after their release. Particle measurements taken before the reactor door was opened (6.1×10^4 particles/cm^3) increased to 9.2×10^4 particles/cm^3 when it was opened. After a 24-hour aging process, the silver colloidal suspension was transferred from the reactor, filtered, and deposited in a dryer to remove volatile organic materials and water. Airborne particle concentrations determined after the drying of the silver suspension indicated a doubling in the number of AgNPs that were 60–100 nm in diameter, compared with background particle number measurements. Prior to packaging, the dried AgNPs were ground to reduce agglomeration; measurements taken at the opening of the grinder detected the release of airborne AgNPs 30–40 nm in diameter.

Lee et al. [2011a, b] reported on the airborne release of engineered AgNPs during their synthesis at two different facilities. Facility A used a large-scale pilot reactor operated at negative pressure in which various silver-containing precursors (wire, powder, liquid) were fed through an inductively coupled argon plasma (ICP) torch, where they were vaporized in argon plasma. Silver atoms were condensed to predominantly 20–30-nm particles in a temperature gradient and then amassed in a collector. Facility B synthesized silver nanoparticles (1 kg/day) by mixing sodium citrate with silver nitrate and pumping the solution into a reactor that was housed in a ventilated fume hood. Worker and area exposure measurements detected airborne silver concentrations up to 0.1 µg/m in Facility A and 0.4 µg/m^3 in Facility B [Lee et al. 2011a]. Two of five workers who were involved in AgNP manufacturing at Facility A also participated in a health surveillance study [Lee et al. 2011b]. The two had been employed at the facility for 7 years. One worker was reported to have been exposed to an airborne silver concentration of ~0.3 µg/m^3 and the other worker to a concentration of ~1.35 µg/m^3. Levels of silver in the blood of the two workers were 0.0135 and 0.034 micrograms per deciliter (µg/dL), and those in the urine were 0.043 µg/dL and ND. All clinical chemistry and hematologic parameters were found to fall within the normal range, and the workers reported no adverse health effects. A follow-up study was conducted to evaluate

workplace exposures over 3 days [Lee et al. 2012]. Personal and area samples were collected for silver determination and for particle characterization by means of scanning transmission electron microscopy (STEM) and energy-dispersive X-ray spectroscopy (EDS). Real-time airborne particle size and count concentrations were also determined, with an SMPS and a condensation particle counter (CPC). The highest airborne concentrations for silver were detected in the injection room, where silver powder along with acetylene and oxygen gas were introduced into the reactor to manufacture AgNPs. Workers who spent a total of 10–20 minutes per day in the injection room had TWA silver concentrations that ranged from 0.04 to 2.43 μg/m^3 during those time periods. The use of exposure controls was not reported, but workers were required to wear half-facepiece respirators. TWA silver concentrations determined from area samples collected in the injection room ranged from 5 to 288.7 μg/m^3, whereas area samples collected for silver at other locations in the facility had concentrations ≤1.3 μg/m^3. Analysis of area and personal airborne samples by STEM showed the preponderance of AgNPs as agglomerates. Real-time aerosol monitoring with the SMPS revealed particle number concentrations that ranged from 224,622 to 2,328,608 particles/cm^3, whereas measurements by CPC revealed concentrations of 533 to 7,770 particles/cm^3, indicating that the majority of the aerosol particles were <100 nm.

Airborne exposure to AgNPs was also reported to occur during the melting and electro-refining of silver feedstock [Miller et al. 2010]. A survey of worker exposures at a precious metals refinery yielded results from personal and area samples collected for metal determination as well as airborne particle number concentrations via a Fast Mobility Particle Sizer (FMPS). A handheld ESP was also used to collect airborne aerosols for TEM characterization. Concentrations in personal airborne samples for total silver (from use of NIOSH Method 7303) ranged from 13 to 94 μg/m^3, whereas those in area samples ranged from 4 to 39 μg/m^3. Concentrations in all area samples analyzed for soluble silver compounds (with use of ISO Method 15202) were <2 μg/m^3. TEM and EDS analysis of ESP samples indicated the presence of silver, lead, selenium, antimony, and zinc, with all metals in the nanometer size range. AgNPs were the primary aerosol, with a mean diameter of ~10 nm, in samples collected near the

furnace; samples collected at other worksites contained agglomerated AgNPs with diameters of ~100 nm. Airborne particle number measurements made with an FMPS in work areas on the electro-refining floor and around the furnaces during mold pours were >10^6/cm^3, representing up to a 1,000-fold increase in particle number concentration over baseline background particle concentrations.

Table 2-1. Summary of occupational exposures to silver.

Source of Exposure	Exposure Details and Airborne Silver Concentrations	Comments	Reference
Brazing, silver soldering, and milling at an air conditioning equipment facility	Personal samples (7): ND–6.0 µg/m^3 TWA Area samples (4): ND–6.0 µg/m^3 TWA	➢ No clinical signs of argyria ➢ No local exhaust ventilation (LEV) used	NIOSH [1973]
Brazing, milling, and sanding at a metal fabrication facility	Personal samples (20): 0.001–0.01 µg/m^3 TWA	➢ No clinical signs of argyria ➢ LEV used	NIOSH [1981]
Brazing at a manufacturer of construction equipment	Personal samples (99): ND–15 µg/m^3 TWA	➢ No clinical signs of argyria ➢ LEV used	NIOSH [1998]
Casting of a silver alloy at a silver jewelry manufacturing facility	Personal sample (1): 54 µg/m^3 (84 min)	➢ No medical assessment performed ➢ LEV used	NIOSH [1992]
Silver recovery from photographic fixer solutions	Personal sample (1): 140 µg/m^3 TWA Area samples (5): 9–190 µg/m^3 TWA	➢ No medical assessment performed ➢ Local exhaust in furnace room not operating correctly	NIOSH [2000]

Manufacturing of silver nitrate and silver oxide	Personal samples (6): 39–378 µg/m^3 TWA	➢ No mention of exposure controls ➢ Medical assessment of 30 workers found • 6 workers with generalized argyria • 20 workers with argyrosis • 10 workers with decreased vision	Rosenman et al. [1979]
Silver processing facility (silver salts and metallic silver)	Area samples: 1–310 µg/m^3 TWA (soluble silver compounds), 3–540 µg/m^3 TWA (insoluble silver compounds)	➢ No mention of exposure controls ➢ Medical assessment of 50 workers found • 9 workers with argyrosis (soluble silver exposure) • No symptoms of argyrosis in workers exposed to insoluble silver	Wolbling et al. [1988]
Reclamation of silver from photographic film, paper, and liquid wastes (insoluble silver halides)	Personal and area samples (>100) over a 30-yr period: 5–240 µg/m^3 TWA	➢ No mention of exposure controls ➢ Medical assessment of 27 workers found • No cases of argyria • 7 workers with some form of ocular argyrosis	Pifer et al. [1989]
Smelting and refining of silver and the preparation of silver salts for photosensitized products	Personal and area samples (62) over a 2-month period: 1–100 µg/m^3 TWA	➢ No mention of exposure controls ➢ Biologic samples for silver in blood, urine, and feces measured for 37 workers • Low levels of silver in blood in 80% of	DiVincenzo et al. [1985]

		workers; none detected in controls	
Manufacturing precious metal powder (silver nitrate, silver oxide, silver chloride, silver cadmium oxide)	Personal samples (OSHA inspection): 40–350 µg/m^3 TWA	➢ No mention of exposure controls; some workers reported to wear respirators ➢ Biologic samples for blood and urine silver showed raised levels in >90% of studied workers ➢ Acute irritation found for eyes and kidney	Rosenman et al. [1987]
Six worksites: Silver reclamation, bullion production, jewelry manufacture, bullion/coin/tableware production, and chemical production (two factories)	No assessment of airborne silver concentrations reported	➢ No mention of exposure controls ➢ Blood silver levels measured for workers at all six worksites • Reclamation workers: 1.3–20 µg/L • Workers from the other 5 worksites: 0.1–16 µg/L • Jewelry workers had lowest levels: 0.2–2.8 µg/L	Armitage et al. [1996]
Two worksites: silver reclamation from X-rays and photographic film, and silver refinery	Samples taken during silver reclamation (3): Area, 85 µg/m^3 (3 hrs) at incinerator; Personal, 1030 and 1360 µg/m^3 (<15 min) at pulverizing area Samples taken during silver refining:	➢ Improvements in exposure control instituted ➢ Medical assessment of a worker at each site for argyrosis and argyria: • Worker involved in silver reclamation (silver halides and oxide): no argyrosis • Worker involved in silver refining (soluble	Williams and Gardner [1995]

	Area, 110–170 µg/m^3 (229 min) at silver refining casting area; Personal, 100 µg/m^3 (224 min) and 59–96 µg/m^3 (28 min) at silver refining casting area	compounds; silver nitrate): argyrosis	
Production of nanoscale silver (liquid-phase production process; silver nitrate with nitric acid)	No quantitative silver exposure measurements; only particle count concentrations	➢ Improvements in exposure control instituted	Park et al. [2009]
Production of nanoscale silver at two facilities: Facility A used inductively coupled plasma torch with electric atomizer; Facility B used sodium citrate and silver nitrate	Personal and area samples (10) at Facility A: 0.02–1 µg/m^3 Personal and area samples (10) at Facility B: 0.03–0.4 µg/m^3	➢ Facility A: The reactor and collector process was performed under vacuum to control release of airborne silver ➢ Facility B: The wet process reacting silver nitrates with citrate prevented release of airborne silver particles	Lee et al. [2011a]
Production of nanoscale silver at Facility A, as described in Lee et al. [2011a]	Facility A personal samples (2): Worker 1, 0.35 µg/m^3 Worker 2, 1.35 µg/m^3	➢ Biologic samples for silver • Worker 1: blood (0.034 µg/dl); urine (0.043 µg/dl) • Worker 2: blood (0.030 µg/dl); urine (ND) Some engineering controls used as well as PPE	Lee et al. [2011b]

Production of nanoscale silver at Facility A, as described in Lee et al. [2011a,b]	Facility A samples were collected over 3 days. Personal samples (6): Worker 1, 1.55–4.99 µg/m^3 (2.43 µg/m^3 TWA) Worker 2, 0.09–1.35 µg/m^3 (0.04 µg/m^3 TWA) Area samples (28): 0.07–426.43 µg/m^3	➢ Highest silver concentrations found in the injection room, in which silver powder and acetylene/oxygen gas were injected into the reactor ➢ Particle number concentration ranged from 911,170 to 1,631,230 cm^3 during reactor operation ➢ Particle size: 15–710 nm during reactor operation ➢ Natural ventilation used; workers wore half-mask respirators	Lee at al. [2012]
Precious metal processing facility; melting and electro-refining of silver	Total silver Personal full-shift samples (6): 13–94 µg/m^3 Area samples (14): 4–39 µg/m^3	➢ Highest personal exposures to silver found on electro-refining floor ➢ Particle number concentrations >10^6, with highest at furnaces/pouring ➢ ~10-nm-diameter particles ➢ Ventilation controls during pouring of molten metal	Miller et al. [2010]

3 Human Evidence of Internal Dose and Potential Adverse Health Effects

3.1 Background

The majority of study reports on workplace and health assessments of workers exposed to silver lack sufficient detail to adequately determine the physical-chemical characteristics (such as particle size and silver species) of the aerosol to which workers were exposed. However, it's reasonable to infer that some workers had exposure to nanometer-sized particles, on the basis of known characteristics of particles that are typically present (1) in fumes generated during brazing and soldering or the melting of silver alloys or silver recycled materials, (2) during the recovery of silver from photographic fixer solutions, and (3) during the handling of colloidal silver. Because of silver's many potential uses, workers can be exposed to a range of particle sizes and forms of silver that have the potential for entry into the body by different routes of exposure [Drake and Hazelwood 2005]. Ingestion can be a significant route of entry for silver compounds and colloidal silver [Silver 2003], whereas the inhalation of dusts or fumes containing silver occurs primarily in occupational settings [ATSDR 1990]. Skin contact can also occur in occupational settings from the handling of silver and silver-containing materials [ATSDR 1990].

Several factors are known to influence the ability of a metal to produce toxic effects on the body; these include the solubility of the metal at the biologic site (affected by particle size and pH of the surrounding media), the nature of any surface coat or binding material, the surface activity of the metal, the ability of the metal to bind to biologic sites, and the degree to which metal complexes are formed and sequestered or metabolized and excreted. Published studies appear to indicate that some forms of silver may be more toxic than others. The majority of health data from workers exposed to silver indicate that long-term inhalation or ingestion of silver compounds (especially soluble

forms of silver) can cause irreversible pigmentation of the skin and mucus membranes (argyria) and/or the eyes (argyrosis), in which the affected area becomes bluish-gray or ash gray [ATSDR 1990; Drake and Hazelwood 2005; Wijnhoven et al. 2009; Johnston et al. 2010; Lansdown 2012]. Generalized argyria has often been reported to occur in individuals following the ingestion or application of silver-containing medicines, but it has also been observed to varying degrees in workers exposed to silver compounds during the production, use, and handling of silver nitrate and silver oxide [Moss et al. 1979; Rosenman et al. 1979; Williams 1999] and silver salts (nitrate and chloride) [Wobling et al. 1988]; during the reclamation of silver from photographic film [Buckley 1963; Pifer et al. 1989; Williams and Gardner 1995]; and during the handling of silver in photosensitized products [DiVincenco et al. 1985]. Localized argyria has also been reported due to the following causes: application of burn creams containing silver [Wan et al. 1991]; silver soldering [Scrogges et al. 1992]; contact with silver jewelry [Catsakis and Sulica 1978]; use of silver acupuncture needles [Tanita et al. 1985; Sato et al. 1999], catheters [Saint et al. 2000], or dental amalgams [Catsakis and Sulica 1978]; and accidental puncture wounds [Rongioletti et al. 1992].

3.2 Human Studies of Lung Deposition of Airborne Silver Nanoparticles

Limited data are available on the deposition of inhaled AgNPs in humans and absorption from the lungs (i.e., transport across epithelial cell membranes and entry into the lymph or blood circulatory system) [Muir and Cena 1987; Cheng et al. 1996]. Muir and Cena [1987] exposed three male volunteers to air containing AgNPs with an average particle diameter of 9 nm (geometric standard deviation [GSD] = 2.0) and at a concentration of 2×10^5 particles/cm^3. Airborne particles were measured with a nucleus particle counter for size and concentration. The particle size of the aerosol was obtained before and after each inhalation experiment and differed only slightly from 9 nm. The sampling of inhaled and exhaled air was undertaken at a fixed flow rate of 2 L/min. Particle deposition in the respiratory tract was determined by relating the concentrations

of particles inhaled to the concentrations of particles exhaled by the subjects. The subjects breathed at a normal resting lung volume. Particle deposition was found to increase from 20% to 90% as the breathing cycle (duration of breath, including both inspiration and expiration) increased from 2 to 10 seconds, but it was not affected by tidal volume (volume of air inhaled and exhaled at each breath; 0.5–3 L tested).

In another lung deposition study with AgNPs, 10 male human subjects were exposed to four different particle sizes (4, 8, 20, and 150 nm diameters) of silver wool (99.9% pure) via an evaporation–condensation method at two constant flow rates of 167 and 333 cm^3 per second [Cheng et al. 1996]. Airborne concentrations of AgNPs were measured with a CPC. Each subject was repeatedly measured for aerosol deposition during 32 combinations of experimental conditions. Lung deposition efficiencies for 4-nm particles ranged from about 25% to 65% with nose-in/mouth-out breathing and 25% to 62% with mouth-in/nose-out breathing. For 8-nm particles, respective deposition efficiencies were 14% to 49% and 14% to 45%. The respective ranges for 20-nm particles were 2% to 35% and 3% to 28%. Although the values of deposition efficiencies varied among the 10 subjects, particle deposition in the lung appeared to result from diffusion, with AgNP deposition observed to increase as the particle diameter and flow rate decreased. The inter-individual variability of particle deposition efficiencies was correlated with the inter-subject variations in nasal dimensions (as measured by total surface area), smaller cross-sectional area, and complexity of the airway shape.

3.3 Health Effects in Workers with Exposure to Silver

Rosenman et al. [1979] reported findings of respiratory symptoms and argyria in workers (*n* = 30) involved with the manufacturing of silver nitrate and silver oxide. Sixteen of the 30 had worked for 5 or more years. All the workers were white males, and the average age was 34.6 years. Chest radiographic findings and results of clinical examination of respiratory function were predominantly normal. Two workers were found to have small irregular opacities on chest x-rays; one of the workers was reported

to have had previous exposure to asbestos. None of the workers had evidence of restrictive pulmonary disease, and obstructive changes in pulmonary function were attributed to smoking. Ten of the 30 workers complained of abdominal pain, which appeared to be associated ($p < 0.25$) with silver found in the blood. There was a history of x-ray-documented ulcers in six of these workers and a history of upper gastrointestinal bleeding in two others. Decreased vision at night was also reported by 10 workers and was associated with the length of employment; however, no changes in visual performance could be attributed to silver deposits. The cross-sectional study did identify six workers with generalized argyria and 20 with argyrosis. At the time of the study, no exposure measurements were taken; however, personal airborne measurements made 4 months before the study revealed 8-hour TWA silver concentrations ranging from 39 to 378 µg/m^3 (total mass). A follow-up study of these 30 workers [Moss et al. 1979] also revealed evidence of argyrosis and burns of the skin from contact with silver nitrate in 27 and a history of ocular burns in 11. An in-depth ophthalmic examination was conducted to determine if workers suffered from any visual deficits from their exposure. A direct relationship was shown between the amount of discoloration of the cornea and the length of time worked. Although some workers complained of decreased night vision, no functional deficits were found.

Wobling et al. [1988] reported on a cross-sectional study of 50 workers (44 males and 6 females employed ≥1 year) at a silver processing plant to determine if symptoms of exposure differed between those exposed predominantly to insoluble silver ($n = 26$) and those exposed exclusively to soluble silver compounds of silver nitrate and silver chloride ($n = 23$). Ten subjects, not occupationally exposed to silver, were used as a control group. Length of exposure ranged from 3 to 20 years. Exposure concentrations ranged from 1 to 310 µg/m^3 for workers exposed to soluble silver compounds and from 3 to 540 µg/m^3 for those exposed to insoluble silver compounds. Among workers in the soluble exposure group, discoloration (argyrosis) was observed in the eyes of 5, the mouths of 2, the nose of 1, and the nape of the neck of 1. No symptoms of argyria or argyrosis were seen in workers in the insoluble exposure group. Skin biopsies analyzed for silver revealed a concentration of 0.03 to 13.48 ppm for the soluble group (median of

0.115 ppm), 0.03 to 0.77 ppm for the insoluble group (median of 0.085 ppm), and 0.01 to 0.11 ppm for the control group (median of 0.02 ppm). Silver concentrations found in the skin biopsies and air did not correlate with either ocular deposits or duration of exposure. The authors concluded that the occurrence of argyria and argyrosis is dependent upon individual susceptibility.

Pifer et al. [1989] reported on a clinical assessment of 27 silver reclamation workers exposed primarily to insoluble silver halides. An equal number of workers not occupationally exposed were selected as a control group. Airborne silver concentrations ranged from 5 to 240 µg/m^3 (total mass). Silver was found in the blood of 21 silver reclamation workers, with a mean concentration of 0.01 µg/mL. Only one worker had a detectable level of urinary silver; silver was not detected in the blood or the urine of the control group. Silver was measured in all fecal samples collected, with a mean concentration of 16.8 µg/g found for exposed workers (*n* = 18) and 1.5 µg/g for unexposed workers (*n* = 22). Clinical examinations and skin biopsies revealed no cases of generalized argyria. Twenty of the 27 reclamation workers exhibited some degree of internal nasal septal pigmentation, and 7 of 24 workers were found to have ocular silver deposits in the conjunctiva and/or cornea. Optometric and contrast sensitivity test results revealed no significant deficits in visual performance. No abnormalities were revealed during tests of renal and pulmonary function or on chest radiographs. The researchers concluded there was no evidence that chronic exposure to insoluble silver halides had detrimental health effects on exposed workers at the concentrations measured.

DiVincenzo et al. [1985] reported on workers exposed to different species of silver during the smelting and refining of silver and preparation of silver salts for use in photosensitized products. The absorption and excretion of silver were monitored by measuring blood, urine, fecal, and hair concentrations in 37 male workers occupationally exposed primarily to insoluble silver compounds; a group of 35 unexposed workers served as a control population. Personal and area airborne samples were collected for silver. The 8-hr TWA exposure to silver over a 2-month monitoring

period (62 samples) ranged from about 1 to 100 µg/m^3 (total mass). Measured concentrations of silver in the blood, urine, and feces were 0.011 µg/mL, <0.005 µg/mL, and 15 µg/mL, respectively. The concentration of silver in the hair was higher for the silver workers than for controls (130 ± 160 vs. 0.57 ± 0.56 µg/g). Using fecal excretion as an index of exposure for calculating body burden of silver and assuming that 1% to 5% of the silver was retained in the body, the authors concluded that a minimum of 24 years of continuous workplace exposure would be necessary for workers to retain enough silver to develop argyria.

Williams and Gardner [1995] reported on the medical evaluation of two workers who were employed by a company involved in the reclamation of silver from old X-rays and photographic film. The reclamation and refining process required incineration of the film, pulverization of the ash, and extraction of the silver, followed by an electrolytic process involving nitric acid to obtain the desired purity prior to casting of the silver. The two workers had been employed for less than 7 years and were reported to be asymptomatic, with no evidence of argyria. A personal exposure measurement for one of the workers (Case 1) during the incineration of films was 85 µg/m^3 (180 minutes), and airborne concentrations of 1030 and 1360 µg/m^3 (<115 minutes) were measured in the pulverizing area. A blood silver determination for this worker at the time of environmental exposure assessments was 49 µg/L. The second worker (Case 2) was mainly involved in silver refinement and was reported to have airborne concentrations of 110 to 170 µg/m^3 (229 minutes) and 100 µg/m^3 (224 minutes) during the casting of silver. Short-term personal samples indicated exposure concentrations of 59 to 96 µg/m^3 (28 minutes), and background airborne concentrations in the electrolytic area of the refinery were 30 to 70 µg/m^3. The background concentrations of silver were attributed to the presence of silver compounds from the electrolytic tanks rather than from the casting process. Follow-up visits to the plant revealed no change in the clinical outcome of the first worker (Case 1) exposed to silver halides and silver oxide. This was consistent with the report of Pifer et al. [1989] that exposure to insoluble silver compounds appeared to be relatively benign in causing argyria. Follow-up clinical assessment of the second worker (Case 2) revealed the onset of argyria, attributed to

exposure to soluble silver compounds (silver nitrate) and metallic silver. Subsequent follow-up of this worker over a 5-year period [Williams 1999] indicated an average blood silver concentration of 11.2 µg/L (range, 6–19 µg/L). During this period, no progression of argyria was noted.

In a cross-sectional study of workers manufacturing silver (silver nitrate, silver oxide, silver chloride, silver cadmium oxide) and other metal powders, Rosenman et al. [1987] observed upper respiratory irritation, such as sneezing, stuffy or runny nose, and chest tightness, in 15 of 27 workers (56%). The average age of the 27 workers was 41, and they had worked at the plant for an average of 8.1 years. Kidney function was also evaluated, and the level of urinary enzyme N-acetyl-B-D glucosaminidase (NAG) was found to be significantly raised in four workers. The increase in NAG levels was correlated with blood silver concentrations and age, suggesting a possible toxic effect of silver on the kidney. In addition, the group's average NAG concentration was significantly higher ($p < 0.01$) than that found in the control population. Because of concurrent exposure to known nephrotoxins, such as cadmium and solvents, the authors could not definitively determine if exposure to silver was responsible. Also, 96% of the workers had elevated urine silver concentrations (0.5–52.0 µg/L), and 92% had elevated blood silver concentrations (0.05–6.2 µg/100 ml). No correlation was found between raised blood and urine silver concentrations and the work area. However, this lack of an association may have been due to the workers' use of respiratory protection. An OSHA health inspection conducted at the plant revealed 8-hr TWA silver concentrations ranging from 40 to 350 µg/m^3 (total mass).

Although it is unclear whether there is a relationship between airborne exposure to silver and blood silver concentrations, Armitage et al. [1996] suggested that blood silver concentrations determined on a group level could be used to evaluate the overall effectiveness of workplace control measures. A total of 98 blood samples from occupationally exposed workers and 15 control blood samples from agricultural workers were analyzed for silver. Samples were collected from workers at factories involved in silver reclamation, jewelry manufacture, bullion production, silver chemical manufacture,

and the production of tableware. A normal range of blood silver concentrations was found for the agricultural workers, with a mean of <0.1 µg/L. Reclamation workers were found to have some of the highest silver concentrations in the blood, ranging from 1.3 to 20 µg/L (average, 6.8 µg/L), whereas workers involved in refining silver to produce bullion, coins, and chemicals had blood silver concentrations that ranged from 0.1 to 16 µg/L (average, 2.5 µg/L). Workers employed in industries as silver refiners and those involved in the production of silver nitrate had the highest blood silver concentrations, whereas workers in jewelry production had the lowest, ranging from 0.2 to 2.8 µg/L. No evidence of argyria was found in any of these workers.

Likewise, Cho et al. [2008] reported normal hematology and clinical chemistry values for a subject whose serum silver level reached 15.44 µg/dL (normal range, 1.1–2.5 µg/dL) and urinary silver level reached 243.2 µg/L (normal range, 0.4–1.4 µg/L) after exposure to aerosolized silver at a mobile telephone subunit facility. The aerosolized silver, which was reported to contain alcohol, acetone, and silver, was used for plating metal parts. Exposure controls were not used during the plating of silver, and the worker did not wear respiratory protection. No information was provided on silver species or particle size. The worker developed generalized argyria of the face, and a biopsy of the epidermal basal layer of the skin revealed the presence of silver granules.

3.4 Reports of Workers Exposed to Silver Nanoparticles and Potential Health Effects

Published reports on the exposure–response relationship—that is, between workplace exposure to AgNPs and health effects—are limited to those by Lee et al. [2011a,b] and those concerning workers using Acticoat™ dressings [Trop et al. 2006; Vlachou et al. 2007].

The potential for silver nanoparticles to induce harmful effects in humans occupationally exposed to AgNPs has not been studied to any great extent, and the available data

have not indicated any significant adverse effects under the prevailing exposure conditions. Lee et al. [2011a,b (described in Section 2)] reported on workers exposed to airborne engineered AgNPs during their synthesis (via an inductively coupled argon plasma process in Facility A and the mixing of sodium citrate/silver nitrate in Facility B). Although traces of silver were detected in their blood and urine, all clinical chemistry and hematologic parameters were found to fall within the normal range and no adverse health effects were reported for these workers.

Trop et al. [2006] reported on a burn victim who had an argyria-like condition and elevated activities of liver-specific plasma enzymes when an Acticoat™ dressing (containing ionic AgNPs) was applied to his wound. No mention was made of silver being sequestered in the liver, although this was possible since levels of the metal were elevated in plasma and urine. As reported by the authors, local treatment with Acticoat™ dressings for 7 days caused the plasma activities of alanine aminotransferase (ALT) and aspartate aminotransferase (AST) to rise incrementally to 233 and 78 units per liter (U/L), respectively (upper limits of normal: 33 U/L for ALT and 37 U/L for AST). The concentration of silver in blood plasma was 107 micrograms per kilogram (µg/kg); this value subsequently dropped toward normal levels (13.3 µg/kg after 97 days) when Acticoat™ dressings were changed on day 8 to dressings containing betadine ointment. C-reactive protein level was also elevated, in parallel with plasma silver levels, reaching a maximum concentration of 128 milligrams per liter (mg/L) after 4 days. The level of this liver-synthesized marker for acute inflammation was back to normal (5 mg/L) after 8 silver treatment–free days.

In a prospective study of 30 patients with graft-requiring burns, Vlachou et al. [2007] found increased concentrations of silver in serum (median, 56.8 micrograms per liter [µg/L]; range, 4.8–230 µg/L) when Acticoat™ dressings were applied to the wounds. The authors found no changes in hematologic or clinical chemistry parameters indicative of toxicity associated with the silver absorption, and at the 6-month follow-up, the median serum level had declined to 0.8 µg/L. However, the absence of any toxicological effects of silver deposition from Acticoat™ dressings reported by Vlachou

et al. [2007] contrasts with the findings of Trop et al. [2006], who reported elevated silver levels in plasma and changes in liver-related clinical chemistry parameters when the wounds of a patient with 30% mixed-depth burns were treated with Acticoat™ dressings. The patient developed argyria-like symptoms, including a grayish discoloration of the face. Plasma silver levels, clinical chemistry results, and the patient's appearance improved on cessation of treatment. However, it is unclear whether the liver perturbations were caused by silver deposition or were a response to the burns themselves. Thus, a review by Jeschke [2009] drew attention to the profound structural and metabolic changes undergone by the liver of burn victims. Hepatic responses to thermal injury such as the formation of edema, release of proinflammatory cytokines, and activity of AST, ALT, and alkaline phosphatase (AP) have been shown to increase by up to 200% in the rat burn model [Jeschke et al. 2009].

The findings from workers treated with Acticoat™ do not provide adequate data to determine a threshold level of plasma silver that might be associated with the elevation of AST and ALT. The fluctuation in these markers of liver function deficits in the worker described by Trop et al. [2006] might be a consequence of thermal injury rather than wound treatment with silver [Jeschke 2009; Jeschke et al. 2009].

4 Cellular and Mechanistic Studies Overview

The comparative in vitro cytotoxicity of elemental AgNPs and ionic silver has been examined in studies with mammalian cells, including human mesenchymal stem cells [Greulich et al. 2009; 2011], human monocytic cells [Foldbjerg et al. 2009], human HEPG2 hepatoma cells [Kawata et al. 2009; Kim et al. 2009c], human HeLa S3 cells [Miura and Shinohara 2009], human lung cells [Gliga et al. 2014], Neuro-2A and HepG2 cells [Kennedy et al. 2014], rat alveolar macrophages [Hussain et al. 2005b; Carlson et al. 2008], and mouse spermatogonia stem cells [Braydich-Stolle et al. 2010]. The results from these studies indicate that (1) the cellular uptake and toxicity can be modulated when AgNPs are functionalized with monosaccharides [Kennedy et al. 2014], (2) the mammalian cytotoxic response to elemental AgNPs appears to be influenced by the particles' physical and chemical characteristics, and (3) the response is similar to that observed with ionic silver, especially for AgNPs with small diameters (less than ~30 nm) [Park et al. 2011c; Kim et al. 2012; Gliga et al. 2012, 2014].

A wide range of cellular assays have also been used to examine the oxidative stress and apoptotic effects of AgNPs in vitro. Key findings following exposure to either AgNPs or ionic silver include increased levels of ROS [Hussain et al. 2005a; Carlson et al. 2008; Foldbjerg et al. 2009; Kim et al. 2009c], induction of oxidative-stress-management genes [Kim et al. 2009c; Miura and Shinohara 2009], increased percentage of apoptotic cells [Hsin et al. 2008; Foldbjerg et al. 2009; Miura and Sinohara 2009], and attenuation of cytotoxic effects of silver by N-acetylcysteine (a glutathione precursor, ligand for ionic silver, and ROS scavenger) [Hsin et al. 2008; Kawata et al. 2009; Kim et al. 2009c]. A number of studies indicate that ionic silver can be more potent than AgNPs in some cellular assays for causing apoptosis [Foldbjerg et al. 2009] and reducing cell viability [Carlson et al. 2008; Greulich et al. 2009; Kim et al. 2009c; Miura and Shinohara 2009], whereas other studies provide evidence of a correlation between the increase in intracellular ROS and particle size [Carlson et al. 2008], and high levels of apoptosis and necrosis for both AgNPs and ionic silver [Foldbjerg et al. 2009, 2011]. Exposure to

AgNPs has also been found to generate more ROS than silver ions, suggesting that the ROS production is due to specific characteristics of AgNPs and not only to ion release [Liu et al. 2010b]. Although the dissolution of AgNPs accounts for at least a degree of toxicity observed with AgNP exposure, the effects cannot always be fully apportioned to the measured dissolved fraction of silver. Although certain AgNPs may have low solubility in certain media and conditions, their contact with biologic receptors may cause the release of ions that could be sustained over a long period. Information is limited on the role of particle shape in the capacity to induce toxicity, but Stoehr et al. [2011] found AgNWs (length, 1.5–25 μm; diameter, 100–160 nm) to be more toxic to alveolar epithelial A549 cells than AgNPs (30 nm) and silver microparticles (<45 μm) at concentrations that overlapped in both mass and surface area. No effects were observed with AgNPs and silver microparticles on A549 cells, whereas AgNWs induced strong cytotoxicity, loss in cell viability, and early calcium influx that appeared to be independent of the length of the AgNWs.

Comparatively few reports of in vivo studies of AgNPs in experimental animals are available, whereas information on in vitro (cellular) studies with AgNPs is extensive. The in vitro studies indicate that AgNP uptake and localization in the cell appear to be dependent on the cell type and specific analysis method applied. The surface properties and size of AgNPs also appear to be important factors. In summary, adverse physiologic and biochemical responses have been observed with AgNPs in isolated cells, including (1) formation of ROS, (2) cellular disruption, (3) impairment of cellular respiration, (4) DNA perturbation, and (5) stimulation of apoptosis. Unfortunately, insufficient information is available to compare the effective concentrations for the toxicological effects of AgNPs in the in vitro studies with the exposure concentrations and doses that brought about the agent-related responses in the in vivo studies. One of the reasons for this is the lack of sufficient characterization of the AgNPs used in experiments under the exposure conditions utilized, which makes it difficult to correlate any observed effect to the AgNP properties and the available dose (which may be affected by media components). The studies do indicate, however, that the higher surface volume ratio of AgNPs, compared with larger respirable-size silver particles, is a

cause of concern because it makes AgNPs potentially more reactive than larger silver particles and makes it more difficult to predict how they will interact with biologic systems [Reidy et al. 2013]. AgNP-induced oxidative stress and the resulting high level of ROS are potential reasons for the observed DNA perturbations causing DNA breaks and oxidative adducts. However, it is not clear to what extent the mechanism of action for AgNP toxicity is related to the physical-chemical properties, including particle size and shape, surface area, release rate of silver ions, or a combination of these properties. Results of limited in vitro studies [Stoehr et al. 2011] and in vivo studies [Schinwald et al. 2012; Kenyon et al. 2013] with AgNWs suggest that inhalation exposure to AgNWs may pose a greater health risk than that to AgNPs because of their high aspect ratio and biopersistence in the lung. Further research on kinetics, toxicity, and risks, with an emphasis on chronic exposure, is necessary to resolve health concerns regarding exposure to AgNWs.

A more detailed description of the in vitro studies on silver is provided in Appendix E.

5 Animal Studies Overview

5.1 Toxicokinetic Findings

Available data suggest that AgNPs or silver ions eluted from AgNPs can be absorbed via the inhalation, oral, parenteral, or dermal routes in humans and experimental animals. However, there appears to be some variation in absorption intensity, depending on particle size, degree of aggregation, dissolution potential, and/or nature of any surface coating or binding material. For example, gastrointestinal absorption of orally administered citrate-coated AgNPs in Sprague-Dawley rats was low, although a small portion of the load was sequestered in the liver [Park et al. 2011a]. Cumulative evidence on the distribution of internalized silver from AgNPs has implicated the liver, spleen, and kidneys as the primary target organs [Lankveld et al. 2010; Park et al. 2011a; Dziendzikowska et al. 2012; Lee et al. 2013c]. However, silver has also been shown to deposit in the brain, ovaries/testes, and lung (Figure 5.1) [Ji et al. 2007; Kim et al. 2008; Tang et al. 2008, 2009; Takenaka et al. 2001; Sung et al. 2008; Lankveld et al. 2010; Park et al. 2010b; Park et al. 2011a; Dziendzikowska et al. 2012; van der Zande et al. 2012; Xue et al. 2012; Lee et al. 2013a,c], and differences in silver distribution may be affected by gender, possibly because of sex-dependent biokinetics [Kim et al. 2008; Sung et al. 2008; Xue et al. 2012].

Silver leached from Acticoat™ dressings applied to the wounds of a burn victim was shown to become elevated in the bloodstream and to be associated with changes in the activity of such liver-related serum enzymes as AST and ALT [Trop et al. 2006]. Forging a causative link between silver internalization and hepatic impacts is difficult, because it is unknown how much—if any—silver was deposited in the liver in this patient. Of strong relevance to occupational exposure, the data of Takenaka et al. [2001] showed inhaled AgNPs to be a source of internalized silver, with ready distribution and uptake by the kidney, heart, and intratracheal lymph nodes, as well as the liver. Smaller nanoparticles (<100 nm diameter) appear to be more readily distributed to susceptible sites than

larger silver particles [Lankveld et al. 2010; Park et al. 2010a; Dziendzikowska et al. 2012].

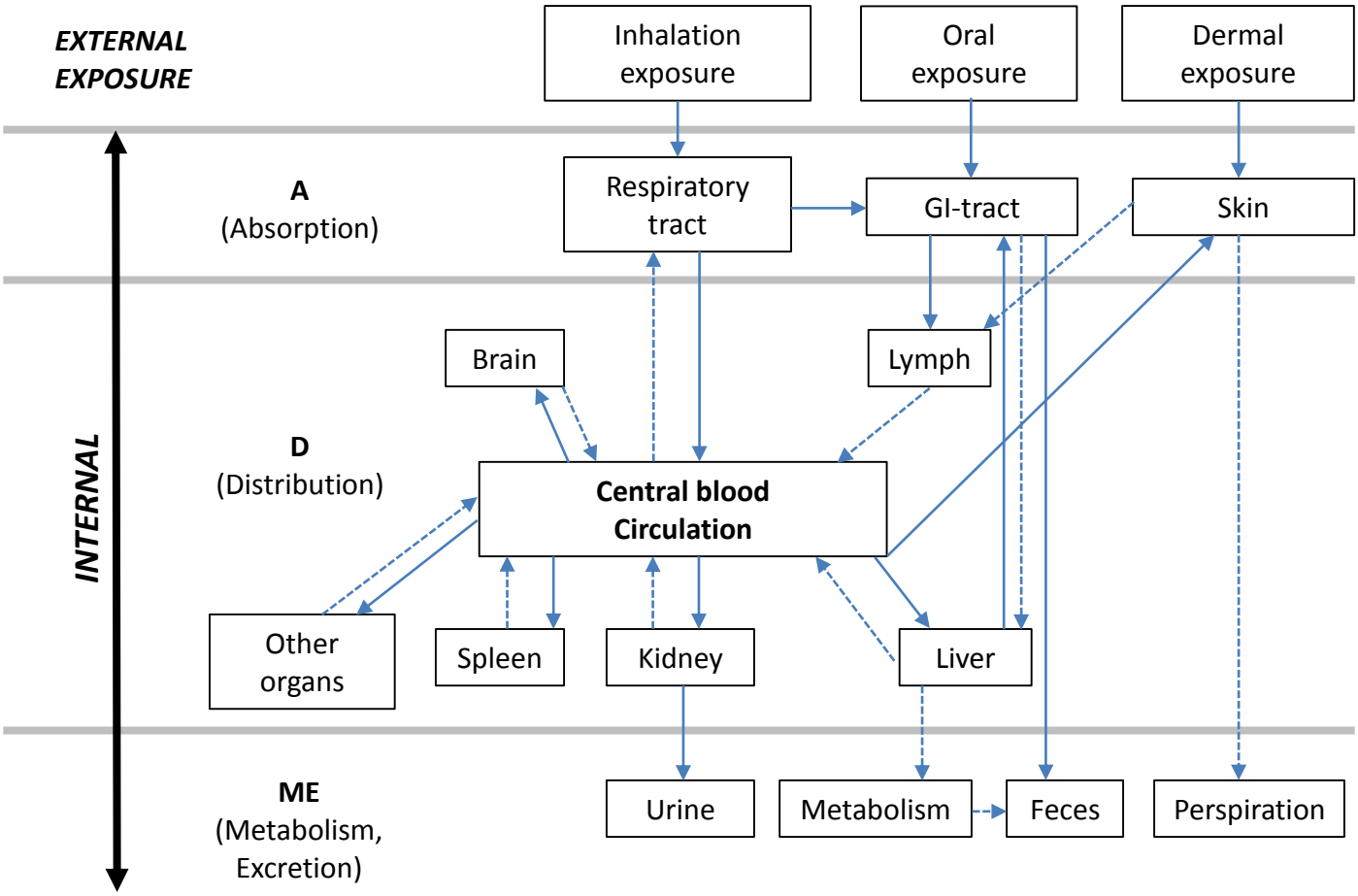

Figure 5.1. Systemic distribution of silver. The bold lines represent confirmed routes for silver (including AgNPs); the dashed lines represent possible routes and other organ sites (such as the heart and reproductive organs). Adapted from Hagens et al. [2007].

5.2 Toxicological Effects

The toxicity of a metal can be influenced by its physical and chemical properties, including (1) the dissolution potential of the metal (which is affected by its particle size, the pH of the surrounding biologic media, and the nature of any surface coat or binding material); (2) the reactivity of the metal surface; (3) the ability of the metal to bind to biologic sites; and (4) the degree to which metal complexes are sequestered or metabolized and excreted [Wijnhoven et al. 2009]. Studies appear to indicate that some forms (such as soluble) and small particle sizes of silver may be more toxic than others. These studies indicate that AgNPs, because of their small particle size and large surface area per unit mass, facilitate the more rapid dissolution of ions than the equivalent bulk material, potentially leading to increased toxicity [Johnston et al. 2010; Park et al. 2011a; Kim et al. 2012; Gliga et al. 2014]. This, coupled with the particles' capacity to adsorb biomolecules and interact with biologic receptors, can mean that AgNPs can reach subcellular locations, leading to potentially higher localized concentrations of ions once those particles start to dissolve or degrade in situ.

The most comprehensive dataset on the potential toxicity of silver comes from studies of animals exposed by subchronic inhalation to silver nanoparticles [Sung et al. 2008, 2009; Song et al. 2013]. No chronic carcinogenicity, reproductive toxicity, or developmental toxicity studies have been reported. Subchronic and acute studies with rodents exposed to AgNPs have provided evidence of the potential health risks to exposed workers (Appendix F, Table F-5). Results from in vivo studies show (1) the uptake of silver and AgNPs to the blood and their subsequent distribution to all major organs and tissues (Figure 5.1); (2) perturbation of lung function and induction of inflammatory responses; and (3) histopathologic changes in the kidney and especially in the liver, in which bile duct hyperplasia was identified as the principal toxicological effect. Evidence is available from inhalation studies with rats that silver can deposit in the lungs and be transported via the blood to the liver [Sung et al. 2008. 2009] and that dissolved silver can clear from the lungs in a manner similar to poorly dissolving AgNPs, a characteristic suggesting that both entities can be readily absorbed via the lungs and

systemically distributed [Takenata et al. 2001]. Significant increases in the amount of silver have been observed in major organs and tissues following exposure to AgNPs, including the lungs, liver, spleen, kidneys, olfactory bulb, brain, and blood in both male and female rats [Ji et al. 2007b; Kim et al. 2008; Sung et al. 2009; Kim et al. 2010a; Lankveld et al. 2010; Lee et al. 2013c]. The accumulation of silver in the kidneys appears to be gender-specific, on the basis of results from 28-day, 90-day, and 12-week inhalation studies [Sung et al. 2009; Kim et al. 2011; Song et al. 2013; Dong et al. 2013] and 90-day oral studies [Kim et al. 2010a]. Both inhalation and oral exposure studies indicate that female rats have two to four times more silver accumulation than males in all kidney regions. In particular, the glomerulus in the kidney cortex was found to contain a higher accumulation in females than in males [Kim et al. 2009a]. The AgNPs were also preferentially accumulated in the basement membranes of the renal tubules in the cortex, in the medium and terminal parts of the inner and outer medulla of female rats; they also were detected in the cytoplasm and nuclei of the interstitial cells in the inner medulla of the kidneys [Kim et al. 2009a]. These gender differences have been suggested to be associated with metabolism and hormonal regulation, because the kidneys are a target organ for several hormones, such as thyroid hormones and testosterone [Kim et al. 2009a]. Although exposure to AgNPs results in the distribution of silver to many organ and tissue sites, the results from animal studies [Klaassen et al. 1979; Kim et al. 2010a; Park et al. 2011a; Dziendzikowska et al. 2012; Lee et al. 2013c] indicate that biliary excretion to feces is the primary route for the elimination of silver.

A common feature of the systemic toxicological effects of AgNPs, irrespective of the exposure route, is the reported histopathologic effects to the liver in both Sprague-Dawley and F344 rats [Sung et al. 2009; Kim et al. 2010a]; liver effects were not reported by Song et al. [2013]. High-dose animals in both studies developed bile duct hyperplasia and signs of hepatic necrosis. In the 90-day oral study, these effects were accompanied by changes in some clinical chemistry parameters indicative of perturbations in liver metabolism, including increases in serum cholesterol concentration and AP activity [Kim et al. 2010a]. In the 90-day inhalation study of Sung et al. [2008, 2009], these systemic effects were accompanied by lung function deficits (decreased

tidal volume, minute volume, and peak inspiration flow), development of inflammation responses, and alveolar accumulation of macrophages [Sung et al. 2008]. In a follow-up inhalation study by the same group [Song et al. 2013], lung function decrease and lung inflammation were observed in male rats, and these effects persisted in the high-dose group at 12 weeks after cessation of exposure. In female rats, no consistent decrease in lung function was observed, and the lung inflammation gradually resolved after cessation of exposure [Song et al. 2013].

A more detailed description of the experimental animal studies of silver can be found in Appendix F.

6 Hazard and Risk Evaluation of OELs for Silver

6.1 Human Health Basis for the NIOSH REL

The NIOSH REL of 10 µg/m^3 (total dust) for silver (metal dust and soluble compounds) [NIOSH 2007] was set to prevent argyria and was based on findings in workers exposed to airborne silver. The NIOSH REL is the same as the OSHA PEL and uses the same evidence basis [OSHA 1988, 2014]. The derivation of the REL and PEL [OSHA 1988] are based on an earlier ACGIH TLV, as described below.

These OELs in the United States are based on early case reports of argyria in humans ingesting silver [Hill and Pillsbury 1939]. A total mass body burden of approximately 3.8 g (1 to 5 g) of silver was associated with arygria [OSHA 1988]. The occupational airborne exposure concentration was calculated that would result in an equivalent body burden of silver. Assuming a worker air intake of 10 m^3/day and 25% deposition and retention of inhaled silver in the body, ACGIH estimated a total deposition of approximately 1.5 g if a worker were exposed at the TLV of 100 µg/m^3 for 25 years [ACGIH 2001]. That is,

$$1.5\ g = 0.1\ mg/m^3 \times 10\ m^3/8\text{-hr d} \times 5\ d/wk \times 50\ wk/yr \times 25\ yr \times 0.25\ [RF] \times (1g/1{,}000mg)$$

Although it is not stated explicitly in the documentation of the PEL and REL, the "body retention fraction" (RF) is a constant factor that represents the assumed total fraction of the inhaled dose of silver that is retained in the body (e.g., 0.25), which includes the fraction deposited in any region of the respiratory tract and also retained in the lungs or other tissues (i.e., following absorption into the blood or lymph and transported and retained in other organs); likewise, 0.75 of the inhaled dose is assumed to be cleared from the body. The use of the factor in the total dose estimate means that a constant proportion of the Ag is retained, regardless of the inhaled dose. No uncertainty factors (UFs) appear to have been used in deriving this TLV. Over a full working lifetime of 45 years, the body burden of silver would be estimated to be higher (i.e., ~2.8 g, assuming

45 years worked at 8 hours/day, 40 hours/week, 50 weeks/year, as well as the same volume of air inhaled per day [10 m^3] and total RF). If a higher RF of 0.50 is assumed (as discussed below), the 45-year body burden would be estimated to be ~5.6 g, which exceeds the average (3.8 g) and minimum (1 g) body burdens associated with argyria in humans [OSHA 1988; ACGIH 2001].

The OSHA PEL [OSHA 1988] and NIOSH REL [NIOSH 1988] are based on an earlier ACGIH TLV of 10 µg/m^3 for silver, which was derived from the same human data [Hill and Pillsbury 1939] but assumed an estimate of 50% body retention of inhaled silver. The PEL of 10 µg/m^3 was based on the following estimates [OSHA 1988]. The retained body burden of silver associated with argyria in humans was estimated to be 1 to 5 g (from Hill and Pillsbury [1939]). Based on the assumption of the lower value of 1 g silver body burden, an 8-hr TWA concentration of 50 µg/m^3 was estimated for a 20-year exposure duration [NIOSH 1988; OSHA 1988]. The PEL was set at 10 µg/m^3 to provide a margin of safety [NIOSH 1988; OSHA 1988]. A 45-year working lifetime was not used in deriving the PEL.

These calculations of the airborne exposure concentration (X mg/m^3) associated with the target human body burden (as reported above) can be calculated as follows:

> X mg/m^3 = Body burden (mg) / [Exposure duration (d) × Air intake per work day (m^3/d) × Body retention fraction, RF]

An example calculation based on the equation above and using the information provided [NIOSH 1988; OSHA 1988] suggests a slightly lower 8-hr TWA concentration associated with a lower body burden estimate for argyria:

> 0.042 mg/m^3 = 1,000/ (5,000*9.6*0.5)

where 1 g (or 1,000 mg) is the minimum estimated body burden associated with argyria [NIOSH 1988; OSHA 1988]; 5,200 is the number of exposure days in 20 years (5 d/wk*50 wk/yr*20 yr); 9.6 m^3/d is the volume of air inhaled per workday (light activity, reference worker value); and 0.5 is the RF (unitless).

Using the same target human body burden (1 g) of silver, retention fraction, and air intake but assuming 45 years of exposure (5 days/week, 50 weeks/year) would result in an estimated airborne concentration of 18 µg/m^3 (8-hr TWA), resulting in a lower factor of <2 (margin of safety) at the current NIOSH REL and OSHA PEL of 10 µg/m^3 (8-hr TWA).

Airborne sampling for silver according to the NIOSH REL and other OELs (Table 1-2) is based on the total airborne mass concentration (NIOSH Methods 7300 and 7301) [NIOSH 2013a]. These sampling criteria include collection of all particle sizes that can be inhaled in the human respiratory tract (approximately 1 nm to 100 µm in diameter). Inhaled particles depositing anywhere in the respiratory tract could potentially contribute to the body burden of silver either at the site of deposition (if retained) or at distal sites (if absorbed).

6.2 Animal Data on Silver Nanoparticles

6.2.1 Lung effects

In the absence of data on human exposure to AgNPs, the findings from subchronic inhalation studies in rats [Sung et al. 2008, 2009; Song et al. 2013] were determined to be the best available data to evaluate the potential occupational health hazard of AgNPs. Lung inflammation and lung function deficits occurred in both male and female Sprague-Dawley rats following inhalation of AgNPs for 13 and 12 weeks, respectively, as reported by Sung et al. [2008, 2009] and Song et al. [2013]. The inflammation (chronic, alveolar) was reported to be of minimal severity on the basis of histopathologic evaluation [Sung et al. 2009; Song et al. 2013]. The NOAEL for lung inflammation was 133 µg/m^3 in male and female rats in a study by Sung et al. [2009]. Song et al. [2013] reported that 117 µg/m^3 was the LOAEL in male rats and a NOAEL in female rats. In male rats, lung inflammation was observed at 117 µg/m^3, which had resolved by 12 weeks post-exposure (but was persistent in the 381-µg/m^3 group). In female rats, lung inflammation was not observed at 117 µg/m^3, and the inflammation observed in the 381-µg/m^3 exposure group had resolved by 12 weeks post-exposure.

Lung function deficits were reported in both of the subchronic inhalation studies in rats [Sung et al. 2008; Song et al. 2013], including decreases in tidal volume, minute volume, peak inspiration flow, and peak expiration flow. The 49 µg/m^3 exposure concentration was a LOAEL for lung function deficits in female rats in the study by Sung et al. [2008], but in the study by Song et al. [2013], 381 µg/m^3 was the NOAEL (that is, no lung function deficits were observed) in female rats. These results show large variability in the female lung function responses in the two studies. For male rats, 133 µg/m^3 was the NOAEL for lung function deficits, according to Sung et al. [2008], whereas it was 49 µg/m^3 according to Song et al. [2013]. The difference in the number of rats in each exposure group (*n* = 10 males and *n* = 10 females in Sung et al. [2008]; *n* = 5 males and *n* = 4 females in Song et al. [2013]) may have contributed to the variability in responses observed in the two studies. Although the effects were dose-related, it is unclear whether the level of reduced lung function reported from these rat studies would be considered clinically significant in humans (discussed in Christensen et al. [2010]).

6.2.2 Liver effects

Silver is eliminated from the blood via biliary excretion and is eliminated from the body primarily in the feces, as noted in studies of workers [DiVincenzo et al. 1985; Wölbling et al. 1988]. The finding of bile duct hyperplasia in rats [Sung et al. 2009] is consistent with that clearance pathway. Bile duct hyperplasia can be caused by exposure to a toxic substance, although it is also associated with aging in rats when it is accompanied by inflammatory cells and/or oval cell proliferation [NTP 2014]. The clinical significance of bile duct hyperplasia itself is not clear, but some evidence suggests that cholangiocellular carcinoma can develop from bile duct hyperplasia [Kurashina et al. 2006]. On the basis of these findings, NIOSH considers the response of bile duct hyperplasia in a subchronic inhalation study in rats [Sung et al. 2009] to be a potential adverse effect. Bile duct hyperplasia of minimum severity was reported to occur in male rats exposed by inhalation to 515 µg/m^3 and in female rats exposed to 133 µg/m^3 or 515 µg/m^3, and single-cell hepatocellular necrosis was observed in 3/10 females in the high

dose group, including one female with bile duct hyperplasia of moderate severity (with concurrent moderate centrilobular fibrosis, necrosis, and pigmentation). Hepatic inflammation was not reported to occur in rats at the silver exposure concentrations associated with hyperplasia of moderate severity and associated fibrosis and necrosis [Sung et al. 2009].

6.3 Biologic Mode of Action and Physical-chemical Properties

Both poorly soluble and soluble particles can potentially cause adverse effects when inhaled into the lungs. The ions are typically associated with acute effects, which may resolve if the exposure does not continue [Roberts et al. 2013], although repeated exposures could result in higher doses of both ions and particles (which may also release ions over time, depending on site of disposition in the body and reaction with cellular proteins and other compounds). Ions released from soluble particles (such as $AgNO_3$) can react with cells and damage cell membranes, resulting in cell death [Cronholm et al. 2013; Zhang et al. 2014]. Smaller particles with greater surface area per unit mass would have a greater potential for ion release [Johnston et al. 2010]. One of the key complexities in hazard and risk assessment of silver particles, including nanoparticles, is uncertainty about the dissolution of various types of silver particles or silver compounds and the extent to which any potential adverse effects may be due to the ionic vs. particulate forms of silver.

Poorly soluble particles that are deposited in the pulmonary region of the lungs at doses that are not effectively cleared can trigger inflammatory responses, and particles that interact with epithelial cells lining the alveoli and translocate to the lung interstitial tissue can elicit fibrotic responses [NIOSH 2011, 2013]. Pulmonary fibrosis has not been found in the animal subchronic inhalation studies of inhaled AgNPs [Sung et al. 2008, 2009; Song et al. 2013] or in studies of workers in silver production or processing [DiVincenzo et al. 1985]. Inhalation may be the route associated with the highest potential for exposure in the workplace [Park et al. 2009; Miller 2010; Lee et al. 2011a, b]. In addition

to inhalation, workers may be exposed to silver particles or ions through dermal exposure or ingestion (for instance, as a result of mucociliary clearance of silver particles from the respiratory tract).

The size and composition of silver to which workers may be exposed can vary, depending on the product being manufactured, production method, and job/task within the facility. Workers can be exposed to a mixture of silver particle sizes (nanoscale or larger respirable or inhalable sizes) [Lee et al. 2011a]. In addition, workers can potentially be exposed to silver compounds (such as silver nitrate, silver acetate), which can exhibit different biologic availability and activity depending on the associated moieties. Potential worker exposure can occur during the use of silver in various applications and depends on the form of the silver or silver compound (such as dry powder or colloidal silver) [Drake et al. 2005]. In the case of colloidal silver compounds (such as used for disinfectant sprays), the ionic silver component can vary with the age of the product [Liu and Hurt 2010].

A primary goal of occupational health risk assessment is to evaluate exposure-related adverse effects in experimental animals that are relevant to humans and to estimate exposure levels that would not likely result in adverse health effects in workers, even if exposed for up to a 45-year working lifetime. Understanding the physico-chemical properties that influence their uptake and bioactivity is important to assessing the health risk of exposure to airborne particles. The inhalable mass fraction that deposits in the respiratory tract can be estimated with relatively low uncertainty, based on aerosol measurement data and deposition models (e.g., MPPD, [ARA 2011]). In contrast, the fate of AgNPs after deposition in the respiratory tract is an area of higher uncertainty, which pertains to the potential adverse effects of exposure to silver dust or fumes (including nanoparticles), especially with chronic exposure. Animal studies have measured silver in various organs in the body, including lungs, liver, kidneys, and brain. The adverse effects observed in rats following subchronic inhalation exposures to AgNPs include persistent pulmonary inflammation and reduced lung function as well as biliary hyperplasia [Sung et al. 2008, 2009; Song et al. 2013], suggesting that effects

occur at both the site of entry and systemically. The extent to which these effects were due to the AgNPs and/or ions cannot be determined from these studies.

6.4 Biomonitoring Data on Humans

Although no data are available on the body burdens in workers resulting from inhaled silver nanoparticles, some biomonitoring data are available on workers exposed to airborne silver (particle size not specified) (Section 3 and further discussion below). Such information provides the best available data on internal doses for comparison to the animal studies.

Following a study of 35 to 37 male silver-production workers (most with 5 or more years of experience in production areas), DiVincenzo et al. [1985] reported workplace airborne exposure measurements of 1 to 100 µg/m^3. These researchers compared the estimated total silver dose in workers to the estimated dose associated with argyria (that is, approximately 2.3 g by intravenous injection [Hill and Pillsbury 1939, cited in DiVincenzo et al. 1985], or 23–115 mg, on the assumption of 1%–5% silver retention in the body [Scott and Hamilton 1948, 1950; Fruchner et al. 1968, cited in DiVincenzo et al. 1985]). They estimated an annual dose of 14 µg/kg in workers, by assuming 1% retention of silver that was absorbed in the body by diet (oral) or workplace (inhalation) exposure [DiVincenzo et al. 1985]. They then estimated a worker airborne exposure concentration of 30 µg/m^3 from fecal excretion data, which is within the measured air concentration range. The estimated annual dose of retained silver in a 70-kg worker was approximately 1 mg. Given the 23 to 115 mg retained dose estimated to be associated with argyria, DiVincenzo et al. [1985] estimated that at least 22 years of workplace exposure would be required for development of argyria. Although different assumptions were used in deriving these estimates, the results are similar to the estimates used as the basis for the NIOSH REL (Section 6.1).

A study of 50 workers in the silver processing industry (44 males, 6 females) investigated associations between the airborne exposure concentration and duration and the clinical symptoms or silver concentrations in skin samples [Wölbling et al.

1988]. About half of the workers (52%) handled only metallic silver and 46% were exposed to silver salts (silver nitrate or silver chloride); one worker was exposed to both forms of silver. No cases of generalized argyria were observed, although 8 of the 23 silver salt workers had localized argyria (especially in mucous membranes of the eyes, mouth, and nose). No cases of localized argyria were observed among the metallic silver workers. Airborne concentrations ranged from 1 to 310 µg/m^3 in the "salts" group and from 3 to 540 µg/m^3 in the "metal" group. Worker exposure durations were 3 to 20 years. The lowest concentration associated with localized argyria (ocular) was 2 to 4 µg/m^3, although no relationship was observed between the exposure concentration or duration and the signs of argyrosis. The silver concentrations in skin (0.01–0.11 µg/g) were within the range of previously reported values and were not associated with argyria. In another study, argyria was observed in a worker (silver polisher) with 3.7 µg/g silver in skin [Treibig and Valentin 1982, cited in Wölbling et al. 1988].

6.5 Evaluation of Health Risk of Exposure to Silver Nanoparticles at the NIOSH REL for Silver

6.5.1 Animal study findings

NIOSH has determined that the best available evidence for evaluating the potential adverse health effects associated with occupational inhalation exposure to AgNPs includes the study findings from acute and subchronic AgNP exposure in animals and the data from human biomonitoring.

6.5.1.1 Acute inhalation exposure

In an acute (5-hr) inhalation study of two types of silver (ionic and AgNP) in rats (male, Sprague-Dawley), no adverse pulmonary effects were observed 1 day or 7 days post-exposure [Roberts et al. 2013]. The ionic silver was a commercial antimicrobial spray, administered at an exposure concentration of 100 µg/m^3 (mass median aerodynamic diameter [MMAD] of 33 nm). The AgNP sample was a NIST reference material of total silver nanoparticles with low ionic content, administered at 1,000 µg/m^3 (MMAD of 39

nm). A transient significant increase in blood monocytes was observed 1 day after exposure to the high dose (AgNP), but not in rats exposed to the low dose (ionic Ag). Slight cardiovascular changes (significant reduction in vascular responsiveness to Ach-induced re-dilation) were observed at the low dose (ionic Ag) at 1 day post-exposure, but not at the high dose (AgNP). Both of these responses had resolved by 7 days post-exposure. Given the minimal, transient responses, each of these doses could be considered NOAELs for the respective types of silver. The estimated human-equivalent single-day (8-hr) exposure concentration is 620 µg/m^3 or 7.7 mg/m^3, respectively, for the commercial spray (ionic Ag) or NIST reference material (AgNP) (Table A-13). These human-equivalent concentrations to the rat acute NOAELs are more than 60 or 700 times lower (margin of safety) than the current NIOSH REL of 10 µg/m^3 (8-hr TWA), for the ionic Ag or AgNP, respectively. Although adverse lung or cardiovascular effects in workers would not be expected to result from a human-equivalent acute inhalation exposure (8-hr, 1 day) to these ionic or nanoparticulate silver materials, it is not known if repeated exposures could result in adverse health effects.

6.5.1.2 Subchronic inhalation exposure

Two subchronic (13-week) inhalation studies of AgNPs (15–20 nm) have been published to date [Sung et al. 2008, 2009; Song et al. 2013]. Exposure-related lung and liver effects were observed in male and female Sprague Dawley rats; these effects were of relatively minimal severity [Sung et al. 2008, 2009; Song et al. 2013]. The NOAELs for lung inflammation were 133 µg/m^3 in male and female rats in the study of Sung et al. [2009] and were 117 µg/m^3 in female rats and 49 µg/m^3 in male rats in the study of Song et al. [2013]. Lung function deficits were also reported following subchronic exposure in both studies [Sung et al. 2008; Song et al. 2013], including decreases in tidal volume, minute volume, peak inspiration flow, and peak expiration flow. A LOAEL for lung function deficits of 49 µg/m^3 was observed in female rats, whereas in male rats the NOAEL was 133 µg/m^3, as noted by Sung et al. [2008]. These results contrasted with those of Song et al. [2013], who noted a NOAEL for lung function deficits of 49 µg/m^3 in male rats and a NOAEL of 381 µg/m^3 in female rats. These highly variable results for lung function deficits were not used in the risk estimates for the OEL

evaluation (Section 6.5.3). The number of rats per exposure group was relatively small in each study (*n* = 10 males and 10 females in Sung et al. [2008, 2009]; 5 males and 4 females in Song et al. [2013]). Liver bile duct hyperplasia was reported by Sung et al. [2009], and the NOAEL was 133 µg/m^3 in both male and female rats; this endpoint was not reported by Song et al. [2013].

The finding of bile duct hyperplasia in rats [Sung et al. 2009] from exposure to AgNPs is consistent with the pathway in which silver is eliminated from the blood via biliary excretion, and eventually from the body in the feces [DiVincenzo et al. 1985; Wölbling et al. 1988]. Although bile duct hyperplasia is often associated with aging in rats when it is accompanied by inflammatory cells and/or oval cell proliferation, it can be caused by exposure to a toxic substance [NTP 2014]. The clinical significance of bile duct hyperplasia is not clear, although some evidence suggests that cholangiocellular carcinoma can develop from bile duct hyperplasia [Kurashina et al. 2006]. On the basis of these findings, NIOSH considers the response of bile duct hyperplasia observed in a subchronic inhalation study in rats [Sung et al. 2009] to be a potential adverse effect. Bile duct hyperplasia of minimum severity was reported to have occurred in male rats exposed by inhalation to 515 µg/m^3 and in female rats exposed to 133 µg/m^3 or 515 µg/m^3, although single-cell hepatocellular necrosis was observed in 3/10 female rats in the high-dose group, including one female with bile duct hyperplasia of moderate severity (with concurrent moderate centrilobular fibrosis, necrosis, and pigmentation).

6.5.2 Human-equivalent exposure estimates

6.5.2.1 Argyria

NIOSH used the results from PBPK modeling [Bachler et al. 2013] to estimate the 45-year working lifetime exposure concentrations associated with argyria at the lowest silver skin-tissue dose reported in humans (Section A.2). These estimates were 47 µg/m^3 for ionic silver, 78 µg/m^3 for 15-nm-diameter AgNPs, and 253 µg/m^3 for 100-nm-diameter AgNPs (Table A-10). These estimates suggest that the current NIOSH REL of 10 µg/m^3 (8-hr TWA, total mass sample) of soluble or insoluble silver [NIOSH 2007]

should be health protective against argyria in workers exposed to AgNPs, with margins of exposure of approximately 5 to 25.

6.5.2.2 Lung and liver effects

NIOSH also estimated the 45-year working lifetime AgNP exposure concentrations that would result in equivalent tissue doses that were associated with minimal lung and liver effects in the rat subchronic inhalation studies of AgNPs (Appendix A, Sections A.2.2–A.2.4). PBPK model estimates of human-equivalent concentrations to the rat NOAELs for lung and liver effects were <1 to 3.8 µg/m^3 for total silver, and 6.2 to 195 µg/m^3 for soluble/active tissue doses for 15-nm- or 100-nm-diameter AgNPs (Table A-12). These estimates of the human-equivalent concentrations associated with no or low-level early-stage adverse liver or lung effects of minimal severity are used in the derivation of REL estimates for AgNPs utilizing PBPK modeling (Section 6.5.3.2).

6.5.3 OEL estimates for silver nanoparticles

6.5.3.1 OEL Estimates based on a default uncertainty factor approach

Table 6-1 shows OEL estimates for AgNPs using a UF approach, applied to the human-equivalent point of departure (POD) extrapolated from the rat subchronic inhalation studies. These estimates use the airborne exposure concentration in rats at the NOAEL for lung inflammation or liver bile duct hyperplasia (i.e., the highest exposure concentration at which these responses were not observed in rats). The derived OELs depend on the assumed UF, either less than the current REL (0.6 or 1.7 µg/m^3) assuming a UF of 60 (based on values used in other risk assessments using these same or similar types of rat data) (Section A.1, Table A-3) or greater than the current REL (18 or 51 µg/m^3) assuming a UF of 2 (i.e., the UF implicit in the current REL for the prevention of argyria, after adjusting for a 45-year working lifetime) (Section 6.1). Other UFs could also be applied, depending on the interpretation of the data and appropriate UFs.

Table 6-1. Summary of OELs derived by applying uncertainty factors to points of departure (PODs) from rat subchronic inhalation studies (adjusted for human daily exposure duration).

Rat response and type of effect level, gender, *n* per group [study reference]	Rat POD ($\mu g/m^3$)	Human-equivalent POD ($\mu g/m^3$)*	UFs (Source)	Derived OEL (8-hr TWA), $\mu g/m^3$
Lung inflammation (NOAEL), males, *n* = 5 [Song et al. 2013]	49	37	60 (Section A.1) 2 (Section 6.1)	0.6 18
Liver bile duct hyperplasia (NOAEL), male & females, *n* = 10 [Sung et al. 2009]	133	100	60 (Setion A.1) 2 (Section 6.1)	1.7 51

*Estimated by adjusting for difference in rat and human exposure day, that is, rat POD (Table A-1) × 6 hour/8 hour.

6.5.3.2 OEL estimates utilizing PBPK modeling

6.5.3.2.1 Evidence on the role of particle size and solubility on toxicity

A recent study in rats showed that ionic silver is more toxic than a similar mass concentration of silver nanoparticles, with pulmonary inflammation observed in rats when exposed to 15-nm-diameter particles but not when exposed to 410-nm-diameter particles, following subacute exposure (4 days, 6 hours/day) to similar airborne concentrations (179 or 167 mg/m^3, respectively) [Braakhuis et al. 2014]. The inflammation in the rats exposed to the 15-nm-diameter AgNPs resolved by 7 days post-exposure. The 15-nm particles were shown to have a higher alveolar (pulmonary) deposition fraction than the 410-nm particles, resulting in 3.5 times higher deposited mass dose (and 66,000 higher particle number dose). The 15-nm particles were observed to have been reduced in size to <5 nm within 24 hours, illustrating their relatively rapid dissolution in the rat lungs. The PBPK model includes differences in the deposition fraction and dissolution rate by particle size (15 nm and 100 nm particle sizes), as modeled in Section A.2 on the basis of the Bachler et al. [2013] model. This model also accounts for particle size–specific differences in the alveolar deposition

fraction and species-specific differences in the clearance of inhaled particles that deposit in the lungs [Bachler et al 2013].

The NIOSH REL is intended to protect workers exposed for up to 8-hr TWA concentrations during a 40-hour work week for up to 45 years. Evidence from acute inhalation studies in rodents [Braakhius et al. 2014; Roberts et al. 2013] suggests that soluble forms of silver are more biologically active and inflammogenic than poorly soluble silver particles, although the nanoparticle forms also had effects. Some in vitro studies found that soluble silver was more bioactive than AgNPs (including reduction in mitrochondrial functon and decreased cell viability) [Foldbjerg et al. 2011; van der Zande et al. 2012]. However, at least one in vitro study showed that AgNP was more damaging to cells than was silver in solution [Piao et al. 2011]. The mechanism of AgNP activity may be different from that of soluble silver.

Studies in workers have shown that soluble forms of silver have been more frequently associated with the development of argyria than poorly soluble forms [as reviewed in ATSDR 1990; Drake and Hazelwood 2005; Wijnhoven et al. 2009] (Chapters 2 and 3). If the inflammation response is related to the release rate of ions during dissolution of the AgNP, then the soluble/active portion of the dose estimates from the PBPK model [Bachler et al. 2013] may be more closely associated with the inflammation responses in the lungs, including with repeated exposures (up to a 45-year working lifetime). Thus, the soluble/active AgNP tissue doses were selected as potentially the most biologically relevant dose metric for evaluation of the current NIOSH REL to AgNPs (Section 6.5.3.2.2).

6.5.3.2.2 OEL estimates derived from soluble/active tissue dose estimates

Current OELs for silver including the NIOSH REL are evaluated for adequacy in protecting workers exposed to AgNPs by comparing those values with estimated OELs for AgNPs based on the findings in rat subchronic inhalation studies [Sung et al. 2008, 2009; Song et al. 2013]. Those estimates were derived by extrapolating the rat effect-level estimates to workers, assuming airborne exposure to AgNP (8-hr TWA concentrations) for up to a 45-year working lifetime. The rat effect levels were based on

the measured tissue doses of silver in the lungs or liver that were associated with no or low adverse effects following subchronic inhalation of AgNP (i.e., the NOAEL or $BMDL_{10}$ estimates). For lung inflammation, the study-reported NOAEL estimates (i.e., the highest experimental dose that was not associated with lung inflammation) are used in this evaluation. The $BMDL_{10}$ estimate for lung inflammation (Table A-12) was not used because those data on male rats (n = 5) [Song et al. 2013] were minimally acceptable for dose-response modeling (Appendix B). For liver bile duct hyperplasia, the data were adequate for BMD modeling and the $BMDL_{10}$ estimates are used (i.e., the dose associated with a 10% additional response of chronic alveolar inflammation, minimal severity). The estimates of the human working lifetime exposure concentration that would result in an equivalent tissue dose of silver in rats and humans were derived from the PBPK model by Bachler et al. [2013] for both the soluble/active form and the total silver (Section A.2) (Table A-12).

On the basis of the evidence of potentially greater toxicity of the soluble/active form (Section 6.5.3.2.1), the soluble/active silver dose metrics are selected for evaluation here. Table 6-2 summarizes the estimate of the human-equivalent concentrations associated with rat NOAEL or $BMDL_{10}$ estimates for the soluble/active AgNP. The human-equivalent working lifetime exposure concentration (8-hr TWA) estimates depend on the particle size (15 or 100 nm diameter) and the effective dose metric assumption (soluble/active or total silver nanoparticles). The estimates of the 45-year working lifetime exposure concentrations (8-hr TWA) of 15 nm AgNPs associated with the rat NOAEL for lung inflammation were 9.7 or 61 $\mu g/m^3$ depending on the rat study (Song et al. [2013] or Sung et al. [2009], respectively). These estimates were 31 or 195 $\mu g/m^3$ for the 100-nm AgNP. When the $BMDL_{10}$ estimates of liver bile duct hyperplasia were used as the POD, these estimates were 6.2 or 11.4 $\mu g/m^3$ (15 nm AgNP) and 20 or 37 $\mu g/m^3$ (100 nm AgNP) (Table 6-2). It should be noted that these estimates do not include UFs.

The lowest derived OEL estimates were for the 15-nm AgNP and were based on the assumption of a UF of 60, i.e., 0.1 to 1.0 $\mu g/m^3$ ($BMDL_{10}$ for liver bile duct hyperplasia or NOAEL for lung inflammation, across studies or genders) (Table 6-2); these OEL

estimates were 3.1 to 30 µg/m^3 based on the assumption of a UF of 2 (Section 6.1). The derived OEL estimates for the 100 nm AgNP based on the assumption of a UF of 60 were 0.33 to 3.2 µg/m^3 ($BMDL_{10}$ for liver bile duct hyperplasia or NOAEL for lung inflammation in rats, across studies or genders) (Table 6-2); these OEL estimates were 10 to 98 µg/m^3 based on the assumption of a UF of 2 (Table 6-2).

Table 6-2. Summary of human-equivalent airborne mass exposure concentration estimates associated with rat no or low effect levels. Estimates were calculated through the human-equivalent tissue concentration estimates of soluble/active silver associated with early-state lung or liver adverse effects of minimal severity in rats following subchronic inhalation exposure to silver nanoparticles (based on Table A-12).

Rat response and type of effect level, gender, *n* per group [study reference]	Rat POD (Ag tissue dose ng/g)	Modeled AgNP diameter (nm)	Human-equivalent POD (µg/m^3)*	UF (Sections 6.1 and A.1)	Derived OEL (8-hr TWA) µg/m^3
Lung inflammation (NOAEL of 117 µg/m^3), female, *n* = 5 [Song et al. 2013]	672*	15	9.7	60 2	0.16 4.85
		100	31	60 2	0.52 15.5
Lung inflammation (NOAEL of 133 µg/m^3), female, *n* = 10 [Sung et al. 2009]	4,241*	15	61	60 2	1.02 30.5
		100	195	60 2	3.25 97.5
Liver bile duct hyperplasia ($BMDL_{10}$), female, *n* = 10 [Sung et al. 2009]	6.3†	15	6.2	60 2	0.10 3.10
		100	20	60 2	0.33 10.0
Liver bile duct hyperplasia ($BMDL_{10}$), male, *n* = 10 [Sung et al. 2009]	11.6†	15	11.4	60 2	0.19 5.7
		100	37	60 2	0.62 18.5

* Measured in rats; assumed equivalent Ag tissue concentration in humans.
† Estimated by modeling the measured Ag tissue dose in rats; assumed equivalent Ag tissue concentration in humans.

6.5.3.2.3 Evaluation of silver tissue dose estimates at the NIOSH REL

An evaluation of estimated human Ag tissue concentrations after a 45-year working lifetime exposure at the current REL for silver (10 µg/m^3) resulted in estimates both above and below the rat NOAEL tissue doses. These estimates were based on the PBPK model based on the Bachler et al. (2013) model (Section A.2 and Table A-11). The female rat Ag lung-tissue doses at the NOAEL (no pulmonary inflammation) were 672 ng/g [Song et al. 2013] and 4,242 ng/g [Sung et al. 2009] (Table A-4). The rat liver-tissue doses of silver at the NOAEL (no bile duct hyperplasia) were 12 ng/g in females and 14 ng/g in males, as reported by Song et al. [2009] (Table A-4). The rat $BMDL_{10}$ estimates for bile duct hyperplasia were somewhat lower (6.3 and 12 ng/g) (Table A-4).

Lungs: The PBPK model-based estimates of the human lung tissue dose after 45 years of exposure to silver at the REL of 10 µg/m^3 depended on particle size and form (i.e., 222, 690, or 1,640 ng/g for 100-nm, 15-nm, or ionic silver, respectively) (Table A-11). Thus, the estimated soluble/active Ag tissue dose from a working lifetime exposure to 15-nm or ionic silver was estimated to exceed the rat NOAEL for pulmonary inflammation from one of the subchronic inhalation studies (672 ng/g) [Song et al. 2013] but did not exceed the rat NOAEL lung Ag tissue dose (4,241 ng/g) from the other rat study [Sung et al. 2009] (Table A-4).

Liver: The PBPK model-based estimates of the human liver tissue dose after 45 years of exposure to silver at the REL of 10 µg/m^3 also depended on particle size and form (i.e., 3, 10, or 40 ng/g for 100-nm, 15-nm, or ionic silver, respectively) (Table A-11). Thus, the estimated soluble/active Ag tissue dose from a working lifetime exposure to 100-nm AgNP did not exceed the NOAEL or $BMDL_{10}$ tissue dose estimates (6–14 ng/g), although those for the 15-nm AgNP or ionic silver (Table A-11) were similar to or higher than those rat effect level estimates (Tables A-4).

No UFs were applied to these comparisons. These results could suggest that workers exposed to ionic silver or to 15-nm AgNPs for a full working lifetime at the REL might have a risk of developing liver bile duct hyperplasia. However, it should be noted that the rat effect level estimates for silver liver tissue concentrations (6–14 ng/g) are lower

than the background silver liver tissue concentrations measured in the general population (17 ng/g [ICRP 1960]) and in unexposed workers (32 ng/g [Brune 1980]) (Section A.2.5.2.3). In addition, the exposure concentrations associated with these human-equivalent Ag liver tissue estimates are below those estimated to be associated with argyria. The few studies that have examined workers have not shown liver function abnormalities in workers with argyria (no information was available on hyperplasia in these workers). These findings suggest uncertainty in the human relevance of the rat effect-level estimates based on the silver tissue dose measurements.

6.5.3.2.4 Sources of uncertainty

The quantitative exposure estimates derived for humans from the rat data include a number of uncertainties: (1) adverse lung or liver effects are estimated at doses below those causing argyria, although such effects have not been reported in humans with argyria in the few studies that have investigated these effects (Section 3.2); (2) the rat liver NOAEL estimates are lower than the background silver concentrations (from dietary sources) that have been measured in human liver tissues (Section A.2.5.2.3); (3) information is lacking on the influence of dissolution and clearance of AgNPs on the doses associated with the observed lung and liver effects; (4) the clinical relevance to humans is unknown at the minimal lung and liver effects observed in rats; and (5) the potential for adverse effects following chronic exposure to AgNPs is poorly understood, including the possible role of particle size (Section A.2.5.3). Additional data are needed to reduce these uncertainties.

6.5.4 Conclusions of evaluation of REL for silver nanoparticles

Depending on the variables used, the OEL estimates range from less than 1 µg/m^3 to greater than 10 µg/m^3 (Tables A-3 and A-12). The factors that influence these OEL estimates include the POD and the total UF used. PBPK model-based estimates on the risk of argyria associated with exposure to AgNPs predict that working lifetime exposure concentrations would need to be 5 to 25 times higher than the current REL of 10 µg/m^3 to reach the minimal skin-tissue dose associated with argyria in humans (Table A-10).

On the basis of the evaluation of available animal and human data, NIOSH has determined that workers would be unlikely to develop argyria if airborne concentrations are maintained below the current NIOSH REL of 10 µg/m^3 (8-hr TWA) for soluble and insoluble silver dusts and fumes. After evaluation of the available human and animal evidence on effects other than argyria, NIOSH has determined that the current evidence is insufficient to support the development of a nanoparticle-specific REL for silver. Limitations in the current evidence include the large variability in the animal tissue doses associated with the lung and liver effects and uncertainty in the silver dose metric (soluble versus total silver) associated with those effects. More data are needed to further evaluate the dose-response relationships associated with silver particle size and solubility.

NIOSH recommends that effective risk management control practices be implemented so that worker exposures to silver nanomaterials do not exceed the NIOSH REL of 10 µg/m^3 (8-hour time-weighted average) for silver metal dust, fume, and soluble compounds, measured as a total airborne mass concentration. NIOSH based this conclusion on the following evidence: (1) worker exposure to silver fumes (containing nanoscale and microscale particles) was inherently included in the derivation of the current REL based on human studies of occupational exposure to silver dust and fume; (2) the lung and liver effects observed in the rat subchronic inhalation studies were of minimal severity at the doses extrapolated to humans; (3) the estimates of the tissue dose-effect levels were highly variable and included silver tissue concentrations in the range of background silver tissue concentrations in the general population; and (4) the range of worker-equivalent exposure concentration estimates associated with the rat-based NOAELs or BMDL$_{10}$ includes the NIOSH REL of 10 µg/m^3. Uncertainties in the evaluation of the health risks from nanoscale silver may be reduced depending on findings from ongoing research studies (e.g., research under way in the NIEHS nanoGo consortium) [Schug et al. 2013]. As new data become available, NIOSH will assess the results and determine whether additional recommendations are warranted.

6.6 Other OELs Proposed for Silver Nanoparticles

6.6.1 EU Calculation of INELs

Christensen et al. [2010] calculated INELs (indicative no effect levels) for silver nanoparticles by using EU European Chemicals Agency guidelines [ECHA 2008], based on findings from the subchronic (90-day) inhalation study in rats [Sung et al. 2008, 2009].

The lowest exposure concentration (49 µg/m^3) [Sung et al. 2008, 2009] was considered a LOAEL [Christensen et al. 2010] for decreased lung function in female rats [Sung et al. 2008]. A NOAEL of 133 µg/m^3 was proposed [Christensen et al. 2010], reportedly based on the lung and liver effects [Sung et al. 2009].

According to the ECHA [2008] criteria, Christensen adjusted the NOAEL or LOAEL for the difference in exposure duration in the rats (6 hours/day) and in humans (8 hours/day), as well as adjusting for resting (comparable to rat study) versus light work activity in workers (that is, 6.7 m^3 vs. 10 m^3) (Table 6-3).

Thus, the human-equivalent LOAEL of 49 µg/m^3 was calculated as

$$49\ \mu g/m^3 \times 6\ hrs/8\ hrs \times 6.7\ m^3/10\ m^3 = 25\ \mu g/m^3.$$

(The same adjustments result in 67 µg/m^3 as the human-equivalent concentration to 133 µg/m^3 in rats.)

Uncertainty factors of 3 and 10 were used for adjusting the rat subchronic LOAEL to estimate a NOAEL. Additional factors included 2.5 for interspecies toxicodynamics and 1 for interspecies toxicokinetics (since the local effects did not depend on metabolic rate); a factor of 5 for interspecies extrapolation to workers; and a factor of 2 for subchronic to chronic uncertainty.

Thus, the human-equivalent concentration of 25 µg/m^3 was divided by these factors:

$$3 \times 2.5 \times 5 \times 2 = 75;\ or\ 10 \times 2.5 \times 5 \times 2 = 250.$$

Thus, the derived INELs for the rat LOAEL of 49 µg/m^3 were calculated by dividing the human-equivalent LOAEL of 25 µg/m^3 by an overall adjustment factor of 75 or 250:

25 µg/m^3 / 75 = 0.33 µg/m^3

25 µg/m^3 / 250 = 0.1 µg/m^3.

Similar calculations were applied to the NOAEL of 133 µg/m^3 for lung inflammation (male and female rats) from Sung et al. [2009] (Table 6-3). In this case, the worker-equivalent concentration was 67 µg/m^3. The assessment factors included 10 for interspecies (animal to human, TK and TD) systemic liver effects; 5 for intraspecies variability; and 2 for subchronic to chronic extrapolation:

10 × 5 × 2 = 100

67 µg/m^3 / 100 = 0.67 µg/m^3.

Table 6-3. Proposed OELs for silver nanoparticles, based on rat subchronic inhalation studies* and European Chemicals Agency (ECHA) guidelines [Christensen et al. 2010].

Rat POD (µg/m^3)	POD type	Worker-equivalent POD (µg/m^3)†	Total UF	Proposed OEL (µg/m^3)
49	LOAEL	25	250 or 75	0.1 or 0.33
133	NOAEL	67	100	0.67

POD = point of departure; UF = uncertainty factor.
*Sung et al. [2008, 2009] and Song et al. [2013] (respective diameters: 18 nm, GSD 1.5; 14 nm, GSD 1.7).
†8-hr TWA concentration.

6.6.2 Other estimates of human-equivalent concentration

Ji and Yu [2012] used a rat POD of 100 µg/m^3, which they estimated on the basis of subchronic inhalation studies in their group [Sung et al. 2008, 2009; Song et al. 2013]. They estimated a worker-equivalent POD of 59 µg/m^3 (light exercise) by adjusting the 100 µg/m^3 rat POD by interspecies differences in the deposition fraction of silver nanoparticles (18 nm in diameter; GSD, 1.5) in the alveolar region (0.4 m^2 for rats; 62.7 m^2 for humans) over a total of 13 weeks (5 days/week) of exposure [Ji and Yu 2012]. The alveolar deposition fractions in rats and humans were estimated with multiple-path particle dosimetry (MPPD) 2.0 [ARA 2009]. This worker-equivalent concentration estimate is similar to those estimated according to ECHA [2008] guidelines (Table 6-3). No OELs were proposed by Ji and Yu [2012].

6.6.3 U.S. EPA margin of exposure evaluation

The U.S. EPA [2012a] used a margin of exposure (MOE) approach to evaluate the potential health hazard concern for workers handling a commercial product containing AgNPs (Table 6-4). MOE was defined as the ratio of the occupational exposure concentration to the rat NOAEL (adjusted for daily exposure duration) [EPA 2012a]. NIOSH used the same method to evaluate the MOE for workers at a facility refining silver feedstock [Miller et al. 2010]. EPA selected a NOAEL for lung inflammation or functional deficits in rats [Song et al. 2013] as the POD for its MOE evaluation. EPA concluded that workers performing a job in a closed system and wearing a respirator had an adequate MOE at 2,500, whereas workers performing the same job without a respirator may not be adequately protected with an MOE of 200.

Comparison of AgNP exposures found in ‘Nanosilva’ (1% nanosilver by weight [silica-sulfur-nanosilver complex]) production jobs [U.S. EPA 2013] to those found for workers in silver production and refining jobs [Miller et al. 2010] showed that the production/refining workers have exposures near the rat NOAEL for lung inflammation and functional deficits [Song et al. 2013], which is the same rat dose that was a LOAEL for lung function deficits in female rats in an earlier subchronic inhalation study of

AgNPs by the same group [Sung et al. 2008, 2009]. Thus, there is little or no MOE for workers in these silver production and refining jobs [Miller et al. 2010], indicating the need for a higher level of exposure containment or control of silver exposures in those facilities. It should be noted that the highest airborne silver concentrations for workers reported by Miller et al. [2010] exceeded the current NIOSH REL and OSHA PEL of 10 µg/m^3 for silver dust and fumes (soluble or insoluble metal).

Table 6-4. Margins of exposure between the rat NOAEL [Song et al. 2013] and worker exposure to concentrations of airborne silver particles, including nanoparticles.

Job	Worker exposure (µg/m^3), adjusted to 8-hr TWA	Rat NOAEL* (µg/m^3)	Margin of exposure (MOE)† 8-hr TWA	Reference
Closed system loading, without respirator	0.25	49	200‡	Nanosilva [EPA 2013]
Closed system loading, with respirator	0.02		2,500‡	Nanosilva [EPA 2013]
Furnace floor, forklift operator	49–94		1–2	Miller et al. [2010]
Electro-refining floor, cell maintenance	13		~4	Miller et al. [2010]

*****As evaluated by EPA [U.S. EPA 2013].

†Definition of MOE: ratio of the occupational exposure concentration and the rat NOAEL [Song et al. 2012], adjusted for the daily exposure duration. The occupational exposure concentrations were either predicted from an exposure model [EPA 2013] or based on personal sampling [Miller et al. 2010].

‡Worker exposure concentration to silver estimated on the basis of mass of silver handled per 8-hr day (1.2 lb) and the estimated exposure concentration per mass (lb) of silver handled, with or without the use of a respirator (0.21 or 0.016 µg/m^3/lb, respectively); also assumes freely available nanosilver and aerosol behavior like that in the 2012 rat study of Song et al. [U.S. EPA 2013, Sections 5.1.1 and 5.1.2, pages 28–30].

7 Recommendations

In light of current scientific evidence on the hazard potential of silver, appropriate steps should be taken to minimize worker exposure through the development of standard operating procedures (SOPs). These SOPs should contain written instructions on how to safely perform processes and job tasks, with guidance on establishing a risk management program that includes management commitment and employee involvement. Elements of a good risk management program should include the following:

(1) Identification of processes and job tasks where there is potential for exposure to silver

(2) Comprehensive assessment of exposures (including exposures to other potential hazards) as part of an overall hazard surveillance program

(3) Development of criteria and guidelines for selecting, installing, and evaluating engineering controls (such as LEV, dust collection systems), with the objective of controlling worker airborne exposure to silver below the NIOSH REL of 10 µg/m^3 as an 8-hr TWA

(4) An education and training program for recognizing potential exposures and using good work practices to prevent airborne and dermal exposure to silver, in particular, the safe handling of silver nanomaterials in a free (powder) form

(5) Development of procedures for selecting and using personal protective equipment (PPE; clothing, gloves, respirators)

(6) Implementation of a medical surveillance program for workers potentially exposed to silver (including silver nanomaterials)

(7) Routine (such as annual), systematic evaluation of worker exposure to silver whenever there is a change in a process or task associated with potential exposure to silver, such as soldering/brazing procedures or other high-temperature applications using silver (such as melting), or the manufacturing/synthesis of silver nanomaterials (such as drying and handling of free [powder] forms)

(8) Provision of facilities for hand washing to reduce the potential for exposure (e.g., dermal and oral exposure) and encouragement of workers to make use of these facilities before eating and leaving the worksite. A smoke-free workplace should also be established in concert with tobacco cessation support programs [NIOSH 2015].

(9) Provision of facilities for showering and changing clothes, with separate facilities for storage of non-work clothing, to prevent the inadvertent cross-contamination of non-work areas (including take-home contamination).

7.1 Exposure Assessment

NIOSH is recommending that a 10-µg/m^3 8-hr TWA (total mass) airborne concentration measurement be used to control worker exposure to all forms of silver. Personal exposure concentrations to silver should be determined with use of NIOSH Method 7300 or 7301 (elements by ICP) [NIOSH 2003] or an equivalent method. These methods prescribe the collection of an airborne sample with use of a cellulose ester membrane or polyvinyl chloride membrane filter (in a closed-faced cassette sampler) and analyzed by inductively coupled argon plasma atomic emission spectroscopy (ICP/AES). Measurement results from NIOSH Methods 7300 and 7301 should provide a reasonable estimate of a worker's exposure to silver at the NIOSH REL of 10 µg/m^3 (8-hr TWA).

7.1.1 Exposure Monitoring Program

An exposure-monitoring program should be established to ensure that worker exposures to silver are maintained below the NIOSH REL of 10 µg/m^3 (8-hr TWA). The program should consist of a plan designed to do the following: (1) identify sources of exposures to silver; (2) characterize exposures of all potentially exposed workers; (3) identify specific work areas or job tasks where worker exposures exceed or may exceed the NIOSH REL; and (4) evaluate the effectiveness of engineering controls, work practices, PPE, training, and all other methods and techniques used in reducing worker airborne exposures. To implement the plan, an exposure assessment strategy should be developed. The details of the strategy will depend on a number of factors, including the number of workers potentially exposed to silver and information on the variability in airborne concentrations of silver (that is, day-to-day and worker-to-worker exposure variability).

An important first step in applying any exposure monitoring strategy is to develop an inventory of the processes and job activities that place workers at risk of exposure (such as handling of bulk nanoscale silver, silver brazing/soldering operations, and other high-temperature processes involving silver). When applicable, this inventory should include an initial assessment of a bulk sample of the material and/or documentation from the manufacturer to determine the presence of nanoscale silver. The inventory can be used to determine the number of workers potentially exposed and to qualitatively determine which workers and processes are likely to have the greatest potential for exposure.

The strategy should also incorporate provisions to measure the airborne release of silver that may be occurring at specific processes or job activities, to provide “activity pattern data” [Duan and Mage 1997]. Activity pattern data (such as exposure measurements made near processes or job tasks handling silver) are useful for identifying possible causes of high exposure for remediation such as the need for exposure controls. However, these data are vulnerable to spatial variation in exposure concentrations and should not be used in predicting worker exposures. Because activity

pattern exposure data are often not predictive of personal exposure, extrapolating personal exposure from exposure measurements made at processes or from general area exposure concentrations should not be done without a thorough assessment of the workplace to establish whether a valid extrapolation is possible. NIOSH [2009a] and others [Brouwer et al. 2009; Kuhlbusch et al. 2011; Ramachandran et al. 2011] have developed guidance for determining workplace exposures to nanomaterials that can be used in identifying sources of exposure to silver, including silver nanomaterials.

To ensure that worker airborne exposures to silver are being maintained below the REL of 10 µg/m^3 8-hr TWA, there are several exposure-measurement strategies that can be used for obtaining exposure data that provide statistical confidence for determining whether worker exposures are below the REL [NIOSH 1977; Corn and Esmen 1979; Leidel and Busch 1994; Rappaport et al. 1995; Lyles et al. 1997; Bullock and Ignacio 2006; Ramachandran et al. 2011; McNally et al. 2014]. These strategies can be tailored to a specific workplace, depending on available resources, the number of workers, and the complexity of the work environment (such as process type and rate of operation, exposure control methods, and physical state and properties of material). One approach for determining worker airborne silver concentrations would be to initially target similarly exposed groups (SEGs) of workers [Corn and Esmen 1979; Leidel and Busch 1994]. This initial sampling effort may be more time efficient and require fewer resources for identifying workers with exposures to silver above the REL. However, this measurement strategy may produce incomplete and upwardly biased exposure estimates if the exposures are highly variable [Kromhout 2009]. Therefore, repeated measurements on randomly selected workers may be required to account for between- and within-worker variations in exposure concentrations [Rappaport et al. 1995; Lyles et al. 1997]. If workplace exposure measurement data for silver are available, as well as information on exposure variability, it may be possible to use a “Bayesian” model that combines expert knowledge with existing exposure measurement data to estimate workers’ exposures [McNally et al. 2014]. Because there is no “best” exposure measurement strategy that can be applied to all workplaces, multi-day random sampling of workers (all workers, if the exposed workforce is small) may be needed to accurately assess the

airborne concentrations of silver to which workers are being exposed. In cases where resources and/or health and safety expertise are limited, consultation with an expert may be required.

7.2 Engineering Controls

One of the best ways to prevent adverse health effects from exposure to a hazardous material is to eliminate exposure and minimize risks early in the design or redesign of manufacturing and downstream user processes (see NIOSH Prevention through Design [PtD], at www.cdc.gov/niosh/topics/PtD/). The concept of PtD is to design out or minimize hazards, preferably early in the design process. This can be accomplished through the establishment of a process safety management (PSM) program that is consistent with the requirements of the OSHA Process Safety Management Standard [29 CFR 1910.119]. PSM entails the development and implementation of programs or systems to ensure that the practices and equipment used in potentially hazardous processes are adequate and appropriately maintained. An integral part of the PSM program is a process hazard analysis prior to the initiation of work, to identify where sources of exposure to silver and other hazardous materials may occur so that process equipment can be designed or redesigned to minimize the risk of exposure. As part of the assessment, the health and safety professional should evaluate the potential magnitude and extent of emissions to determine the risk of exposure to workers. This initial assessment is an important first step toward identifying possible exposure control strategies.

Controlling exposures to occupational hazards is the fundamental method of protecting workers. Traditionally, a hierarchy of controls has been used as a means of determining how to implement feasible and effective control measures. Following the hierarchy normally leads to implementation of inherently safer systems, where the risk of illness or injury has been substantially reduced. Elimination and substitution are generally most effective if implemented when a process is in the design or development stage. If done early, implementation is simple, and in the long run it can result in substantial savings

(such as in the cost of protective equipment and the initial and operation costs for the ventilation system) [NIOSH 2013b]. For an existing process, elimination or substitution of the material may require major changes in equipment and/or procedures in order to reduce the potential hazard. When elimination or substitution is not feasible, the use of engineering controls can be an effective control strategy for minimizing exposure to hazards associated with processes and job tasks. Well-designed engineering controls can be highly effective in protecting workers and will typically be independent of worker interactions. The use of engineering controls to reduce worker exposure to all forms and particle sizes of silver is an effective means of minimizing health concerns and works best when it is part of an overall risk management program that includes education/training, administrative controls, and use of PPE.

There are a number of different types of exposure control systems that can be used, depending on the configuration of the process and the degree of exposure control required [ACGIH 2013; NIOSH 2013]. For example, exposure control systems such as source enclosure (that is, isolating the generation source from the worker) and well-designed local exhaust ventilation (LEV), equipped with high-efficiency particulate air (HEPA) filters, can be effective for capturing airborne silver particles at the source of exposure [NIOSH 2013b]. The selection of an appropriate exposure control system should take into account the extent to which the airborne concentration of silver is to be reduced (such as below the NIOSH REL of 10 μg/m^3), the quantity and physical form of the material (such as dispersible silver powder, a liquid slurry, or contained in a matrix), the task duration, the frequency with which workers may come into contact with silver or silver-containing material, and the characteristics of the task itself (e.g., an assessment as to how much energy is imparted to the material during sonication or powered sanding/cutting). For instance, working with materials containing nanoscale silver (such as encapsulated in a fabric or solid material) may require a different type of exposure control system than would working with large quantities of silver nanomaterials in a highly dispersed free (powder) form. Specific processes (such as high temperature melting of silver) and job tasks (such as silver brazing/soldering) have the potential to generate an aerosol or fume containing silver and therefore should incorporate

exposure controls at the exposure source. Likewise, the manufacturing/synthesis of engineered silver nanomaterials and the handling of dry powders should be performed in enclosed systems and, when warranted, HEPA-ventilated systems. HEPA filtration has been shown to be effective in capturing nanoscale particles and should be considered in situations where emissions may be regular, where processes are repeated, and where higher quantities are used in a way that may lead to emissions. Research quantities of nanoscale silver in laboratories can be safely handled if appropriate exposure-containment systems are used, such as a constant-velocity (variable air-volume) laboratory fume hood or air-curtain hood [Tsai et al. 2010] or a glove box to minimize worker exposure [NIOSH 2012]. These exposure control systems should be properly designed, tested, and routinely maintained and evaluated to ensure maximum efficiency [ACGIH 2010].

The use of an occupational exposure band (OEB) of 1 to 10 µg/m^3 as an exposure control strategy [Naumann et al. 1996] should also be considered as a means for determining the types of engineering controls that could be used to maintain silver nanomaterial exposures below 10 µg/m^3 (8-hr TWA). Table 7-1 provides examples of the types of engineering and other exposure control measures that could be used at various processes and job tasks to help control worker exposures to silver below 10 µg/m^3 (8-hr TWA). In some cases, a combination of approaches may be necessary to accomplish exposure control goals (such as installing a continuous liner system inside a ventilated booth).

Table 7-1. Engineering controls to reduce silver exposures below the NIOSH REL*

Process and/or Task Activity	Potential Sources of Exposure	Exposure Containment/Control Options
A. Pilot and Research & Development Operations	Potential exposures are generally to small quantities of AgNPs/AgNWs (such as µg and mg) during ▪ Synthesis of AgNPs/AgNWs, including chemical vapor deposition, solution phase synthesis, and dry powder dispersion ▪ Harvesting of AgNPs after synthesis ▪ Removal of nanosilver from a substrate ▪ Powder transfer (AgNPs/AgNWs) ▪ Reactor cleaning	**Exposure Controls:** ▪ Constant-velocity fume hood or nanomaterial enclosure with HEPA-filtration exhaust when warranted ▪ HEPA-filtration exhaust enclosure (such as glove box isolators) ▪ Biologic safety cabinet ▪ Note: local exhaust ventilation or some type of enclosure control (glove box) may be required at the reactor and during the harvesting of material.
B. Research Laboratories	Potential exposures are generally to small quantities of AgNPs/AgNWs (such as µg and mg) during ▪ Handling (such as mixing, weighing, blending, transferring) of AgNPs/AgNWs in free powder form or sonication of AgNP or AgNW liquid suspension	**Exposure Controls:** ▪ Constant-velocity fume hood or nanomaterial-handling enclosure with HEPA-filtration exhaust when warranted ▪ HEPA-filtration exhaust enclosure (such as glove box isolators) ▪ Biologic safety cabinet
C. Manufacturing and Synthesis of AgNPs and AgNWs	Potential exposures are generally to large quantities of AgNPs/AgNWs (≥ kg amounts) during ▪ Synthesis of AgNPs (chemical vapor deposition, solution phase synthesis, and dry powder dispersion) ▪ Harvesting of AgNPs after synthesis ▪ Removal of nanosilver from a substrate ▪ Powder transfer of nanosilver ▪ Drum and bag filling ▪ Reactor cleaning ▪ Coating of AgNPs/AgNWs	**Exposure Controls:** ▪ Dedicated ventilated room (such as a down-flow room) for reactor with HEPA-filtration exhaust, potentially in conjunction with localized controls listed below ▪ LEV at source of potential exposure when isolation or total enclosure of the process is not possible ▪ Ventilated bagging/weighing stations and/or unidirectional down-flow ventilation booth ▪ Non-ventilation options, including a continuous liner off-loading system for bagging operations ▪ Ventilated bag dumping stations for product transfer

Process and/or Task Activity	Potential Sources of Exposure	Exposure Containment Options
D. Use of AgNPs and AgNWs to produce enabled materials	**1.** Potential exposures are generally to <u>small quantities</u> of AgNP/AgNW powder or liquid suspensions during ▪ Mixing, weighing, and transferring of AgNPs/AgNWs ▪ Incorporation of AgNPs/AgNWs into matrices and coatings ▪ Spraying of AgNPs/AgNWs on surfaces	**1. Exposure Controls:** ▪ Transfer of AgNPs/AgNWs in sealed, unbreakable, labeled containers ▪ Constant velocity fume hood or nanomaterial handling enclosure (with filtered exhaust when warranted) ▪ HEPA-filtration exhaust enclosure (such as glove box isolators) ▪ Biologic safety cabinet
	2. Potential exposures are generally to <u>large quantities</u> of AgNPs or AgNWs in powder or liquid suspensions during ▪ Blending or pouring into other matrices ▪ Impregnating of textile materials and spray coating of surfaces	**2. Exposure Controls:** ▪ Isolation techniques such as a dedicated ventilated room or process enclosure with HEPA-filtration exhaust ▪ Process-based controls such as ventilated bagging/weighing station and unidirectional down-flow booth ▪ Non-ventilation options such as continuous liner off-loading systems for bagging operations ▪ Ventilated bag dumping stations for product transfer
	3. Potential exposures during handling of <u>small pieces</u> of AgNP- and AgNW-enabled textiles, fabrics, materials and composites: ▪ Grinding, sanding, cutting, drilling, or other mechanical energy applied to materials containing AgNPs or AgNWs	**3. Exposure Controls:** **<u>Small pieces of AgNP/AgNW-enabled textiles, fabrics, materials, and composites</u>** ▪ Constant-velocity fume hood or nanomaterial handling enclosure with filtered exhaust when warranted ▪ HEPA-filtration exhaust enclosure (such as glove box isolators) ▪ Biologic safety cabinet ▪ Localized dust-suppression techniques, including ventilation-based (power tool–type) or mist/water-based, where appropriate **<u>Large pieces of AgNP/AgNW-enabled materials/composites, where use of isolation techniques (such as large ventilated enclosures) are not feasible</u>**

		▪ Ventilated process enclosure or unidirectional down-flow booth with HEPA-filtered exhaust ▪ LEV at exposure source with HEPA-filtered exhaust ▪ Localized dust-suppression techniques, including ventilation-based (power tool–type) or mist/water-based, where appropriate
E. Processes requiring the application of high temperatures to Ag metals and alloys	Potential exposure to fumes generated during brazing, soldering, welding, and melting of Ag and Ag alloys	**Exposure Controls:** • LEV-based welding fume control approaches should be used, including ventilated enclosing hoods, fixed slot/plenum ventilated worktables, or moveable capture hoods (such as a welding fume extraction unit) • Process-based controls, such as ventilated production welding booths, may be required for large-scale applications where fumes may be generated

*****Note: Factors that influence the selection of appropriate engineering controls and other exposure control strategies include the physical form (such as dry dispersible powder, fume, liquid slurry, or a matrix/composite), task duration, frequency, quantity of the Ag (including AgNPs and AgNWs) handled, and the task characteristics (how much energy is imparted to the material). The airborne concentration of silver at the potential source of emission should be measured to confirm the effectiveness of the exposure control measures. See NIOSH documents *Current Strategies for Engineering Controls in Nanomaterial Production and Downstream Handling Process* [NIOSH 2013b] and *General Safe Practices for Working with Engineered Nanomaterials in Research Laboratories* [NIOSH 2012] for guidance on the selection of appropriate exposure control strategies.

7.3 Worker Education and Training

Establishing a safety and health program that includes educating and training workers on the potential hazards of silver, including exposure to silver nanomaterials, is critical to preventing adverse health effects from exposure. Research has shown that immediate and long-term objectives can be attained with training when (1) workers are educated about the potential hazards of their job, (2) knowledge and work practices become improved, (3) workers are provided the necessary skills to perform their jobs safely, and (4) management shows commitment and support for workplace safety [NIOSH 2010]. Requirements for the education and training of workers, as specified in the OSHA Hazard Communication Standard (29 CFR 1910.1200) and the Hazardous Waste Operation and Emergency Response Standard (29 CFR 1910.120), and as described by Kulinowski and Lippy [2011] for workers exposed to nanomaterials, provide a minimum set of guidelines that can be used for establishing an education and training program. The establishment and oversight of the program should be described in the SOP to (1) ensure management's commitment to control exposures; (2) identify and communicate potential hazards to workers; (3) evaluate workplace exposures to silver; (4) identify and implement engineering controls and effective work practices; (5) establish documentation; and (6) periodically review the adequacy of exposure controls and other preventive practices. Management should systematically review and update these procedures and convey to workers the actions taken to resolve and/or improve workplace conditions.

A program for educating workers should also include both instruction and "hands on" training that addresses the following:

- The potential health risks associated with exposure to silver
- The safe handling of silver nanomaterials and nanoscale silver–containing materials to minimize the likelihood of inhalation exposure and skin contact, including the proper use of engineering controls, PPE (such as respirators and gloves), and good work practices.

7.4 Cleanup and Disposal

Procedures should be developed to protect workers from exposure to silver, with special emphasis on the safe cleanup and removal of silver nanomaterials from contaminated surfaces. Inhalation and dermal exposures will likely present the greatest risks. The potential for inhalation exposure during cleanup will be influenced by the likelihood of silver nanomaterials becoming airborne, with bulk silver nanomaterials (powder form) presenting a greater inhalation potential than silver nanomaterials in solution (liquid form), and liquids in turn presenting a greater potential risk than silver nanomaterials in encapsulated materials.

It would be prudent to base strategies for dealing with spills and contaminated surfaces on the use of current good practices, together with available information on exposure risks. Standard approaches for cleaning powder spills can be used for cleaning surfaces contaminated with silver. These include using HEPA-filtered vacuum cleaners, wiping up silver (in powder form) with damp cloths, and wetting the powder before wiping. Liquid spills containing silver nanomaterials can typically be cleaned up with absorbent materials or liquid traps. If vacuum cleaning is employed, extreme caution should be taken that HEPA filters are installed properly and that bags and filters are changed according to the manufacturer's recommendations. Dry sweeping or air hoses should not be used to clean work areas. There may need to be the use of different PPE (from the norm) depending on the amount of the spill and its location. A plan should be in place describing the steps that should be taken to address the issue and the type of PPE that should be used.

The handling and disposal of waste (including all cleaning materials) and other contaminated materials (such as gloves) should comply with all applicable regulations (federal, state, and local).

7.5 Dermal Protection

Although there are no regulations or guidelines for the selection of clothing or other apparel protective against exposure to silver, OSHA requires employers to ensure that employees wear appropriate PPE for their work tasks [OSHA 29 CFR 1910.132 (d)(1)]. Results from experimental studies with various types of nanoparticles showed that dermal penetration of nanoparticles can occur under certain conditions of exposure (such as flexing of skin) [Ryman-Rasmussen et al. 2006; Rouse et al. 2007] and that factors such as size, shape, water solubility, and surface coating directly affect a nanoparticle's potential to penetrate the skin [Sayes et al. 2004; Ryman-Rasmussen et al. 2006]. In addition, the flexing of skin may enhance skin penetration [Smijs and Bouwstra 2010]. Currently, only limited information is available to assess the exposure and health hazards of skin exposure to AgNPs. Studies of the dermal toxicity of AgNPs in pigs [Samberg et al. 2010] and guinea pigs [Korani et al. 2011] revealed little sign of gross irritation to the skin; however, AgNPs were found in the upper stratum corneum layers of the skin, with some focal inflammation (intracellular and intercellular epidermal edema) after 14 days of topical application [Samberg et al. 2010]. In guinea pigs receiving dermal applications of AgNPs at doses of 100, 1000, and 10,000 µg/mL in a subchronic study, overproduction of Kupffer cells and degeneration of hepatocytes occurred and increased with nanosilver concentrations; the highest dose caused necrosis [Korani et al. 2011].

Ling et al. [2012] reported on the potential dermal risk to workers exposed to nanoscale silver colloid (average diameter, 9.87 nm) and silver liquid (average diameter, 13.04 nm) and several other nanomaterials. On the basis of the criteria of OECD [2004], WHO [2010], and EPA [2004], two skin exposure techniques (transdermal Franz diffusion cell drive and tape stripping) were used to evaluate dermal absorption of AgNPs. Excised porcine skin was used as a model for human skin in the transdermal Franz diffusion cell test and tape stripping. Results of the tape-stripping analysis showed that the distribution of silver colloid and silver liquid was predominantly on the first and second strippings of the stratum corneum. This occurred at both the 20-µg/mL and 300-µg/mL

concentrations, indicating a low rate of skin penetration over a short period of exposure. In addition, the experiments showed that organic modifiers affected the infiltration of AgNPs. When a less polar solvent such as isopropyl alcohol was used, the penetration rate was higher than for other polar solvents. In a few case studies of workers, localized argyria was observed when burn creams containing silver were applied to the skin [Wan et al. 1991], during the handling of silver jewelry [Catsakis and Sulica 1978], and during dermal exposure to silver nitrate [Moss et al. 1979].

Given the data on dermal exposure to AgNPs, PPE (such as protective clothing, including gloves) is recommended when

- all technical measures to eliminate or control exposure to Ag, including silver nanomaterials, have not been successful, or
- there is a potential for dermal exposure to damaged or abraded skin.

Several factors (performance criteria) should be considered when selecting the appropriate PPE [Gao et al., 2014]:

- Penetration potential
- Durability (resistance to wear, tear, abrasions, and punctures; resistance to chemical degradation)
- Dexterity/flexibility
- Decontamination ability (for multi-use PPE)
- Comfort
- Compatibility with other equipment and interface regions (such as the glove/coat interface)

If protective clothing and gloves are worn, particular attention should be given to preventing silver nanomaterial exposure to abraded or lacerated skin. The limited experimental evidence suggests that airtight fabrics made of nonwoven textiles are more efficient in protecting workers against nanoparticles than fabrics made of woven cotton or polyester [Golanski et al. 2009; Golanski et al. 2010]. A study of the

penetration of nanoparticles and submicron particles (30–500 nm) through various nonwoven fabrics showed penetration levels up to 90% for some of the fabrics tested [Gao et al. 2011]. Particle penetration was observed to increase with increasing particle size, up to 300 to 500 nm.

The challenge when selecting appropriate protective clothing is to strike a balance between comfort and protection. Garments that provide the highest level of protection (such as an impermeable Level A suit) are also the least comfortable to wear for long periods of time, whereas garments that are probably the least protective (such as a thin cotton laboratory coat) are the most breathable and comfortable to wear. The efficiency of commercial gloves in preventing dermal exposure to nanoparticles varies, depending on the glove material, its thickness, and the manner in which it is used (such as long exposure times and other chemical exposures) [NanoSafe 2008; Golanski et al. 2009, 2010]. The proper selection of gloves should take into account their resistance to chemical attack by the nanomaterial and, if it is suspended in liquids, by the liquid itself [USDOE 2008]. If protective gloves (such as powder-free nitrile, neoprene, and latex gloves) are used, then “double gloving” may be needed when the worker requires physical protection (such as when working with sharp instruments), in addition to chemical protection [http://nioshsciencepolicy.cdc.gov/PDF/97-135.pdf]. Special attention should also be given to the proper removal and disposal of contaminated gloves to prevent skin contamination. Gloves should also be visually inspected for tears and routinely replaced.

7.6 Respiratory Protection

The decision to use respiratory protection should be based upon a hazard assessment and risk management practices to keep worker inhalation exposure below prescribed occupational exposure limits. Published reports of workers exposed to silver [Rosenman et al. 1979, 1987; Wobling et al. 1988; Pifer et al 1989; Lee et al. 2011a; Lee et al. 2012a,b; Miller et al. 2010] indicate that workplace airborne concentrations to silver can exceed the NIOSH REL and OSHA PEL of 10 µg/m^3 as an 8-hr TWA when appropriate

exposure control measures are not used. When engineering controls and work practices cannot reduce worker airborne exposures to silver below the NIOSH REL of 10 µg/m^3 (8-hr TWA), workers should be provided respiratory protection. The use of respirators may also be advisable for certain tasks that place workers at risk of potentially high peak concentrations of silver, such as the cleanup of silver nanomaterial spills or debris (free form); maintenance of equipment used to process silver nanomaterials; large processes involving the electro-refining of silver; and the cleaning and/or disposal of filtration systems used to capture airborne silver nanomaterials. When selecting the appropriate respirator, the respirator program manager should consider the presence of other potentially hazardous aerosols (such as chemicals) [Rengasamy and Eimer 2011]. On the basis of this information, the respirator program manager may decide to choose a respirator with a higher assigned protection factor (APF) or one with a higher level of filtration performance (such as changing from an N95 to a P100). Studies on the filtration performance of N95 filtering facepiece respirators have found that the mean penetration levels for 40-nm particles range from 1.4% to 5.2%, indicating that N95 and higher-performing respirator filters would be effective at capturing airborne AgNPs [Bałazy et al. 2006; Rengasamy et al. 2007, 2008]. Recent studies show that nanoparticles <20 nm are also effectively captured by NIOSH-approved filtering facepiece respirators [Rengasamy et al. 2008, 2009]. Other classes of respirators also can provide a higher level of protection (Table 8-2). The publication *NIOSH Respirator Selection Logic 2004* provides guidance for selecting an appropriate respirator [NIOSH 2005].

The OSHA respiratory protection standard (29 CFR 1910.134) requires establishment of a respiratory program for both voluntary and required respirator use. Elements of the standard include (1) a medical evaluation of each worker's ability to perform the work while wearing a respirator; (2) regular training of personnel; (3) periodic workplace exposure monitoring; (4) respirator fit-testing; and (5) respirator maintenance, inspection, cleaning, and storage. The program should be evaluated regularly and respirators should be selected by the person who is in charge of the program and

knowledgeable about the workplace and the limitations associated with each type of respirator.

Table 7-2. Respiratory protection for exposure to silver.

Workplace Airborne Concentrations of Silver or Conditions of Use* Options	Minimum Respiratory Protection
10–100 µg/m^3 (10 × REL)	Any filtering facepiece respirator or air-purifying, elastomeric half-facepiece respirator equipped with appropriate type of particulate filter†; any negative-pressure (demand), supplied-air respirator equipped with a half-mask
≤250 µg/m^3 (25 × REL)	Any powered, air-purifying respirator equipped with a hood or helmet and a HEPA filter; any continuous-flow supplied-air respirator equipped with a hood or helmet
≤500 µg/m^3 (50 × REL)	Any air-purifying full-facepiece respirator equipped with N-100, R-100, or P-100 filter; any powered air-purifying respirator equipped with a tight-fitting half-facepiece and a HEPA filter; any negative-pressure (demand) supplied-air respirator equipped with a full facepiece; any continuous-flow supplied-air respirator with a tight-fitting half-facepiece; any negative-pressure (demand) self-contained respirator equipped with a full facepiece

(Continued)

Table 7-2 (Continued)

Workplace airborne concentrations of silver or conditions of use options	Minimum respiratory protection
≤10,000 μg/m^3 (1,000 × REL)	Any pressure-demand supplied-air respirator equipped with a full facepiece

*The protection offered by a given respirator is contingent upon (1) the respirator user adhering to complete program requirements (such as those required by OSHA in 29 CFR 1910.134), (2) the use of NIOSH-certified respirators in their approved configuration, and (3) individual fit testing to rule out those respirators for which a good fit cannot be achieved.

†The appropriate type of particulate filter means any 95- or 100-series (N, R, or P) filter. Note: N-95 or N-100 series filters should not be used in environments where there is potential for exposure to oil mists.

Note: complete information on the selection of respirators can be found at (1) OSHA 3352-02 2009, *Assigned Protection Factors for the Revised Respiratory Protection Standard*, at http://www.osha.gov/Publications/3352-APF-respirators.html, and (2) NIOSH [http://www.cdc.gov/niosh/docs/2005-100/default.html].

7.7 Medical Screening and Surveillance

The evidence summarized in this document leads to the conclusion that workers occupationally exposed to silver (including silver nanomaterials) may potentially be at risk of argyria when exposed to airborne concentrations greater than 10 µg/m^3 (8-hr TWA). These workers may benefit from inclusion in a medical screening and surveillance program to help protect their health. Evidence indicates that excessive occupational exposure to silver may also lead to adverse effects on the pulmonary, renal, and hepatic systems. Although not focused on these other organ systems, the medical screening and surveillance described below may also be helpful in early detection and prevention should clinical effects occur in those organ systems.

7.7.1 Worker Participation

Workers who could receive the greatest benefit from such a medical surveillance program include those exposed to concentrations of silver (including AgNPs and AgNWs) in excess of the REL (that is, workers exposed to airborne silver at concentrations above 10 µg/m^3 as an 8-hr TWA) or those workers assigned to tasks qualitatively assessed to have a higher potential for exposure to silver.

7.7.2 Program Oversight

Oversight of the medical surveillance program should be assigned to a qualified health-care professional who is informed and knowledgeable about potential workplace exposures, routes of exposure, and potential health effects related to silver.

7.7.3 Screening Elements

Initial evaluation

- An initial (baseline) evaluation of all participating workers potentially exposed to silver should be conducted by a qualified health-care professional and should consist of the following:

- An occupational and medical history, with special attention given to potential occupational exposure to silver and to other sources of silver exposure (such as medications or previous occupational exposure to silver)
- A physical examination with an emphasis on evaluation of the nasal septum, eyes, throat, and skin for changes in pigmentation that might be early signs of argyria
- Other examinations or medical tests deemed appropriate by the responsible health-care professional on the basis of factors such as abnormal findings on initial examination. For example, findings consistent with localized or generalized argyria in a worker potentially exposed to silver could prompt a test for silver in blood or feces to help confirm the diagnosis.

Periodic evaluations

- Evaluations should be conducted at regular intervals and at other times (such as after an unintentional spill or other exposure), as deemed appropriate by the responsible health-care professional on the basis of data from the initial evaluation, ongoing work history, or signs or symptoms of silver toxicity following work process changes (such as a change in how silver nanomaterials are manufactured or used).
- Evaluations should include the following:
    - An occupational and medical history update and focused physical examination, performed annually, as well as any other examinations or medical tests deemed appropriate by the responsible health-care professional.

Written reports of medical findings

- The health-care professional should give each worker a written report containing the following:

    - The individual worker's medical examination results
    - Medical opinions and/or recommendations concerning any relationships between the individual worker's medical conditions and occupational exposures, any special instructions on the individual's exposures and/or use of personal protective equipment, and any further evaluation or treatment
- For each examined employee, the health-care professional should give the *employer* a written report specifying the following:
    - Any work or exposure restrictions based on the results of medical evaluations
    - Any recommendations concerning use of personal protective equipment
    - A medical opinion as to whether any of the worker's medical conditions are likely to have been caused or aggravated by occupational exposures
- Findings from the medical evaluations having no bearing on the worker's ability to work with silver should not be included in any reports to employers. Confidentiality of the worker's medical records should be enforced in accordance with all applicable regulations and guidelines.

7.7.4 Worker education

Workers should be provided information sufficient to allow them to understand the nature of potential workplace exposures, potential health risks, routes of exposure, and instructions for reporting health symptoms. Workers should also be provided with information about the purposes of medical screening, the health benefits of the program, and the procedures involved.

7.7.5 Periodic evaluation of data and screening program

- Standardized medical screening data should be periodically aggregated and evaluated to identify patterns of worker health that may be linked to work activities and practices that require additional primary prevention efforts. This

analysis should be performed by a qualified health professional or other knowledgeable person to identify worker health patterns that may be linked to work activities or exposures. Confidentiality of workers' medical records should be enforced in accordance with all applicable regulations and guidelines.

- Employers should periodically evaluate the screening elements to ensure that the program is consistent with current knowledge related to exposures and health effects associated with occupational exposure to silver (including silver nanomaterials).

Other important components related to occupational health surveillance programs, including medical surveillance and screening, are discussed in Appendix C.

8 Research Needs

Additional data and information are needed to ascertain the occupational safety and health concerns of working with all forms of silver. Data are particularly needed on sources of exposure to silver nanomaterials (such as AgNPs and AgNWs) and on factors that influence workers' exposure; exposure control measures (such as engineering controls) and work practices that are effective in reducing worker exposures below the NIOSH REL; and appropriate measurement methods and exposure metrics for characterizing workplace exposures. The conduct of in vitro and in vivo studies with silver of different physical-chemical properties are needed to better understand the role of particle size, shape, surface charge, chemical composition, dissolution potential, and surface treatment in causing toxicity. Chronic inhalation studies in animals may provide information about the long-term potential for adverse health effects in workers.

Information gathered from the following research is needed to determine the appropriate risk management practices for protecting workers occupationally exposed to silver, including silver nanomaterials:

(1) Identification of industries or occupations in which exposures to silver may occur
(2) Trends in the production and use of silver nanomaterials
(3) Description of work tasks and scenarios with a potential for exposure to silver nanomaterials
(4) Workplace exposure measurement data from various types of industries and jobs where silver nanomaterials are manufactured and used
(5) Case reports or other health information demonstrating potential health effects in workers exposed to silver nanomaterials
(6) Epidemiology studies of workers including quantitative exposure estimates by silver type and particle size

(7) Research studies (e.g., in vitro) that provide sufficient characterization (physical and chemical) of AgNPs used in the same solution and under the same conditions (temperature, time) to obtain a better understanding of what actually interacts with cells/organisms.

(8) Complementary in vivo and in vitro studies with AgNPs to ascertain the role of particle size and other physical-chemical properties on the toxicity of silver, including quantitative dose measures in vitro that are comparable to in vivo doses. Physical-chemical properties that should be examined include: particle size and size dispersion (monodispersity, polydispersity), shape, zeta potential, surface coating, agglomeration, age of the sample, ion-producing potential, and dissolution rate. Studies should include the use of an accepted Ag reference material (e.g., National Institute of Standards and Technology) as a control.

(9) Studies to determine whether AgNPs could be genotoxic in vivo

(10) Information on the types and effectiveness of control measures (such as engineering controls, work practices, PPE) being used in the workplace to minimize worker exposure to silver, including silver nanomaterials

(11) Information on measurement methods and exposure metrics that could be used to quantify worker exposure to silver nanomaterials, including information on the limitations of those methods in quantifying exposures

(12) Long-term animal inhalation studies with AgNPs and AgNWs of different compositions and dimensions to assess biodistribution/accumulation and chronic effects. Studies should include the use of an accepted AgNP reference material (e.g., National Institute of Standards and Technology [NIST 2015]) as a control.

(13) Further validation of the PBPK model used in the risk assessment [Bachler et al. 2013] (Appendix A) to estimate silver tissue doses by particle size and solubility.

9 References

ACGIH [2001]. Silver and compounds. In: Documentation of threshold limit values and biological exposure indices. 7th Ed., Vol. 1. Cincinnati, OH: American Conference of Governmental Industrial Hygienists.

ACGIH [2010]. Industrial ventilation: a manual of recommended practice for operation and maintenance. Cincinnati, OH: American Conference of Governmental Industrial Hygienists.

ACGIH [2013]. Industrial ventilation: a manual of recommended practice for design. Cincinnati, OH: American Conference of Governmental Industrial Hygienists.

Ahamed M, Karns M, Goodson M, Rowe J, Hussain SM, Schlager JJ, Hong Y [2008]. DNA damage response to different surface chemistry of silver nanoparticles in mammalian cells. Toxicol Appl Pharmacol *233*(3):404–410.

Amato C, Hussain S, Hess K, Schlager J [2006]. Interaction of nanomaterials with mouse keratinocytes. The Toxicologist *90*(1-S0):168.

ARA [2011]. Multiple-path particle deposition (MPPD 2.1): a model for human and rat airway particle dosimetry. Raleigh, NC: Applied Research Associates, Inc.

Armitage SA, White MA, Wilson HK [1996]. The determination of silver in whole blood and its application to biological monitoring of occupationally exposed groups. Ann Occup Hyg *40*(3):331–338.

Arora S, Jain J, Rajwade JM, Paknikar KM [2008]. Cellular responses induced by silver nanoparticles: in vitro studies. Toxicol Lett *179*(2):93–100.

Arora S, Jain J, Rajwade JM, Paknikar KM [2009]. Interactions of silver nanoparticles with primary mouse fibroblasts and liver cells. Toxicol Appl Pharmacol *236*(3):310–318.

AshaRani PV, Mun GLK, Hande MP, Valiyaveettil S [2009]. Cytotoxicity and genotoxicity of silver nanoparticles in human cells. ACS Nano *3*(2):279–290.

ATSDR [1990]. Toxicological profile for silver. TP-90-24. Atlanta, GA: Agency for Toxic Substances and Disease Registry.

Austin CA, Umbreit TH, Brown KM, Barber DS, Dair BJ, Francke-Carroll S, Feswick A, Saint-Louis MA, Hikawa H, Siebein KN, Goering PL [2012]. Distribution of silver nanoparticles in pregnant mice and developing embryos. Nanotoxicology *6*(8):912–922.

Bachler G, von Goetz N, Hungerbühler K [2013]. A physiologically based pharmacokinetic model for ionic silver and silver nanoparticles. Intl J Nanomed *8*:3365–3382.

Baker EL, Matte TP [2005]. Occupational health surveillance. In: Rosenstock L, Cullen E, Brodkin R, eds. Textbook of clinical occupational and environmental medicine. Philadelphia, PA: Elsevier Saunders Company [http://www.osha.gov/SLTC/medicalsurveillance/surveillance.html].

Bałazy A, Toivola M, Reponen T, Podgorski A, Zimmer A, Grinshpun SA [2006]. Manikin-based performance evaluation of N95 filtering facepiece respirators challenged with nanoparticles. Ann Occup Hyg *50*(3):259–269.

Beer C, Foldbjerg R, Hayashi Y, Sutherland DS, Autrup H [2012]. Toxicity of silver nanoparticles: nanoparticle of silver ion? Toxicol Lett *208:*286-292.

Bell RA, Kramer JR [1999]. Structural chemistry and geochemistry of silver-sulfur compounds: critical review. Environ Toxicol Chem *18*(1):9–22.

Braakhuis H, Gosens I, Krystek P, Boere J, Cassee F, Fokkens P, Post J, van Loveren H, Park M [2014]. Particle size dependent deposition and pulmonary inflammation after short-term inhalation of silver nanoparticles. Particle Fibre Toxicology *11*:49.

Braydich-Stolle LK, Lucas B, Schrand A, Murdock RC, Lee T, Schlager JJ, Hussain SM, Hofmann MC [2010]. Silver nanoparticles disrupt GDNF/Fyn kinase signaling in spermatogonial stem cells. Toxicol Sci *116*(2):577–589.

Brouwer D, van Duuren-Stuurman B, Berges M, Jankowska E, Bard D, Mark D [2009]. From workplace air measurement results toward estimates of exposure? Development of a strategy to assess exposure to manufactured nano-objects. J Nanopart Res *11*(8):1867–1881.

Brune D, Nordberg G, Wester PO [1980]. Distribution of 23 elements in the kidney, liver and lungs of workers from a smeltery and refinery in North Sweden exposed to a number of elements and of a control group. Sci Total Environ *16*(1):13-35.

Buckley WR [1963]. Localized argyria. Arch Derm *88:*531–539.

Bullock W, Ignacio JS, eds. [2006]. A strategy for assessing and managing occupational exposures. 3rd ed. Fairfax, VA: AIHA Press.

Carlson C, Hussain SM, Schrand AM, Braydich-Stolle LK, Hess KL, Jones RL, Schlager JJ [2008]. Unique cellular interaction of silver nanoparticles: size-dependent generation of reactive oxygen species. J Phys Chem B *112*(43):13608–13619.

Catsakis LH, Sulica VI [1978]. Allergy to silver amalgams. Oral Surg *46:*371-375.

Chang AL, Khosravi V, Egbert B [2006]. A case of argyria after colloidal silver ingestion. J Cutan Pathol *33*(12):809–811.

Chen X, Schluesener HJ [2008]. Nanosilver: a nanoproduct in medical application. Toxicol Lett *176*(1):1–12.

Cheng KH, Cheng YS, Yeh HC, Guilmette RA, Simpson SQ, Yang YH, Swift DL [1996]. In vivo measurements of nasal airway dimensions and ultrafine aerosol deposition in the human nasal and oral airways. J Aerosol Sci *27*(5):785–801.

Cho EA, Lee WS, Kim KM, Kim S-Y [2008]. Occupational generalized argyria after exposure to aerosolized silver. J Dermatol *35*:759–760.

Cho W-S, Duffin R, Donaldson K [2012]. Zeta potential and solubility to toxic ions as mechanisms of lung inflammation caused by metal/metal oxide nanoparticles. Toxicol Sci *126*(2):469–477.

Corn M, Esmen N [1979]. Workplace exposure zones for classification of employee exposure to physical and chemical agents. Am Ind Hyg Assoc *40*:47–57.

Chrastina A, Schnitzer JE [2010]. Iodine-125 radiolabeling of silver nanoparticles for in vivo SPECT imaging. Int J Nanomed *5*:653–659.

Christensen FM, Johnston HJ, Stone V, Aitken RJ, Hankin S, Peters S, Aschberger K. [2010]. Nano-TiO_2: feasibility and challenges for human health risk assessment based on open literature. Nanotoxicology *5*(2):110–124.

Chronholm P, Karlsson HL, Hedberg J, Lowe TA, Winnberg L, Elihn K, Wallinder IO, Moller L [2013]. Intracellullar uptake and toxicity of Ag and CuO nanoparticles: a comparison between nanoparticles and their corresponding metal ions. Small *9*(7):970–982.

Crump KS [1984]. A new method for determining allowable daily intakes. Fund Appl Toxicol *4*(5):854–871.

Deng F, Olesen P, Foldbjerg R, Dang DA, Guo X, Autrup H [2010]. Silver nanoparticles upregulate connexin43 expression and increase gap junctional intercellular communication in human lung adenocarcinoma cell line A549. Nanotoxicol *4*:186–195.

DiVincenzo GD, Giordano CJ, Schriever LS [1985]. Biologic monitoring of workers exposed to silver. Int Arch Occup Environ Health *56*:207–215.

DFG [2013]. Deutsche Forschungsgemeinschaft. List of MAK and BAT values 2013. Weinheim, Germany: Wiley-VCH Veriag GmbH & Co. KGaA. ISBN: 978-3-527-33616-6.

Dong MS, Choi JY, Sung JH, Kim JS, Song KS, Ryu HR, Lee JH, Bang IS, An K, Park HM, Song NW, Yu IJ [2013]. Gene expression profiling of kidneys from Sprague-Dawley rats following 12-week inhalation exposure to silver nanoparticles. Toxicol Mech Methods *23*(6):437–448.

Drake PL, Hazelwood KJ [2005]. Exposure-related health effects of silver and silver compounds: a review. Ann Occup Hyg *49*(*7*):575–585.

Duan N, Mage T [1997]. Combination of direct and indirect approaches for exposure assessment. J Expo Anal Environ Epidemiol *7*(4):439–470.

Dziendzikowska K, Gromadzka-Ostrowska J, Lankoff A, Oczkowski M, Krawczynska A, Chwastowska J, Sadowska-Bratek M, Chajduk E, Wojewodzka M, Dusinska M, Kruszewski M [2012]. Time-dependent biodistribution and excretion of silver nanoparticles in male Wistar rats. J Appl Toxicol *32*:920–928.

ECHA [2008]. REACH Guidance on Information Requirements and Chemicals Safety Assessment. Chapter R.8. European Chemicals Agency (ECHA), http://guidance.echa.europa.eu/.

Elzey S, Grassian VH [2010]. Agglomeration, isolation, and dissolution of commercially manufactured silver nanoparticles in aqueous environments. J Nanoparticle Res *12*:1945–1958.

Eustis SL, Boorman GA, Harada T, Popp JA [1990]. Liver. In: Boorman GA, Eustis SL, Elwell MR, Montgomery CA Jr, MacKenzie WF, eds. Pathology of the Fischer Rat: Reference and Atlas. New York: Academic Press.

Evanoff DD, Chumanov G [2005]. Synthesis and optical properties of silver nanoparticles and arrays. Chem Phys Chem *6*:1221–1231.

Foldbjerg R, Olesen P, Hougaard M, Dang DA, Hoffmann HJ, Autrup H [2009]. PVP-coated silver nanoparticles and silver ions induce reactive oxygen species, apoptosis and necrosis in THP-1 monocytes. Toxicol Lett *190*(2):156–162.

Foldbjerg R, Dang DA, Autrup H [2011]. Cytotoxicity and genotoxicity of silver nanoparticles in the human lung cancer cell line, A549. Arch Toxicol *85*(7):743–750.

Foldbjerg R, Irving ES, Hayaski Y, Sutherland DS, Thorsen K, Autrup H, Beer C [2012]. Global gene expression profiling of human lung epithelial cells after exposure to nanosilver. Toxicol Sci *130*(1):145–157.

Furchner JE, Richmond CR, Drake GA [1968]. Comparative metabolism of radionuclides in mammals-IV. Retention of silver 110m in the mouse, rat, monkey and dog. Health Physics *15*:505–514.

Future Markets, Inc. [2013]. The global nanotechnology and nanomaterials industry. Technology Report No. 68, www.futuremarketsinc.com.

Gao P, Jaques PA, Hsiao T, Shepherd A, Eimer BC, Yang M, Miller A, Gupta B, Shaffer R [2011]. Evaluation of nano- and submicron particle penetration through ten nonwoven fabrics using a wind-driven approach. J Occup Environ Hyg *8*(1):13–22.

Gao P, Behar JL, Shaffer R [2014]. Considerations for selection of PPE to protect against nanoparticle dermal exposure. In Daniel Anna, ed. Chemical Protective Clothing. 2nd printing of 2nd ed. Fairfax, VA: AIHA Press, pp. 511–555.

Gliga AR, Skoglund S, Wallinder IO, Fadeel B, Karisson HL [2014]. Size-dependent cytotoxicity of silver nanoparticles in human lung cells: the role of cellular uptake, agglomeration and Ag release. Particle and Fibre Toxicology, doi:10.1186/1743-8977-11-11.

Golanski L, Guiot A, Rouillon F, Pocachard J, Tardif F [2009]. Experimental evaluation of personal protection devices against graphite nanoaerosols: fibrous filter media, masks, protective clothing, and gloves. Hum Exp Toxicol *28*(6-7):353–359.

Golanski L, Guiot A, Tardif F [2010]. Experimental evaluation of individual protection devices against different types of nanoaerosols: graphite, TiO_2 and Pt. J Nanopart Res *12*(1):83–89.

Gopinath P, Gogoi SK, Sanpui P, Paul A, Chattopadhyay A, Ghosk SS [2010]. Signaling gene cascade in silver nanoparticle induced apoptosis. Colloids and Surface B: Biointerfaces *77*:240–245.

Gregoratto, D., Bailey, M.R., Marsh, J.W. [2010]. Modelling particle retention in the alveolar-interstitial region of the human lungs. J Radiol Prot *30*(3):491–512.

Greulich C, Kittler S, Epple M, Muhr G, Koller M [2009]. Studies on the biocompatibility and the interaction of silver nanoparticles with human mesenchymal stem cells (hMSCs). Arch Surg *394*:495–502.

Greulich C, Diendorf J, Simon T, Eggeler G, Epple M, Koller M [2011]. Uptake and intracellular distribution of silver nanoparticles in human mesenchymal stem cells. Acta Biomaterialia *7:*347–354.

Gromadzka-Ostrowska J, Dziendzikowska K, Lankoff A, Dobrzynska M, Instanes C, Brunborg G, Gajowik A, Radzikowska J, Wojewodzka M, Kruszewski M [2012]. Silver nanoparticles effects on epididymal sperm in rats. Toxicol Lett *214:*251–258.

Hackenberg S, Scherzed A, Kessler M, Hummel S, Technau A, Froelich K, Ginzkey C, Koehler C, Hagen R, Kleinsasser N [2011]. Silver nanoparticles: evaluation of DNA damage, toxicity and functional impairment in human mesenchymal stem cells. Toxicol Lett *201*(1):27–33.

Hadrup N, Loeschner K, Bergstrom A, Wilcks A, Gao X, Vogel U, Frandsen HL, Larsen EH, Lam HR, Mortensen A [2012a]. Subacute oral toxicity investigation of nanoparticulate and ionic silver in rats. Arch Toxicol *86*:543–551.

Hadrup N, Loeschner K, Mortensen A, Sharma AK, Qvortrup K, Larsen EH, Lam HR [2012b]. The similar neurotoxic effects of nanoparticulate and ionic silver *in vivo* and *in vitro*. Neurotoxicology *33*:416–423.

Hagens WI, Oomen AG, de Jong WH, Cassee FR, Sips A [2007]. What do we (need to) know about the kinetic properties of nanoparticles in the body? Reg Tox Pharm *49:*217–229.

Hansen RE, Roth D, Winther JR [2009]. Quantifying the global cellular thiol-disulfide status. Proc Natl Acad Sci USA *106*(2):422–427.

Harber P, Conlon C, McCunney RJ [2003]. Occupational medical surveillance. In: McCunney RJ, Ed. A practical approach to occupational and environmental medicine. Philadelphia, PA: Lippincott, Williams, and Wilkins.

Harker JM, and Hunter D [1935]. Occupational argyria. British Journal of Dermatology and Syphilis. November, 441–455.

Hathaway GJ, Proctor NH [2004]. Chemical Hazards of the Workplace. 5th ed. Hoboken, NJ: John Wiley & Sons, 632–634.

Hendren CQ, Mesnard X, Droge J, Wiesner MR [2011]. Estimating production data for five engineered nanomaterials as a basis for exposure assessment. Environ Sci Technol *45*:2562–2569.

Hill WR, Pillsbury DM [1939]. Argyria: The Pharmacology of Silver. Baltimore, MD: The Williams and Wilkins Company.

Hsin YH, Chen CF, Huang S, Shih TS, Lai PS, Chueh PJ [2008]. The apoptotic effect of nanosilver is mediated by a ROS- and JNK-dependent mechanism involving the mitochondrial pathway in NIH3T3 cells. Toxicol Lett *179*(3):130–139.

Hubbs AF, Mercer RR, Benkovic SA, Harkema J, Sriram K, Schwegler-Berry D, Goravanahally MP, Nurkiewicz TR, Castranova V, Sargent LM [2011]. Nanotoxicology – a pathologist's perspective. Toxicologic Pathology *39*:301-324.

Hussain SM, Hess KL, Gearhart JM, Geiss KT, Schlager JJ [2005a]. In vitro toxicity of nanoparticles in BRL 3A rat liver cells. Toxicol In Vitro *19*(7):975–983.

Hussain S, Hess K, Gearhart JM, Geiss KT, Schlager JJ [2005b]. Toxicity assessment of silver nanoparticles (Ag 15, 100 nm) in alveolar macrophages. Toxicol Sci *84*(1-S):350.

Hyun J-S, Lee BS, Ryu HY, Sung JH, Chung KH, Yu IJ [2008]. Effects of repeated silver nanoparticles exposure on the histological structure and mucins of nasal respiratory mucosa in rats. Toxicol Lett *182*:24–28.

ICRP [1960]. Report of Committee II on permissible dose for internal radiation, 1959. Annals of the ICRP/ICRP Publication *2*:1–40.

ICRP [1994]. Human respiratory tract model for radiological protection. In: Smith H, ed. Annals of the ICRP. Tarrytown, NY: International Commission on Radiological Protection, ICRP Publication No. 66.

ISO [2006]. Workplace atmospheres; ultrafine, nanoparticle and nano-structured aerosols, exposure characterization and assessment. Geneva, Switzerland: International Standards Organization. Document No. ISO/TC 146/SC2/WGI N324.

ISO/TS [2008]. Nanotechnologies: terminology and definitions for nano-object, nanoparticle, nanofibre and nanoplate. ISO/TS 27687:2008. Vienna, Austria: International Organization for Standardization.

Jeong GN, Jo UB, Ryu HY, Kim YS, Song KS, Yu IJ [2010]. Histochemical study of intestinal mucins after administration of silver nanoparticles in Sprague-Dawley rats. Arch Toxicol *84*:63–69.

Jeschke MG [2009]. The hepatic response to thermal injury: is the liver important for postburn outcomes? Mol Med *15*:337–351.

Jeschke MG, Gauglitz GG, Song J, Kulp GA, Finnerty CC, Cos RA, Barral JM, Herndon DN, Boehning D [2009]. Calcium and ER stress mediate hepatic apoptosis after burn injury. J Cell Mol Med *13*:1857–1865.

Ji JH, Jung JH, Yu IJ, Kim SS [2007a]. Long-term stability characteristics of metal nanoparticle generator using small ceramic heater for inhalation toxicity studies. Inhal Toxicol *19*(9):745–751.

Ji JH, Jung JH Kim SS, Yoon J-U, Park JD Choi BS, Chung YH, Kwon IH, Jeong J, Han BS, Shin JH, Sung JH, Song KS, Yu IJ [2007b]. Twenty-eight-day inhalation toxicity study of silver nanoparticles in Sprague-Dawley rats. Inhalation Toxicol *19*:857–871.

Ji JH, Yu IJ [2012]. Estimation of human equivalent exposure from rat inhalation toxicity study of silver nanoparticles using multi-path particle dosimetry model. Toxicology Research, The Royal Society of Chemistry, DOI: 10.1039/c2tx20029e.

Johnston HJ, Hutchison G, Christensen FM, Peters S, Hankin S, Stone V [2010]. A review of the in vivo and in vitro toxicity of silver and gold particulates: particle attributes and biological mechanisms responsible for the observed toxicity. Crit Rev Tox *40*(4):328–346.

Jun E-A, Lim K-M, Kim K, Bae O-N, Noh J-Y, Chung K-H, Chung J-H [2011]. Silver nanoparticles enhance thrombus formation through increased platelet aggregation and procoagulant activity. Nanotoxicology *5*:157–167.

Kalishwaralal K, Banumathi E, Pandian SBRK, Deepak V, Muniyandi J, Eom SH, Gurunathan S [2009]. Silver nanoparticles inhibit VEGF induced cell proliferation and migration in bovine retinal endothelial cells. Colloids Surf B Biointerfaces *73*(1):51–57.

Kawata K, Osawa M, Okabe S [2009]. In vitro toxicity of silver nanoparticles at noncytotoxic doses to HepG2 human hepatoma cells. Environ Sci Technol *43*:6046–6051.

Kennedy DC, Orts-Gil G, Lai C-H, Miller L, Haase A, Luch A, Seeberger PH [2014]. Carbnhydrate functionalization of silver nanoparticles modulates cytotoxicity and cellular uptake. J Nanobiotechnology *20*:59.

Kenyon A, Antonini JM, Mercer RR, Schwegler-Berry D, Schaeublin NM, Hussain SM, Oldenburg SJ, Roberts JR [2012]. Pulmonary toxicity associated with different aspect ratio silver nanowires after intratracheal instillation in rats. Society of Toxicology Annual Meeting, San Francisco, CA, March 11–15, 2012. Toxicol Sci: The Toxicologist *126*(1):A652, p. 141.

Kim J, Kuk E, Yu K, Kim J, Park S, Lee H, Kim S, Park Y, Park YH, Hwang C, Kim Y, Lee Y, Jeong D, Cho M [2007]. Antimicrobial effects of silver nanoparticles. Nanomedicine *3*:95–101 (as cited in Hackenberg et al. [2011]).

Kim YS, Kim JS, Cho HS, Rha DS, Park JD, Choi BS, Lim R, Chang HK, Chung YH, Kwon IH, Jeong J, Han BS, Yu IJ [2008]. Twenty-eight day oral toxicity, genotoxicity, and gender-related tissue distribution of silver nanoparticles in Sprague-Dawley rats. Inhal Toxicol *20*:575–583.

Kim W-Y, Kim J, Park JD, Ryu HY, Yu IJ [2009a]. Histological study of gender differences in accumulation of silver nanoparticles in kidneys of Fischer 344 rats. J Toxicol Environ Health Part A *72*:1279–1284.

Kim E, Maeng J-H, Lee DH, Kim JM [2009b]. Correlation of biomarkers and histological responses in manufactured silver nanoparticle toxicity. Toxicol Environ Health Sci *1*:8–16.

Kim S, Choi JE, Choi J, Chung KH, Park K, Yi J, Ryu DY [2009c]. Oxidative stress-dependent toxicity of silver nanoparticles in human hepatoma cells. Toxicol In Vitro *23*(6):1076–1084.

Kim YS, Song MY, Park JD, Song KS, Ryu HR, Chung YH, Chang HK, Lee JH, Oh KH, Kelman BJ, Hwang IK, Yu IJ [2010a]. Subchronic oral toxicity of silver nanoparticles. Particle Fibre Toxicol *7*:20.

Kim E, Chu YC, Han JY, Lee DH, Kim YJ, Kim H-C, Lee SG, Lee SJ, Jeong SW, Kim JM [2010b]. Proteomic analysis of silver nanoparticle toxicity in rat. Toxicol Environ Health Sci *2*:251–262.

Kim JS, Sung JH, Ji JH, Song KS, Lee JH, Kang CS, Yu IJ [2011]. In vivo genotoxicity of silver nanoparticles after 90-day silver nanoparticle inhalation exposure. Saf Health Work (2):34–38.

Kim TH, Kim M, Park HS, Shin US, Gong MS, Kim HW [2012]. Size-dependent cellular toxicity of silver nanoparticles. J Biomed Mater Res Part A *100A:*1033–1043.

Kim JS, Song KS, Sung JH, Ryu HR, Choi BG, Cho HS, Lee JK, Yu IJ [2013]. Genotoxicity, acute oral and dermal toxicity, eye and dermal irritation and corrosion and skin sensitization evaluation of silver nanoparticles. Nanotoxicology *7*(5):953–960.

Kitter S, Greulich C, Diendorf J, Koller M, Epple M [2010]. Toxicity of silver nanoparticles increases during storage because of slow dissolution under release of silver ions. Chem Mater *22:*4548–4554.

Klaassen CD [1979]. Biliary excretion of silver in the rat, rabbit, and dog. Tox Applied Pharm *5:*49–55.

Korani M, Rezayat SM, Gilani K, Arbabi Bidgoli S, Adeli S [2011]. Acute and subchronic dermal toxicity of nanosilver in guinea pig. Int J Nanomed *6*:855–862.

Kreyling WG, Hirn S, Möller W, Schleh C, Wenk A, Celik G, Lipka J, Schäffler M, Haberl N, Johnston BD, Sperling R, Schmid G, Simon U, Parak WJ, Semmler-Behnke M [2014]. Air-blood barrier translocation of tracheally instilled gold nanoparticles inversely depends on particle size. ACS Nano *28*;8(1):222–233.

Kromhout H [2009]. Design of measurement strategies for workplace exposures. Occup Environ Med *59*(5):349–354.

Kuempel ED, Tran CL [2002]. Comparison of human lung dosimetry models: implications for risk assessment. Ann Occup Hyg *46*(Suppl.1):337-341.

Kuhlbusch TA, Asbach C, Fissan H, Gohler D, Stintz M [2011]. Nanoparticle exposure at nanotechnology workplaces: A review. Part Fibre Toxicol *8*:22.

Kulinowski K, Lippy B [2011]. Training workers on risks of nanotechnology. Washington, DC: National Clearinghouse for Worker Safety and Health Training, National Institute of Environmental Health Sciences (NIEHS) Worker Education and Training Program (WETP), http://tools.niehs.nih.gov/wetp/index.cfm?id=537.

Kurashina M, Kozuka S, Nakasima N, Hirabayasi N, Masafumi I [2006]. Relationship of intrahepatic bile duct hyperplasia to cholangiocellular carcinoma. Cancer *61*(12):2469–2474.

Landsiedel R, Fabian E, Ma-Hock L, et al. [2012]. Toxico-/biokinetics of nanomaterials. Arch Toxicol *86*(7):1021–1060.

Lankveld DP, Oomen AG, Krystek P, Neigh A, Troost-de Jong A, Noorlander CW, Eijkeren JC, Geertsma RE, De Jong WH [2010]. The kinetics of the tissue distribution of silver nanoparticles of different sizes. Biomaterials *31*:8350–8361.

Lansdown ABG [2012]. Silver and gold. In: Bingham and Cohrssen, eds. Patty's Toxicology. 6th ed. Vol. 1. New York: John Wiley & Sons.

Larese FF, D'Agostin F, Crosera M, Adami G, Renzi N, Bovenzi M, Maina G [2009]. Human skin penetration of silver nanoparticles through intact and damaged skin. Toxicology *255*:33–37.

Lee H-Y, Choi Y-J, Jung E-J, Yin H-Q, Kwon J-T, Kim J-E, Im H-T, Cho M-H, Kim, J-H, Kim H-Y, Lee B-H [2010]. Genomics-based screening of differentially expressed genes in the brains of mice exposed to silver nanoparticles via inhalation. J Nanopart Res *12*:1567–1578.

Lee YS, Kim DW, Lee YH, Oh JH, Yoon S, Choi MS, Lee SK, Kim JW, Lee K, Song CW [2011]. Silver nanoparticles induce apoptosis and G2/M arrest via PKCzeta-dependent signaling in A549 lung cells. Arch Toxicol, doi: 10.1007/s00204-011-0714-1.

Lee JH, Kwon M, Ji JH, Kang CS, Ahn KH, Han JH, Yu IJ [2011a]. Exposure assessment of workplaces manufacturing nanosized TiO_2 and silver. Inhalation Toxicol *23*:226–236.

Lee JH, Mun J, Park JD, Yu IJ [2011b]. A health surveillance case study of workers who manufacture silver nanomaterials. Nanotoxicology *6*:667–669.

Lee JH, Ahn K, Kim SM, Jeon KS, Lee JS, Yu IJ [2012]. Continuous 3-day exposure assessment of workplace manufacturing silver nanoparticles. J Nanopart Res *14*:1134.

Lee JH, Kim YS, Song KS, Ryu HR, Sung JH, Park JD, Park HM, Song NW, Shin BS, Marshak D, Ahn K, Lee JE, Yu IJ [2013a]. Biopersistence of silver nanoparticles in tissues from Sprague-Dawley rats. Particle Fibre Toxicol *10*:36.

Lee TY, Liu MS, Huang LJ, Lue SI, Lin LC, Kwan AL, Yang RC [2013b]. Bioenergetic failure correlates with autophagy and apoptosis in rat liver following silver nanoparticle intraperitoneal administration. Particle Fibre Toxicol *10*:40.

Lee Y, Kim P, Yoon J, Lee B, Choi K, Kil K-H, Park K [2013c]. Serum kinetics, distribution and excretion of silver in rabbits following 28 days after a single intravenous injection of silver nanoparticles. Nanotoxicology *7*(6):1120-1130.

Leidel NA, Busch KA [1994]. Statistical design and data analysis requirements. In: Harris RL, Cralley LJ, Cralley LV, eds. Patty's Industrial Hygiene and Toxicology, 3rd ed. Vol. 3, Part A. New York: John Wiley and Sons, pp. 453–582.

Levard C, Reinsch BC, Michel FM, Oumahi C, Lowry GV, Brown GE [2011]. Sulfidation processes of PVP-coated silver nanoparticles in aqueous solution: impact on dissolution rate. Environ Sci Technol *45*(12):5260–5266.

Levard C, Hotze EM, Lowry GV, Brown GE [2012]. Environmental transformations of silver nanoparticles: impact on stability and toxicity. Environ Sci Technol *46*(13):6900–6914.

Li M, Panagi Z, Avgoustakis K, Reineke J [2012]. Physiologically based pharmacokinetic modeling of PLGA nanoparticles with varied mPEG content. Int J Nanomedicine 7:1345–1356.

Li S-D, Huang L [2008]. Pharmacokinetics and biodistribution of nanoparticles. Mol Pharm *5*(4):496-504.

Li PW, Kuo TH, Chang JH, Yeh JM, Chan WH [2010]. Induction of cytotoxicity and apoptosis in mouse blastocysts by silver nanoparticles. Toxicol Lett *197*(2):82–87.

Ling MP, Lin WC, Liu CC, Huang YS, Chueh MJ, Shih TS [2012]. Risk management strategy to increase the safety of workers in the nanomaterials industry. J Hazardous Materials, http://dx.doi.org/10.1016/j.jhazmat.2012.05.073.

Li Y, Chen DH, Yan J, Chen Y, Mittelstaedt RA, Zhang Y, Biris AS, Heflich RH, Chen T [2012]. Genotoxicity of silver nanoparticles evaluated using the Ames test and *in vitro* micronucleus assay. Mutation Research *745*:4–10.

Ling MP, Lin WC, Liu CC, Huang YS, Chueh MJ, Shih TS [2012]. Risk management strategy to increase the safety of workers in nanomaterials industry. J Hazard Mater, http://dx.doi.org/10.1016/j.jhazmat.2012.05.073.

Liu J, Hurt RH [2010]. Ion release kinetics and particle persistence in aqueous nano-silver colloids. Environ Sci Technol *44*(6):2169-2175.

Liu W, Wu Y, Wang C, Li HC, Wang T, Liao CY, Cui L, Zhou QF, Yan B, Jiang GB [2010a]. Impact of silver nanoparticles on human cells: effect of particle size. Nanotoxicology *4*(3):319–330.

Liu J, Sonshine DA, Shervani S, Hurt RH [2010b]. Controlled release of biologically active silver from nanosilver surfaces. ACS Nano *4:*6903–6913.

Liu P, Huang Z, Gu N [2013]. Exposure to silver nanoparticles does not affect cognitive outcome or hippocampal neurogenesis in adult mice. Ecotoxicol Environ Safety *87*:124–130.

Loeschner K, Hadrup N, Qvortrup K, Larsen A, Gao X, Vogel U, Mortensen A, Lam HR, Larsen EH [2011]. Distribution of silver in rats following 28 days of repeated oral exposure to silver nanoparticles or silver acetate. Particle Fibre Toxicol *8*:18.

Lok C-N, Ho C-M, Chen R, He Q-Y, Yu W-Y, Sun H, Tam PK-H, Chiu J-F, Che C-M [2006]. Proteomic analysis of the mode of antibacterial action of silver nanoparticles. J Proteome Res *5*:916–924.

Lyles RH, Kupper LL, Rappaport SM [1997]. A lognormal distribution-based exposure assessment method for unbalanced data. Ann Occup Hyg *41*(1):63–76.

Ma J, Lü X, Huang Y [2011]. Genomic analysis of cytotoxicity response to nanosilver in human dermal fibroblasts. J Biomed Nanotechnol *7*:263–275.

Mahabady MK [2012]. The evaluation of teratogenicity of nanosilver on skeletal system and placenta of rat fetuses in prenatal period. Afr J Pharmacy Pharmacol *6*(6):419–424.

Maneewattanapinyo P, Banlunara W, Thammacharoen C, Ekgasit S, Kaewamatawong T [2011]. An evaluation of acute toxicity of colloidal silver nanoparticles. J Vet Med Sci *73*(11):1417–1423. E-pub June 29.

Mathias FT, Romano RM, Kizys ML, Kasamatsu T, Giannocco G, Chiamolera MI, Dias-da-Silva MR, Romano MA [2014]. Daily exposure to silver nanoparticles during prepubertal development decreases adult sperm and reproductive parameters. Informa Healthcare, 17 February, doi:10.3109/17435390.2014.889237.

Maynard AD, Kuempel ED [2005]. Airborne nanostructured particles and occupational health. J Nanopart Res *7*:587–614.

McNally K, Warren N, Fransman W, Entink RK, Schinkel J, van Tongeren M, Cherrie JW, Kromhout H, Schneider T, Tielemans E [2014]. Advanced REACH Tool: a Bayesian model for occupational exposure assessment. Ann Occup Hyg *55*(5):551–565.

Mei N, Zhang Y, Chen Y, Guo X, Ding W, Ali SF, Biris AS, Rice P, Moore MM, Chen T [2012]. Silver nanoparticle-induced mutations and oxidative stress in mouse lymphoma cells. Environ Molecular Mutagenesis *53*:409–419.

Miller A, Drake PL, Hintz P, Habjan M [2010]. Characterizing exposures to airborne metals and nanoparticle emissions in a refinery. Ann Occup Hyg *54*(5):504–513.

Miura N, Shinohara Y [2009]. Cytotoxic effect and apoptosis induction by silver nanoparticles in HeLa cells. Biochem Biophys Res Commun *390*(3):733–737.

Moss AP, Sugar A, Hargett NA, Atkin A, Wolkstein M, Rosenman KD [1979]. The ocular manifestations and functional effects of occupational argyrosis. Arch Ophthalmol *97*:906–908.

Muir DC, Cena K [1987]. Deposition of ultrafine aerosols in the human respiratory tract. Aerosol Sci Technol *6*:183–190.

Nallathamby PD, Xu X-HN [2010]. Study of cytotoxic and therapeutic effects of stable and purified silver nanoparticles on tumor cells. Nanoscale *2*(6):942–952.

NanoSafe [2008]. Are conventional protective devices such as fibrous filter media, respirator cartridges, protective clothing and gloves also efficient for nanoaerosols? DR-325/326-200801-1. Brussels, Belgium: European Commission (EC), http://www.nanosafe.org/home/liblocal/docs/Dissemination%20report/DRI_s.pdf.

Naumann BD, Sargent EV, Starkman BS, Fraser WJ, Becker GT, Kirk GD [1996]. Performance-based exposure control limits for pharmaceutical active ingredients. Am Ind Hyg Assoc J *57:*33–42

NIOSH [1973]. Health Hazard Evaluation (HHE) report: Dunham-Bush, Incorporated, West Hartford, Connecticut. By Vandervort R, Polakoff PL, Flesch JP, Lowry LK. Cincinnati, OH: U.S. Department of Health and Human Services, National Institute for Occupational Safety and Health (NIOSH). NIOSH HHE Report No. 72-84-31, NTIS No. PB 229627.

NIOSH [1977]. Occupational exposure sampling strategy manual. Cincinnati, OH: U.S. Department of Health and Human Services, Centers for Disease Control, National institute for Occupational Safety and Health, DHHS (NIOSH) Publication No. 77-173.

NIOSH [1981]. Health Hazard Evaluation (HHE) report: General Electric Company, Lynn, Massachusetts. By McManus KP, Baker EL. Cincinnati, OH: U.S. Department of

Health and Human Services, Centers for Disease Control, National Institute for Occupational Safety and Health (NIOSH), NIOSH HHE Report No. 80-084-927.

NIOSH [1988]. Silver (metal dust and fume). CDC-NIOSH 1988 OSHA PEL Project Documentation: List by Chemical Name: Silver, http://www.cdc.gov/niosh/pel88/7440-22.

NIOSH [1992]. Hazard Evaluation and Technical Assistance (HETA) report: Langers Black Hills Silver Jewelry, Inc., Spearfish, South Dakota. By Kiefer M. Cincinnati, OH: U.S. Department of Health and Human Services, Centers for Disease Control and Prevention, National Institute for Occupational Safety and Health (NIOSH), NIOSH HETA Report No. 92-097-2238.

NIOSH [1998]. Hazard Evaluation and Technical Assistance (HETA) report: Caterpillar Inc., York, Pennsylvania. By Tepper A, Blade LM. Cincinnati, OH: U.S. Department of Health and Human Services, Centers for Disease Control and Prevention, National Institute for Occupational Safety and Health (NIOSH), NIOSH HETA Report No. 95-0001-2679.

NIOSH [2000]. Hazard Evaluation and Technical Assistance (HETA) report: OmniSource Corporation, Precious Metal Recycling Facility, Ft. Wayne, Indiana. By Gwin KK, Nemhauser JB. Cincinnati, OH: U.S. Department of Health and Human Services, Centers for Disease Control and Prevention, National Institute for Occupational Safety and Health (NIOSH), NIOSH HETA Report No. 2000-0041-2796.

NIOSH [2003]. Method 7300 and 7301 Elements by ICP (supplement issued March 15, 2003). In: NIOSH manual of analytical methods (NMAM®). Cincinnati, OH: U.S. Department of Health and Human Services, Public Health Service, Centers for Disease Control and Prevention, National Institute for Occupational Safety and Health, DHHS (NIOSH) Publication No. 94-113.

NIOSH [2005]. NIOSH respirator selection logic. Cincinnati, OH: U.S. Department of Health and Human Services, Centers for Disease Control and Prevention, National Institute for Occupational Safety and Health, DHHS (NIOSH) Publication No. 2005-100.

NIOSH [2006]. Criteria for a recommended standard: occupational exposure to refractory ceramic fibers. Cincinnati, OH: U.S. Department of Health and Human Services, Centers for Disease Control and Prevention, National Institute for Occupational Safety and Health, DHHS (NIOSH) Publication No. 2006-125.

NIOSH [2007]. NIOSH Pocket Guide to Chemical Hazards. Cincinnati, OH: U.S. Department of Health and Human Services, Centers for Disease Control and Prevention, National Institute for Occupational Safety and Health, DHHS (NIOSH) Publication No. 2005-149, http://www.cdc.gov/niosh/pel88/7440-22.html.

NIOSH [2009]. Approaches to safe nanotechnology: managing the health and safety concerns with engineered nanomaterials. Cincinnati, OH: U.S. Department of Health and Human Services, Centers for Disease Control and Prevention, National Institute for Occupational Safety and Health, DHHS (NIOSH) Publication No. 2009-125.

NIOSH [2010]. A systematic review of the effectiveness of training and education for the protection of workers. Toronto: Institute for Work & Health. Cincinnati, OH: U.S. Department of Health and Human Services, Centers for Disease Control and Prevention, National Institute for Occupational Safety and Health, DHHS (NIOSH) Publication No. 2010-127.

NIOSH [2011]. Occupational exposure to titanium dioxide. Cincinnati, OH: U.S. Department of Health and Human Services, Centers for Disease Control and Prevention, National Institute for Occupational Safety and Health, DHHS (NIOSH) Publication No. 2011-160.

NIOSH [2012]. General safe practices for working with engineered nanomaterials in research laboratories. Cincinnati, OH: U.S. Department of Health and Human Services, Centers for Disease Control and Prevention, National Institute for Occupational Safety and Health, DHHS (NIOSH) Publication No. 2012-147.

NIOSH [2013]. Current strategies for engineering controls in nanomaterial production and downstream handling processes. Cincinnati, OH: U.S. Department of Health and Human Services, Centers for Disease Control and Prevention, National Institute for Occupational Safety and Health, DHHS (NIOSH) Publication No. 2014-102.

NIOSH [2015]. Promoting health and preventing disease and injury through workplace tobacco policies. Cincinnati, OH: U.S. Department of Health and Human Services, Centers for Disease Control and Prevention, National Institute for Occupational Safety and Health, DHHS (NIOSH) Publication No. 2015-113.

NIST [2015]. National Institute of Standards and Technology (NIST): silver nanoparticle test material, https://www-s.nist.gov/srmors/view_report.cfm?srm=8017.

Nowack B, Kurg HF, Height M [2011]. 120 Years of nanosilver history: implications of policy makers. Environ Sci Technol *45*:1177–1183.

NTP [2014]. National Toxicology Program: NTP nonneoplastic lesion atlas. Liver, bile duct-hyperplasia, http://ntp.niehs.nih.gov/nnl/hepatobiliary/liver/bdhyperp/index.htm.

Oberdorster G, Stone V, Donaldson K [2007]. Toxicology of nanoparticles: a historical perspective. Nanotoxicology *1*:2–25.

OECD (Organisation for Economic Co-operation and Development) [2004]. OECD guideline for the testing of chemicals. Skin absorption: in vitro method, http://www.oecd-ilibrary.org/docserver/download/9742801e.pdf?expires=1423779844&id=id&accname=guest&checksum=EEEB10E26F1C4EFFC7A40DBF2F9E39F6.

OSHA (Occupational Safety and Health Administration) [1988]. Silver (metal dust and fume). Federal Register *53*(109):21215. Proposed rules Air Contaminants: Federal Register 53:20960-21393.

OSHA (Occupational Safety and Health Administration) [2012]. Safety Data Sheets. Hazard Communication Standard (HCS). Washington, DC: U.S. Department of Labor. https://www.osha.gov/Publications/OSHA3514.html.

OSHA (Occupational Safety and Health Administration) [2014]. Silver, metal and soluble compounds (as Ag): chemical sampling information. Washington, DC: U.S. Department of Labor, http://www.osha.gov/dts/chemicalsampling/data/CH_267300.html.

Park J, Kwak BK, Bae E, Lee J, Kim Y, Choi K Yi J [2009]. Characterization of exposure to silver nanoparticles in a manufacturing facility. J Nanopart Res *11*:1705–1712.

Park EJ, Bae E, Yi J, et al. [2010a]. Repeated-dose toxicity and inflammatory responses in mice by oral administration of silver nanoparticles. Environ Toxicol Pharmacol *30*(2):162–168.

Park EJ, Yi J, Kim Y, Choi K, Park K [2010b]. Silver nanoparticles induce cytotoxicity by a Trojan-horse type mechanism. Toxicol In Vitro *24*(3):872–878.

Park K, Park E-J, Chun IK, Choi K, Lee SH, Yoon J, Lee BC [2011a]. Bioavailability and toxicokinetics of citrate-coated silver nanoparticles in rats. Arch Pharm Res *34*:153–158.

Park E-J, Choi K, Park K [2011b]. Induction of inflammatory responses and gene expression by intratracheal instillation of silver nanoparticles in mice. Arch Pharm Res *34*(2):299–307.

Park M, Neigh AM, Vermeulen JP, de la Fonteyne L, Verharen HW, Briede JJ, van Loveren H, de Jong WH [2011c]. The effect of particle size on the cytotoxicity, inflammation, developmental toxicity and genotoxicity of silver. Biomaterials *32*:9810-9817.

Park K [2013]. Toxicokinetic differences and toxicities of silver nanoparticles and silver ions in rats after single oral administration. J Toxicol Environ Health, Part A *76*(22):1246–1260.

Piao MJ, Kang KA, Lee IK, Kim HS, Kim S, Choi JY, Choi J, Hyun JW [2011]. Silver nanoparticles induce oxidative cell damage in human liver cells through inhibition of reduced glutathione and induction of mitochondria-involved apoptosis. Toxicol Lett *201*(1):92–100.

Pifer JW, Friedlander BR, Kintz RT, Stockdale DK [1989]. Absence of toxic effects in silver reclamation workers. Scand J Work Environ Health *15*:210–221.

OSHA [2013]. United States Code of Federal Regulations, 29CFR Part 1910.1000, Air Contaminants, final rule. Vol. 54. Washington, DC: Occupational Safety and Health Administration, p. 2702.

OSHA [2012]. Hazard Communication Standard (HCS). Occupational Safety and Health Administration. 29 CFR 1910.1200, http://www.osha.gov/publications/OSHA3514.htm.

Quadros ME, Marr LC [2010]. Environmental and human health risks of aerosolized silver nanoparticles. J Air Waste Mgmt *60*:770–781.

Rahman MF, Wang J, Patterson TA, Saini UT, Robinson BL, Newport GD, Murdock RC, Schlager JJ, Hussain SM, Ali SF [2009]. Expression of genes related to oxidative stress in the mouse brain after exposure to silver-25 nanoparticles. Toxicol Lett *187*:15–21.

Ramachandran G, Ostraat M, Evans DE, Methner MM, O'Shaughnessy P, D'Arcy J, Geraci CL, Stevenson E, Maynard A, Rickabaugh K [2011]. A strategy for assessing workplace exposures to nanomaterials. J Occup Environ Hyg *8*:673–685.

Rappaport SM, Lyles RH, Kupper LL [1995]. An exposure-assessment strategy accounting for within—and between—worker sources of variability. Ann Occup Hyg *39*(4):469–495.

Reidy B, Haase A, Luch A, Dawson KA, Lynch I [2013]. Mechanisms of silver nanoparticle release, transformation and toxicity: a critical review of current knowledge and recommendations for future studies and applications. Materials *6*:2295-2350.

Rengasamy S, Verbofsky R, King WP, Shaffer RE [2007]. Nanoparticle penetration through NIOSH-approved N95 filtering-facepiece respirators. J Int Soc Respir Protect *24*:49–59.

Rengasamy S, King WP, Eimer B, Shaffer RE [2008]. Filtration performance of NIOSH-approved N95 and P100 filtering-facepiece respirators against 4-30 nanometer size nanoparticles. J Occup Environ Hyg *5*(9):556–564.

Rengasamy S, Eimer BC, Shaffer RE [2009]. Comparison of nanoparticle filtration performance of NIOSH-approved and CE-marked particulate filtering facepiece respirators. Ann Occup Hyg *53*(2):117–128.

Rengasamy S, Eimer BC [2011]. Total inward leakage of nanoparticles through filtering facepiece respirators. Ann Occup Hyg *55*(3):253–263.

Roberts JR, Kenyon A, Young SH, Schwegler-Berry D, Hackley, VA, MacCuspie RI, Stefaniak AB, Kashon ML, Chen BT, Antonini JM [2012]. Pulmonary toxicity following repeated intratracheal instillation of dispersed silver nanoparticles in rats. The Toxicologist *126*(Suppl 1):141.

Roberts JR, McKinney W, Kan H, Krajnak K, Frazer DG, Thomas TA, Waugh S, Kenyon A, MacCuspie RI, Hackley VA, Castranova V [2013]. Pulmonary and cardiovascular responses of rats to inhalation of silver nanoparticles. J Toxicol Environ Health, Part A *76*:651–668.

Rongioletti F, Buffa RE [1992]. Blue nevi-like dotted occupational argyria. J Am Acad Dermatol *27:*1015–1016.

Rosenman KD, Moss A, Kon S [1979]. Argyria: clinical implication of exposure to silver nitrate and silver oxide. J Occup Med *21*:430–435.

Rosenman KD, Seixas N, Jacobs I [1987]. Potential nephrotoxic effects of exposure to silver. Br J Ind Med *44*:267–272.

Rouse JG, Yang J, Ryman-Rasmussen JP, Barron AR, Monteiro-Riviere NA [2007]. Effects of mechanical flexion on the penetration of fullerene amino acid-derivatized peptide nanoparticles through skin. Nano Lett *7*(1):155–160.

Ryman-Rasmussen JP, Riviere JE, Monteiro-Riviere NA [2006]. Penetration of intact skin by quantum dots with diverse physicochemical properties. Toxicol Sci *91*(1):159–165.

Saint S, Veenstra DL, Sullivan SD [2000]. The potential clinical and economic benefits of silver alloy urinary catheters in preventing urinary tract infection. Arch Intern Med *160:*2670–2675.

Samberg M, Oldenburg SJ, Monteiro-Riviere NA [2010]. Evaluation of silver nanoparticle toxicity in skin in vivo and keratinocytes in vitro. Environ Health Perspect *118*:407–413.

Samberg ME, Loboa EG, Oldenburg SJ, Monteiro-Riviere NA [2012]. Silver nanoparticles do not influence stem cell differentiation but cause minimal toxicity. Nanomedicine *7*(8):1197–1209.

Sato S, Sueki H, Nishijima A [1999]. Two unusual cases of argyria: the application of an improved tissue processing method for X-ray microanalysis of selenium and sulphur in silver-laden granules. Br J Dermatol *140:*158–163.

Sayes CM, Fortner J, Guo W, Lyon D, Boyd AM, Ausman KD, Tao YJ, Sitharaman B, Wilson LJ, Hughes JB, West JL, Colvin VL [2004]. The differential cytotoxicity of water soluble fullerenes. Nano Lett *4*(10):1881–1887.

Schaeblin NM, Estep CA, Roberts JR, Hussain SM [2011]. Silver nanowires induced inflammation in an in vitro human alveolar lung model. Society of Toxicology Annual Meeting, Washington, DC, March 6–10, 2011. Toxicol Sci: The Toxicologist *120*(Suppl 2):A2181, p. 468.

Schinwald A, Chernova T, Donaldson K [2012]. Use of silver nanowires to determine thresholds for fibre length-dependent pulmonary inflammation and inhibition of macrophage migration in vitro. Particle Fibre Toxicol *9*:47.

Schug TT, Nadadur SS, Johnson AF [2013]. Nano GO Consortium-a team science approach to assess engineered nanomaterials: reliable assays and methods. Environ Health Perspect 121:A176–A177, http://dx.doi.org/10.1289/eph.1306866.

Scott KG, Hamilton JG [1948]. The metabolism of silver. J Clin Invest *27*:555–556.

Scott KG, Hamilton JG [1950]. The metabolism of silver in the rat with radiosilver used as an indicator. Univ Calif (Berk) Publ Pharmacol *2*:241–262.

Scrogges MW, Lewis JS, Proia AD [1992]. Corneal argyrosis associated with silver soldering. Cornea *11*(3):264–269.

Sharma HS, Hussain S, Schlager J, Ali SF, Sharma A [2010]. Influence of nanoparticles on blood–brain barrier permeability and brain edema formation in rats. Acta Neurochir Suppl *106*:359–364.

Silver S [2003]. Bacterial silver resistance: molecular biology and uses and misuses of silver compounds. FEMS Microbiol Rev *27*:341–353.

Sleiman HK, Romano RM, de Oliveira CA, Romano MA [2013]. Effects of prepubertal exposure to silver nanoparticles on reproductive parameters in adult male Wistar rats. J Toxicol Environ Health Part A *76:*1023–1032.

Smijs TGM, Bouwstra JA [2010]. Focus on skin as a possible post of entry for solid nanoparticles and the toxicological impact. J Biomed Nanotechnol *6*(5):469–484.

Song KS, Sung JH, Ji JH, Lee JH, Lee JS, Ryu HR, Lee JK, Chung YH, Park HM, Shin BS, Chang HK, Kelman B, Yu lJ [2013]. Recovery from silver-nanoparticle-exposure-induced inflammation and lung function changes in Sprague Dawley rats. Nanotoxicology *7*(2):169–180.

Soto K, Garza KM, Murr LE [2007]. Cytotoxic effects of aggregated nanomaterials. Acta Biomaterialia *3*:351–358.

Sriram MI, Kanth SBM, Kalishwaralal K, Gurunathan S [2010]. Antitumor activity of silver nanoparticles in Dalton’s lymphoma ascites tumor model. Int J Nanomed *5*:753–762.

Stebounova LV, Adamcakova-Dodd A, Kim JS, Park H, O'Shaughnessy PT, Grassian VH, Thorne PS [2011]. Nanosilver induces minimal lung toxicity or inflammation in a subacute murine inhalation model. Particle Fibre Toxicol *8*:5.

Stoehr LC, Gonzalez E, Stampfl A, Casals E, Duschl A, Puntes V, Oostingh GJ [2011]. Particle Fibre Toxicol *8*:36, http://www.particleandfibretoxicology.com/content/8/1/36.

Stone KC, Mercer RR, Freeman BA, Chang LY, Crapo JD [1992]. Distribution of lung cell numbers and volumes between alveolar and nonalveolar tissue. Am Rev Respir Dis *146*(2):454–456

Sung JH, Ji HJ, Yoon JU, Kim DS, Song MY, Jeong J, Han BS, Han JH, Chung YH, Kim J, Kim TS, Chang HK, Lee EJ, Lee JH, Yu IJ [2008]. Lung function changes in Sprague-Dawley rats after prolonged inhalation exposure to silver nanoparticles. Inhalation Toxicol *20*:567–574.

Sung JH, Ji, JH, Park JD, Yoon, JU, Kim DS, Jeon KS, Song MY, Jeong J, Han BS, Han JE, Chung YH, Chang HK, Lee JH, Cho MH, Kelman BJ, Yu IJ [2009]. Subchronic inhalation toxicity of silver nanoparticles. Toxicol Sci *108*:452–461.

Sung JH, Ji JH, Song KS, Lee JH, Choi KH, Lee SH, Yu IJ [2011]. Acute inhalation toxicity of silver nanoparticles. Toxicol Ind Health *27*:149–154.

Takenaka S, Karg E, Roth C, Schulz H, Ziesenis A, Heinzmann U, Schramel P, Heyder J [2001]. Pulmonary and systemic distribution of inhaled ultrafine silver particles in rats. Environ Health Perspect *109*:547–551.

Tang J, Xiong L, Wang S, Wang J, Liu L, Li, J, Yuan F, Xi T [2009]. Distribution, translocation and accumulation of silver nanoparticles in rats. J Nanosci Nanotech *9*:4924–4932.

Tang J, Xiong L, Wang S, Wang J, Liu L, Li J, Wan Z, Xi T [2008]. Influence of silver nanoparticles on neurons and blood–brain barrier via subcutaneous injection in rats. Applied Surface Sci *255:*502–504.

Tang J, Xiong L, Zhou G, Wang S, Wang J, Liu L, Li J, Yuan F, Lu S, Wan Z, Chou L, Xi T [2010]. Silver nanoparticles crossing through and distribution in the blood–brain barrier in vitro. J Nanosci Nanotechnol *10*:6313–6317.

Tanita Y, Kato T, Hanada K, Tagami H [1985]. Blue macules of localized argyria caused by implanted acupuncture needles. Arch Dermatol *121:*1550–1552.

Tejamaya M, Romer I, Merrifield RC, Lead JR [2012]. Stability of citrate, PVP, and PEG coated silver nanoparticles in ecotoxicology media. Environ Sci Technol, dx.doi.org/10.1021/es2038596.

Trickler WJ, Lantz SM, Murdock RC, Schrand AM, Robinson BL, Newport GD, Schlager JJ, Oldenburg SJ, Paule MG, Slikker W Jr, Hussain SM, Ali SF [2010]. Silver nanoparticle induced blood–brain barrier inflammation and increased permeability in primary rat brain microvessel endothelial cells. Toxicol Sci *118*:160–170.

Triebig G, Valentin H [1982]. Berufskrankheit Argyrose? – Aktuelle Aspekte [Occupational disease argyrosis? - Current aspects]. In German. Verhandlungen der Deutschen Gesellschaft für Arbeitsmedizin *22*:239–243.

Trop M, Novak M, Rodl S, Hellbom B, Kroell W, Goessler W [2006]. Silver-coated dressing Acticoat caused raised liver enzymes and argyria-like symptoms in burn patient. J Trauma *60*:648–652.

Trout DB, Schulte PA [2009]. Medical surveillance, exposure registries, and epidemiologic research for workers exposed to nanomaterials. Toxicology *269*(2-3):128–135.

Tsai S, Huang RF, Ellenbecker MJ [2010]. Airborne nanoparticle exposures while using constant-flow, constant-velocity, and air-curtain isolated fume hoods. Ann Occup Hyg *54*(1):78–87.

Tiwari DK, Jin T, Behari J [2011]. Dose-dependent in-vivo toxicity assessment of silver nanoparticle in Wistar rats. Toxicol Mech Methods *21*(1):13–24.

U.S. DOE [2008]. Approach to nanomaterial ES & H. Washington, DC: U.S. Department of Energy, Nanoscale Science Research Centers, http://science.energy.gov/~/media/bes/pdf/doe_nsrc_approach_to_nanomaterial_esh.pdf.

U.S. EPA [1994]. Methods for derivation of inhalation reference concentrations and application of inhalation dosimetry. Washington, DC: U.S. Environmental Protection Agency, Office of Research and Development. EPA/600/8-90/066F, http://nepis.epa.gov/EPA/html/Pubs/pubtitleORD.html.

U.S. EPA [2002]. A review of the reference dose and reference concentration processes. Washington, DC: U.S. Environmental Protection Agency, Risk Assessment Forum. EPA/630/P-02/002F.

U.S. EPA [2004]. Risk assessment guidance for superfund, Vol. I: Human Health Evaluation Manual, http://www.epa.gov/oswer/riskassessment/ragse/index.htm. U.S. EPA/540/R/99/005.

U.S. EPA [2012]. Nanosilver: summary of human health data for registration review. Washington, DC: Office of Chemical Safety and Pollution Prevention. PC Code: 072599, Case No. 5042.

U.S. EPA [2012a]. Science review of the AEATF II Liquid Pour Human Exposure Monitoring Study, October 9, http://www.epa.gov/hsrb/riles /meeting-materials/nov-1-2012-public-meeting/AEATF-Liquid-Pour-Study.pdf.

U.S. EPA [2013]. Draft decision document: proposed conditional registration of nanosilver as a materials preservative in textiles and plastics. August 27. Washington, DC: Environmental Protection Agency, Office of Pesticide Programs, Antimicrobials Division.

USGS [2014]. U.S. Geological Survey, Mineral Commodity Summaries, January 2013, http://minerals.usgs.gov/minerals/pubs/commodity/silver/index.html.

Van der Zande M, Vandebriel RJ, Van Doren E, Kramer E, Rivera ZH, Serrano-Rojero CS, Gremmer ER, Mast J, Peters RJB, Hollman PCH, Hendriksen PJM, Marvin HJP, Peijnenburh ACM, Bouwmeester H [2012]. Distribution, elimination, and toxicity of silver nanoparticles and silver ions in rats after 28-day oral exposure. ACS Nano *6*(8):7427–7442.

Vlachou E, Chipp E, Shale E, Wilson YT, Papini R, Moiemen NS [2007]. The safety of nanocrystalline silver dressings on burns: a study of systemic silver absorption. Burns *33*:979–985.

Wagner GR, Fine LJ [2008]. Surveillance and health screening in occupational health. In: Wallace RB, ed. Maxcy-Rosenau-Last Public Health and Preventive Medicine. 15th ed. New York: McGraw-Hill Medical Publishing, pp. 759–793.

Wadhera A, Fung M [2005]. Systemic argyria associated with ingestion of colloidal silver. Dermatol Online J *11*(1):12.

Wahlberg JE [1965]. Percutaneous toxicity of metal compounds. Arch Environ Health *11*:201–204.

Wan AT, Conyers RAJ, Coombs CJ, Masterton JP [1991]. Determination of silver in blood, urine and tissue of volunteers and burn patients. Clin Chem *37*:1683–1687.

Wang XQ, Chang HE, Francis R, et al. [2005]. Silver deposits in cutaneous burn scar tissue is a common phenomenon following application of a silver dressing. J Cutan Pathol *36*(7):788–792.

Wei L, Tang J, Zhang Z, Chen Y, Zhou G, Xi T [2010]. Investigation of the cytotoxicity mechanism of silver nanoparticles in vitro. Biomed Mater *5*(4):044103.

Wheeler MW, Bailer AJ [2007]. Properties of model-averaged BMDLs: a study of model averaging in dichotomous response risk estimation. Risk Anal *27*(3):659–670.

WHO [2005]. Chemical-specific adjustment factors for interspecies differences and human variability: guidance document for use of data in dose/concentration-response assessment. Geneva, Switzerland: World Health Organization.

WHO (World Health Organization) [2010]. Draft Environmental Health Criteria (EHC): Dermal Exposure, http://www.who.int/ipcs/methods/dermal.exposure.pdf.

Wijnhoven S, Peijnenburg W, Herberts C, Hagens WI, Oomen A, Heugens EHW, Roszek B, Bisschops J, Gosens I, Van De Meent D, Dekkers S, De Jong WH, Van Zijverden, Sips AJAM, Geertsma RE [2009]. Nano-silver: a review of available data and knowledge gaps in human and environmental risk assessment. Nanotoxicology *3*(2):109–138.

Williams N, Gardner I [1995]. Absence of symptoms in silver refiners with raised blood silver levels. Occup Med *45*(4):205–208.

Williams N [1999]. Longitudinal medical surveillance showing lack of progression of argyrosis in a silver refiner. Occup Med *49*(6):397–399.

Wolbling RH, Milbradt R, Schopenhauer-Germann E, Euler G, Konig KH [1988]. Argyria in employees in the silver processing industry: dermatological investigations and

quantitative measurements using atomic absorption spectrometry. Arbeitsmed Sozialmed Praventivmed *23*:293–297.

Xue Y, Zhang S, Huang Y, Zhang T, Liu X, Hu Y, Zhang Z, Tang M [2012]. Acute toxic effects and gender-related biokinetics of silver nanoparticles following an intravenous injection in mice. J Appl Toxicol *32*:890–899.

Zook JM, Long SE, Cleveland D, Geronimo CL, MacCuspie RI [2011]. Measuring silver nanoparticle dissolution in complex biological and environmental matrices using UV-visible absorbance. Anal Bioanal Chem *401*:1993–2002.

APPENDIX A

Risk Assessment Methods for REL Evaluation

A detailed overview of the toxicological literature is provided in Appendix F, and the evidence available for risk assessment and REL development of silver nanoparticles is evaluated in Section 6.3. The current OELs for silver (dust and fumes, soluble and insoluble) are measured as total mass concentration, which includes all airborne particle sizes, including nanoparticles. The basis for these existing OELs, as well as for the proposed OELs for silver nanoparticles, is discussed in Section 6.4.

This Appendix describes the process used for assessing the risk of occupational exposure to silver nanoparticles and evaluating the applicability of the current NIOSH REL for silver particles. This evaluation was based on results from the subchronic inhalation studies in rats, using the following methods: (1) a simple adjustment of the airborne exposure concentrations identified as the no observed adverse effect level (NOAEL) or the lowest observed adverse effect level (LOAEL) in the rat studies [Sung et al. 2008, 2009; Song et al. 2013]; and (2) a dosimetric adjustment of the rat effect levels based on the measured silver doses in the rat lung or liver tissues using a physiologically-based pharmacokinetic (PBPK) model for silver nanoparticle disposition in humans and rats [Bachler et al. 2013]. Appendix B provides benchmark dose (BMD) estimates, which are risk-based estimates of the effect levels derived from modeling the dose-response data. The BMD estimates were used as target tissue doses in the PBPK modeling. Tables and figures are at the end of Appendix A.

A.1 Method I: Simple Adjustment of Rat NOAEL and Default Uncertainty Factors

A simple default method for estimating an OEL is to apply standard uncertainty factors (e.g., Table A-2) to the animal effect level or point of departure (POD) (such as a NOAEL or BMDL):

$$OEL = POD / UFs$$

For inhalation exposures, a prior step is to adjust the animal POD for the difference in exposure time compared to a reference work day (8-hr TWA). For example,

$$PODhum = PODrat \times 6\ hr/8\ hr$$

$$OEL = PODhum / UFs$$

When the airborne particle size data are available, the 'PODhum' may be estimated as the equivalent total deposited dose in the respiratory tract or a specific region (such as pulmonary) by using respiratory tract deposition models (discussed in next section). This approach does not account for dissolution or clearance of silver nanoparticles, although it does account for interspecies and particle size–related differences in the initial internal dose of silver to the respiratory tract and other organs. A physiologically based pharmacokinetic (PBPK) model that accounts for both clearance and dissolution of silver can provide a more biologically relevant estimate of dose. A PBPK model for silver based on rat data has been developed and extrapolated to humans [Bachler et al. 2013].

Table A-1 lists the points of departure from the subchronic inhalation studies [Sung et al. 2008, 2009; Song et al. 2013] and the health endpoints observed in male or female rats. Table A-2 lists standard uncertainty factors typically applied to PODs to derive OELs. Uncertainty factors depending on both science and policy considerations (e.g.,

as shown in Table 6-3). Derivation of the proposed OELs in Table 6-3 started with the same rat study data but used different rat PODs and different uncertainty factors to extrapolate the rat data to humans.

In the subchronic inhalation studies in rats (Table A-1), 49 µg/m^3 was a LOAEL in female rats since lung function deficits were observed in this lowest exposure group [Sung et al. 2008]. However, the severity of those effects at the LOAEL was not entirely clear [Christensen et al. 2010]; and there was a high degree of variability in the female rat lung function response between the two studies from the same laboratory (i.e., 49 µg/m^3 was a LOAEL in Sung et al. [2008]; and 381 µg/m^3 was a NOAEL in Song et al. [2013]) (Table A-1). A NOAEL of 133 µg/m^3 was observed for bile duct hyperplasia in both male and female rats in the study of Sung et al. [2009]. NOAELs were observed at 49 µg/m^3 for lung inflammation and lung function deficits in male rats [Song et al. 2013]. However, the authors interpreted the alveolar inflammation at the LOAEL of 117 µg/m^3 in male rats to be minimal and proposed that 117 µg/m^3 was the NOAEL in males, as in females (see specific results in Table A-1). The authors then rounded down to 100 µg/m^3 as the NOAEL for lung and liver effects [Song et al. 2013].

On the basis of these studies, the following NOAELs were selected as PODs in this assessment:

- 49 (or 117) µg/m^3 for no observed lung inflammation and lung function deficits
- 133 µg/m^3 for no observed liver bile duct hyperplasia.

Standard uncertainty factor examples are shown in Table A-2, which could be applied to the PODs. The UFs are values of 1–10 for each of four main areas of variability and uncertainty: (1) use of a LOAEL instead of a NOAEL as the POD; (2) animal to human extrapolation of the dose and response; (3) human inter-individual variability in dose and response; and (4) use of subchronic data to estimate chronic response. UF2 (interspecies) and UF3 (intraspecies) contain toxicokinetic and toxicodynamic sub-factors that equal a value of 10 when multiplied together (Table A-2). Other UFs have been proposed for specific cases. For example, Oberdörster [1989] proposed a value of 1 for UF2 (interspecies) for respirable poorly-soluble particles (PSPs), based on using

dose-response data in the rat, which has been shown to be the most sensitive rodent species for lung effects from PSPs compared to the mouse or hamster (also shown in Bermudez et al. [2002, 2004]; and Elder et al. [2005]). As such, Oberdörster [1989] assumed an equal response to equivalent lung doses of PSPs in animals and humans. NIOSH selected the following uncertainty factors (from Table A-2) as being the most applicable to the silver nanoparticle data to apply to the PODs in Table A-1:

(1) NOAEL to LOAEL: 1 (for NOAEL or $BMDL_{10}$ used as POD), or
3 (for LOAEL used as POD)

(2) Animal to human extrapolation: 4 (toxicokinetics and toxicodynamics combined)
Toxicokinetics: 4 (using exposure concentrations)
Toxicodynamics: 1 (assuming equal average response at equivalent dose in workers)

(3) Human inter-individual variability in workers: 5 (toxicokinetics and toxicodynamics combined)

(4) Subchronic to chronic (that is, uncertainty that the POD could be lower with chronic exposure): 3

The total uncertainty factors (UF1–4) as described for these data would be

$1 \times 4 \times 5 \times 3 = 60$ (NOAEL or BMDL); or

$3 \times 4 \times 5 \times 3 = 180$ (LOAEL).

In this approach,

$OEL = POD/UFs$.

Thus, the PODs in Table A-1 were first adjusted for the difference in the daily exposure duration (6 hr/8 hr), and then divided by the total uncertainty factor to derive the OEL

(Table A-3). These OEL estimates (ranging from 0.2 to 1.6 µg/m^3, 8-hr TWA concentration) could be interpreted as no-effect levels in workers. These estimates are based on a simple UF factor approach using the rat subchronic inhalation data of AgNPs. It should be noted that the lung and liver effects observed in the rat studies were of minimal severity (if any) at the doses extrapolated to workers. The clinical significance to workers of the rat lung and liver effects of minimal severity is uncertain. No adverse lung or liver effects have been reported in workers exposed to silver dust or fumes in the few studies that have been performed (Section 3); however, the number of workers examined was low (e.g., few dozen) and none of these studies was specific to silver nanoparticle exposures. In addition, some of the rat doses and responses were highly variable (e.g., lung dose and lung function in female rats) in Sung et al. [2008] and Song et al. [2013] (Tables A-1 and A-12), and the number of rats studied was small (especially in Song et al. [2013] with n=5 per group), resulting in uncertainty in the effect level estimates in those studies. OELs based on these NOAELs or LOAELs could be considered highly health protective. However, an area of uncertainty is the severity and persistence of these biologic effects if exposure to AgNPs is long-term (i.e., up to a 45-year working lifetime). The OEL estimates in Table A-3 depend on the total UF assumed. As discussed in Section 6.1, the margin of safety factor that was used in the derivation of the current NIOSH REL and OSHA PEL for silver based on argyria in humans was ~2 after adjusting for a 45-year working lifetime.

A.2 Method II: Silver Nanoparticle Internal Dose and PBPK Modeling

A.2.1 Background

In risk assessment using rodent bioassay data, estimates are needed of the human-equivalent exposure concentration to the animal effect level (e.g., the NOAEL or $BMDL_{10}$). A simple (default) risk assessment approach, when data are limited, uses standard uncertainty factors to estimate the human-equivalent NOAEL or LOAEL (Section A.1 and Table A-2). When estimating the risk of adverse health effects over a working lifetime (e.g., up to 45 years), the dose rate is an additional source of uncertainty, especially when these estimates are based on short-term exposures in animal studies (e.g., 13 wks). Factors that can influence the retained tissue dose over time include the clearance and retention processes for inhaled particles and the physical-chemical properties of the particles (e.g., size, shape, solubility) or changes to the particles (e.g., dissolution or chemical transformation such as to silver-sulfur nanocrystals) after deposition or uptake in the body [Bachler et la. 2013]. These processes can influence the internal dose of the soluble, more biologically active form of the particles.

Silver is processed in the body through various mechanisms including sulfidation (binding with sulfur) or opsonization (binding with protein), which results in stabilization of the silver, although it is not known if these processes occur within or outside cells (e.g., macrophages). In human skin and eyes, precipitated granules (micrometer scale) can occur regardless of the form of silver taken/administered including metallic, ionic, or colloidal silver/nanosilver (Scroggs et al. 1992; Wang et al. 2009; Wadhera and Fung 2005, Chang et al. 2006; respectively). In a 28-d oral administration study of silver nanoparticles or silver acetate in rats, Loeschner et al. 2011 measured sulfur and selenium in the precipitated granules of silver in cells (e.g., macrophages). In an *in vitro* study, silver reacted with sulfur, forming "bridges" between the nanoparticles – resulting in decreased dissolution rate and decreased toxicity [Levard et al. 2011, 2012].

Silver nanoparticles have been shown to undergo dissolution in the lungs, translocation to blood, liver, skin and other organs. Human exposures to silver resulting in argyria (bluish coloration of skin) have been reported [Hill and Pillsbury 1939; ATSDR 1990; Drake and Hazelwood 2005; Wijnhoven et al. 2009; Johnston et al. 2010; Lansdown 2012]. To better estimate the airborne exposures and tissue doses associated with argyria in humans, physiologically-based pharmacokinetic (PBPK) modeling is needed to estimate the relationship between external (airborne) exposure and internal tissue dose of Ag nanoparticles after inhalation.

The Bachler et al. [2013] PBPK model was developed based on rat data and extrapolated to humans. It consists of two sub-models, one for ionic silver and one for silver nanoparticles. Both sub-models were validated with independent data from the literature. Figure 1 of Bachler et al. [2013] shows the structures and inter-dependencies between these sub-models. The PBPK models in Bachler 2013 were designed as membrane-limited models (vs. flow limited), as also used by Li et al. [2012]. In this model, both silver ions and nanoparticles can translocate from the lungs to the blood (Figures 2A and 2B in Bachler et al. 2013). In the blood, both ionic and nanoparticle silver are predicted to translocate to other organs including the liver, kidney, and spleen (Figure 7A and B in Bachler et al. [2013]). Soluble silver is considered to be the active form, from which silver ions are released at a rate that depends on various factors including the particle form and size and the tissue compartment. Some evidence indicates that silver ions readily react with sulfhydryl groups to form silver-sulfur complexes. Glutathione (GSH) is the most common mercaptan (source of sulfhydryl groups) in many cells and therefore, plays a major role in the biodistribution of ionic silver [Bell and Kramer 1999; Hansen et al. 2009]. Since liver has by far the highest levels of GSH of any organs, most ionic silver is taken up by the liver. Bachler et al. [2013] defined organ silver uptake as being proportional to the relative organ GSH concentration, thus allowing for a reduction in the number of model parameters.

In the general population, less than 0.5 g of silver is estimated to be stored in the human body within a lifetime, although 100 g or more of silver was been reported to be stored in extreme cases [ICRP 1960; East et al. 1980; Wadhera and Fung 2005]. Based

on this information, Bachler et al. [2013] modeled the storage compartments for each organ (except blood) as sinks from which no silver is released and which have infinite capacity. The total storage of ionic silver in the rat's body was set to 0.5%, based on experimental results after intravenous injection of an ionic silver solution [Furchner et al. 1968].

In the Bachler et al. [2013] PBPK model, two possible scenarios were considered for the metabolism of AgNPs (as shown in Figure 3 of that paper): (1) AgNPs dissolve and release soluble silver species, which are described in the ionic silver PBPK model; and (2) AgNPs are directly transformed to silver sulfide particles. Scenario 2 was found to result in the best model fit to the data. Bachler et al. [2013] attribute their model finding of no significant dissolution of AgNPs to silver ions to the stabilization of the nanoparticles by proteins adsorbed to the particle surface; and/or to the transformation of silver to silver-sulfur nanocrystals (either of which would reduce the dissolution rate). Scenario 2 was considered to be supported by the evidence that silver readily reacts with mercaptans, that silver sulfide is detected in tissue samples after exposure to ionic silver, and that the silver tissue burdens predicted by that model scenario agrees well with the tissue burden data from Kim et al. [2008] after oral exposure to AgNPs in rats [Bachler et al. 2013, including supplementary material]. Thus, a direct storage mechanism of silver to silver sulfide particles (i.e., bypassing ion formation) was used in the main model calculations [Bachler et al. 2013].

The rat silver nanoparticle and ionic models in Bachler et al. [2013] were calibrated with data from Lankveld et al. [2010] and Klaassen [1979], respectively, with some of the individual rate parameters from other studies, as noted in Bachler et al. [2013]. Lankveld et al. [2010] and Klaassen [1979] administered silver intravenously to rats and measured the silver excretion or tissue doses for up to 16 or 7 days post-exposure, respectively. Silver particles of 20, 80, or 110 nm diameter were used in Lankveld et al. [2010], and an ionic silver solution was administered in Klaassen [1979]. Bachler et al. [2013] reported that in the calibration and validation of their model, they utilized experimental data of only easily soluble silver species (silver nitrate and silver acetate) or ionic silver solutions. [Note: the form and solubility of the silver in Lankveld et al.

[2010] was not verified as it was not found to be reported in the paper]. Data from four additional studies in rats were compared to the rat model predictions in Bachler et al [2013] (Figures 4 and 5 in that paper), including two inhalation studies of AgNPs in rats [Takenaka et al. 2001; Ji et al. 2007]. Bachler et al. [2013] then extrapolated the rat model to humans by adjusting for species-specific differences in the respective physiological factors and body or organ weights [ICRP 2002]. This rat-extrapolated human PBPK model showed good correlation with the limited human biomonitoring data [DiVincenzo et al. 1985] (Figure 6C in Bachler et al. [2013]). Human model parameter values were based on those for the reference worker (adult male) [ICRP 2002]; possible kinetic differences by gender or age were not considered. The human model-predicted [Bachler et al. 2013] and measured values of silver in blood and feces (reported in a worker biomonitoring study) [Di Vincenzo et al 1985] were shown to be in good agreement [Bachler 2013, Figure 6C].

In addition to the Ag tissue estimates from PBPK modeling in rats based on short-term exposures, silver tissue doses have been measured in rats following subchronic (13 or 12 wk) inhalation of AgNPs (~19 or 15 nm diameter, respectively) [Sung et al. 2009; Song et al. 2013]. As described in this section, the rat tissue burden data were used to estimate the human-equivalent tissue doses and working lifetime exposures associated with the adverse effects observed in the rat subchronic inhalation studies. These adverse effects included pulmonary inflammation and bile duct hyperplasia (see Section 5.1). Thus, the lung and liver tissue dose data in rats were used to estimate the human-equivalent lung and liver doses of silver, assuming occupational airborne exposure to silver nanoparticles for up to a 45-year working lifetime.

The objectives of this evaluation are to (1) examine the relationship between the exposure concentrations and the lung and liver tissue doses in rats after subchronic inhalation exposure; (2) estimate the rat effect levels based on lung and liver tissue doses, including the NOAELs, LOAELs, and benchmark dose (BMD) estimates; and (3) estimate the human-equivalent working lifetime exposure concentrations (up to 45 years) associated with the rat adverse effect levels, based on either the active/soluble (i.e., able to release ions and/or form complexes such as silver sulfide) or the total silver

concentrations (i.e., both the active/soluble and the complexed silver) in tissues. The PBPK model of Bachler et al. [2013] was used to estimate the occupational exposures (as 8-hr time-weighted average, TWA, concentrations) of AgNPs for up to a 45-year working lifetime associated with the estimated equivalent tissue doses to those in rats with no or minimal adverse effects in the lungs or liver.

Before estimating the human-equivalent concentrations to the rat subchronic effect levels, analyses were performed to compare the airborne exposure and tissue dose concentrations of silver in the two rat subchronic inhalation studies. Analyses were also performed to compare the Bachler et al. [2013] model predictions of the measured tissue doses of silver in both rat studies [Sung et al. 2009; Song et al. 2013].

A.2.2 Silver Tissue Doses in Rats

The relationships between the airborne cumulative exposure concentration of AgNPs (19 or 15 nm diameter) and the measured silver burden in lung or liver tissues in rats (male and female) following subchronic inhalation (13 or 12 weeks) [Sung et al. 2009; Song et al. 2013] was examined (Sections A.2.2.1 and A.2.2.2). The cumulative exposure metric was used to adjust for the exposure duration difference in these two studies (13 vs. 12 weeks in Sung et al. [2009] and Song et al. [2013], respectively). In both lung and liver, the variability in the silver tissues burdens increased with increasing exposure concentration.

The finding of non-constant (heterogeneous) variance in the tissue burdens given exposure may be due to the inter-individual rat differences in the clearance and retention of silver nanoparticles (toxicokinetics). Despite the increased variability in the silver tissue doses at the highest dose, the two lower doses – which are associated with no or minimal adverse effects – are most relevant to human health risk assessment.

A.2.2.1 Lungs

The rat lung tissue burdens of silver also varied by study [Sung et al. 2009; Song et al. 2013] and by gender (Figure A-1). The measured burdens are higher in Sung et al. [2009] at all doses for both male and female rats, and a disproportionally higher Ag lung

tissue dose is seen in rats at the highest exposure concentration (515 µg/m^3) [Sung et al. 2009]. The higher burdens observed at all airborne exposure concentrations in Sung et al. [2009] could be due to higher deposition efficiencies of inhaled AgNPs in the lungs of rats in that study, although this is considered unlikely since rats in both studies were exposed to similar sized particles (~19 nm diameter vs. ~15 nm median diameter in Sung et al. [2009] and Song et al. [2013], respectively). Particles of similar diameter would be expected to have similar deposition efficiencies. Other, unexplained differences in the animals and/or experimental conditions may have resulted in these between-study differences. The relatively low number of animals also needs to be taken into account when comparing tissue burdens across groups (i.e., n=3-5 rats per lung or liver tissue group in male or female rats in Sung et al. [2009]; n=9 male rats and n=4 female rats per lung or liver tissue group in Song et al. [2013]).

The steeper increase in the lung tissue burdens at the higher exposure concentration in the Sung et al. [2009] (Figure A-1) is consistent with the possibility that impairment of lung clearance resulted in a disproportionate increase in the lung retention of silver particles at the highest exposure concentration (515 µg/m^3). In general, the within-study lung tissue burdens (among males or females) were less variable than the between-study (Sung et al. [2009] or Song et al. [2013]) Ag lung tissue burdens, at the same (or similar interpolated) airborne exposure concentrations.

A.2.2.2 Liver

The rat silver tissue burdens in the liver are generally more consistent across study and gender (Figure A-2) than those in the lungs (Figure A-1). At the two lower concentrations, the rat liver tissue burdens are relatively similar between the two studies [Sung et al. 2009; Song et al. 2013] and between males and females within each study. As was also observed in the lungs, the liver silver burdens seem to increase disproportionately at the highest concentration (515 µg/m^3 [Song et al. 2013]), suggesting increased tissue retention of silver at that concentration, especially in female rats. Male and female rat liver tissue doses of silver are similar in the Sung et al. [2009] study at the lower exposure concentrations, and varied by a factor of approximately

three between the studies [Sung et al. 2009; Song et al. 2013] at the lowest exposure concentration (49 μg/m^3) (Figure A-2).

A.2.3 Effect Level Estimates in Rats and Humans

The rat subchronic inhalation studies [Sung et al. 2008, 2009; Song et al. 2013] reported NOAELs or LOAELs for minimal adverse lung or liver effects. The lung response of chronic pulmonary inflammation (minimal) and the liver response of bile duct hyperplasia (minimal) were selected as potentially adverse responses of relevance to humans. The silver tissue doses associated with either no significant increase (NOAEL) or a low (10%) increase ($BDML_{10}$) in these responses were selected as the target doses for risk assessment based on PBPK modeling [Bachler et al. 2013]; this model was used to estimate the working lifetime exposure concentrations that would result in the equivalent lung or liver tissue concentrations. In addition, for endpoints with sufficient data (at least one intermediate dose group with a response between that of the controls and the highest response), $BMDL_{10}$'s were estimated using dose-response modeling (as discussed in Appendix B).

Table A-4 shows estimated doses of silver in lung and liver tissues in rats after subchronic inhalation (12 or 13 wk), at the NOAEL and $BMDL_{10}$ estimates. Dose-response data were not sufficient for modeling the chronic alveolar inflammation response in male or female rats in Sung et al. [2009] or in female rats in Song et al. [2013]. In those cases, the NOAELs only are provided in Table A-4. Dose-response data for chronic alveolar inflammation in male rats in Song et al. [2013] were minimally acceptable for $BMDL_{10}$ estimation (Appendix B). The highlighted doses are selected as representative target tissue doses of silver associated with either no or low estimated risk of adverse effects in the lungs or liver. These doses were selected as being the lowest estimates for a given study, response endpoint, or gender, and were used as target doses in the PBPK modeling.

As shown in Table A-4, the NOAEL lung tissue doses of silver vary substantially between the two studies [Song et al. 2013; Sung et al. 2009] (up to an order of magnitude or more); although the exposure concentrations and durations were similar.

This suggests that rats in the Sung et al. [2009] study retained considerably more silver in their lungs during the 13 week exposure than did the rats in the Song et al. [2013] study (to a greater extent than the one additional week would suggest) but did not develop adverse lung effects at those doses. The generation method and particle size of the silver was similar between the two studies, which were performed in the same laboratory. The reason for the large difference in silver lung tissue burdens in the two studies is not known, and it contributes to uncertainty in the lung tissue dose level for use in risk assessment. Gender differences in the mean lung tissue silver dose are also observed, although these gender differences are smaller than the between-study differences in silver lung tissue dose. It is also possible that there may have been an unknown difference in solubility of the AgNP used in the two studies [Sung et al. 2009, diameter ~19 nm; Song et al. 2013, diameter ~15 nm], which could have resulted in different rates of clearance of AgNP from the lungs, or that the analytical method used for quantifying silver in tissues gave varying results.

Unlike the results for the lungs, the liver tissue doses of silver at the NOAEL were quite similar in male and female rats in Sung et al. [2009] (Table A-4) and in rats at the lower doses in Song et al. [2013] study (which did not report any findings on bile duct hyperplasia) (see Figure A-4).

A.2.4 PBPK Model Estimates

A.2.4.1 Overview of PBPK Modeling Runs

A recently developed PBPK model for silver uptake and disposition in the body [Bacher et al. 2013] was used to estimate the internal tissue doses of silver in workers after up to 45 years of inhalation exposure to AgNPs [Bachler 2015, report to NIOSH]. Model simulations were performed to estimate the following:

- Occupational exposure concentration (8-hr TWA, time-weighted average) concentration of AgNP over a 45-year working lifetime (8 hr/d, 5 d/wk) associated with the retention of Ag in the skin at the target dose of 3.2 µg Ag/g skin, which is reported to be the lowest dose associated with argyria in humans [Bachler et al.

2013]; estimates are provided for AgNPs of different diameters and for ionic silver. The purpose of these estimates is to evaluate whether working lifetime exposures to AgNPs at the current NIOSH REL for silver (10 µg/m^3, 8-hr TWA concentration) would be likely to result in argyria.

- Tissue dose levels of silver in humans assuming inhalation exposure to AgNPs (either 15 or 100 nm diameter) or ionic silver over a 45-year working lifetime at 10 µg/m^3 (8-hr TWA) concentration. The purpose of these estimates is to evaluate whether working lifetime exposures to AgNPs would result in lung and liver tissue concentrations of silver above the rat adverse effect levels.

- Occupational exposure concentration (8-hr TWA) of AgNPs over a 45-year working lifetime that would result in the human-equivalent lung or liver tissue dose to that in the rat associated with adverse (early-stage) effects; estimates for either 15 or 100 nm diameter AgNPs. No tissue dose data are available in humans exposed to AgNPs; thus, the rat subchronic inhalation data of AgNPs (median diameter ~15-20 nm) are extrapolated to humans to estimate the target tissue doses associated with early-stage adverse lung or liver effects in rats.

All human model simulations are for adult male, assuming light exercise (typically 1.2 m^3/d for 8-hr), and nasal breathing pattern, using the parameter values reported in Bachler et al. [2013]. Prior to these human model simulations, rat model simulations were performed of compare estimates from the rat model calibrated using other rat data on AgNP kinetics by inhalation and other routes of exposure [Bachler et al. 2013] (see Section 3.2). The parameters used in the rat model and the human model are reported in Tables A-5 and A-6, respectively.

Additional model runs (results not shown) included: evaluations of rat models with increased lung clearance rate; human model estimates for mixed particle sizes of 1-100 nm, assuming uniform particle size distribution (these estimates are shown for argyria estimates only); and human model estimates for other rat-based target tissue doses, including the rat NOAEL estimates of 100 or 117 µg/m^3 and human-equivalent tissue

dose estimates of 47 or 23 µg/m^3 (adult male, light exercise, nose breathing) estimated in Sung et al. [2013] [Bachler 2015, report to NIOSH].

A.2.4.2 Comparison of model-predicted and measured lung and liver tissue burdens in rats

The Bachler et al. [2013] PBPK model was calibrated and validated based on data of silver nanoparticles in rat studies, including inhalation exposure studies by Ji et al. [2007] (same laboratory as the Sung et al. [2008, 2009] and Song et al. [2013] studies) and by Takenaka et al. [2001]. These studies reported tissue burden/kinetics data only, not biological response. Other rat studies [Sung et al. 2008, 2009; Song et al. 2013] reported both tissue burden and response data, which are used in this risk assessment. As discussed in this section, the lung and liver tissue burdens reported in those four rat studies [Takenaka et al. 2001; Ji et al. 2007; Sung et al. 2009; Song et al. 2013] are compared to each other, and the model-predicted tissue burdens are compared to the data in Sung et al. [2009] and Song et al. [2013], which had not been used in the calibration or validation of the Bachler et al. [2013] model.

Ji et al. [2007] was a 28-day inhalation exposure study in rats (male and female, 6-wk of age, specific-pathogen-free (SPF) Sprague-Dawley) exposed to 0, 0.5, 3.5, or 61 µg/m^3 AgNPs (6 h/day, 5 days/wk, 4 wk). Takenaka et al. [2001] was a 1-day inhalation exposure study in rats (female Fischer 344 rats; body weight 150–200 g) exposed for 6 hr at 133 µg/m^3 of silver nanoparticles (15 nm modal diameter) and were sacrificed on days 0, 1, 4, and 7. The silver lung burden immediately after exposure was 1.7 µg Ag, which decreased rapidly to 4% of the initial lung burden by day 7.

Lungs: Figure A-3 show the end-of-exposure silver lung tissue burdens in these four rat studies by cumulative exposure (µg/m^3 x hours) (normalized) to account for the differences in exposure concentration and duration. These plots do not account for differences in the clearance of silver from the lungs during the exposure time (ranging from 1 day (6-hr) in Takenaka et al. [2001]; 28 days in Ji et al. [2007]; 12 wk in Song et al. [2013]; or 13 wk in Sung et al. [2009]. The results show much higher lung silver burdens in Takenaka et al. [2001] and Ji et al. [2007], which is likely due to the minimal

lung clearance of the AgNPs during the 1 day exposure [Takenaka et al. 2001] and the lower clearance of silver during 4 wk [Ji et al. 2007] compared to 12 or 13 wk [Sung et al. 2009; Song et al. 2013], even at equivalent cumulative exposures.

Liver: Figure A-4 shows the end-of-exposure silver liver tissue burdens in these four rat studies, also plotted by cumulative exposure (μg/m^3 x hours) (normalized) to account for the differences in exposure concentration and duration. Again, these plots do not account for differences in the amount of silver cleared from the liver during the exposure time (as mentioned above for the lungs). These results show similar liver silver burdens in the 4, 12, and 13 wk exposure studies (Ji et al. [2007]; Song et al. [2013]; Sung et al. [2009], respectively), suggesting similar build-up rates of silver in liver over time. The highest liver silver burden is observed in the Takenaka et al. [2001] study relative to similar cumulative exposure concentration in the other studies, which may reflect the rapid initial translocation to the liver in this acute exposure. These findings illustrate the importance of accounting for the clearance pathways in the estimation of tissue doses over time. Cumulative exposure may be a good surrogate for the total deposited lung dose, but a PBPK model is needed to account for particle dissolution and clearance from the lungs and translocation to other organs.

The PBPK model-predicted tissues burdens of silver based on the Bachler et al. [2013] rat model were higher than the measured rat burdens of silver in lung and liver tissues at the end of the subchronic (12 or 13 wk) inhalation exposure [Sung et al. 2009; Song et al. 2013] (Figures A-5 and A-6). For example, at the middle exposure concentration (133 μg/m^3 in Sung et al. [2009] or 117 μg/m^3 in Song et al. [2013]), the model-predicted rat lung burdens were higher by a factor of approximately 3 compared to the measured lung burdens in Sung et al. [2009] and by a factor of approximately 4-7 compared to the lung burdens in Song et al. [2013], among male and female rats. The model-predicted rat liver burden of silver was approximately 1.5 to 3 fold higher than the measured rat liver burdens in male and female rats in both studies [Sung et al. 2009; Song et al. 2013]. The number of rats per tissue burden group were: n = 3-5 male rats and n=5 female rats in Sung et al. [2009]; and n=9 male rats and n=4 female rats in Song et al. [2013]. The sample sizes for the Monte Carlo simulations in the PBPK model estimates

was assumed to be equal to that of the same observed groups [Note: Bachler et al. 2013 used 1,000 model iterations in the Monte Carlo simulations. Background levels of silver were not considered (although these would typically be low compared to the levels of silver from the inhalation exposure)].

The reason for the over-prediction of the lung and liver tissue burdens to the measured tissues burdens in the rat subchronic inhalation studies may be due to several factors. First, between-study variability and small number of animals could contribute to the apparent differences. Second, the PBPK model was calibrated and validated against rat data of shorter duration of exposure (1 or 28 day inhalation) at exposure concentrations of 133 $\mu g/m^3$ (1 d) or 0, 0.5, 3.5, or 61 $\mu g/m^3$ (28 days) in Takenaka et al. [2001] or Ji et al. [2007], respectively. By comparison, rats were exposed to generally higher concentrations (0, 49, 117 or 133, and 381 or 515 $\mu g/m^3$) over longer durations (12 or 13 wk), respectively, in Song et al. [2013] or Sung et al. [2009]. The higher tissue burdens in the shorter-term inhalation studies [Takenaka et al. 2001; Ji et al. 2007] used in the PBPK modeling, extrapolated to longer-term exposures, may have contributed to the over-estimation of the tissue burdens in the subchronic inhalation studies, in which there was apparently a higher clearance rate of silver from the rat lungs and liver [Sung et al. 2009; Song et al. 2013]. Another possibility is the AgNPs differed (e.g., in solubility) across the studies; however, the particle sizes were similar (15 or 19 nm diameter), and the Ji et al. [2007] study was performed in the same laboratory as the subchronic studies [Sung et al. 2009; Song et al. 2013].

An area of uncertainty is how this apparent model over-prediction of rat silver tissue doses would influence the estimates of human-equivalent exposure concentrations. Other model uncertainties suggest the silver tissue burdens could be underestimated, for example, extrapolating the rat subchronic data to human working lifetime exposures based on a long-term clearance model (ICRP 1994), as used in Bachler et al. [2013]. Human studies have shown that the ICRP [1994] model under-predicts the long-term retention of poorly-soluble particles in the lungs of humans [Kuempel and Tran 2002; Gregoratto et al. 2010], although these models do not include particle dissolution pathways.

A.2.4.3 Human-equivalent working lifetime exposure concentrations

Estimation of working lifetime exposure concentrations of silver depend on the occupational exposure concentration and duration. The occupational route of exposure for these simulations is assumed to be inhalation. The deposited dose in the respiratory tract depends on the airborne particles size. The retained dose in the lungs and in other organs depends on the absorption rate of Ag from the lungs to the systemic circulation [Bachler et al. 2013].

A.2.4.4 Worker body burden estimates of silver from diet and occupational exposures

Apart from the potential occupational exposure to silver in some workers, humans take in a certain amount of silver in the daily diet. The routes of exposure differ, which is assumed to be primarily inhalation in the workplace and oral from diet. Some studies of intravenous silver administration have also been reported [e.g., Park et al. 2011a]. Regardless of the route of exposure, silver nanoparticles can be absorbed into the adjacent tissue, enter the systemic circulation, and be taken into all organs in the body, including liver, kidney, spleen, bone marrow, and brain [Bachler et al. 2013; Song et al. 2013; Brune 1980].

A few studies have measured or estimated the tissue dose or body burdens of silver from diet [Snyder et al. 1975; Kehoe et al. 1940] or occupational exposures [DiVincenzo et al. 1985; Wölbling et al. 1988]. Table A-7 show results from DiVincenzo et al. [1985] of Ag body burden in humans from diet and from occupational exposure and retention estimates based on Ag biomonitoring results in workers at a U.S. facility that produced silver for photographic processes and products. The study included workers with airborne exposure to silver (n=30) and control workers at the same facility without airborne exposures to silver (n=35) (randomly selected) (sample sizes from Table 2 of DiVincenzo et al. 1985). Most of the workers with silver exposure had worked for 5 or more years in a production area with the highest potential exposure to airborne silver. Job descriptions included burner operators, maintenance workers, smelter operators, mechanics, as well as other jobs. The mean duration of employment in both groups

was approximately 20 years, and the mean age was approximately 45 years in both groups.

The annual body burden of silver from the diet in unexposed workers (controls) estimated by DiVincenzo et al. [1985] (assuming 1% intestinal absorption) was 2 µg Ag/kg BW, or storage/retention of 1% silver (form of silver not reported) (Table A-7). Based on the Bachler et al. [2013] PBPK model (assuming 4% intestinal absorption) the estimated annual body burden of silver nanoparticles or ionic silver, respectively, are 1 or 3 µg Ag/kg BW (corresponding to either 0.77 or 0.25% storage/retention after 45 years). These similar estimates reported in DiVincenzo et al. [1985] and calculated from the Bachler et al. [2013] model provide some information relevant to validation of the PBPK model predictions.

Table A-7 (as well as Table 5 of DiVincenzo et al. 1985) provides information from which to estimate the average airborne concentration of the workers in that study. The estimated exposed worker daily Ag uptake (as reported in Table 5 of DiVincenzo et al. 1985) is 0.054 µg Ag / kg BW (assuming 1% uptake), or 3.78 µg Ag/d for a 70 kg adult male. Thus, the estimated daily airborne exposure concentration can be estimated as follows, assuming a reference worker air intake of 9.6 m^3 in an 8-hr day:

3.78 µg/d uptake in Ag worker = X µg/m^3 * 9.6 m^3/d * 0.01 absorption fraction

Or,

X µg/m^3 = 3.78 µg/d / [9.6 m^3/d * 0.01]

Where X = 39.4 µg/m^3.

This estimate is consistent with the airborne exposure concentrations of 1 – 100 µg/m^3 measured over a two-month period, as reported by DiVincenzo et al. [1985]. Insoluble silver was considered to be the primary form of silver to which workers were exposed in that study. The worker annual body burden of silver was approximately 6-fold higher (12 µg Ag / kg BW) than that from diet (2 µg Ag / kg BW) (total of (14 µg Ag / kg BW in exposed workers), although the route of exposure and internal organs exposed differ.

No adverse health effects were reported in the DiVincenzo et al. [1985] study (among workers with ~20 yr exposure, age ~45 yr). However, the purpose of that study was to estimate Ag body burdens based on measurements in feces, urine, blood, and hair), and did not report any biomedical findings. Thus, there is uncertainty about whether any adverse health effects occurred in those workers associated with their occupational exposure to silver.

Silver tissue burden estimates in humans, based on measurements or model predictions, are provided in Tables A-8 and A-9. Measured tissue burden of silver are reported in Table A-8 in smelter workers and in workers without occupational exposure to silver (controls), as reported in Brune [1980]. Estimates of silver tissue burdens from dietary intake are provided in Table A-9 based on PBPK model estimates of silver tissue burden assuming an average dietary intake of 80 µg/d (based on upper estimate of the 60 – 80 µg/d from Snyder et al. 1975; Kehoe et al. 1940, as reported in DiVincenzo et al. 1985) for up to 45 years, based on the Bachler et al. [2013] PBPK model.

A.2.4.5 Estimated working lifetime exposure concentrations associated with argyria

Argyria (bluish pigmentation of the skin) has been observed in humans with Ag burdens of 3.2 µg / g skin tissue; this skin tissue dose was measured in an individual that developed argyria at the lowest administered dose of 1.84 g (intravenous) of silver arsphenamine [Triebig and Valentin 1982; Wadhera et al. 2005; Gaul and Staud 1935, as reported in Bachler et al. 2013].

Table A-10 shows the working lifetime exposure concentrations (8-hr/d, 5-d/wk, and 52 wk/yr, for up to 45 yr) estimated to result in an Ag skin concentration that has been associated with argyria at the lowest dose in humans (3.2 µg/g, as reported in Bachler et al. 2013). These estimated working-lifetime exposure concentrations associated with argyria depend on the particle diameter (1-100, 15, 100 nm) and physical-chemical form (ionic, nanoparticle). The estimated average airborne exposure concentrations to reach the minimum skin tissue dose associated with argyria over a 45-yr working lifetime range from 47 µg/m^3 for exposure to ionic silver to 78 µg/m^3 for exposure to 15 nm

diameter Ag nanoparticles or 253 µg/m^3 for exposure to 100 nm diameter Ag nanoparticles. These estimated concentrations are based on the skin tissue dose in a sensitive human, i.e., at the lowest administered dose reported to be associated with argyria.

All of these estimates of working lifetime exposure concentrations associated with argyria exceed the current NIOSH REL and OSHA PEL of 10 µg/m^3 (for any particle size; soluble or insoluble), by factors of approximately 5 to 25. These PBPK model-based estimates suggest that the current NIOSH REL and OSHA PEL of 10 µg/m^3 (8-hr TWA concentration, up to 45-yr working lifetime) would be protective against the development of argyria in workers exposed to airborne AgNPs or ions. These estimates are consistent with the estimates of silver body burdens not expected to result in argyria that were used as the basis for the OSHA PEL and NIOSH REL (see Section 6.1).

A.2.4.6 Estimated silver tissue burdens in workers with inhalation exposure to 10 µg/m^3 of AgNP

The estimated tissue doses of silver in workers with airborne exposures at the current NIOSH REL for silver (i.e., 10 µg/m^3, as an 8-hr TWA concentration; total airborne particle size sampling; soluble or insoluble particles) are shown in Table A-11. These Ag tissue doses (ng/g) in workers (up to a 45-year working lifetime) are then compared to the rat Ag target tissue dose estimates (Ag ng/g) (NOAEL or $BMDL_{10}$) associated with no or low adverse (early-stage) lung or liver effects in the rat subchronic inhalation studies. These estimated tissue doses are also compared to those reported in smelter workers (for whom airborne exposure concentration data were not available).

As shown in Table A-11, the lung tissue doses for both particle diameters (15 and 100 nm) and types (nanoparticle or ionic, 15 nm) following 45-yr working lifetime exposure at the current NIOSH REL of 10 µg/m^3 exceeds the target tissue dose in rats based on the NOAEL for chronic pulmonary inflammation in male rats (0.081 µg/g) (Song et al. 2013). In addition, the total Ag in the lung tissue – but not the soluble/active Ag – exceeded the rat target tissue dose based on the lowest NOAEL in an earlier subchronic inhalation study (i.e., 4.2 µg/g, in female rats) (Sung et al. 2009) for both silver sizes (15 and 100

nm) and types (nanoparticle and ionic, 15 nm). The number of rats per group (approx. 10) was greater in Sung et al. (2009) study, but BMD estimation was not feasible due to the absence of intermediate responses between background and 100%; thus, the lowest tissue dose (i.e., in female rats) associated with the NOAEL was selected as the lung target tissue dose in that study.

Some of the lung tissue estimates of Ag (Table A-11) also exceeded those reported in smelter workers (0.28 µg Ag/g lung tissue) (Table A-8) by more than two orders of magnitude; however, silver exposures were not reported in smelter workers [Brune 1980]. Comparison of the estimated cumulative exposures to 10 µg/m^3 silver for 45-yr (i.e., 450 µg/m^3 x yr) to the average cumulative exposures reported in DiVincenzo et al. [1985] (estimated in Section 3.3.1 at ~39 µg/m^3 for 20 yr, i.e., 788 µg/m^3 x yr) suggests that workers in DiVincenzo et al. [1985] had nearly two-fold higher cumulative exposures compared to those estimated at the REL. Medical results were not reported in DiVincenzo et al. [1985].

As shown in Table A-11, the estimated liver tissue burdens of total Ag (for either 15 or 100 AgNPs or ionic silver) in workers exceeded the rat target tissue burden associated with 10% added risk of bile duct hyperplasia (minimal severity) after 45-yr working lifetime exposure to 10 µg/m^3 (8-hr TWA). This level was also exceeded for the soluble/active AgNP of 15 nm diameter, but not AgNP of 100 nm diameter.

The soluble/active Ag tissue dose appears to reach an approximate steady-state tissue concentration in the lung, liver, and other tissues shown in Table A-11 (presumably due to first-order rate of transformation of active/soluble silver to insoluble silver). The total silver tissue doses appear to continue increasing up to the 45 yr working lifetime (presumably due to the slow pulmonary clearance of insoluble particles).

A.2.4.7 Estimated 45-yr working lifetime airborne exposure concentrations of AgNP to result in tissue burdens associated with no or low (early-stage) adverse lung or liver effects in rats.

Estimated human-equivalent 45-yr working lifetime exposures of AgNP (8-hr TWA) to the rat effect levels ($BMDL_{10}$ or NOAEL) are shown in Table A-12, by particle size and type. Assuming total AgNP (both soluble and insoluble) is the relevant tissue dose metric, the 45-yr working lifetime exposure concentrations estimates that result in human lung or liver tissue doses equivalent to the rat target tissue doses (NOAEL or $BMDL_{10}$ estimates in Table A-4) are all lower than 10 µg/m^3. The airborne concentration estimates for the 15 nm Ag are lower than those for the 100 nm Ag (Table A-12).

Assuming that soluble/active AgNP is the relevant tissue dose metric, some of these working lifetime 8-hr TWA concentration estimates are less than the current NIOSH REL of 10 µg/m^3 (i.e., those at the $BMDL_{10}$, which are the most sensitive target tissue dose estimates). Other estimates for the soluble/active Ag tissue burden are greater than 10 µg/m^3 (Table A-12).

A.2.5 Discussion

A.2.5.1 Use of PBPK modeling methods

PBPK modeling permits evaluation of the predicted lung and liver doses in workers to those measured in rat subchronic inhalation studies of silver nanoparticles (15-19 nm diameter) and associated with no or low level of early-stage adverse effects in the lungs or liver. This PBPK model also permits evaluation of the skin tissue burden associated with argyria in humans, and to estimates of silver in workers based on occupational (inhalation) or dietary (oral) exposure.

The Bachler et al. [2013] PBPK model was calibrated from AgNP kinetics data in rats and extrapolated to humans based on interspecies adjustment of physiological and morphological parameters that influence the deposition and disposition of silver particles

following inhalation. The human model was shown to provide good prediction of the limited biomonitoring data in workers exposed to silver [Bachler et al. 2013].

Bachler et al. [2013] report certain limitations in their PBPK model that could bias an evaluation of the particle dissolution. These limitations include: model calibration with the experimental data could have incorporated some dissolution that was not accounted for in the model (i.e., that may have occurred during the 5 days of intravenous administration of silver or during the 16 days post-exposure until Lankveld et al. [2013] investigated the silver tissue burdens and kinetics). In addition, since the Bachler et al. [2013] ionic PBPK model was also calibrated with data after the intravenous injection (in this case of an ionic silver solution with rats examined 7 days post-exposure [Klaassen 1979]), the model accounts only for silver ions that are able to freely distribute within the body. That means those that dissolve and transform to silver sulfide within cells would be outside of the application domain of the model, according to Bachler et al. [2013].

Another area of uncertainty in the human PBPK model [Bachler et al. 2013] is the pulmonary or intestinal absorption fraction of Ag ions or nanoparticles. Although no human data are known to be available on these parameters, the sensitivity of the model estimates to the assumed parameter values could be investigated. Another area of uncertainty is whether the smaller AgNPs (e.g., <15 nm) may translocate more efficiently from the lungs to the blood. If this occurs, as was shown recently for gold nanoparticles [Kreyling et al. 2014], the silver burdens in the lungs and other organs may depend to a greater extent on the particle size. A key data gap in the evaluation of this PBPK model is the lack of chronic inhalation exposure data of AgNPs in rats on which to further test it.

A.2.5.2 Evaluation of the NIOSH silver REL for its applicability to nanoparticles

Data are limited on which to evaluate the health risk of occupational exposure to AgNPs and the adequacy of the current NIOSH REL of 10 µg/m^3 (8-hr TWA concentration of soluble and insoluble particles; total airborne particle size fraction) in protecting the health of workers exposed to airborne silver nanoparticles. In the absence of data in humans on the dose-response relationship of inhaled AgNPs, data from the two rat

subchronic inhalation studies of silver nanoparticles were used to estimate the human-equivalent airborne exposures and associated tissue burdens.

Although most of the studies in workers did not report the specific airborne particle sizes of silver, exposure to AgNPs would be anticipated at some production processes [e.g., in DiVincenzo et al. 1985]. Miller et al. [2010] did measure and report airborne exposures to AgNPs in workers' breathing zones, including airborne concentrations that exceed the NIOSH REL.

No studies have reported adverse health effects other than argyria in workers with long-term inhalation exposures to silver (e.g., ~20 yr at ~39 µg/m^3 [DiVincenzo et al. 1985], which is greater than the NIOSH REL (10 µg/m^3 for up to 45-yr); however, few studies have performed medical evaluations in workers exposed to silver dust and fumes (e.g., Pifer et al. [1989]; Rosenman et al. [1979, 1987], discussed in Sections 2 and 3). Studies that have reported argyria in workers have not reported adverse lung or liver effects associated with exposure to silver (although these studies were relatively small, e.g., few dozen workers). Adverse lung or liver effects are predicted from the rat studies to develop at similar or lower Ag tissue doses than those associated with argyria (Table A-10; Table A-12), and therefore adverse lung or liver effects would be expected to be observed in workers with sufficient exposures to cause argyria. This absence of reported lung or liver effects in workers (including those with argyria) suggests that the lung and liver effects in rats could be early-stage, pre-clinical effects that are not associated with adverse function. On the other hand, the absence of reported adverse health effects in workers could be due to insufficient study, especially of workers exposed to silver nanoparticles.

An evaluation of the available evidence from the human and rat studies, and from PBPK-modeling, is discussed in detail below. Comparisons are made between the tissue dose levels of silver reported in the rat studies and as estimated in humans exposed for up to a 45-year working lifetime, including at the current NIOSH REL for silver of 10 µg/m^3. These findings are discussed for the measured and/or estimated silver tissues dose and responses in the skin, lungs, and liver of rats and humans.

A.2.5.2.1 Risk of argyria

Comparison of the PBPK model [Bachler et al. 2013] estimates of skin tissue burdens to those associated with argyria in humans suggests that workers exposed for up to a 45-yr working lifetime at the current NIOSH REL for silver would not likely develop argyria (Table A-10). That is, the estimated working lifetime airborne exposure concentrations (8-hr TWA) resulting in the lowest skin tissue dose reported to be associated with argyria in humans (3.2 µg/g [Triebig et al. 1982]) were higher than the REL of 10 µg/m^3 for all particle sizes and types evaluated. These exposure estimates were 47, 78, or 253 µg/m^3, respectively, for ionic silver, AgNPs of 15 nm diameter, and AgNPs of 100 nm diameter.

These PBPK model-based estimates suggest an approximately 5 to 25-fold margin of exposure between the current REL and the lowest reported human skin tissue dose of silver associated with argyria. As discussed previously, no other adverse effects associated with silver exposure have been reported in humans with argyria.

A.2.5.2.2 Risk of lung inflammation

The rat effect levels (NOAEL or $BMDL_{10}$) based on the lung tissue dose of silver (Table A-4) can be compared to the predicted human tissue doses of silver given workplace exposure at the NIOSH REL of 10 µg/m^3 (Table A-11). These predictions depend on particle size and solubility. According to the Bachler et al. [2013] model, the human total silver doses in lung tissue after a 45-year working lifetime at the REL are estimated to be 11, 36, or 85 µg/g for 100 nm diameter AgNPs, 15 nm diameter AgNPs, or ionic Ag, respectively. The estimated human soluble/active silver doses in lung tissue are lower at 0.22, 0.69, or 1.6 µg/g for the same particle size and form. These human silver lung tissue dose estimates exceed the rat $BMDL_{10}$ estimate of 0.033 µg/g and the rat NOAEL of 0.081 µg/g in male rats in Song et al. [2013] (Table A-4). The estimated human soluble/active silver doses in lung tissue do not exceed the NOAELs of 0.672 or 4.2 µg/g silver in lung tissue in female rats in Song et al. [2013] or Sung et al. [2009], respectively.

Available data on human background lung tissue dose of silver in unexposed workers is 0.032 µg/g (Table A-8) [Brune 1980]. In smelter workers, the average lung tissue dose was 0.33 µg/g, although the no data were available on exposures to silver or on adverse lung effects associated with that dose.

These findings indicate that the risk estimates of developing adverse lung effects after a working lifetime exposure to silver nanoparticles at the current REL depend on the assumed dose metric (total or soluble/active) and the rat effect level estimate. The rat lung tissue silver dose estimates ($BMDL_{10}$ or NOAEL) for pulmonary inflammation vary widely depending on the study and gender (Table A-4). These large differences in the quantitative estimate of the rat lung tissue dose of silver associated with adverse pulmonary effects contributes to the uncertainty in the estimated human equivalent lung tissue dose after a working lifetime exposure at the current silver REL.

A.2.5.2.3 Risk of bile duct hyperplasia

The rat liver effect levels (NOAEL or $BMDL_{10}$) (Table A-4) can be also compared to the predicted dose of silver in human liver tissue at the NIOSH REL of 10 µg/m^3 (Table A-11). These predictions depend on particle size and solubility, as seen also for the lung tissue dose estimates. Based on the Bachler et al. [2013] model, the human total silver dose in liver tissue after a 45-year working lifetime at the REL is estimated to be 0.077, 0.25, or 0.50 µg/g for 100 nm diameter AgNPs, 15 nm diameter AgNPs, or ionic Ag, respectively. The estimated soluble/active silver tissue doses are lower at 0.003, 0.01, or 0.04 µg/g for the same particle size and form. The total silver doses exceed the rat effect levels ($BMDL_{10}$ estimates of 0.006 µg/g in females and 0.012 µg/g in males). The rat NOAELs for bile duct hyperplasia, 0.012 µg/g in females and 0.014 µg/g in males, are similar to the $BMDL_{10}$ estimates (Table A-4). The human estimated liver tissue doses of soluble/active silver are similar to the rat effect levels, with some estimates in humans above or below those in rats. These results suggest that the estimated risk for developing bile duct hyperplasia (minimal or higher severity) depend on whether the relevant dose metric is the total silver or the soluble/active silver, as well as on the particle size and type.

Available data on human background liver dose of silver (from dietary sources) indicate background silver levels of approximately 0.017 µg/g [ICRP 1960] or 0.032 µg/g [Brune 1980]. These human liver tissue concentrations of silver are similar to or higher than the rat liver tissue silver concentrations at the NOAEL and $BMDL_{10}$. These findings suggest that workers exposed at the human-equivalent working lifetime concentrations to the rat subchronic effect levels (Table A-12) would be unlikely to develop bile duct hyperplasia. The estimated equivalent 45-year working lifetime exposures to the rat no adverse liver effect levels range from 0.3 to 1.5 µg/m^3 based on a total silver dose metric, and 6 to 37 µg/m^3 based on soluble/active silver (8-hr TWA airborne concentrations).

These findings indicate that the risk estimates at the NIOSH REL depend on the assumed dose metric (total or soluble/active) for silver. However, some evidence suggests that the rat may be more sensitive or the effect level may be underestimated. First, the human predicted liver doses after dietary exposure to silver (0.023 µg/g total silver after 45 years) (Table A-9) exceed the rat effect levels. Second, the background concentrations of silver in liver tissue (from dietary sources) reported in the general US population (~0.017 µg/g) also exceed the rat effect levels of 0.006 or 0.012 µg Ag/g tissue. Thus, the quantitative estimates from the rat data are uncertain, and may be due to: (1) measurement error of silver in rat tissue, (2) higher sensitivity of the rat to silver tissue levels, and/or (3) these effects being subclinical.

A.2.5.2.4 Form of silver nanoparticles

The form of the silver in the human or rat tissues is not known. It may be reasonable to assume that the proportion of active/soluble silver in the rat subchronic inhalation studies would be greater than that in the humans over a lifetime. This assumption is based on the hypothesis that opsonization (protein binding) of silver occurs essentially immediately in mammals, forming a “protein corona” that stabilizes the particles [Bachler et al. 2013; Landsiedel et al. 2011]. Thus over time, the proportion of total silver that is in the soluble/active form would be smaller. If the soluble/active form of silver is more relevant to the toxicity, then it may be more relevant to use an equivalent

active/soluble silver dose in the rat and human tissues based on the PBPK model estimates. On the other hand, if the insoluble nanoparticle dose is related to the toxicity, then the total silver tissue dose should be used to estimate the airborne concentration. The role of the physical-chemical form of the silver on its toxicity is a major area of uncertainty.

A.2.5.3 Uncertainty in the risk evaluation

Areas of uncertainty in hazard and risk assessment based on the rat subchronic inhalation studies [Sung et al. 2011; Song et al. 2013] include:

- Clinical significance of the early-state lung and liver effects in the rat subchronic inhalation study to humans.
- Quantification of the tissue doses associated with the adverse effects in rats, and extrapolation of those doses to humans for up to a working lifetime.
- Role of the soluble/active vs. total silver tissue burden on the dose-response relationships for lung or liver effects.
- Lack of chronic studies in rats, and potential for other adverse effects (e.g., neurotoxicity)

Information is lacking on whether the early-stage adverse lung and liver effects in the rat studies result in functional impairment. Inconsistent results were reported in the two studies within the same rat gender [Sung et al. 2008, 2009; Song et al. 2013]. For example, lung function deficits were measured in female rats at 49 $\mu g/m^3$ (LOAEL) [Sung et al. 2008] but not at 381 $\mu g/m^3$ (NOAEL) [Song et al. 2013]. The variability in these and other lung responses results in uncertainty about the functional significance of the lung effects in rats or as extrapolated to humans. No data are available on whether bile duct hyperplasia is a clinically adverse effect. These uncertainties, in addition to risk estimates that include the current NIOSH REL, indicate that the data are insufficient at this time to derive a REL for silver based on particle size.

The wide difference in the effect level estimates for pulmonary inflammation in the same rat gender across the two studies raises in uncertainty about the doses associated with

that response (e.g., female rat NOAEL of 0.67 or 4.2 ng/g, associated with 117 or 133 mg/m^3 exposure concentration, in Song et al. [2013] or Sung et al. [2009]) (Table A-4). Thus, for similar airborne exposure concentrations, the associated silver lung tissue doses were nearly an order of magnitude different. This difference in tissue dose could be due to differences in the particles between the two studies (although these were generated by the same method and had similar characteristics) or to difficulties in obtaining consistent analytical results for quantifying the tissue burdens. The challenge of obtaining adequate recovery of the silver administered to rodent lungs was reported in the NIEHS NanoGo consortium [http://ehp.niehs.nih.gov/1306866/] at SOT 2015 [http://www.toxicology.org/AI/MEET/am2015/ss.asp]. High variability in the recovery amounts were also reported in the NIEHS studies, and it was difficult to achieve mass balance in many cases. The Sung et al. [2009] and Song et al. [2013] studies did not report mass balance (nor did the study design permit that estimate since the initial deposited dose was not reported).

Data on the chemical composition and physical state of AgNPs is limited in the rat studies and in the human studies as well. Thus, there is uncertainty about the extent to which the total silver or the soluble silver portion contributed to the adverse lung and liver effects associated with inhalation exposure to silver nanoparticles in the rat studies.

Concern about potential for neurotoxic effects inhalation of silver nanoparticles [Hubbs et al. 2011] is based on the exposure-related, statistically significant increase of the silver in the brain tissue in one of the rat subchronic inhalation studies [Sung et al. 2009]. However, the lack of an exposure-related increase in the brain tissue dose in the other rat subchronic inhalation study [Song et al. 2013] raises uncertainty about the extent of translocation of silver to the brain following inhalation exposure to the nanoparticles and/or the reliability of quantifying silver in tissue. In the latter study, the silver tissue concentration in the brain of unexposed (control) rats was four-fold higher (0.004 µg/g in females; not measured in males) compared to the control brain tissue doses in rats in the Sung et al. [2009] study (0.001 µg/g in female or male rats); those measurements in both studies were at the end of the 12 or 13 week study.

A.2.6 Quantitative Evaluation of Short-term Inhalation Exposure to Silver Nanoparticles

In order to evaluate the short-term effects of exposure to silver nanoparticles, data from an acute (5-hr) inhalation study in rats was used to identify the rat NOAELs for airborne exposure to two type of silver (ionic and nanoparticles) [Roberts et al. 2013]. No adverse pulmonary effects were observed at 1 or 7 day post-exposure [Roberts et al. 2013]. A significant increase (1.7 fold) in blood monocytes observed 1 day after exposure to the high dose (particulate form) was no longer significant at 7 day post-exposure. Slight cardiovascular changes (significant reduction in vascular responsiveness to Ach-induced redilation) were observed at the low dose (ionic form) at 1 day post-exposure, but not at the high dose (particulate form); that response was not significant at 7 day post-exposure [Roberts et al. 2013]. Given the minimal, transient responses, each of these doses could be considered NOAELs for the respective types of silver.

Human-equivalent NOAELs were calculated by adjusting for the rat and human lung weights (i.e., 1.5 g assumed for 9-wk male Sprague-Dawley rats, approximately 300 g body weight; human lung weight of 1,200 g [ICRP 2002]), and by using a human alveolar deposition fraction of 0.17 (33 nm) or 0.15 (39 nm) based on the MPPD human deposition (Yeh and Schum) model [ARA 2011]. Lung dose estimates are shown for the pulmonary regions in rats and humans (Table A-13). Table A-13 also shows the equivalent single-day (8-hr) exposure concentration. The current NIOSH REL (10 $\mu g/m^3$) is approximately 60 or 700 times lower than the human-equivalent acute no-adverse effect concentrations (8-hr) based on the rat acute (5-hr) inhalation study [Roberts et al. 2013]. Based on this evaluation, adverse lung effects in workers are not expected from human-equivalent acute exposure (8-hr, 1 day) to either of these investigated silver nanoparticle (ionic and nanoparticle). However, the potential for adverse effects of repeated exposure to these ionic or nanoparticle silver sprays is unknown.

A.2.7 Summary of Risk Evaluation Findings

A PBPK model for silver nanoparticles [Bachler et al. 2013] was used to evaluate the potential adverse health effects of working lifetime exposure to silver nanoparticle at the current NIOSH REL for silver (10 µg/m^3, 8-hr TWA concentration of soluble or insoluble silver, total airborne particle mass sampling). This PBPK model was developed based on data in rats, extrapolated to humans, and validated wthi limited bioassay data in humans [Bachler et al. 2013]. The estimated human tissue doses of silver were compared to those measured in two rat subchronic inhalation studies of silver nanoparticles and associated with no or low adverse effects in the rat lungs or liver [Sung et al. 2009; Song et al. 2013]. The rat adverse effects evaluated were pulmonary inflammation (minimal severity) or bile duct hyperplasia (minimal or greater severity).

Comparison of the estimated working lifetime tissue doses of silver in the lungs or liver to those in rats showed different results depending on the particle size and form and on assumptions about the predictive dose metric. If the total silver tissue dose is the dose metric associated with the adverse lung or liver effects in rats (and by extrapolation, in humans), then most estimates of the associated working lifetime exposure concentration exceeded the NIOSH REL. If the soluble/active silver tissue dose is the dose metric most predictive of the adverse lung or liver effects, then the similar or lower human-equivalent tissue doses to the rat NOAEL suggest that the current REL for silver may be adequate to protect workers exposed to AgNPs over a working lifetime. Additional uncertainty in these estimates include the clinical significance of the early-stage effects in the rat and the possible adverse effects with chronic exposure.

In contrast to the findings on possible lung and liver effects, comparisons of the PBPK-model estimates of skin tissue burdens to those associated with argyria in humans suggest that workers exposed to silver nanoparticles for up to a 45-year lifetime exposure at the current REL would not likely develop argyria. The working lifetime exposure concentrations estimated to result in the lowest skin tissue concentration of silver associated with argyria in humans were 5 to 25 times higher than the current REL of 10 µg/m^3. Moreover, the AgNP exposure concentrations estimated to be associated

with adverse lung or liver effects based on rat data were similar or lower than those associated with argyria in humans; yet adverse lung or liver effects have not been reported in humans with argyria in the few studies that included medical tests on lung and liver function in workers (Section 3).

The rat-based estimates of liver tissue effect levels of silver are lower than the human background silver liver tissue doses, suggesting uncertainty in the analytical methods to measure silver in tissues and/or the sensitivity of rats compared to humans. The working lifetime estimates of lung tissue silver dose generally exceeded the rat effect levels for adverse lung effects, although those rat estimates varied by an order of magnitude across gender and study. These findings suggest uncertainty in estimating the risk of adverse lung effects in workers based on the rat subchronic inhalation data.

NIOSH concludes that the current evidence is insufficient to derive a REL for silver based on particle size. Thus, NIOSH recommends that until more data become available, the current REL of 10 μg/m^3 (8hr-TWA) for silver should be applied to both dust and fumes of silver (soluble and insoluble), measured as the total airborne mass concentration of silver. Uncertainties in this evaluation may be reduced following completion of ongoing studies with silver (e.g., the NIEHS nanoGo consortium research) [Schug et al. 2013].

A.3 Sensitivity Analysis of Risk Assessment

Because of the limited available data for risk assessment of silver nanoparticles, a comprehensive sensitivity analysis was not feasible. However, the risk assessment included consideration of several alternative estimates of dose associated with the adverse effects observed in the rat studies and included alternative assumptions in the estimation of the human-equivalent dose. Several response endpoints were evaluated from the rat study for possible points of departure (PODs) (Table A-1 and A-4) for estimation of human-equivalent concentration. A range of POD estimates was evaluated, including NOAEL, LOAEL, as well as $BMCL_{10}$ or $BMDL_{10}$ estimates (based, respectively, on either airborne exposure concentrations or internal tissue doses of silver) (Tables A-1 and A-4). In risk assessment Method I, a set of standard uncertainty

factor values were evaluated (Table A-2) and selected for that assessment (Table A-3). In Method II, alternative assumptions on particle size and solubility were considered in the PBPK model-based estiamtes of Ag tissue dose and equivalent airborne exposure concentrations; different durations of exposure (i.e., 15, 30, or 45-years) were evaluated; and comparisons were made of the PBPK model estimates to limited available data on silver tissue doses in humans.

The sources of uncertainty that could not be evaluated quantitatively were also considered. These included (1) the role of particle dissolution and clearance of AgNPs on the doses associated with the adverse effects observed in rats; (2) the clinical significance of the adverse effects observed in the rat studies to humans; and (3) the potential for chronic adverse effects not observed in the subchronic studies. As new data become available and further validation of the PBPK model becomes feasible, the uncertainties in this risk assessment could be reduced, resulting in improved OEL estimates for AgNPs.

TABLES AND FIGURES FOR APPENDIX A

Table A-1. Points of departure from the animal subchronic inhalation studies: NOAELs or LOAELs.

Study	Type of Effect Level	Exposure Concentration (µg/m^3)	Group (Gender)	Adverse Health Endpoint
Sung et al. [2008]	LOAEL	**49**	Females	Lung function deficits (decreased minute volume and peak inspiration flow) at all doses
	NOAEL	133	Males	Lung function deficit (decreased minute volume and peak inspiratory flow) at 515 µg/m^3 (LOAEL)
Sung et al. [2009]	NOAEL	133	Male and Female	Lung inflammation (chronic alveolar) in males and females, and mixed cell perivascular infiltrate in females, at 515 µg/m^3 (LOAEL)
	NOAEL	**133**	Male and Female	Liver–bile duct hyperplasia (significantly increased incidence) at 515 µg/m^3 (LOAEL)
Song et al. [2013]	NOAEL	**49**	Male	Lung inflammation at 117 µg/m^3 after 12-wk exposure (LOAEL) (persistent during post-exposure in 381-µg/m^3 group)
	NOAEL	49	Male	Lung function deficits (decreased tidal volume, minute volume, peak inspiration flow, and peak expiration flow) at 117 µg/m^3 (LOAEL)
	NOAEL	**117**	Female	Lung inflammation at 381 µg/m^3 (LOAEL), which resolved by 12 weeks post-exposure
	NOAEL	381	Female	No lung function deficits observed

LOAEL = Lowest observed adverse effect level; NOAEL = No observed adverse effect level.

Table A-2. Examples of standard Uncertainty Factors (UFs)

Factor	Source of Uncertainty or Variability	Value	Reference
UF1	LOAEL vs. NOAEL used as POD	3 3 to 10	Christensen et al. [2010] (EU Echa) EPA [1994]
UF2	Animal to human: Interspecies differences in toxicokinetic (TK) & toxicodynamic (TD)	Up to 10: 4.0 & 2.5 3.3 each 1*	 WHO [2005] EPA [1994] Oberdörster [1989]
UF3	Human inter-individual variability in TK & TD: Workers General population	5 10: 3.3 each, TK & TD	Christensen et al. [2010] (EU Echa) WHO [2005] EPA 1994
UF4	Subchronic to chronic exposure and effects	2 3 3-10	Christensen et al. [2010] (EU Echa) Naumann et al. [1996] Doursen et al. ; EPA [1994]

LOAEL = lowest observed adverse effect level; NOAEL = no observed adverse effect level; POD = point of departure.

*Following dosimetric adjustment to estimate equivalent dose of poorly soluble respirable particles in animals and humans, and the use of most sensitive animal model for the endpoint of interest.

Table A-3. OELs derived from applying uncertainty factors to PODs from rat subchronic inhalation studies (with daily exposure duration adjustment).

Rat Study	Endpoint in Rats	POD (µg/m³)*	UFs 1–4	OEL (8-hr TWA) µg/m³
Sung et al. [2008]	Lung function deficits, females (LOAEL)	49 (rat) 37 (human)	180 (3 × 4 × 5 × 3)	0.2
Song et al. [2013]	Lung inflammation, males (NOAEL)	49 (rat) 37 (human)	60 (1 × 4 × 5 × 3)	0.6
Song et al. [2013]	Lung inflammation, females (NOAEL)	117 (rat) 88 (human)	60 (1 × 4 × 5 × 3)	1.5
Sung et al. [2009]	Liver–bile duct hyperplasia, male and females (NOAEL)	133 (rat) 100 (human)	60 (1 × 4 × 5 × 3)	1.7

*Estimated by adjusting for difference in rat and human exposure day, that is, rat POD (Table A-1) × 6 hr/8 hr.

Table A-4. Estimated target tissue doses of silver nanoparticles based on rat subchronic inhalation studies

Target organ	Adverse endpoint	Gender	Exposure concentration (μg/m³)	Tissue dose, measured or estimated (ng/g)[a]	Type of effect level
Song et al. 2013					
Lung	Chronic alveolar inflammation, minimal	M	49	**33**[b]	**$BMDL_{10}$**
				81	NOAEL
		F	117	**672**	**NOAEL**
Sung et al. 2009					
Lung	Chronic alveolar inflammation, minimal	M	133	5,450	**NOAEL**
		F		**4,241**	
Liver	Bile duct hyperplasia, minimal	M	133	**12**	**$BMDL_{10}$**
				14	NOAEL
		F		**6.3**	**$BMDL_{10}$**
				12	NOAEL

[a] Tissue doses of silver, as NOAEL or $BMDL_{10}$.

[b] Estimate was excluded from evaluation due to limited data and modeling options (see Appendix B).

NOAEL: No observed adverse effect level. The NOAEL is the highest dose group above the control (unexposed) group that did not have a significantly greater proportion of rats with an adverse lung or liver response. NOAELs are as reported in: Sung et al. 2009 - Table 7 (M), Table 8 (F); Song et al. 2013 - Table II (M), Table III (F).

$BMDL_{10}$: Benchmark dose (95% lower confidence limit) associated with a 10% response ($BMDL_{10}$), derived from benchmark dose modeling (US EPA BMDS version 2.5) of the measured tissue dose and response data, including: liver bile dust hyperplasia - Sung et al. Table 9 (M), Table 10 (F); lung inflammation - Song et al. Table XII (M). (See Appendix B for the BMD modeling results).

Notes: The human-equivalent tissue dose is assumed to be equal to the rat target tissue dose expressed as ng Ag/g tissue. PBPK modeling was used to estimate the occupational airborne exposure to Ag (as 8-hr time-weighted average concentration, 40 hr/wk, up to 45-yr) that would result in the same target tissue burden in humans (Section A.2). Human-equvialent estimates to those in bold type are shown in Table A-12.

Table A-5. Physiological parameters for rat used in silver nanoparticle PBPK model [Bachler et al. 2013].

RAT	Organ weight [% of total body weight]	SD	Blood Flow amount [% of total Blood Volume]	SD	GSH concentration [µmol/g]	SD
Skin°	19.0	2.620	5.80	0.09	0.37	0.08
Liver	3.66	0.650	18.30	2.50	9.37	0.86
Kidneys	0.730	0.110	14.10	1.90	2.45	0.14
Muscles°	40.4	7.170	27.80	13.34	0.73	0.20
Spleen*	0.200	0.050	0.85	0.26†	2.12	0.09
Heart	0.330	0.040	5.10	0.10	2.12	0.52
Brain	0.570	0.140	2.00	0.30	1.64	0.11
Lung	0.500	0.090	2.10	0.40	2.04	0.01
Testes°	1.03	0.060	0.79	0.16	3.41	0.20
Small Intestines°	1.40	0.390	10.14	2.43	1.78	0.24
Large Intestines°	0.840	0.040	1.64	0.44	2.10	0.22
Thymus^	0.102	0.057	0.42	0.21	1.90	0.15
Remainder	31.2	7.67	26.26	13.94	1.22	0.09
Cardiac Output [L/min]	0.095	0.013		**Average:**	1.22	0.09
Blood [L]	0.022	0.002				
Body Weight [kg]	0.300					

Reference values taken from Brown et al 1997, blood flow: *Davies et al 1993, °Stott et al 2006
^ Hatai et al 1914, Alhamdan & Grimble 2003, Jansky & Hart 1968
† Estimate based on the distribution of other organs; no exact values available.
[Note: these parameters are used in Monte Carlo runs based on a new (unpublished) version of Bachler et al. [2013] model; the new version also includes a remainder compartment to account for the discrepancies observed between administered doses of silver and recovered doses measured in the tissues; the remainder compartment includes muscles and bone marrow].

Table A-6. Physiological parameters for humans used in silver nanoparticle PBPK model [Bachler et al. 2013].

HUMAN	Organ weight [% of total body weight]	SD	Blood Flow amount [% of total Blood Volume]	SD	GSH concentration [µmol/g]	SD
Skin	4.36	0	5.92	1.13	0.46	0.20
Liver	2.47	0	21.3	4.84	6.40	0.40
Kidneys	0.420	0	18.1	2.32	4.00	0.30
Muscles	39.7	0	14.2	5.10	1.80	0.08
Spleen	0.210	0	3.43	1.24	2.12[a]	0.09[a]
Heart	0.450	0	4.91	1.32	1.20	0.20
Brain	1.99	0	11.8	1.77	1.40	0.30
Lung	0.680	0	3.38	2.49	2.04[a]	0.01[a]
Testes	0.048	0	0.10	0.00	3.41[a]	0.20[a]
Small Intestines	1.40	0	9.10	2.20	1.78[a]	0.24[a]
Large Intestines	0.490	0	3.80	0.40	2.10[a]	0.22[a]
Thymus^	0.034	0	0.42[a]	0.21[a]	1.90[a]	0.15[a]
Remainder	47.7	0	18.3	8.59	1.87	0.06
Cardiac Output [L/min]	6.5	1.300		**Average:**	1.87	0.06
Blood [L]	5.6	0.810				
Body Weight [kg]	73					

Reference values taken from, weight: ICRP 2002, blood flow: Williams and Legget 1989, GSH: various see Bachler et al 2013.

^ Hatai et al 1914, Alhamdan & Grimble 2003, Jansky & Hart 1968

[a] Values from the rat.

[Note: these parameters are used in Monte Carlo runs based on a new (unpublished) version of Bachler et al. [2013] model; the new version also includes a remainder compartment to account for the discrepancies observed between administered doses of silver and recovered doses measured in the tissues; the remainder compartment includes muscles and bone marrow].

Table A-7. Estimated annual body burden of silver in humans – based on biomonitoring measurements and estimates [DiVincezo et al. 1985] or PBPK model predictions [Bachler et al. 2013].

Study	Ag Form	Annual body burden (µg Ag/kg body wt)	Retention (%)
DiVincenzo et al. [1985]*			
Workers (workplace + diet)	nr	14	1
Controls (diet)	Nr	2	1
Bachler et al. [2013] – Controls (diet)	Nanoparticle	3	0.77
	Ionic	1	0.25

nr: not reported.
*As reported in Table 5 of that DiVincenzo et al. [1985].

Table A-8. Silver tissue doses in smelter workers who had exposures to silver and in workers without silver exposures [Brune 1980].

Organ	**Ag-exposed workers: Organ dose (µg Ag/g tissue)**	**Unexposed workers: Organ dose (µg Ag/g tissue)**
Lung	0.28	0.06
Liver	0.33	0.032
Kidney	0.18	0.045
Skin	Nr	Nr

nr: not reported.

Table A-9. Estimated silver tissue burdens after *dietary intake* of 80 µg/day in adult male (BW: 70 kg) for up to 45-yr, by silver particle size and physical form) – based on Bachler et al. [2013] human model.

Duration (yr)	LUNG (µg Ag/g tissue)		LIVER (µg Ag/g tissue)		KIDNEY (µg Ag/g tissue)		SKIN (µg Ag/g tissue)	
	Sol/Activ	Total	Sol/Activ	Total	Sol/Activ	Total	Sol/Activ	Total
Nanoparticles (average diameter 15 nm)								
15	0.000	0.000	0.001	0.008[d]	0.002	0.020	0.000	0.008
30	0.000	0.001	0.001	0.015[d]	0.002	0.038	0.000	0.016
45	0.000	0.001	0.001	0.023[d]	0.002	0.056[a]	0.000	0.024
Ionic silver								
15	0.002	0.014	0.010[d]	0.048[a,d]	0.003	0.027	0.000	0.036
30	0.002	0.026	0.010[d]	0.086[a,d]	0.003	0.050[a]	0.000	0.071
45	0.002	0.038	0.010[d]	0.124[a,d]	0.003	0.074[a]	0.000	0.107

Notes: Intestinal absorption of silver estimated to be 4% for silver nanoparticles, assuming that nanosilver is formed after the oral intake of soluble silver salts [Bachler et al. 2013]; this may be an upper estimate, given that the rat intestinal absorption closer to 1%. Ionic silver absorption also estimated to be 4%.

For either silver nanoparticles or ions, model-predictions include: Intake: 1,314 mg; and uptake: 52.6 mg (at 4% absorption). Predicted retained dose was 3.27 mg for ionic silver and 10.2 mg for silver nanoparticles over 45 years.

[a] Higher than the Ag tissue burdens in unexposed workers [Brune 1980] (Table A-8).

[b] Higher than the Ag tissue burdens in Smelter workers [Brune 1980] (Table 5).

[c] Exceeds the lung tissue level of 0.081 µg Ag/g (male rats) associated with the estimated NOAEL for lung effects, following subchronic inhalation of Ag nanoparticles [Song et al. 2013] (Table A-4).

[d] Similar to or higher than the rat liver tissue levels (0.006 or 0.012 µg/g) associated with lower 95% confidence interval estimate of the benchmark dose ($BMDL_{10}$) associated with 10% of bile duct hyperplasia, minimal severity, (Table A-4). Also exceeds the human reference level of silver in liver (~0.017 µg/g), based on a study in deceased persons in the USA [ICRP 1960] (Bachler et al. [2013], Figure 6).

Table A-10. Estimated working lifetime (45-yr) exposure concentrations associated with argyria (retained skin dose of 3.2 µg Ag/g skin, minimum dose) [Bachler et al. 2013, citing Triebig et al. 1982].

Physical-chemical form	Particle diameter (nm)	Airborne concentration (8-hr TWA) (µg/m^3)
Ionic	NA	46.8
Nanoparticle	15	77.6
Nanoparticle	100	253
Nanoparticle	1 – 100	204

Assumptions: adult male (8hr/d, 5 d/wk), 1.2 m^3/hr breathing rate, nose breather.
NA: not applicable

Table A-11. Estimated silver tissue burdens after a 45-yr working lifetime inhalation exposure to 10 µg/m³ (current NIOSH REL for silver particles, soluble and insoluble), by particle size and physical form of Ag (assuming adult male, air intake 1.2 m³/hr, 8 hr/d, 5 d/wk) – based on Bachler et al. [2013] human model.

Duration (yr)	LUNG (µg Ag/g tissue)		LIVER (µg Ag/g tissue)		KIDNEY (µg Ag/g tissue)		SKIN† (µg Ag/g tissue)	
	Sol/Activ	Total	Sol/Activ	Total	Sol/Activ	Total	Sol/Activ	Total
Particle average diameter: 15 nm								
15	0.67[a,*]	25[a,b,*]	0.01[c]	0.090[c,d]	0.024	0.22*	0.0008	0.088
30	0.68[a,*]	31[a,b,*]	0.01[c]	0.17[c,d]	0.025	0.42*	0.0008	0.18
45	0.69[a,*]	36[a,b,*]	0.01[c]	0.25[c,d]	0.026	0.62*	0.0008	0.26
Particle average diameter: 100 nm								
15	0.21[a]	7.8[a,b,*]	0.003	0.028[c,d]	0.007	0.068	0.002	0.027
30	0.21[a]	9.8[a,b*]	0.003	0.052[c,d]	0.008	0.13	0.002	0.054
45	0.22[a]	11[a,b,*]	0.003	0.077[c,d]	0.008	0.19*	0.002	0.810
Ionic silver								
15	1.59[a,*]	58.8[a,b,*]	0.04[c,d]	0.19[c,d]	0.016	0.11	0.00	0.14
30	1.61[a,*]	74.4[a,b,*]	0.04[c,d]	0.35[c,d,*]	0.016	0.22*	0.00	0.29
45	1.64[a,*]	84.8[a,b,*]	0.04[c,d]	0.50[c,d,*]	0.016	0.32*	0.00	0.44

[a] Exceeds the lung tissue level of 0.081 µg Ag/g (male rats) associated with the estimated NOAEL for lung effects, following subchronic inhalation of Ag nanoparticles [Song et al. 2013] (Table A-4).

[b] Exceeds the lung tissue level of Ag of 4.2 µg Ag/g lung tissue (female rats) associated with the NOAEL (no observed adverse effect level), following subchronic inhalation of Ag nanoparticles [Sung et al. 20009] (Table A-4).

[c] Similar to or exceeds the liver tissue levels (0.006 µg/g females; 0.012 µg/g males) associated with lower 95% confidence interval estimate of the benchmark dose ($BMDL_{10}$) associated with 10% of bile duct hyperplasia, minimal severity, in rats [Sung et al. 2009] (Table A-4) .

[d] Exceeds the liver tissue level of silver in the general population (0.017 µg/g) [ICRP 1960] and/or that reported in unexposed workers (0.032 µg/g) [Brune 1980].

* Exceeds tissue levels of Ag reported in smelter workers (Table A-8) by Brune [1980], for whom airborne exposure concentrations of Ag were not reported.

† The estimated skin tissue doses are all less than 3.2 µg/g, which is the minimum estimated Ag dose in skin associated with argyria (as reported in Bachler et al. 2013).

Note: An *in vitro* Ag dose of 1 µg/g was associated with adverse effects [as discussed in Bachler et al. 2013].

Table A-12. Working lifetime (45-yr) exposure concentration of silver (Ag) nanoparticles (soluble/active or total; 15 or 100 nm diameter) associated with Ag target tissue doses (NOAEL or BMDL) in the rat subchronic inhalation studies [Sung et al. 2009; Song et al. 2013] (adult male; reference worker air intake, 1.2 m^3/hr).[a]

Rat Study, Gender	Type of Effect Level	Silver Tissue Dose (ng/g)	Particle Diameter (nm)	Airborne Exposure (8-hr TWA) (μg/m^3)	
				Assuming Tissue Dose Metric of Soluble/Active Ag	Assuming Tissue Dose Metric of Total Ag
Lung – Chronic alveolar inflammation, minimal					
Song 2013, male	$BMDL_{10}$	33	15	0.48 [b]	0.0092 [b]
			100	1.5 [b]	0.029 [b]
Song 2013, female	NOAEL (117 μg/m^3)	672	15	9.7	0.19
			100	31	0.60
Sung 2009, female	NOAEL (133 μg/m^3)	4,241	15	61	1.2
			100	195	3.8
Liver – Bile duct hyperplasia, minimal					
Sung 2009, female	$BMDL_{10}$	6.30	15	6.2	0.26
			100	20	0.83
Sung 2009, male	$BMDL_{10}$	11.6	15	11.4	0.47
			100	37	1.5

[a] Based on Ag absorption rate from lungs to systemic circulation in humans as determined from an *in vivo* animal studies [Takenaka et al. 2001], which is 7-fold higher than the Ag absorption rate from Ji et al. [2007] that was used in simulations of Sung et al. 2009 and Song et al. 2013 studies.

[b] Estimates considered to be of higher uncertainty due to minimally acceptable dose-response data and limited modeling options (Appendix B); not included in the OEL evaluation (Sections 6.5.2.2 and 6.5.3).

Table A-13. Acute (5-hr) inhalation exposure in rats – No observed adverse effect level (NOAEL) [Roberts et al. 2013] and human-equivalent exposure concentration*

Type of Ag	CMAD (nm)	Rat Ag lung dose (µg) [NOAEL]	Human-equivalent Ag lung dose (µg)	Airborne concentration (mg/m^3) in 1 d (8-hr TWA) resulting in human-equiv. lung dose
Commercial spray (ionic)	33	1.4	1,000	0.62
NIST reference (particulate)	39	14	11,000	7.7

*Calculations based on the following: Rat (male rat Sprague-Dawley, 9-wk old) estimated body weight: 300 g; estimated lung weight: 1.5 g. Human lung weight 1,200 g [ICRP 2002]. Human alveolar deposition fraction (DFalv): 0.17 (33 nm) or 0.15 (39 nm) MPPD Yeh and Schum model [ARA 2011]. Reference worker air inhaled (AI) of 9.6 m^3/8-hr d [ICRP 1994]. Calculated the 8-hr time weighted average (TWA) airborne concentrations as:
X mg/m^3 = Lung dose (mg) / [DFalv x AI].

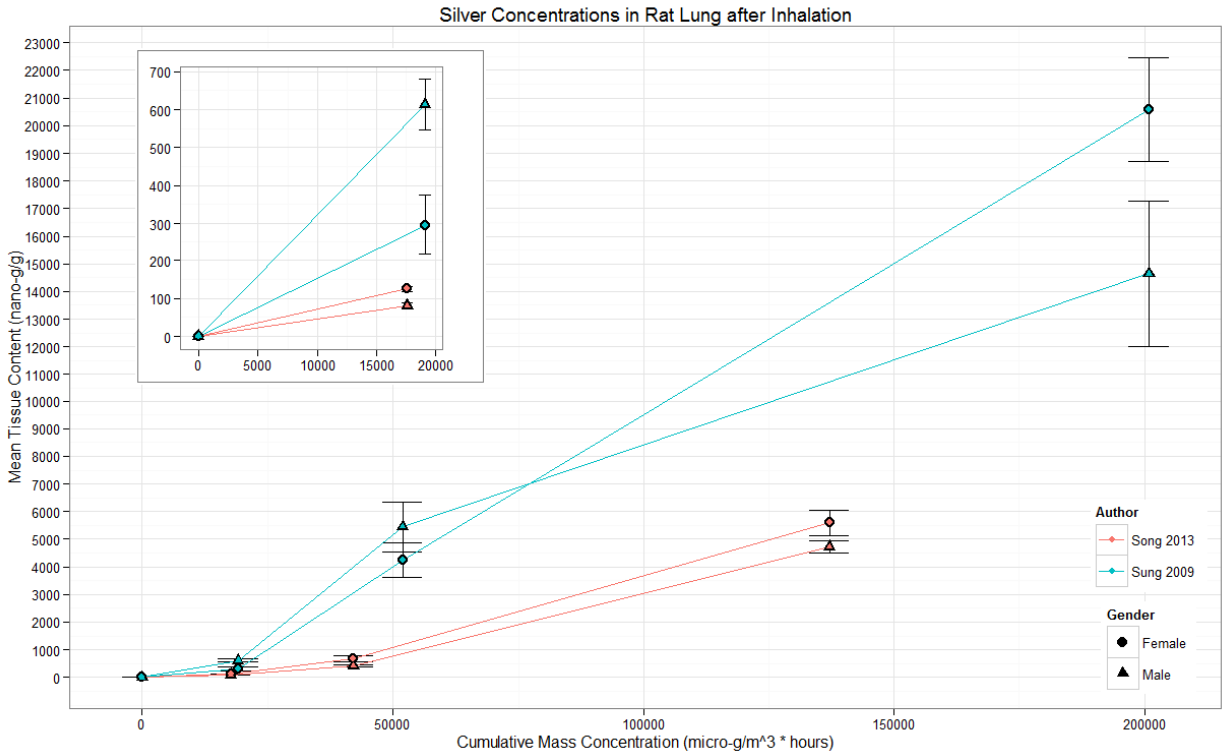

Figure A-1. Lung silver burden (µg Ag/g wet tissue) by cumulative exposure (µg/m³ x hours) in male and female rates, measured at the end of the 13 or 12 week exposure [Sung et al. 2009 or Song et al. 2013], respectively. Tissue concentrations are means ± 1 standard error. Lines fit to data, not modeled. Insert shows low exposure concentration (49 µg/m³) and control (unexposed) data only.

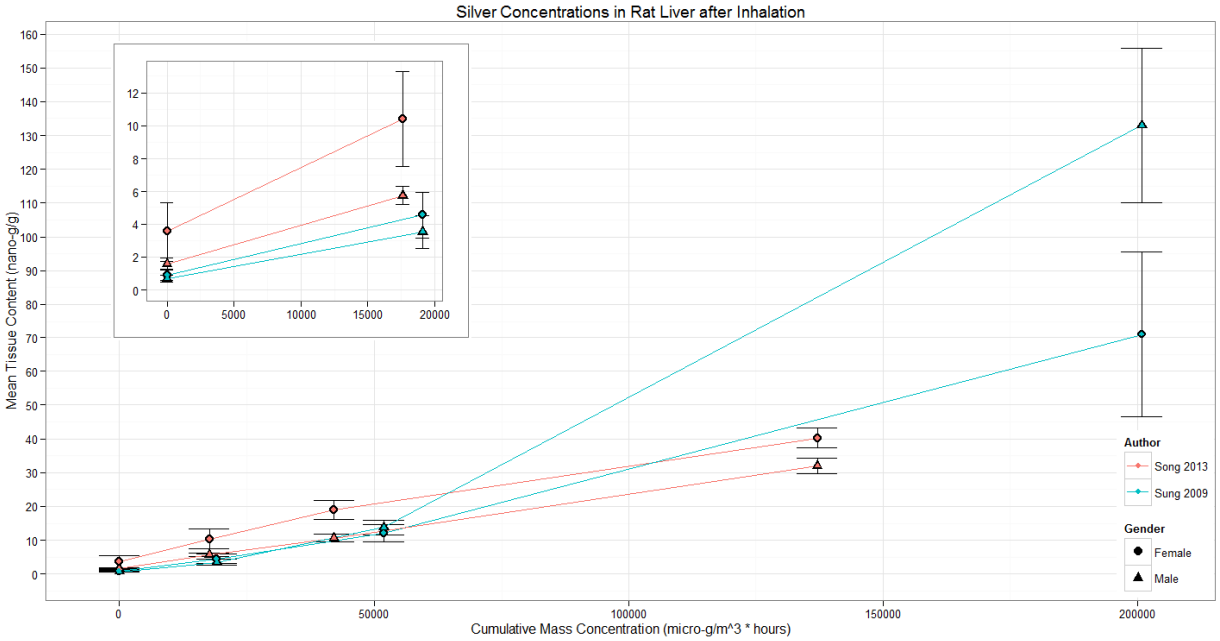

Figure A-2. Liver silver burden (µg Ag/g wet tissue) by cumulative exposure (µg/m³ x hours) in male and female rates, measured at the end of the 13 or 12 week exposure [Sung et al. 2009 or Song et al. 2013], respectively. Tissue concentrations are means ± 1 standard error. Lines fit to data, not modeled. Insert shows low exposure concentration (49 µg/m³) and control (unexposed) data only.

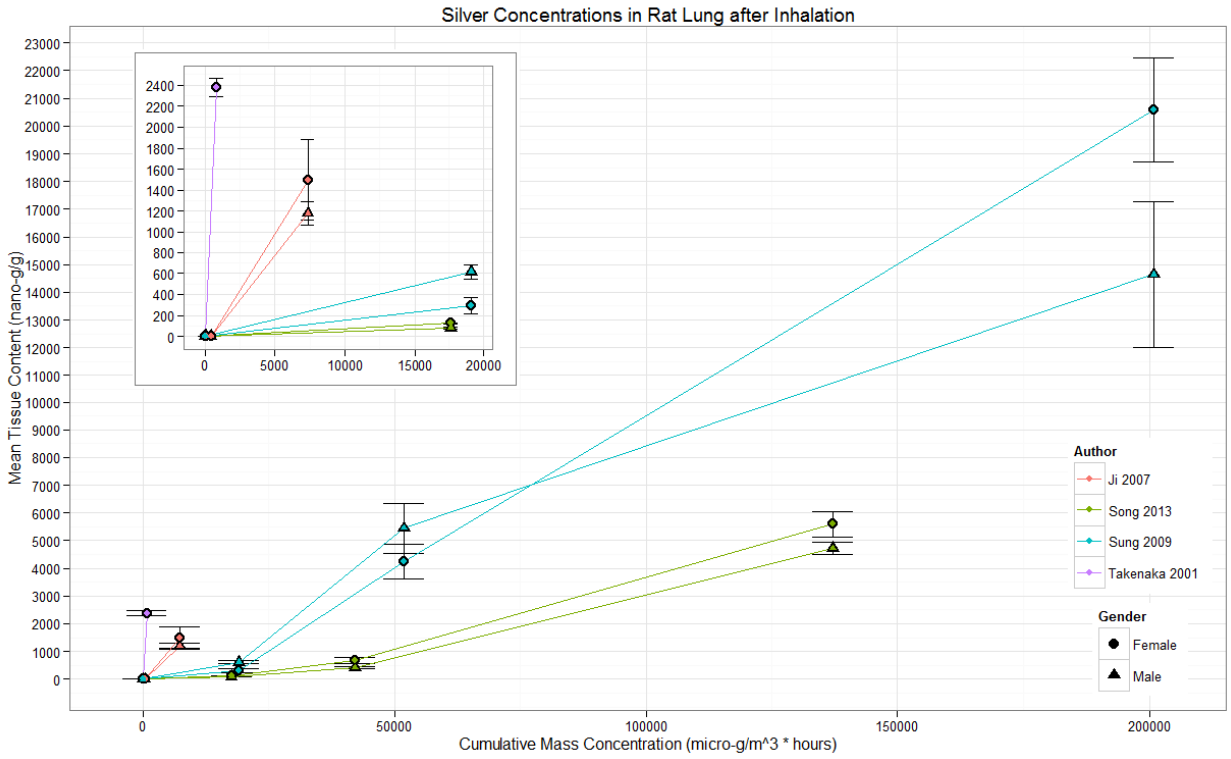

Figure A-3. Comparison of lung silver burden (µg Ag/g wet tissue) by cumulative exposure (µg/m³ x hours) in male and female rates, measured at the end of inhalation exposure (day 0 "immediately" after 6-hr in Takenaka et al. [2001]; 4 wk in Ji et al. [2007]; 13 wk in Sung et al. [2009]; or 12 wk in Song et al. [2013]. Tissue concentrations are means ± 1 standard error. Lines fit to data, not modeled. Insert shows data at lowest exposure concentration only (i.e., 133, 0.5, 49, 49 µg/m³, respectively, as cited above) and control (unexposed) data only.

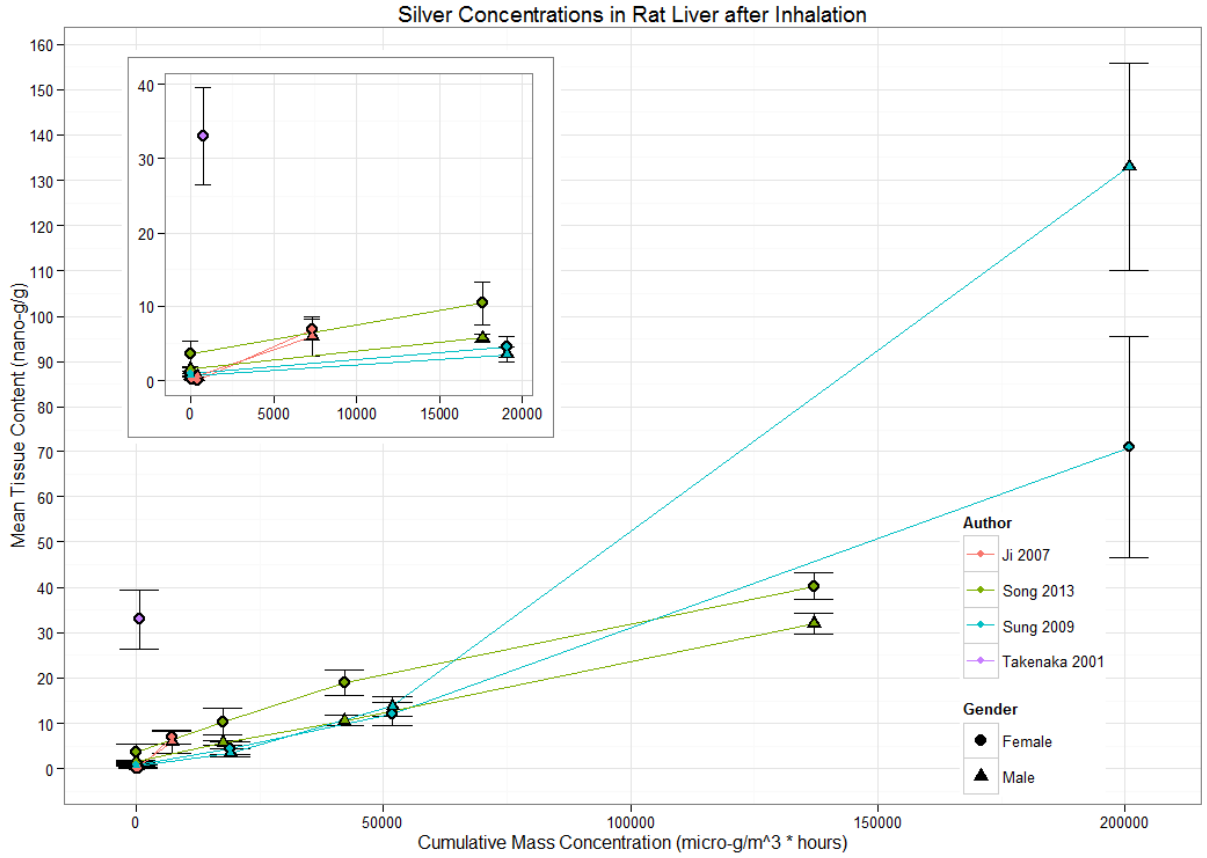

Figure A-4. Comparison of liver silver burden (µg Ag/g wet tissue) by cumulative exposure (µg/m³ x hours) in male and female rates, measured at the end of inhalation exposure (day 0 "immediately" after 6-hr in Takenaka et al. [2001]; 4 wk in Ji et al. [2007]; 13 wk in Sung et al. [2009]; or 12 wk in Song et al. [2013]. Tissue concentrations are means ± 1 standard error. Lines fit to data, not modeled. Insert shows data at lowest exposure concentration only (i.e., 133, 0.5, 49, 49 µg/m³, respectively, as cited above) and control (unexposed) data only; Takenaka et al. [2001] did not include a control group.

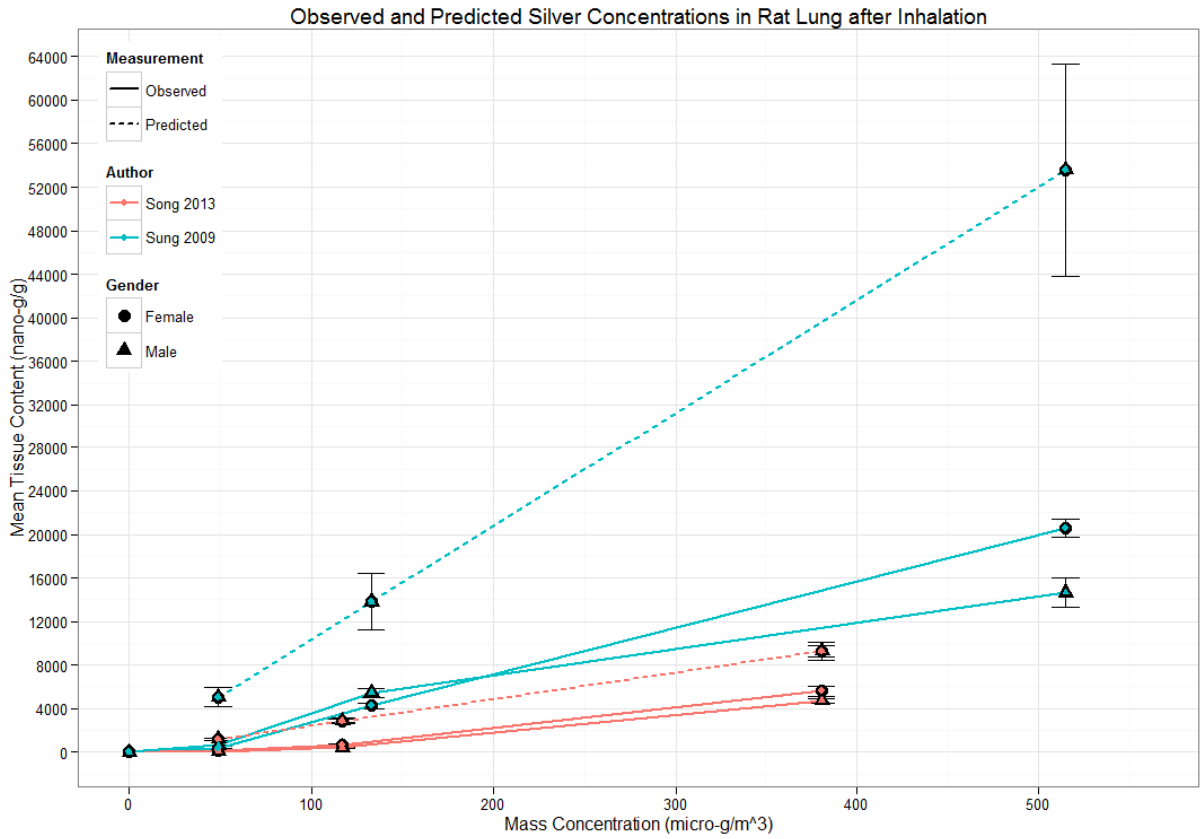

Figure A-5: Observed and PBPK-model predicted lung burdens in male and female rats at the end of the 13 or 12 week inhalation exposure, respectively, in Sung et al. [2009] and Song et al. [2013]. [Note: the model predictions are the same for both genders].

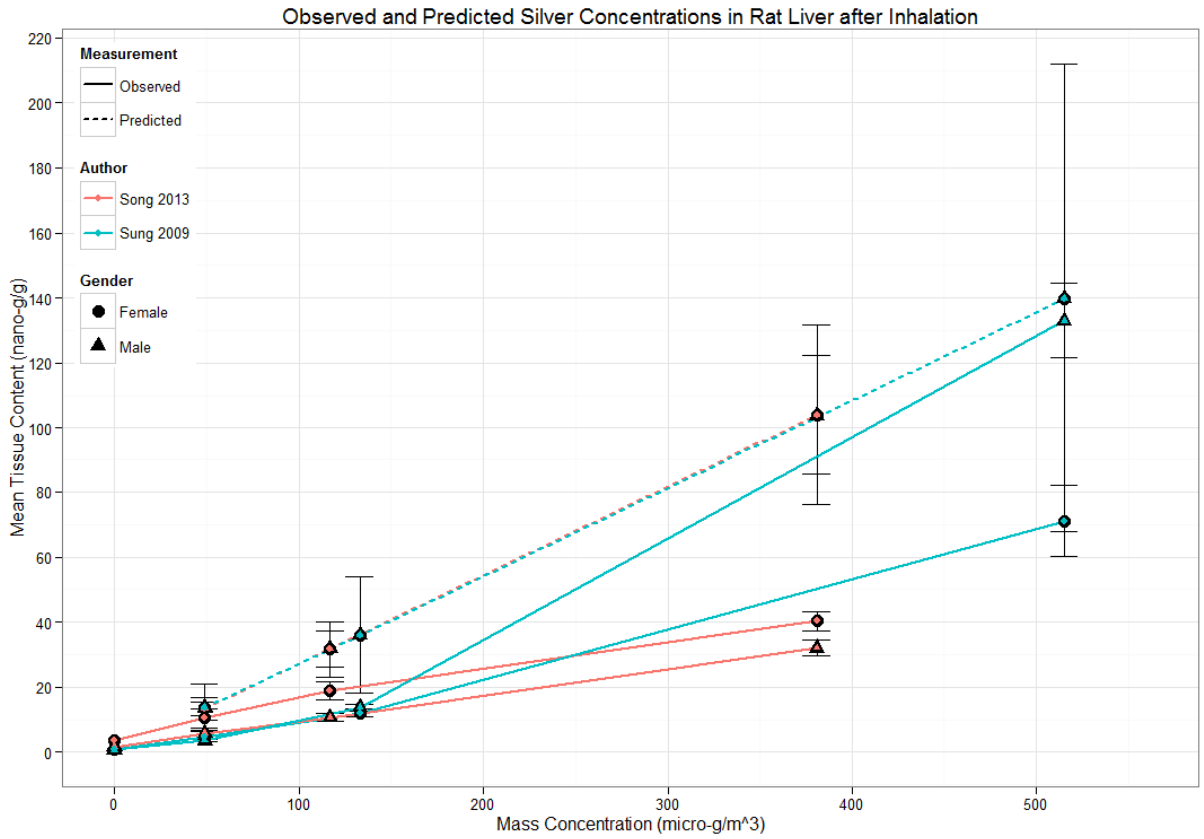

Figure A-6: Observed and PBPK-model predicted liver burdens in male and female rats at the end of the 13 or 12 week inhalation exposure, respectively, Sung et al. [2009] and Song et al. [2013]. [Note: the model predictions are the same for both genders].

APPENDIX B

Benchmark Dose Modeling of Rat Subchronic Inhalation Studies of Silver Nanoparticles

The in vivo toxicological studies on silver nanoparticles in experimental animals are summarized in Appendix F, Table F-5. More detailed accounts of the studies are provided in the text of Appendix F. The studies considered most applicable to the development of an OEL were subchronic inhalation studies in Sprague-Dawley rats reported by Sung et al. [2009] (90 days) and Song et al. [2013] (12 weeks). These studies were evaluated for dose-response data that were sufficient for benchmark dose (BMD) modeling. Criteria include a monotonic dose-response relationship, dichotomous responses, and at least one dose group with response proportion between 0 and 1.

A BMD is a maximum likelihood estimate of the dose associated with a low response (e.g., 10%); a BMDL is the 95% lower confidence limit estimate of the BMD [Crump 1984]. BMDL estimates are often treated as NOAELs for use as PODs to estimate exposure limits in humans [US EPA 2002]. The U.S. Environmental Protection Agency (EPA) benchmark dose software (BDMS) version 2.5 was used to model the data in Sung et al. [2009], and Song et al. [2013].

Both point-of-impact (lung) and systemic (liver) target organ endpoints were evaluated. These response endpoints include: (1) mixed cell perivascular infiltration in the lungs of males or females, accumulation of alveolar macrophages in males, and chronic alveolar inflammation in males; and (2) bile duct hyperplasia in males or females. The dose (as airborne exposure concentration) and response data used in these BMD models are shown in Table B-1 [Sung et al. 2009] and Table B-2 [Song et al. 2013]. Tables B-3 and B-4 show dose as mean tissue concentration for the same responses and studies as Tables B-1 and B-2, respectively.

All of the available BMDS dichotomous response models were evaluated, which included: Gamma, logistic, log-logistic, probit, log-probit, multistage (polynomial degree 1, 2, and/or 3), Weibull, and quantal linear. Model averaging (MADr) per Wheeler and Bailer [2007], using the logistic, log-probit, multistage degree 2, and Weibull models, was also performed for comparison to the BMDS modeling results. All BMDS models were used to estimate a benchmark response of 10% the excess (added) risk of early-stage adverse lung or liver effects in rats following subchronic inhalation of AgNP. The best fitting model(s) were selected based on the optimal goodness-of-fit criteria, i.e., the models with the lowest Akaike Information Criteria (AIC) among the models with Goodness-of-Fit *p* values within the applicable range (> 0.1). Care should be taken when selecting the model with the smallest AIC, as the EPA BMDS does not include parameters that are estimated to be at a boundary value (e.g. the background parameter) in the penalization of the log likelihood, which can misrepresent the best fitting model for the given data.

For some models, such as the multistage, EPA BMDS did not report the standard errors for the parameter estimates, which can be used as an additional check for a statistically significant trend (i.e. the slope parameter). In those cases, the fitted model was compared to the null model using the likelihood ratio test for nested models.

The resulting benchmark concentration (BMC_{10}) and lower 95% confidence interval ($BMCL_{10}$) estimates associated with 10% response, along with the goodness of fit parameters for the best-fitting model(s), are shown in Tables B-5 and B-7 [Sung et al. 2009] and Tables B-6 and B-8 [Song et al. 2013]. The $BMCL_{10}$ estimates for all endpoints and dose metrics utilizing model averaging are provided in Tables B-9 and B-10.

Comparison of the $BMCL_{10}$ estimates based on BMDS and MADr were reasonably similar, but some differences (in part due to different criteria used for the model fit estimates) are observed. For example, for the Sung et al. [2009] endpoints, BMDS estimates of $BMDL_{10}$ are smaller; and for the Song et al. [2013], the MADr estimates of $BMDL_{10}$ are smaller.

These $BMCL_{10}$ and $BMDL_{10}$ estimates are similar to or lower than the NOAELs (or LOAEL) reported in the animal studies (Table A-1). A $BMCL_{10}$ or $BMDL_{10}$ estimate may be considered equivalent to a NOAEL estimate [US EPA 2002], and equivalent uncertainty factors applied as described in Appendix A. The resulting OELs would be similar to or lower than those estimated using the NOAELs (or LOAEL). As discussed in Appendix A, the sources of uncertainty in the estimation of the $BMCL_{10}$ or $BMDL_{10}$ estimates include the small number of rats per group (n=5) for the pulmonary inflammation endpoint and the large variability in the silver lung tissue doses between the two subchronic studies [Sung et al. 2008; Song et al. 2013].

TABLES FOR APPENDIX B

Table B-1. Response proportions in Sprague-Dawley rats following subchronic inhalation exposure to silver nanoparticles [Sung et al. 2009]

Bile duct hyperplasia				
	Concentration (µg/m^3)			
Group	**0**	**49**	**133**	**515**
Males	0/10	0/10	1/10	4/9
Females	3/10	2/10	4/10	9/10

Table B-2. Response proportions in Sprague-Dawley rats following subchronic inhalation exposure to silver nanoparticles [Song et al. 2013]

Chronic alveolar inflammation (minimal)				
	Concentration (µg/m^3)			
Group	**0**	**49**	**117**	**381**
Males[a]	0/5	0/5	3/5	5/5

[a] Female response proportions at same concentrations (0/4, 0/4, 0/4, 4/4) are inadequate for BMD modeling.

Table B-3. Response proportions in Sprague-Dawley rats following subchronic inhalation exposure to silver nanoparticles [Sung et al. 2009]

Bile duct hyperplasia [a]				
	Mean Liver Tissue Concentration (ng/g)			
Group	**0.90**	**4.55**	**12.07**	**71.08**
Females	3/10	2/10	4/10	9/10
	Mean Liver Tissue Concentration (ng/g)			
	0.70	**3.52**	**13.75**	**132.97**
Males	0/10	0/10	1/10	4/9

[a] Severity level in female rats: minimum (3/10, 2/10, 4/10, 8/10) and moderate (0/10, 0/10, 0/10, 1/10), respectively, in increasing dose groups; severity level in male rats: minimum in all dose groups.

Table B-4. Response proportions in Sprague-Dawley rats following subchronic inhalation exposure to silver nanoparticles [Song et al. 2013]

Chronic alveolar inflammation (minimal)				
	Mean Lung Tissue Concentration (ng/g)			
Group	**0.82**	**80.65**	**417.40**	**4715.28**
Males[a]	0/5	0/5	3/5	5/5

[a] Female response proportions at same concentrations (0/4, 0/4, 0/4, 4/4) are inadequate for BMD modeling.

Table B-5. Best-fitting Benchmark Concentration (BMC) models of subchronic inhalation responses to silver nanoparticles in Sprague-Dawley rats [Sung et al. 2009].

Model	**AIC**	***p***	**BMC (µg/m^3)**	**BMCL$_{10}$ (µg/m^3)**
Male: Bile duct hyperplasia				
Log-probit	21.1114	0.9806	155.8	92.5
Female: Bile duct hyperplasia				
Logistic	46.8796	0.7073	78.2	50.5

AIC = Akaike Information Criterion.

Table B-6. Best-fitting Benchmark Concentration (BMC) models of subchronic inhalation responses to silver nanoparticles in Sprague-Dawley rats [Sung et al. 2013].

Model	**AIC**	***P***	**BMC (µg/m^3)**	**BMCL$_{10}$ (µg/m^3)**
Male: Alveolar inflammation (minimal)				
Multistage (Degree = 2)[a]	10.1497	0.843	44.8	13.6

AIC = Akaike Information Criterion.
[a] Multistage model only fit to these data, following the methodology described in Appendix A of NIOSH [2013].

Table B-7. Best-fitting Benchmark Dose (BMD) models of subchronic inhalation responses to silver nanoparticles in Sprague-Dawley rats [Sung et al. 2009].

Model	AIC	*P*	BMD (ng/g)	$BMDL_{10}$ (ng/g)
Male: Bile duct hyperplasia				
Gamma	21.4821	0.9281	22.7	11.6
Female: Bile duct hyperplasia				
Logistic	46.7501	0.7624	10.3	6.3

AIC = Akaike Information Criterion.

Table B-8. Best-fitting Benchmark Dose (BMD) models of subchronic inhalation responses to silver nanoparticles in Sprague-Dawley rats [Sung et al. 2013].

Model	AIC	*p*	BMD (ng/g)	$BMDL_{10}$ (ng/g)
Male: Alveolar inflammation (minimal)				
Multistage (Degree = 2)[a]	9.0622	0.9818	145.8	33.0

AIC = Akaike Information Criterion.
[a] Multistage model only fit to these data, following the methodology described in Appendix A of NIOSH [2013].

Table B-9. Summary of rat Model-Average $BMCL_{10}$ estimates from subchronic inhalation studies in Sprague-Dawley rats

Rat study	Endpoint	$BMCL_{10}$ estimate in rats ($\mu g/m^3$) - BCa	$BMCL_{10}$ estimate in rats ($\mu g/m^3$) – Percentile
Sung et al. [2009]	Bile duct hyperplasia in males	30.20	112.49
	Bile duct hyperplasia in females	32.87	24.52
Song et al. [2013]	Chronic alveolar inflammation in males	48.17	36.86

Table B-10. Summary of rat Model-Average $BMDL_{10}$ estimates from subchronic inhalation studies in Sprague-Dawley rats

Rat study	Endpoint	$BMDL_{10}$ estimate in rats (ng/g) - BCa	$BMDL_{10}$ estimate in rats (ng/g) – Percentile
Sung et al. [2009]	Bile duct hyperplasia in males	2.61	14.55
	Bile duct hyperplasia in females	2.09	2.03
Song et al. [2013]	Chronic alveolar inflammation in males	57.18	43.50

APPENDIX C

Occupational Health Surveillance: Informing Decisions for including Medical Surveillance in the Workplace

Key Terms Related to Medical Surveillance

Occupational health surveillance involves the ongoing systematic collection, analysis, and dissemination of exposure and health data on groups of workers for the purpose of preventing illness and injury. Occupational health surveillance, which includes hazard and medical surveillance, is an essential component of an effective occupational safety and health program [Harber et al. 2003; Baker and Matte 2005; NIOSH 2006; Wagner and Fine 2008; Trout and Schulte 2009], and NIOSH continues to recommend occupational health surveillance as an important part of an effective risk management program.

Hazard surveillance includes elements of hazard and exposure assessment.

- The hazard assessment involves reviewing the best available information concerning toxicity of materials; such an assessment may come from databases, texts, and published literature or available regulations or guidelines (such as from NIOSH or OSHA). Human studies, such as epidemiologic investigations and case series or reports, and animal studies may also provide valuable information. In most instances involving silver nanomaterials, there are limited toxicological data and a lack of epidemiologic data with which to make a complete hazard assessment.

- The exposure assessment involves evaluating relevant exposure route(s) (inhalation, ingestion, dermal, and/or injection), amount, duration, and frequency

(that is, dose), as well as whether exposure controls are in place and how protective they are. When data are not available, this will be a qualitative process.

Medical surveillance

Medical surveillance targets actual health events or a change in a biologic function of an exposed person or persons. Medical surveillance involves the ongoing evaluation of the health status of a group of workers through the collection and aggregate analysis of health data, for the purpose of preventing disease and evaluating the effectiveness of intervention programs (primary prevention). NIOSH recommends medical surveillance of workers when they are exposed to hazardous materials and therefore are at risk of adverse health effects from such exposures. Medical screening is a form of medical surveillance used to detect early signs of work-related illness in individual workers. It involves administering tests to apparently healthy persons to detect those with early stages of disease or risk of disease. Medical screening generally represents secondary prevention.

Medical surveillance is a second line of defense, behind the implementation of engineering, administrative, and work practice controls (including personal protective equipment). Integration of hazard and medical surveillance is key to an effective occupational health surveillance program, and surveillance of disease or illness should not proceed without having a hazard surveillance program in place.

Planning and Conduct of Medical Surveillance

Important factors when considering medical surveillance include:

(1) a clearly defined purpose or objective,
(2) a target population that is clearly defined, and

(3) the availability of testing modalities to accomplish the defined objective (these may include questionnaires, physical examinations, and medical testing).

A clear plan should be established before a medical surveillance program is initiated. The plan should include:

(1) a rationale for the type of medical surveillance,
(2) provisions for interpreting the results,
(3) presentation of the findings to workers and managers of the affected workplace, and
(4) implementation of all the other steps of a complete medical surveillance program [Harber et al. 2003].

The elements for conducting a medical surveillance program generally include the following:

(1) an initial medical examination and collection of medical and occupational histories

(2) periodic medical examinations at regularly scheduled intervals, including specific medical screening tests when warranted

(3) more frequent and detailed medical examinations, as indicated, on the basis of findings from these examinations

(4) post-incident examinations and medical screening following uncontrolled or non-routine increases in exposures, such as spills

(5) worker training to recognize symptoms of exposure to a given hazard

(6) a written report of medical findings

(7) employer's actions in response to identification of potential hazards.

APPENDIX D

Literature Search Strategy

An initial literature search, record retrieval, and evaluation of studies was conducted by the Oak Ridge Institute for Science and Education (ORISE). A report was submitted to NIOSH in June 2012 that provided an evaluation of the experimental in vivo and in vitro studies with silver nanoparticles. Studies cited in the report were identified from literature searches using PubMed, Toxline, Embase, and BIOSIS. Search terms included silver nanoparticles as well as the use of other relevant key words (e.g., toxicology, physical and chemical properties, dosimetry).

In January 2013, NIOSH conducted an updated and expanded literature search to identify studies with exposure to silver and/or silver nanoparticles. Search terms were selected to ensure that all in vivo and in vitro studies with silver and/or silver nanoparticles were identified as well as studies describing workplace exposure. Literature searches were conducted in the on-line databases CINAHL, PubMed, Compendex, Embase, HSDB, NIOSHTIC-2, Risk Abstracts, Toxicology Abstracts, Toxline, and Web of Science. In June 2014 a follow-up literature search was conducted using the same search terms to identify relevant studies published since January 2013.

Articles from the updated literature searches were retrieved if found to be relevant following examination of titles and abstracts by the authors. The articles selected from the updated literature searches for full review included any in vivo studies on silver nanoscale or microscale particles and any in vitro studies that provided new information on the role of particle size and/or solubility on the toxicological effects. Studies cited in retrieved articles, but not identified during the primary and follow-up database searches, were retrieved for evaluation. For each article retrieved, the quality of the study design (including the risk of bias), relevance of the evidence to workers, and quality of the study methodology were assessed by the authors to determine their appropriateness for inclusion in the document.

Appendix E

In Vitro/Mechanistic Studies

A considerable number of research reports address the impacts of AgNPs on isolated cellular systems. These studies provide inferential evidence of the capacity of AgNPs to bring about cellular changes of potential toxicological consequence, and in many cases they contribute to our understanding of what biochemical and physiologic mechanisms might be triggered when AgNPs interact with cellular systems. In an extensive database of in vitro studies, the predominant topic areas for cellular and subcellular changes brought about by AgNPs are (1) development of oxidative stress and the induction of apoptosis and (2) DNA damage/genotoxicity. In the following paragraphs, results of in vitro and mechanistic studies of AgNPs are discussed within these general topic areas. Other relevant studies highlight possible impacts of AgNP exposure on gene expression and regulation, neurologic changes, effects on skin cells, and cytotoxicity.

E.1 Oxidative Stress/Induction of Apoptosis

A wide range of cellular isolates and cultures have been used to examine cellular uptake of AgNPs and the oxidative stress and apoptotic effects of AgNPs in vitro. These studies provide some evidence of the toxic potential of the particles and provide insight into the physiologic and biochemical mechanisms that may be responsible. Among the many cellular systems that have formed a platform for these investigations are liver/hepatoma cells [Piao et al. 2011; Liu et al. 2010; Arora et al. 2009; Kim et al. 2009c; Hussain et al. 2005a]; rat alveolar and mouse peritoneal macrophages [Park et al. 2010b; Carlson et al. 2008; Hussain et al. 2005b]; fibroblasts [Wei et al. 2010; Arora et al. 2009, 2009; Hsin et al. 2008]; HeLa cells [Miura et al. 2009]; human acute monocytic leukemia cell lines (THP-1 monocytes) [Foldbjerg et al. 2009]; rat vascular smooth muscle cells [Hsin et al. 2008]; bovine retinal endothelial cells [Kalishwaralal et al. 2009]; mouse blastocysts [Li et al. 2010]; mouse MC3T3-E1 cells, rat adrenal PC12

cells, human HeLa cervical cancer cells, and hamster ovary CHO cells [Kim et al. 2012]; A549 human lung cells [Lee et al. 2011c; Liu et al. 2010; Foldbjerg et al. 2011; Stoehr et al. 2011]; A431 human skin carcinoma cells [Arora et al. 2008]; SGC-7901 human stomach cancer cells [Liu et al. 2010]; MCF-7 human breast adenocarcinoma cells [Liu et al. 2010]; murine alveolar cell line and human macrophage and epithelial lung cell lines [Soto et al. 2007]; hamster kidney (BHK21) and human colon adenocarcinoma (HT29) cell lines [Gopinath et al. 2010]; human mesenchymal stem cells (hMSCs) [Greulich et al. 2009, 2011; Hackenberg et al. 2011]; A549 lung cells [Beer et al. 2012]; and human adipose-derived stem cells (hASCs) [Samberg et al. 2012].

Examples of the general approach to in vitro experimentation with AgNPs may be found in studies conducted at Wright-Patterson Air Force Base in which rat alveolar macrophages were incubated with different sizes of AgNPs [Hussain et al. 2005b; Carlson et al. 2008]. The cells, at 80% confluence, were incubated for 24 hours with various concentrations of hydrocarbon-coated AgNPs in a physiologic medium. The particles were 15, 30, 55, or 100 nm in diameter. Parameters under investigation included cellular morphology and uptake of AgNPs, mitochondrial function, membrane integrity, generation of ROS, glutathione content, mitochondrial membrane potential, and the inflammatory response. Study results indicated that AgNPs with the smallest diameter were more effective than larger nanoparticles at bringing about physiologic and toxicological changes. For example, at silver concentrations up to 75 μg/mL, 15-nm AgNPs appeared to be more effective at releasing LDH from the cells, as a measure of lowered cell viability. Similarly, when the fluorescence intensity of dichlorofluorescein (DCF) in the presence of AgNPs was assessed for the various incubation products, 15-nm silver nanoparticles appeared to induce a greater intensity of fluorescence, a response indicative of enhanced generation of ROS. Concomitant with the enhanced generation of ROS was a significant depletion of cellular reduced glutathione (GSH) levels, lowered mitochondrial function as indicated in the 3-(4,5-dimethylthiazol-2-yl)-2,5-diphenyltetrazolium bromide (MTT) viability assay, and the loss of mitochondrial membrane potential. Carlson et al. [2008] also demonstrated a treatment-related increase in TNF-α, macrophage inflammatory protein-2, and IL-1β but not IL-6 in the

supernatant of macrophage/AgNP incubations. The authors suggested that the significant depletion of GSH levels may have created an imbalance between antioxidants and ROS, thereby resulting in oxidative stress and cellular damage. However, the degree to which this effect was related to the release of cytokines/chemokines remained unclear, since these responses did not appear to be influenced by particle size.

Given the importance of the liver as an important target organ of toxicity associated with AgNPs, a number of research groups have used cultures of hepatocytes to investigate the possible toxic effects of AgNPs in vitro. For example, the Wright-Patterson Air Force Base group, using BRL 3A rat liver cells, studied a range of endpoints [Hussain et al. 2005a] similar to those previously evaluated with use of rat alveolar macrophages [Hussain et al. 2005b; Carlson et al. 2008]. The two species of AgNPs employed were defined by diameters of either 15 or 100 nm, although little additional information was provided about the method of formation or their potential for aggregation. Using dose concentrations of 5 to 50 μg/mL and incubation times of up to 24 hours, the authors measured cytotoxicity by leakage of LDH and deficits in mitochondrial function in the presence of MTT. Other parameters under investigation included changes in cellular morphology, formation of ROS, depletion of GSH levels, and changes to mitochondrial membrane potential. Both sets of AgNPs appeared to be effective at inducing a concentration-dependent depletion of mitochondrial function and the release of LDH to the culture medium. Under the microscope, the cells displayed a range of distortions in comparison with untreated cells, and by analogy to the same group's results with rat alveolar macrophages, they showed a concentration-dependent increase in ROS and depletion of GSH. Hussain et al. [2005a] concluded that the cytotoxicity of AgNPs was likely to be mediated through oxidative stress.

Many of these same manifestations of oxidative stress and cell viability were evident when cultured HepG2 human hepatoma cells were incubated with commercially obtained 10-nm AgNPs dispersed in an aqueous medium [Kim et al. 2009c]. The researchers ensured that any deficits in these parameters could be unequivocally

assigned to the effect of the AgNPs by using an ion exchange resin to remove any free silver ions that might have been associated with the nanoparticle preparations. Then, in parallel incubations, they compared the capacity of equivalent amounts of silver in AgNPs and solutions of silver nitrate to reduce cell viability and/or induce oxidative stress and DNA damage. Cytotoxicity was measured with MTT and AB reduction assays and by LDH leakage, and data were expressed as median inhibitory concentration (IC_{50}) values. For each parameter under investigation, increasing concentrations of silver brought about a reduction in cell viability in a dose-dependent manner. However, for both dye-reduction assays, free silver ions reduced cell viability to a greater extent than did the silver nanoparticles. By contrast, release of LDH activity was brought about more completely and at a lower silver concentration by incubation with AgNPs as compared with free silver ions (with IC_{50} of 0.53 ± 0.19 versus 0.78 ± 0.10 µg/mL). This difference was not statistically significant. Pre-incubation of the cells with N-acetyl cysteine (NAC) abolished these manifestations of reduced cell viability by a presumed reduction in the oxidative stress that had become apparent whether the cells were incubated with either AgNPs or a silver solution. Moreover, further evidence of the importance of oxidative stress in relation to AgNP toxicity was obtained by including the antioxidant N-acetylcysteine in the incubation medium 2 hours prior to the addition of the AgNP or silver nitrate preparations. Deficits in mitochondrial function and cellular membrane integrity and the occurrence of oxidative stress were largely abolished by this pretreatment. Kim et al [2009c] used intracellular fluorescence as an indicator of the formation of ROS in the presence of either AgNP or silver anion preparations. In each case, ROS formation was abolished by pretreatment with NAC. In an effort to understand the mechanism(s) whereby AgNPs caused intracellular oxidative stress, the authors used RT-PCR to study the expression of oxidative stress–related genes such as glutathione peroxidase 1 (GPx1), catalase, and superoxide dismutase 1 (SOD1). In contrast to the effect of aqueous silver nitrate, AgNPs did not induce messenger ribonucleic acid (mRNA) expression of GPx1. However, the mRNA levels of catalase and SOD1 were increased in response to 24-hour incubation with AgNPs. Detection of phosphorylation on the H2AX gene, indicative of DNA double-strand breaks, was also thought to be associated with oxidative stress, because this effect was

abolished as well after pre-incubation with N-acetylcysteine. Kim et al. [2009c] concluded that silver in free solution or on nanoparticles induced cytotoxicity as a result of oxidative stress. However, because the expression of oxidative stress-related mRNA species appeared to be regulated differently by AgNPs than by silver cations, the precise mechanism of AgNP activity may be different from that of soluble silver.

HepG2 cells were also used as a platform for the study of AgNP toxicity by Liu et al. [2010]. The researchers used PVP-coated nanoparticles with defined sizes of 5, 20, and 50 nm. All AgNP preparations were formed chemically by the reduction of silver nitrate by sodium hypophosphite in the presence of sodium hexametaphosphate and PVP, adjusted to a concentration of 1 g/L in deionized water, and dispersed by ultrasonication. In evaluating HepG2 responses to AgNPs, Liu et al. [2010] observed changes to cell morphology, viability, membrane integrity, and induction of oxidative stress by experimental procedures that were closely similar to those previously described. Ultrastructural analysis using TEM revealed the presence of AgNPs inside the cells, with the smaller particles apparently more effective at penetrating the membrane and inducing the toxic effects. Liu et al. [2010] attempted to distinguish between apoptotic and necrotic cell death as a result of AgNP treatment with the double staining technique, using annexin V-fluorescein isothiocyanate (FITC) for apoptosis and propidium iodide (PI) for necrosis. When HepG2 cells were incubated at 0.5 μg/mL for 24 hours, the relative amounts of apoptotic cells were 4.64%, 8.28%, 6.53%, and 4.58% for silver nitrate and AgNPs (5 nm, 20 nm, and 50 nm), respectively, all compared to an incidence in controls of 2.39%. The authors concluded that despite the increased fraction of apoptotic cells in the silver-exposed groups, there was no difference between the treated and control groups for necrosis. Therefore, the AgNP-induced cell death was caused mainly by apoptosis.

Piao et al. [2011] incubated human Chang liver cells with AgNPs prepared by the THF approach to demonstrate oxidative stress and to probe the biochemical and physiologic mechanisms that might be associated with this phenomenon. The authors reported that the nanoparticles had undergone a degree of aggregation in the incubation medium,

with a size distribution of 28 to 35 nm in diameter, an increase from the original 5 to 10 nm. Cellular morphology, viability, mitochondrial efficiency, intracellular formation of ROS, and GSH levels were measured by means of "standard techniques," with and without N-acetylcysteine. A comparison of equivalent amounts of silver on nanoparticles or in solution in the MTT assay gave IC_{50} that differed by a factor of two. This suggested that silver in nanoparticle form was more damaging to the cells than silver in free solution (IC_{50} of 4 µg/mL for AgNPs, versus 8 µg/mL for silver nitrate). In mechanistic analysis, the spectrum of intracellular proteins was surveyed by Western blot analysis, and a comet assay was performed to determine the degree of oxidative DNA damage. Flow cytometry was used to determine the percentage of apoptotic sub-G1 hypodiploid cells, and the amount of cellular DNA fragmentation was assessed by cytoplasmic histone-associated DNA fragmentation. The expected picture of oxidative-stress-related cytotoxicity and partial blockade with N-acetylcysteine was obtained. The comet assay showed that incubating human Chang liver cells with silver nanoparticles increased the tail length and the percentage of DNA in the tails, as compared to control cells. Other markers of oxidative stress, such as the levels of lipid peroxidation and the degree of protein carbonyl formation, were increased in AgNP-treated cells compared to control cells. The authors of the study compiled an array of mechanistic data that pointed to AgNP-induced induction of apoptosis via a mitochondrial and caspase-dependent pathway. For example, after treatment with AgNPs, the AgNP-associated decrease in Bcl-2 expression and concomitant increase in Bax expression resulted in the following increases in Bax/Bcl-2 ratio with time: 1.0, 7.0, 9.5, 12.8, and 24.5 at 0, 6, 12, 24, and 48 hours, respectively. A change in ratio at this level led to the release of cytochrome from the mitochondrion and the occurrence of active forms of caspases 9 and 3. The authors interpreted their data as indicating that AgNP-induced apoptosis might be mediated through a caspase-dependent pathway with mitochondrial involvement.

The importance of c-Jun NH_2-terminal kinase (JNK) in mediating the apoptotic effects in human Chang liver cells was demonstrated by its time-dependent phosphorylation in the presence of AgNPs. In parallel with the retention of cell viability, the effect was

attenuated by pretreatment with the JNK-specific inhibitor SP600125 or by transfection with small, interfering RNA against JNK [Piao et al. 2011].

Many of the same responses that indicated induction of oxidative stress and apoptosis in macrophages and liver cells have also been observed in fibroblasts when incubated with AgNPs. For example, Arora et al. [2008] used a commercial preparation of AgNPs (7–20 nm in diameter) in an aqueous suspension to challenge HT-1080 human fibrosarcoma cells and A431 human skin carcinoma cells. Using a variant of the MTT assay for mitochondrial function with the compound sodium 3′-[1-(phenylaminocarbonyl)-3, 4-tetrazolium]-bis (4-methoxy-6-nitro) benzene sulfonic acid hydrate, a dose-dependent effect on cell viability was obtained in the concentration range of 6.25 to 50 µg/mL. Subsequent incubation of the cultures at one half the median inhibitory concentration (IC_{50}) of approximately 11 µg/mL gave an array of responses indicative of oxidative stress, including a reduction in GSH content and SOD activity and an increase in lipid peroxidation. An increase in treatment-related DNA fragmentation and a biphasic response in caspase-3 activation (in which the enzyme was induced up to a AgNP concentration of 6.25 µg/mL but suppressed at higher concentrations) indicated that cell death occurred by apoptosis at AgNP concentrations up to 6.25 µg/mL but by necrosis at higher concentrations. However, AgNP-induced oxidative stress and apoptosis were less evident when the same researchers carried out equivalent studies in primary mouse fibroblasts and liver cells [Arora et al. 2009]. Respective IC_{50} values were 61 and 449 µg/mL and little change was seen in intracellular GSH and lipid peroxidation at one half the IC_{50}. The AgNPs in these studies were synthesized by an unspecified proprietary process. They were reported to be stable in culture media, with >90% of the particles with diameters between 7 and 20 nm. Possible agglomeration of the particles in the culture media was not mentioned. The results suggest that the primary cell preparations contained sufficient antioxidant capacity to protect the cells from possible oxidative damage.

Similar to the results reported by Piao et al. [2011] from studies with human Chang liver cells, the study by Hsin et al. [2008] used NIH3T3 fibroblasts to investigate the link

between the mitochondrial-related generation of ROS, the incidence of apoptosis, and the activation of JNK. Incubating mouse L929 fibroblasts with nanoparticles also resulted in an increased incidence of apoptosis and a greater percentage of cells arrested in the G2M phase of the cell cycle [Wei et al. 2010]. Larger-scale silver entities (silver microparticles with a range of shapes and diameters between 2 and 20 µm) did not bring about these changes and were not internalized by the cells to the same extent as AgNPs. Transmission electron micrographs appeared to provide direct evidence that AgNPs but not microparticles entered the cells via an endocytic pathway. The authors concluded that AgNPs were more cytotoxic to L929 cells than silver microparticles. Differences were characterized by the ability of nanoparticles to enter the cells, causing morphologic abnormalities and apoptosis, and the cell cycle being arrested in the G2M phase.

Foldbjerg et al. [2009] used a human acute monocytic leukemia cell line (THP-1 cells) as a platform for studying the relative capacity of AgNPs and ionic silver to induce ROS, apoptosis, and necrosis. As obtained from the supplier, the particles were 30 to 50 nm in diameter and coated with 0.2% PVP. When the AgNPs were prepared in a stock solution, a major peak size of 118 nm was obtained. This preparation, as well as an equimolar solution of silver cations, was used to incubate THP-1 at a dose range of 0 to 7.5 µg/mL (calculated as silver mass), with an incubation time of up to 24 hours. The fluorescent marker, DCF, was used to measure the intracellular generation of ROS, and the annexin V/PI double staining technique was used to discriminate between cells undergoing apoptosis or necrosis. The presence of apoptosis was confirmed with the terminal deoxynucleotidyl transferase dUTP nick end labeling (TUNEL) assay. As indicated by the results of the annexin V/PI assay, both AgNPs and silver cations brought about a significant reduction in the percentage of viable cells after 24 hours' exposure. The median effective concentrations (EC_{50}) were 2.4 and 0.6 µg/mL, respectively, indicating that silver cations were approximately four times more toxic than AgNPs. Silver nanoparticles and silver cations likewise increased the production of ROS, as indicated by the differential formation of DCF. A 35% increase in cells positive for DNA breakage was observed when compared to controls when THP-1 cells were

incubated with AgNPs for 6 hours at a concentration of 5 µg/mL. In general, the findings of this study point to a strong correlation between the increase in intracellular ROS, DNA damage, and high levels of apoptosis and necrosis for both AgNPs and ionic silver. In a follow-up study, Beer et al. [2012] evaluated the degree to which the silver ion fraction of AgNP suspensions contribute to the toxicity of AgNPs, using A549 human lung carcinoma epithelial-like cell line. PVP-coated (0.2%) spherical AgNPs, with dimensions ranging in size from 30 to 50 nm, were exposed to suspensions/supernatants containing either 39% (0.2 µg/mL) or 69% (1.6 µg/mL) silver ions for 24 hours. At 1.6 µg/mL total silver, A549 cells exposed to an AgNP suspension containing a 39% silver ion fraction showed a cell viability of 92%, whereas cells exposed to an AgNP suspension containing a 69% silver ion fraction had a cell viability of 54%, as measured by the MTT assay. At initial silver ion fractions of 5.5% and above, AgNP-free supernatant had the same toxicity as AgNP suspensions. Flow-cytometric analyses of cell cycle and apoptosis confirmed that there was no significant difference between the treatments with AgNP suspension and AgNP supernatant, as measured by MTT assays. A clear association was observed between the amount of silver ions present in the solution and the toxicity of the AgNP suspensions. As found in the study of Foldbjerg et al. [2011], ionic and/or nanoparticulate silver induces ROS in A549 cells.

Liu et al. [2010] examined the impact of different sizes of AgNPs on oxidative stress and incidence of apoptosis in HepG2 cells, also using cultures of SGC-7901 human stomach cancer cells, MCF-7 human breast adenocarcinoma cells, and A549 human lung adenocarcinoma cells to ensure the universality of the toxic effect. This study was followed-up by Lee et al. [2011c] to investigate the cytotoxic potential of AgNPs and the pathways by which they impact A549 cells. In addition to findings that AgNPs induce the reduction in cell viability, increase LDH release, alter cell cycle distribution, and change the expression of Bax and Bcl-2 reflective of increased apoptosis, AgNPs were also found to alter mRNA levels of protein kinase C (PKC) isotypes.

Soto et al. [2007] also used the results from a series of assays with A549 cells to compare the cytotoxicity potential of a wide range of nanoparticle material, including

AgNPs, titanium dioxide (TiO_2), multiwall carbon nanotubes, chrysotile asbestos, Al_2O_3, Fe_2O_3, and ZrO_2, using both a murine lung macrophage cell line (RAW 264.7) and a human lung macrophage cell line (THB-1). Relative cell viabilities were measured at a constant nanoparticulate material concentration of 5 µg/mL for the different cell lines. All of the nanoparticulate materials, except for TiO_2, showed a cytotoxic response, and AgNPs were particularly cytotoxic to the murine lung macrophage cell line. The nanoparticulate materials were observed to have a greater toxic effect in A549 cells, with the TiO_2 samples demonstrating a slight cytotoxic response. The A549 cells were found to be more sensitive than the murine and human macrophages. No correlation was found when particle surface area was used as an index for comparing cytotoxicity. Particle morphology or aggregate morphology was also not correlated with the cytotoxicity response for either the murine or the human cell line exposure, since a variety of morphologies within the nano-size range exhibited equivalent or similar cytotoxicity's.

The degree of cell viability after 24-hour incubation with AgNPs was assessed in HeLa cells with use of Alamar blue reagent as a probe for cell viability [Miura and Shinohara 2009]. An IC_{50} of 92 µg/mL silver was obtained. The AgNPs were provided by the supplier with a specified diameter of 5 to 10 nm and were stabilized with a proprietary protectant. TEM analysis confirmed the particle size but showed the presence of some aggregates as well. To analyze for apoptosis, cells were incubated for 3 hours with various concentrations of AgNPs, double stained with Annexin V (FITC-conjugated) and PI, and then analyzed by flow cytometry. As charted by the authors, AgNPs appeared to induce apoptosis in a dose-dependent manner up to 120 µg/mL. In an effort to assess the expression level of genes potentially associated with apoptosis, Miura and Shinohara [2009] extracted total RNA from HeLa cells that had been incubated with silver nanoparticles for 4 hours and used RT-PCR to determine the expression of stress-related genes such as those for heme oxygenase-1, metallothionein-2A, and heat shock protein 70. Silver nanoparticles were effective in increasing the expression of heme oxygenase-1 and mettothionein-2A several-fold but not heat shock protein-70. This discrepancy was different from the pattern of gene expression obtained when cells

were exposed to cadmium sulfate, in which all three stress-related genes were strongly expressed in response to treatment.

Gopinath et al. [2010] examined the effects of AgNPs on gene expression in an endeavor to assess the fundamental mechanisms that contribute to AgNP-induced cell death through mediated apoptosis. Hamster kidney (BHK21) and human colon adenocarcinoma (HT29) cells were treated with <20-nm-diameter AgNPs from 30 minutes to 6 hours. In order to assess the mode of cell death induced by AgNPs, treated cells were stained with FITC Annein V and PI for flow cytometric analysis. An increase in early apoptotic population was observed in treated BHK21 cells (9%) and HT29 cells (11%), compared to control cells. Expression profiles of apoptotic genes such as, bak, bax, bad, C-myc, and caspase-3 were analyzed, and an upregulation of p53 gene in the AgNP-treated cells was observed. On the basis of these gene expression profiles, the investigators proposed that AgNP treatment of both BHK21 and HT29 cells leads to programmed cell death (that is, apoptosis) as a result of a cascade reaction that activates caspase-3, which penetrates the nuclear membrane to induce DNA fragmentation. This extracellular cytotoxic stress on the cell membrane upregulates p53, which in turn acts on other apoptotic molecules and causes the mitochondria to induce apoptosis.

Schaeublin et al. [2011] evaluated the response to silver nanowires (4 or 20 µm in length; ~90 nm in diameter) in an in vitro co-culture assay with human alveolar lung cells [Schaeublin et al. 2011] 24 hours after exposure to 200 ng/mL. Neither AgNW length was toxic to the cells (on the basis of normal cell morphologic appearance) or decreased the cell viability (on the basis of MTS assay of mitochondrial function). However, both AgNW lengths were associated with an increase in some inflammatory cytokines (IL-6, IL-8, and interferon gamma). These results showed that the AgNWs were not cytotoxic at the dose evaluated but did cause irritant and inflammatory responses.

E.2 DNA Damage/Genotoxicity

Ahamed et al. [2008] used mouse embryonic stem (MES) cells and mouse embryonic fibroblasts (MEF) to study the link between AgNP-induced apoptosis and DNA damage. Two types of AgNPs were used; uncoated plasma gas-synthesized particles and polysaccharide-coated particles, both approximately 25 nm in diameter. As visualized with a Cell Tracker Green fluorescent probe and observed under confocal microscopy, both types of AgNPs were taken up by the cell, although uncoated particles showed a greater tendency to aggregate and were excluded from certain organelles such as the nucleus and mitochondria. Coated particles were distributed throughout the cell. As determined by Western blot analysis, expression of annexin V protein was enhanced by both species of nanoparticles, confirming the role of AgNPs in the induction of apoptosis in these cell lines. This was accompanied by upregulation of the p53 tumor suppressor gene, increased induction of the Rad51 double strand break repair protein, and enhanced phosphorylation of the histone H2AX at the serine-139 residue. Because the latter effect is also thought to occur in response to a DNA double break, the authors interpreted their data as an indication that both types of AgNPs had induced increased p53 expression and double strand DNA breakage, with concomitant apoptosis in MES and MEF cells. Uncoated (and less agglomerated) particles appeared to be more effective in bringing about these responses.

Foldbjerg et al. [2011] detected perturbations in the genetic architecture of the human lung A549 cancer cell line in response to AgNPs and silver in solution. In the former case, the 30- to 50-nm particles were coated with 0.2% PVP. As before, the cytotoxicity of AgNPs and silver in solution was assessed by a decrease in mitochondrial activity with the MTT assay. Silver ions induced dose-dependent reductions in mitochondrial function to a greater extent than equivalent concentrations of silver in nanoparticle form. In both cases, these effects were significantly reduced by pretreating the cells with NAC. However, AgNPs induced greater amounts of ROS, suggesting that these entities could not be solely due to the potential release of silver ions from the nanoparticles. AgNP-induced cytotoxicity and ROS formation were accompanied by the formation of

bulky DNA adducts, as demonstrated by ^{32}P post-labeling. Although the chemical identity of adducts was not determined, the authors speculated that these endogenously formed “I-compounds” were similar to those found to accumulate in an age-dependent manner in the absence of exogenous carcinogens. The strongly correlated responses were both inhibited by pretreatment with the antioxidant N-acetyl-cysteine, suggesting the AgNPs had triggered ROS-induced genotoxicity.

The effect of particle shape and size of Ag particles on causing toxic and immunotoxic effects was investigated by Stoehr et al. [2011]. Silver nanowires (length, 1.5–25 µm; diameter, 100–160 nm), AgNPs (30 nm), and silver microparticles (<45 µm) were tested with alveolar epithelial cells (A549) for cell viability and cytotoxicity. AgNWs and AgNPs were synthesized by wet chemistry, while silver microparticles were synthesized by the reduction of silver salt with sodium citrate. AgNWs, AgNPs, and silver microparticles were all coated with PVP to make them biocompatible and to keep them dispersed in water. TEM analysis of sample preparations confirmed that AgNWs and AgNPs were mostly monodispersed with little agglomeration, while some sedimentation and minor agglomeration of the silver microparticles was observed. Eight different AgNW concentrations (range, 5.05–16.47 mg/mL) as well as single concentrations of AgNPs (0.33 mg/mL) and silver microparticles (13.5 mg/mL) were prepared that overlapped in mass concentration and surface area. Ion release by the tested silver materials was determined by means of inductively coupled plasma mass spectrometry (ICP-MS), and the effects of the released ions on cell viability and LDH generation were measured. To compare the effects on an activated and a resting immune system, the epithelial cells were stimulated with rhTNF-α or left untreated. Changes in intracellular free calcium levels were determined with calcium imaging. No effects were observed with AgNPs and silver microparticles on A549 cells, whereas AgNWs induced a strong cytotoxicity, loss in cell viability, and early calcium influx; however, the length of the AgNWs had minimal effect on the observed level of toxicity. The investigators hypothesized that the increase in toxicity and the absence of specific immunotoxic responses to AgNWs may be a result of its needle-like structure, making it easier to penetrate the cell membrane. Also, because of the lengths of the AgNWs, entry into the cell may have been

incomplete, causing cell membrane damage that resulted in impaired repair and eventually cell death.

Greulich et al. [2009] evaluated the biologic activity of AgNPs on human tissue cells by exposing hMSCs to PVP-coated AgNPs (~100 nm in diameter) and determining their effect on cell viability, cytokine release, and chemotaxis. AgNPs were prepared by the polyol process and hMSCs were exposed either to AgNP concentrations of 0.5, 1, 2.5, 3, 3.5, 4, 5, and 50 µg/mL or to silver ions (silver acetate) for up to 7 days. At AgNP concentrations of 3.5 to 50 µg/mL, no viable cells were detected. When silver acetate was used, the cytotoxic effect of silver was observed at a silver concentration of 2.5 µg/mL, whereas no cytotoxic reactions of hMSC were observed with AgNPs at concentrations of ≤3 µg/mL and with silver acetate at concentrations of ≤1 µg/mL. There was also a significant decrease in the release of IL-6, IL-8, and VEGF (typical set of cytokines from hMSCs) in the presence of AgNPs as well as with silver acetate in the concentration range of 5 to 50 µg/mL. Silver acetate concentrations below 2.5 µg/mL (for ions) and below 5 µg/mL (for AgNPs) did not lead to a decrease in cytokine formation. The findings indicate that AgNPs exert cytotoxic effects on hMSCs at high concentrations but also induce cell activation (as analyzed by the release of IL-8) at high but nontoxic concentrations of nanosilver. The same investigators [Kittler et al. 2010] also studied the effect of aging on the toxicity of PVP- and citrate-coated AgNPs (diameter of metallic core, 50 ± 20 nm), using hMSCs at water-solution concentrations of 50, 25, 20, 15, 5, 2.5, and 1 mg/L. AgNPs were stored at these concentrations for 3 days, 1 month, and 6 months and evaluated for cell viability and morphology. Aged AgNPs (at 50 mg/L) stored for 1 and 6 months caused complete cell death, whereas at 3 days the reduction in viability was 70%. AgNPs that were stored in solution for 6 months had a lethal concentration that was about 20 times smaller than that of freshly prepared AgNPs, indicating the release of silver ions during storage. However, the released silver ions were probably bound by proteins and therefore rendered less toxic. Cell viability at 6 months increased as the concentration decreased. The dissolution rates for the PVP- and citrate-coated AgNPs were studied at different temperatures. Dissolution was only partial for each functionalized AgNP, and the degree of dissolution

did not depend on the absolute concentration of silver nanoparticles but seemed to be an intrinsic (but temperature-dependent) property of the nanoparticles. The rate of dissolution and the final degree of dissolution were higher for the PVP-coated than for the citrate-functionalized AgNPs.

In a follow-up study by the same investigators [Greulich et al. 2011], the uptake of AgNPs into hMSC was examined to determine if more than one endocytotic pathway was involved. PVP-coated AgNPs with a metallic core of 50 ± 20 nm in diameter were used. The uptake of AgNPs into hMSC was determined by exposing hMSC for 24 hours at concentrations of 2.5, 2.0, 1.5, 1.0, or 0.5 µg/mL silver ions (silver acetate) or 50, 30, 25, 20, or 15 µg/mL AgNPs and quantitatively analyzing the intracellular side scatter signal by flow cytometry. AgNP uptake by hMSCs was observed to occur by clathrin-dependent endocytosis and by micropinocytosis, and the ingested nanoparticles subsequently occurred as agglomerates in the perinuclear region and not in the cell nucleus, endoplasmic reticulum, or Golgi complex. The inhibition of the clathrin-mediated pathway did not result in complete suppression of endocytosis, indicating that more than one endocytotic pathway might be involved.

The widespread use of AgNP-treated dressings to heal wounds and prevent infection led Hackenberg et al. [2011] to investigate the dosimetry for the agent's ability to induce toxicity in hMSCs. As supplied, the nanoparticles had a mean diameter of 46 nm, although aggregation to a mean diameter of 404 nm was observed when the particles were dispersed in physiologic medium or situated within the cells. Significant cytotoxicity was observed at a concentration of 10 µg/mL and a degree of DNA damage was indicated in the comet assay and by a significant increase in chromosomal aberrations. Chromosomal aberrations consisting of chromatid deletions and exchanges were induced at concentrations of 0.1 µg/mL and above. Hackenberg et al. [2011] compared this concentration with published data on the growth inhibition of *Staphylococcus aureus*, for which AgNP concentrations of 3.5 µg/mL had been reported [Kim et al. 2007]. This led Hackenberg et al. [2011] to conclude that the cytotoxic and genotoxic

potential of AgNPs in hMSCs occurred at significantly higher doses than did their antimicrobial effects.

Similarly, Samberg et al. [2012] assessed the toxicity and cellular uptake of both undifferentiated and differentiated human adipose-derived stem cells (hASCs) exposed to AgNPs and evaluated their effect on hASC differentiation. The stem cells were exposed to 10- or 20-nm AgNPs (confirmed by TEM analysis) at concentrations of 0.1, 1.0, 10.0, 50.0, and 100.0 µg/mL either before or after differentiation. Baseline-viable hASCs were first differentiated down the osteogenic and adipogenic pathways or maintained in their proliferative state for 14 days and then exposed for 24 hours at concentrations of 0.1 through 100.0 µg/mL. To evaluate potential cellular uptake of AgNPs into hASCs, undifferentiated hASCs were grown to 100% confluency in complete growth medium for 5 days, while the effects of AgNPs on hASC differentiation were determined also with use of undifferentiated hASCs grown to 100% confluency in complete growth medium for 5 days. Exposure to either 10- or 20-nm AgNPs resulted in no significant cytotoxicity to hASCs and minimal dose-dependent toxicity to adipogenic and osteogenic cells at 10 µg/mL. Adipogenic and osteogenic cells showed cellular uptake of both 10- and 20-nm AgNPs without significant morphologic changes to the cells, in comparison with controls. Exposure to 10- or 20-nm AgNPs did not influence the differentiation of the cells at any concentration and only resulted in a minimal decrease in viability at antimicrobial concentrations. Exposure to AgNPs also resulted in no significant cytotoxicity to undifferentiated hASCs, either prior to differentiation or following 14 days of differentiation.

The association of AgNP incubation of IMR-90 human lung fibroblast cells and U251 human glioblastoma cells with genetic perturbations, as well as mitochondrial damage and ROS formation, was demonstrated by AshaRani et al. [2009]. The AgNPs employed in the study were administered at concentrations of 25, 50, or 100 µg/mL and were to have been synthesized by the reduction of silver nitrate solution with sodium borohydride, followed by the addition of a filtered starch solution with constant stirring. The starch-coated particles were 6 to 20 nm in diameter and were stated to have good

stability in water. Consistent with the work of others, the study demonstrated uptake of the particles into the cell cytoplasm and nucleus, causing an alteration in cell morphology and reduced viability, deficits in mitochondrial performance, and ROS production. Whereas annexin-V staining showed that only a small percentage of cells underwent apoptosis, cell cycle arrest in the G2M phase and data from the comet and cytokinesis-blocked MN assays gave an indication of treatment-associated DNA damage. For example, the comet assay of AgNP-treated cells showed a concentration-dependent increase in tail momentum, and chromosomal breaks were detected in the cytokinesis-blocked MN assay. This effect was especially noticeable in the U251 cell line.

Nallathamby and Xu [2010] used a novel approach to chart the changes in cellular growth and subcellular morphology when mouse fibroblast (L929) tumor cells were incubated with AgNPs. The particles were synthesized by chemical reduction of silver chlorate with sodium borohydride and sodium citrate. The product was stable in aqueous solution and inside single living cells with a median diameter of 12 nm. When the cells were incubated in flasks with AgNPs at 0, 11, or 22 µg/mL, the uptake of particles and inhibition of growth occurred as a function of concentration and duration of exposure. However, by culturing the cells on coverslips in Petri dishes, the impact of AgNPs on individual cells could be visualized by microscopy. The result was a dose- and exposure-related formation of cells with single giant nuclei or cells with two, three, or sometimes four nuclei per cell. After incubation for 72 hours, almost all of the L929 fibroblast cells displayed one of these altered nuclear states. The authors interpreted their data as indicating that AgNPs induce malsegregation of the chromosomes rather than having a direct effect on replication.

Mei et al. [2012] evaluated the mutagenic potential of uncoated AgNPs (average size, ~5 nm; range, 4–12 nm), using a mouse lymphoma assay system. Modes of action (MOA) were assessed by means of standard alkaline and enzyme-modified comet assays and gene expression analysis. The mouse lymphoma cells (L5178Y/TK$^{+/-}$) were treated with AgNPs at a concentration of 5 µg/mL for 4 hours, at which time the AgNPs

were observed to be in the cytoplasm of the lymphoma cells. AgNPs induced dose-dependent cytotoxicity and mutagenicity, with a marked increase in the mutation frequency at 4 and 5 µg/mL (<50% cell survival at ≥5 µg/mL), where nanosilver had a clastogenic MOA. In the standard Comet assay there was no significant induction of DNA damage, although the percentage of DNA in the tail increased slightly with increasing dose. However, in the oxidative DNA damage comet assays, addition of lesion-specific endonucleases resulted in significant induction of DNA breaks in a dose-dependent manner. Gene expression analysis with use of an oxidative stress and antioxidant defense polymerase chain reaction (PCR) array, showed that the expressions of 17 of the 59 genes on the arrays were altered in the cells treated with AgNPs. These genes are involved in the production of ROS, oxidative stress response, antioxidants, oxygen transporters, and DNA repair. The investigators concluded that the results from this study indicated that the mutagenicity of AgNPs used in this study resulted from a clastogenic MOA.

Several of the studies cited above have revealed significant toxic effects on cells that often occurred in a dose-dependent manner; however, only a few studies have evaluated AgNPs and the role of particle size on cellular toxicity [Park et al. 2011c; Kim et al. 2012; Gliga et al. 2014]. The effects of AgNPs of different sizes (20, 80, 113 nm) have been compared in in vitro assays for cytotoxicity, inflammation, genotoxicity, and developmental toxicity [Park et al. 2011c]. Cytotoxicity was investigated in L929 murine fibroblasts and RAW 264.7 murine macrophages, and effects of AgNPs were compared to those of silver in ionic form. The role of AgNP size on the generation of ROS and on parameters of inflammation were also evaluated, as well as the dependence of particle size on developmental toxicity and genotoxicity in mouse embryonic cells and embryonic fibroblasts, respectively. Metabolic activity of RAW 264.7 cells, embryonic stem cells, and L929 cells was evaluated with use of WST-1 cell proliferation reagent when the cells were exposed to AgNPs for 24 hours or for 10 days (embryonic stem cells). In both L929 fibroblasts and RAW 264.7 macrophages, metabolic activity was decreased (concentration dependently) by AgNPs as well as by ionic silver. For ionic silver, the decrease in metabolic activity was similar between the two cell types. In

contrast, for AgNPs, the metabolic activity was significantly more affected in 929 fibroblasts than in RAW 264.7 macrophages. In both cell types the 20-nm AgNPs were the most potent in decreasing metabolic activity. In assessing cell membrane integrity (LDH), 20-nm AgNPs were more potent in reducing the cell membrane integrity of L929 fibroblasts than was ionic silver, whereas ionic silver was more potent in RAW 264.7 macrophages. In addition, the cellular generation of ROS was observed to increase for 20-nm AgNPs but only marginally for the larger AgNPs when exposed to RAW 264.7 macrophages. The generation of ROS in macrophages occurred only at concentrations above those decreasing the metabolic activity of macrophages, suggesting a secondary effect rather than causing the onset of cytotoxicity. The 20-nm AgNPs were also found to be the most potent for causing embryonic stem cell differentiation. However, 20-nm AgNPs did not induce an increase in gene mutation frequencies (genotoxicity evaluation) at concentrations up to 3 µg/mL.

Kim et al. [2012] examined the size-dependent cellular toxicity of AgNPs, using three different sizes (~10, 50, and 100 nm in diameter). A series of cell lines, including osteoblastic MC3T3-E1 cells, rat adrenal PC12 cells, human cervical cancer HeLa cells, and hamster CHO cells, were exposed to AgNPs at doses of 10, 20, 40, 80, or 160 µg/mL to investigate the regulation of cell proliferation, ROS production, LDH release, apoptosis induction, and stress-related gene expression. Cell assays were conducted at 24, 48, and 72 hours after treatment with AgNPs. Results from assays suggested that AgNPs exerted significant cytotoxic effects against all cell types, as indicated by decreased mitochondrial function, and that these effects occurred in a dose- and size-dependent manner. Both the MC3T3-E1 and PC12 cell lines were shown to be the most sensitive to toxic effects. In particular, the cytotoxic response to AgNPs was cell-dependent, with apoptosis occurring in MC3T3-E1 and necrosis in PC12 cell lines. Moreover, 10-nm-diameter AgNPs had a greater apoptotic effect against the MC3T3-E1 cells than did AgNPs 50 and 100 nm in diameter.

Gliga et al. [2014] also investigated the size- and coating-dependent toxicity of AgNPs following exposure of human lung cells (BEAS-2B). BEAS-2B cells were exposed to

citrate-coated AgNPs of different sizes (10-, 40-, and 75-nm diameters) as well as to 10-nm PVP-coated and 50-nm uncoated AgNPs, at doses of 5, 10, 20, and 50 µg/mL. Study parameters included evaluation of particle agglomeration, cell viability, ROS induction, genotoxicity, γH_2AX foci formation (a marker for DNA damage and repair), and intracellular localization. To assess cytotoxicity, BEAS-2B cells were exposed to AgNPs for 4 and 24 hours in an AB assay. After 4 hours, no significant signs of toxicity of any of the AgNPs were observed, up to the highest dose tested. Significant cell toxicity was evident only for the 10-nm citrate-coated AgNPs ($P \leq 0.05$) and 10-nm PVP-coated AgNPs ($P \leq 0.01$) after 24 hours for the doses of 20 and 50 µg/mL. No significant alterations of the mitochondrial activity of the BEAS-2B cells were observed at doses of 5 and 10 µg/mL or for the other AgNPs. When the LDH assay was used for cytotoxicity determination, no significant toxicity was observed after 4 hours for any of the AgNPs. However, significant toxicity was observed after 24 hours for the 10-nm citrate-coated AgNPs ($P \leq 0.05$) and the 10-nm PVP-coated AgNPs ($P \leq 0.0001$) at the dose of 50 µg/mL. None of the larger AgNPs altered cell viability. In contrast, all AgNPs tested caused an increase in overall DNA damage after 24 hours when assessed by the comet assay, suggesting an independent mechanism for cytotoxicity and DNA damage. No γH_2AX formation was detected, and no increased production of intracellular ROS was observed. Despite different agglomeration patterns, there was no difference in the uptake or intracellular localization of the citrate- and PVP-coated AgNPs, and there was no coating-dependent difference in cytotoxicity. Furthermore, the 10-nm particles released significantly more Ag^+ than did all other AgNPs (approximately 24% by mass versus 4–7% by mass) following 24 hours in cell medium. The released fraction in cell medium did not induce any cytotoxicity, indicating that intracellular release of Ag could have been responsible for the toxicity.

The genotoxicity of AgNPs (range, 4–12 nm in diameter) was evaluated by Li et al. [2012], using a *Salmonella* reverse mutation assay (Ames) and an in vitro micronucleus test in TK6 human lymphoblastoid cells. The Ames assay was conducted according to OECD test guidelines, with use of *Salmonella typhimurium* tester strains TA98 and TA1537 for detection of frame-shift mutation and the use of tester strains TA100,

TA1535, and TA102 for the measurement of base-pair substitution. For TA98 and TA100, frank toxicity (reduction of background revertant frequency and/or thinning of the background) was detected at 4.8 µg/plate and higher doses; toxicity was observed for TA1535 and TA1537 at 9.6 µg/plate and higher doses. At the highest dose of 76.8 µg/plate, all the bacteria from the five tester strains were killed. In general, AgNPs were found to be negative in the Ames test; this result may have been due to the agglomeration of the nanoparticles, making them too large to transport through the pores in the bacterial cell wall, or possibly due to the insensitivity of most tester strains to oxidative DNA damage. The cytotoxicity of AgNPs was evaluated with use of lymphoblast TK6 cells treated at concentrations of 10 to 30 µg/mL, in accordance with OECD guidelines. Cytotoxicity was measured with relative population doubling, which reflects a combination of cell growth, death, and cytostasis. A dose-response increase in micronuclei was observed at a dose of 25 µg/mL and was reported by the investigators as a weak positive, consistent with findings from other studies that tested various types of nanomaterials with mammalian cells.

To determine the mutagenic potential of colloidal AgNPs (average diameter, 10 nm), four histidine-requiring strains of *S. typhimurium (*TA98, TA100, TA1535, and TA1537) and one tryptophan-requiring strain of *Escherichia coli* (WP2uvrA) were used in the presence and absence of metabolic activation with S9 mix [Kim et al. 2013]. In the absence of metabolic activation (that is, without S9 mix), cytotoxicity was found at ~62.5 µg/plate (TA98, TA1535, TA1537, and WP2uvrA) and at ~31.25 µg/plate (TA100). Cytotoxicity was also exhibited at concentrations of ~125 µg/plate (TA98, TA100, and TA1537) and ~250 µg/plate (TA1535 and WP2uvrA) in the presence of metabolic activation. Precipitation and aggregation of the AgNPs were also observed at a dose level greater than 1.25 µg/plate with and without metabolic activation. No significant number of revertant colonies was observed for any of the bacterial strains, with or without metabolic activation, in comparison with the negative control. No dose-dependent increase of revertant colonies was observed for any of the bacterial strains. Kim et al. [2013] also conducted a chromosome aberration test to identify chromosomal abnormalities. A preliminary cytotoxicity test was carried out at a relative cell count

(RCC) concentration of ~ 50%. At this RCC, AgNPs were found to induce cytotoxicity. For groups treated for 6 and 24 hours without the S9 mix, a cytotoxic effect was induced at about 15.625 µg/mL, whereas for the group treated for 6 hours with the S9 mix, cytotoxicity was induced above 31.25 µg/mL. On the basis of these results, chromosome slide samples were prepared at 3.906, 7.813, and 15.625 µg/mL, with 50% of the RCC concentration as the highest concentration. AgNPs did not produce any statistically significant increase in the number of CHO-k1 cells with chromosome aberrations when compared to the negative controls with or without metabolic activation. AgNPs also did not cause a statistically significant increase in the number of cells with polyploidy or endoreduplication when compared with controls in the presence and absence of the S9 mix.

E.3 Changes in Gene Expression/Regulation

A number of research groups have employed DNA microarray analysis in an attempt to understand the cellular responses to AgNPs at the molecular level. For example, using 7- to 10-nm-diameter nanoparticles stabilized with PVP, Kawata et al. [2009] observed changes in cellular morphology, cell viability, and MN formation when HepG2 human hepatoma cells were incubated with AgNPs at noncytotoxic doses. However, MN formation was greatly reduced in cells incubated with either a polystyrene nanoparticle preparation or a silver carbonate solution, but it was only partially reduced in response to AgNPs where the cells had been pre-incubated with the antioxidant NAC. Accompanying these well-characterized responses was a significant induction of genes associated with cell cycle progression. Thus, AgNPs altered the expression levels of 529 genes at least twofold, with 236 genes being induced and 293 repressed. Patterns of induction featured genes classified as “M phase” (31 genes), microtubule-based processes (19 genes), DNA repair (16 genes), DNA replication (24 genes), and intracellular transport (32 genes). Many of the genes were involved in chromosome segregation, cell division, and cell proliferation. Striking levels of induction were also observed for some stress-inducible gene, including three coding for metallothioneins and three for different heat-shock proteins. Overlapping patterns of gene expression in

this cell line were observed in silver carbonate–altered gene profiles. For example, in comparisons of AgNPs and silver carbonate, 66 upregulated genes and 72 downregulated genes were altered commonly in the same direction with both chemical treatments. Kawata et al. [2009] speculated that the upregulation of a number of genes associated with DNA repair and the increase in MN in AgNP-exposed HepG2 cells might point to the DNA-damaging effects of silver in both nanoparticle and ionic form.

The A549 human lung adenocarcinoma cell line was used by Deng et al. [2010] as a platform for studying increased gap-junction intercellular communication (GJIC) activity and increased expression of connexin43 (Cx43) mRNA in the presence of AgNPs. The particles were a proprietary formulation, 30 nm in diameter and coated with 0.2% PVP, although TEM and dynamic light scattering indicated that a degree of aggregation had occurred when the particles were dispersed in an aqueous medium. Assessment of GJIC was achieved by means of a scrape loading/dye transfer technique, and Cx43 was detected by immunofluorescence. Furthermore, western blot assays were performed to determine the level of expression of Cx43 protein, and RT-PCR analysis showed that silver AgNPs upregulated the expression of Cx43 mRNA in a dose-dependent manner (1.2–1.8 times at concentrations ranging from 0.5 to 4.0 μg/mL after a 24-hour incubation). Deng et al. [2010] speculated that GJIC and Cx43 might mediate some of the biologic effects of AgNPs.

Ma et al. [2011] applied genomic analysis to responses to AgNPs (~20 nm in diameter) in human dermal fibroblasts. The particles employed had been prepared by reduction of a silver nitrate solution with sodium borohydride and were used at 200 micromolar (μM). However, TEM analysis showed a considerable degree of aggregation of the nearly spherical particles. For the microarray analysis, total RNA was isolated, amplified, labeled, and hybridized and cRNA probes were synthesized. A proprietary computer program (BeadStudio) used to survey changes in gene expression showed that 1,593 genes were impacted by AgNPs after 1, 4, or 8 hours' incubation. Only 237 genes were affected after 1 hour, as compared to 1,149 after 4 hours and 684 after 8 hours. Biologic pathway analysis of the affected genes identified five functional clusters associated

primarily with disturbance of energy metabolism, disruption of cytoskeleton and cell membrane, gene expression, and DNA damage/cell cycle arrest.

Foldbjerg et al. [2012] studied the effect of AgNPs (average particle diameter, 15.9 nm) on gene expression, using human lung epithelial cell line A549 exposed to 12.1 µg/mL AgNPs for 24 and 48 hours. Results were compared to control (unexposed) and silver ion (Ag^+)–treated cells (1.3 µg/mL) with Affymetrix microarray analysis. AgNPs exposed for 24 hours altered the regulation of more than 1,000 genes (twofold regulation), compared to only 133 genes that responded to Ag^+ exposure. Nearly 80% of all genes induced by Ag^+ were also upregulated in AgNP-treated cells. Bioinformatic analysis of the upregulated genes in response to the 24-hour exposure with Ag^+ and AgNPs revealed similar functional gene groups that were significantly enriched. Exposure of epithelial cells to AgNP and Ag^+ resulted in intracellular production of ROS but did not induce apoptosis or necrosis at the concentrations used in the study. Exposure to AgNP influenced the cell cycle and led to an arrest in the G2/M phase, while exposure to Ag^+ caused a faster but less-persisting cellular response than did exposure to AgNPs. The investigators concluded that although the transcriptional response to exposure with Ag^+ is highly related to the responses caused by exposure to AgNPs, the particulate form and size of AgNPs "affect cells in a more complex way."

E.4 Modeling the Perturbation of the Blood–Brain Barrier

Tang et al. [2010] used co-cultures of rat brain microvessel vascular endothelial cells and astrocytes that were established on a polycarbonate membrane in a diffusion chamber to model the potential for AgNPs to cross the blood–brain barrier. The researchers used commercial preparations of AgNPs (diameter, 50–100 nm) and contrasted their passage with larger-scale silver microparticles (diameter, 2–20 µm) incubated in the same system. The use of ICP-MS showed that AgNPs readily crossed the barrier, whereas silver microparticles did not. TEM analysis demonstrated the capacity of AgNPs to be taken up by the mixed culture. Some of the endothelial cells

showed signs of morphologic disruption, with large vacuole formation and signs of necrosis of cellular organelles.

Primary brain microvessel endothelial cells isolated from Sprague-Dawley rats were employed by Trickler et al. [2010] to determine the capacity of AgNPs to potentiate the release of proinflammatory mediators, with possible impacts on blood–brain barrier permeability. Obtained from a commercial supplier, the PVP-coated AgNPs used in these experiments conformed to their size requirements of 25, 40, and 80 nm in diameter and were mostly spherical, as indicated by TEM and dynamic light-scattering analysis. Cellular accumulation of silver was greater from the smaller nanoparticles, and cell viability was likewise more severely affected in those cultures exposed to the 25-nm-diameter particles. The cultures also showed a time-dependent preferential release of prostaglandin E_2 and the cytokines TNF-α, IL-1β, and IL-2, in relation to smaller AgNPs. According to the authors, these changes may be linked to ROS generation and an increase in microvascular permeability.

E.5 Impact of Silver Nanoparticles on Keratinocytes

Two research reports have examined the effects of AgNPs on keratinocytes, focusing in particular on the different results that were obtained when the toxicity of particles of different sizes and coatings were compared [Amato et al. 2006; Samberg et al. 2010]. For example, Amato et al. [2006] reported in an abstract that hydrocarbon-coated AgNPs of 15, 25, or 55 nm in diameter induced greater degrees of toxicity than did uncoated forms of silver that were 80 or 130 nm in diameter. The use of a CytoViva 150 Ultra Resolution Imaging system showed AgNP aggregates on the surface of the cells, along with some evidence of particle uptake into the HEL-30 mouse keratinocytes. Measuring caspase activity and using confocal fluorescent microscopy provided evidence of the onset of apoptosis at sublethal doses. These results differed from those of Samberg et al. [2010], who incubated human epidermal keratinocytes for 24 hours with eight different species of AgNPs. As supplied by nanoComposix, Inc. (San Diego, CA), these preparations included three unwashed colloids of 20-, 50-, and 80-nm-

diameter AgNPs, three washed colloids of the same nominal size, and two carbon-coated powders that were 25 and 35 nm in diameter. In contrast to the findings of Amato et al. [2006], the loss of cell viability that was observed with unwashed AgNPs at silver concentrations of 0.34 or 1.7 µg/mL was not seen when the cells were incubated with washed or carbon-coated particles, even though all silver nanoparticles were taken up into cytoplasmic vacuoles to roughly the same extent. The inflammatory potential of AgNPs was demonstrated by increases of IL-1β, IL-6, IL-8, and TNF-α in the media of cells exposed at 0.34 µg/mL. The authors suggested that the toxicity of AgNPs to human epidermal keratinocytes might be influenced by residual contaminants in the AgNP preparations and not necessarily by the particles themselves.

E.6 Effect of Silver Nanoparticles on Platelet Activation

Jun et al. [2011] carried out a series of experiments to investigate the effect of AgNPs on platelet aggregation. The commercial AgNPs averaged slightly less than 100 nm in diameter and were maintained in solution in nonaggregated form by ultrasonication and vortexing. A colloidal dispersion of AgNPs (5,000–8,000 nm in diameter) was used in comparison. The measured parameters that were indicative of platelet activation included platelet aggregation per single-cell counts, TEM analysis, low cytometric analysis of phosphatidylserine exposure (a measure of apoptosis), platelet pro-coagulant activity, serotonin secretion, detection of p-selectin expression, and determination of intracellular calcium levels. There was a dose-dependent increase in platelet aggregation with increased concentration of nanoparticle-borne but not microparticle-borne silver. Aggregation was further enhanced by the presence of thrombin. Other determinants of coagulation dose-dependently associated with the presence of AgNPs included the degree of phosphatidylserine exposure, pro-coagulant activity, expression of p-selectin, and secretion of serotonin. The presence of the calcium chelator ethylene glycol-bis (*β*-amino-ethyl ether) N,N,N′,N′-tetra acetic acid in the incubation medium partially blocked the platelet aggregation activity of AgNPs, implicating a role for calcium ions in the induction of platelet aggregation. Overall, the results pointed to the capacity of AgNPs to enhance platelet aggregation and pro-

coagulant activity, with a possible intermediary role for intracellular calcium and sub-threshold levels of thrombin.

E.7 Antitumor and Antimicrobial Activity of Silver Nanoparticles

The in vivo experiments of Sriram et al. [2010], in which intraperitoneal injected AgNPs appeared to enhance survival time and reduce the volume of ascites tumors in female Swiss albino mice, were supplemented by experiments in which Dalton's lymphoma cell lines were incubated for 24 hours with AgNPs in vitro. As described in Section 5.3.3, the researchers used 50-nm-diameter AgNPs that had been produced in *B. licheniformis* cultures incubated in the presence of silver nitrate. When the MTT assay was used as a measure of cell viability, a silver concentration of 500 nm was calculated for the IC_{50}. Measurement of caspase 3 in cell lysates showed a marked increase in activity compared to that in controls, and fragmentation of DNA indicated the presence of double strand breaks. The authors speculated that their data indicated a potential antitumor property of AgNPs and the relevance of apoptosis to this process.

In light of the extensive use of AgNP-bearing dressings to deter infection in wounds, Lok et al. [2006] used proteomic analysis to examine their mode of antibacterial action by incubating cultures of *E. coli* (wild-type K12 strain MG1655) with samples of spherical, 9.3-nm-diameter bovine serum albumin-stabilized nanoparticles that had been produced by the borohydride reduction method. Two-dimensional electrophoresis was used to separate the spectrum of cellular proteins pre- and post-incubation; the resulting peptides were identified by MALDI-TOF MS and, in some cases, immunoblots. The initial concentrations of AgNPs and silver nitrate that inhibited bacterial proliferation were 0.4 nm and 6 μm, respectively, suggesting that silver presented in the nanoparticle form was more efficient at deterring bacterial growth. With regard to changes in gene expression, induction of some cell envelope and heat-shock proteins appeared to be differentially enhanced, including outer membrane proteins A, C, and F (or their precursors), periplastic oligopeptide binding protein A, D-methionine binding protein (including body binding proteins A and B), and a 30S ribosomal subunit S6. However,

the researchers reported that some of these stimulated proteins appeared to be in their precursor forms, which were said to generally contain a positively charged N-terminal signal sequence of about 2 kDa. In addressing the possible mode of action associated with the antimicrobial effect of AgNPs, the researchers found that short-term incubation of *E. coli* with AgNPs provided evidence of membrane destabilization, reduction in membrane potential, and depletion of intracellular potassium and ATP. These consequences were thought to be manifestations of the proteomic changes observed at the molecular level.

Table E-1. Summary of *in vitro* studies of silver nanoparticles (AgNPs) and nanowires (AgNWs)

Cell Type	Particle Characteristics	Exposure Details		Major Outcomes	NOAEL/ LOAEL	Comments	Reference
		Concentrations/ Doses	Duration				
Human Cells							
HepG2 human hepatoma	AgNPs and Ag^+ ions: 5–10 nm particles dispersed in an aqueous medium; agglomerates 100–300 nm	0.2–1 µg/mL	24- to 28-hr incubation	Release of LDH activity; mRNA levels of catalase and SOD1 increased; detection of phosphorylation on the H2AX gene; ROS formation	NA	AgNPs exhibited cytotoxicity with a potency comparable to that of Ag^+ ions	Kim et al. [2009c]
HepG2 human hepatoma cells; SGC-7901 human stomach cancer cells; MCF-7 human breast adenocarcinoma cells; and A549 human lung adenocarcinoma cells	PVP coated; 5, 20, and 50 nm in diameter	Cell viability test: 0.01 – 100 µg/mL	6-, 12-, or 24-hr incubation	Apoptosis and necrosis test: 0.1, 0.5, 2.5 µg/mL; membrane damage and oxidative stress: 0.01–10 µg/mL	NA	Induced cell death caused by apoptosis; no difference between control group and exposed group for necrosis; smaller particles more effective at penetrating the membrane and inducing toxic effects	Liu et al. [2010]

Cell Type	Particle Characteristics	Exposure Details		Major Outcomes	NOAEL/ LOAEL	Comments	Reference
		Concentrations/ Doses	Duration				
Human Chang liver cells	Particles started at 5–10 nm but aggregated to 28–38 nm after incubation in the medium	4 µg/mL	0- to 24-hr incubation	Increased levels of lipid peroxidation and protein carbonyl formation; decrease in Bcl-2 expression: increase in Bax. ROS formation	NA	Apoptosis via a mitochondrial and caspase-dependent pathway; the importance of JNK in mediating the apoptotic effects was demonstrated by its time-dependent phosphorylation in the presence of AgNPs	Piao et al. [2011]
HT-1080 human fibrosarcoma cells; A431 human skin carcinoma cells	7–20-nm diameter in an aqueous suspension	6.25–50 µg/mL		Reduction in GSH content and SOD activity; increase in lipid peroxidation; increase in treatment-related DNA fragmentation	NA	Oxidative stress; cell death by apoptosis and necrosis	Arora et al. [2008]
Human acute monocytic leukemia cell line (THP-1 cells)	30–50 nm in diameter and coated with 0.2% PVP	0–7.5 µg/mL (calculated as silver mass)	Up to 24-hr incubation	Increase in intracellular ROS, DNA damage		Apoptosis; necrosis; significant reduction of viable cells after 24-hr exposure	Foldbjerb et al. [2009]

Cell Type	Particle Characteristics	Exposure Details		Major Outcomes	NOAEL/ LOAEL	Comments	Reference
		Concentrations/ Doses	Duration				
A549 human lung carcinoma epithelial-like cell line	30–50 nm, spherical, coated with 0.2% PVP	Suspensions/ supernatants containing 39% (0.2 µg/mL silver ions) or 69% (1.6 µg/mL silver ions)	24-hr incubation	Induced ROS	NA / 1.6 µg/mL total silver, suspension containing 39% silver	AgNP-free supernatant had the same toxicity as AgNP suspensions	Beer et al. [2012]
HeLa cells	5–10 nm in diameter, stabilized with a proprietary protectant	IC_{50} of 92 µg/mL silver	3- to 4-hr incubation	Increase in expression of heme oxygenase-1 and mettothionein-2A		Apoptosis	Miura and Shinohara [2009]
A549 cells	~500 nm (agglomerated)	Morphology: 10, 50, 200 µg/mL Cytotoxicity: 5, 10, 50, 200 µg/mL Apoptosis: 50 and 100 µg/mL	Morphology: 24-hr incubation Cytotoxicity: 12, 24, 48, 72 hrs of incubation Apoptotic cell death: 24-hr incubation	Increased LGH release; altered cell cycle distribution; changes to expression of Bax and Bcl-2; altered mRNA levels of protein kinase C isotypes		Reduction in cell viability; increased apoptosis; cytotoxicity at 48 hrs	Lee et al. [2011c]
Human colon adenocarcinoma (HT29) cells	<20 nm in diameter	11 µg/mL	30-min to 6-hr incubation	Cascade reaction, which activates caspase-3, which penetrates nuclear membrane to induce DNA fragmentation		Programmed cell death (apoptosis)	Gopinath et al. [2010]

Cell Type	Particle Characteristics	Exposure Details		Major Outcomes	NOAEL/ LOAEL	Comments	Reference
		Concentrations/ Doses	Duration				
Human lung macrophage cell line (THB-1); human epithelial (A549) cells	Primary particle: 3-100 nm in diameter	5 µg/mL	52-hr incubation	Cytotoxic effect		Epithelial cells more sensitive to effects	Soto et al. [2007]
Human lung A549 cancer cell line	30–50 nm in diameter and coated with 0.2% PVP	AgNPs: 0–20 µg/mL Ag^+: 0–10 µg/mL	24-hr incubation	Induced dose-dependent reductions in mitochondrial function to a greater extent than equivalent concentrations of silver in nano-form		Induced cytotoxicity and ROS formation was accompanied by formation of bulky DNA adducts; responses inhibited by pretreatment with N-acetyl-cysteine	Foldbjerb et al. [2011]
Human mesenchymal stem cells (hMSCs)	Mean diameter of 46 nm; aggregation mean diameter of 404 nm when dispersed in medium	0.1, 1.0, and 10 µg/mL	1-, 3-, and 24-hr incubation	Chromosomal aberrations	NA / 0.1 µg/mL	Cytotoxic and genotoxic potential of AgNPs occurred at significantly higher doses than did their antimicrobial effects	Hackenberg et al. [2011]

Cell Type	Particle Characteristics	Exposure Details		Major Outcomes	NOAEL/ LOAEL	Comments	Reference
		Concentrations/ Doses	Duration				
Human mesenchymal stem cells (hMSCs)	PVP-coated, ~100 nm in diameter	Concentrations of 0.5, 1, 2.5, 3, 3.5, 4, 5 µg/mL or to silver ions (silver acetate)	Up to 7 days	Both types showed a decrease in release of IL-6, IL-8, and VEGF	Silver: 1 µg/mL; 2.5 µg/mL AgNP: 3 µg/mL; 3.5 µg/mL	AgNPs exert cytotoxic effects in hMSCs at high concentrations but also induce cell activation at high but nontoxic concentrations of nanosilver	Greulich et al. [2009]
Human mesenchymal stem cells (hMSCs)	PVP-coated, 50 nm ± 20 nm in diameter	Concentrations of 0.5 , 1.0, 1.5, 2.0, or 2.5 µg/mL silver acetate (ions) or 15, 20, 25, 30, or 50 µg/mL AgNPs	24-hr incubation	80-nm AgNP agglomerates found in perinuclear region of hMSCs (clathrin-mediated endocytosis uptake)		Possibly more than one endocytotic pathway for cell uptake	Greulich et al. [2011]
Human adipose-derived stem cells (hASCs), undifferentiated and differentiated	10 or 20 nm in diameter	0.1, 1.0, 10.0, 50.0, 100.0 µg/mL, either before or after differentiation	Cells were differentiated down the osteogenic or adipogenic pathways or maintained in their proliferative state for 14 days and then exposed for 24 hrs to evaluate potential cellular uptake of AgNPs the	No significant morphologic changes occurred in adipogenic and osteogenic cell uptake of both 10 & 20 nm; no significant cytotoxicity to hASCs when exposed to 10- or 20-nm	NA/ 10 µg/mL	No significant cytotoxicity to undifferentiated hASCs either prior to differentiation or following 14 days of differentiation	Samberg et al. [2012]

Cell Type	Particle Characteristics	Exposure Details		Major Outcomes	NOAEL/ LOAEL	Comments	Reference
		Concentrations/ Doses	Duration				
			hASCs grew in a medium for 5 days				
IMR-90 human lung fibroblasts; U251 human glioblastoma cells	6–20 nm in diameter; starch-coated	25, 50, or 100 µg/mL	2- to 48-hr incubation	Alteration in cell morphology; reduced viability; deficits in mitochondrial performance and ROS production		Small percentage of cells underwent apoptosis; indication of treatment-associated DNA damage	Asharani et al. [2009]
Human lung cells (BEAS-2B)	Citrate-coated: 10, 40, 75 nm in diameter PVP-coated: 10 nm in diameter Uncoated: 50 nm in diameter	5, 10, 20, 50 µg/mL	4- and 24-hr incubation	No cells showed significant signs of cell toxicity after 4 hrs; after 24 hrs, cell toxicity was significant in 10-nm citrate-coated and 10-nm PVP-coated from doses of 20 and 50 µg/mL; all cells showed overall DNA damage after 24 hrs		Independent mechanism for cytotoxicity and DNA damage	Gliga et al. [2014]
TK6 human lymphoblastoid cells	4–12 nm in diameter	10–30 µg/mL		Frank toxicity of TA98 and TA100; toxicity of TA1535 and TA1537; dose-response increase in micronuclei was observed at a dose of 25 µg/mL	Frank toxicity: 4.8 µg/plate; toxicity: 9.6 µg/plate	Results were weak-positive, consistent with results in similar studies	Li et al. [2012]

Cell Type	Particle Characteristics	Exposure Details		Major Outcomes	NOAEL/ LOAEL	Comments	Reference
		Concentrations/ Doses	Duration				
HepG2 human hepatoma cells	7–10 nm in diameter; stabilized by PVP	0, 0.1, 0.2, 0.5, 1.0, 1.5, 2.0, 2.5, 3.0 mg/L	24-hr incubation	Changes in cellular morphology; cell viability; MN formation; significant cytotoxicity at >1.0 mg/L		DNA-damaging effects; altered expression levels of 529 genes at least twofold	Kawata et al. [2009]
A549 human lung adenocarcinoma cell line	30 nm in diameter; coated with 0.2% PVP	0.5–4.0 µg/mL	24-hr incubation	Upregulated the expression of Cx43		GJIC and Cx43 might mediate some of the biologic effects of AgNPs	Deng et al. [2010]
Human dermal fibroblasts	~20 nm in diameter	Reduction of silver nitrate solution with sodium borohydride at 200 micromolar	1-, 4-, or 8-hr incubation	1,593 genes were impacted after 1-, 4-, and 8-hr incubations		Disturbance of energy metabolism; disruption of cytoskeleton, cell membrane, and gene expression; DNA damage/cell cycle arrest	Ma et al. [2011]
A549 human epithelial cell line	AgNPs: 30 nm in diameter; silver microparticles: <45 µm in diameter; AgNWs: 1.5–25 µm in length, 100–160 nm in diameter (all particles coated with PVP)	AgNPs: 0.33 mg/mL; silver nanoparticles: 13.5 mg/mL; AgNWs: 5.05–16.47 mg/mL	24- and 48-hr incubation	Strong cytotoxicity, loss in cell viability, and early calcium influx with AgNWs; AgNPs and silver microparticles had minimal effect on A549 cells		Cell damage and resulting cell death hypothesized by investigator as being caused by the needle-like structure of the AgNWs	Stoehr et al. [2011]

Cell Type	Particle Characteristics	Exposure Details		Major Outcomes	NOAEL/ LOAEL	Comments	Reference
		Concentrations/ Doses	Duration				
Human epithelial cell line	15.9 nm average particle size	12.1 µg/mL	24- and 48-hr incubation	Altered the regulation of more than 1000 genes (twofold regulation); intracellular production of reactive oxygen species		Did not induce apoptosis or necrosis	Foldbjerb et al. [2012]
Human epidermal keratinocytes	Three unwashed colloids of 20, 50, and 80 nm in diameter; 3 washed colloids of 20, 50, and 80 nm in diameter; 2 carbon-coated powders 25 and 35 nm in diameter	0.000544–1.7 µg/mL	24-hr incubation	Loss of cell viability observed in unwashed AgNPs; increases in TNF-α, IL-1β, IL-6, and IL-8; decrease in cell viability for unwashed AgNPs <1.7 µg/mL	NA / 0.34 µg/mL (unwashed AgNPs)	Toxicity of AgNPs might be influenced by residual contaminants in the AgNP preparations and not necessarily by the particles themselves	Samberg et al. [2010]
Human platelets (washed)	100 nm in diameter; solution in nonaggregated form by ultrasonication and vortexing; colloidal dispersion (microparticles 5,000–8,000 nm in diameter)	50, 100, and 250 µg/mL	5 min	Dose-dependent increase in platelet aggregation with increased concentration of nanoparticles but not microparticle-borne silver		Enhance platelet aggregation and pro-coagulant activity, with possible intermediary role for intracellular calcium and sub-threshold levels of thrombin	Jun et al. [2011]

Cell Type	Particle Characteristics	Exposure Details		Major Outcomes	NOAEL/ LOAEL	Comments	Reference
		Concentrations/ Doses	Duration				
	used for comparison						
Animal Cells							
Rat alveolar macrophages	15, 30, 55, 100 nm in diameter	0, 5, 10, 25, 50, and 75 µg/mL	Cells at 80% confluence were incubated 24 hrs	Same as Hussain et al. [2005b]; treatment-related increase in TNF-α, macrophage inflammatory protein-2, IL-1β, in the supernatant of macrophage/ AgNP incubations	NA	Oxidative stress; cellular damage.	Carlson et al. [2008]
Rat alveolar macrophages	15, 30, 55, 100 nm in diameter	5–50 µg/mL	Cells at 80% confluence incubated 24 hrs	Smaller-diameter AgNPs more effective than larger NPs at physiologic and toxicological changes	NA	Oxidative stress; cellular damage	Hussain et al. [2005b]
BRL 3A rat liver cells	15 or 100 nm in diameter	5–50 µg/mL	Incubation times up to 24 hrs	Both cell sizes induced a concentration-dependent depletion of mitochondrial function; release of LDH to culture medium	NA	Cytotoxicity through oxidative stress	Hussain et al. [2005a]
NIH3T3 fibroblasts	Ag 1–100 nm in diameter; non-	50 and 100 µg/mL	24 hrs for AgNPs; up to	Link between mitochondrial-related		Results similar to those for Piao et al. [2011]	Hsin et al. [2008]

Cell Type	Particle Characteristics	Exposure Details		Major Outcomes	NOAEL/ LOAEL	Comments	Reference
		Concentrations/ Doses	Duration				
	nano Ag <250 µm in diameter		72 hrs for non-nano Ag	generations of ROS and incidence of apoptosis and activation of JNK; non-nano Ag not cytotoxic and no effect on apoptosis			
Primary mouse fibroblasts and liver cells	>90% of particles 7–20 nm in diameter	IC50 values were 61–449 µg/mL	24-hr incubation	Primary cell preparations contained sufficient antioxidant capacity to protect cells from possible oxidative damage		Study similar to Arora et al. [2008], but oxidative stress and apoptosis were less evident	Arora et al. [2009]
L929 fibroblasts	AgNPs: 50–100 nm; Ag microparticles: 2–20 µm	10, 25, 50, 100 µg/mL	24-hr incubation	Greater percentage of cells arrested in G2M phase of cell cycle		Increased incidence of apoptosis; AgNPs caused greater level of apoptosis than did Ag microparticles at same dose	Wei et al. 2010
Murine lung macrophage (RAW 264.7)		5 µg/mL				Cytotoxic response	Soto et al. [2007]

Cell Type	Particle Characteristics	Exposure Details		Major Outcomes	NOAEL/ LOAEL	Comments	Reference
		Concentrations/ Doses	Duration				
Mouse embryonic stem cells, mouse embryonic fibroblasts	Uncoated plasma gas-synthesized AgNPs & polysaccharide-coated AgNPs, both approx. 25 nm in diameter	50 µg/mL	4-, 24-, 48-, and 72-hr incubation	Increased induction of the Rad51 double-strand break repair protein; enhanced phosphorylation of the histone H2AX at the serine-139 residue		Increased p53 expression and double DNA breakage, with concomitant apoptosis in both cells within 4 hrs after exposure	Ahamed et al. [2008]
Mouse fibroblast (L929) tumor cells	Median diameter of 12 nm; synthesized by chemical reduction of silver chlorate with sodium borohydride and sodium citrate	0, 11, 22 µg/mL	72-hr incubation	Formation of cells with single giant nuclei or cells with two, three, or sometimes four nuclei per cell		Induced malsegregation of the chromosomes rather than having direct effect on replication	Nallathamby and Xu [2010]
Mouse lymphoma assay system	4–12 nm in diameter; average size ~5 nm; uncoated	5 µg/mL	4-hr incubation	Observed in the cytoplasm of the lymphoma; DNA breaks; expressions of 17 of the 59 genes on the arrays were altered in the cells		Induced dose-dependent cytotoxicity and mutagenicity	Mei et al. [2012]
Rat brain microvessel vascular endothelial cells; astrocytes to model a blood-brain barrier	AgNPs: 50–100 nm in diameter; Ag microparticles: 2–20 µm in diameter	100 µg/mL	4-hr incubation	AgNPs readily crossed the barrier, whereas silver microparticles did not		Morphologic disruption, with large vacuole formation and signs of necrosis of cellular organelles	Tang et al. [2010]

Cell Type	Particle Characteristics	Exposure Details		Major Outcomes	NOAEL/ LOAEL	Comments	Reference
		Concentrations/ Doses	Duration				
Sprague-Dawley rat primary brain microvessel endothelial cells (rBMECs)	25, 40, and 80 nm in diameter; spherical; PVP-coated	Cytotoxicity: 1.95–15.63 µg/cm^2; prostaglandin E_2 and cytokine release in rBMECs: 10.4 µg/cm^2; cell morphology: 5.2 µg/cm^2	24-hr incubation	ROS generation; increase in microvascular permeability; release of prostaglandin E_2 and cytokines TNF-α, IL-1β, and IL-2		Cell viability more severely affected in cultures exposed to the 25- and 50-nm diameters; cerebral microvascular damage	Trickler et al. [2010]
HEL-30 mouse keratinocytes	15-, 25-, or 55-nm diameter (coated with hydrocarbon); 80- or 130-nm diameter (not coated)	25, 40, 50, 65, and 100 µg/mL	24-hr incubation	Onset of apoptosis at 25 µg/mL	NA	The 15-, 25-, and 55-nm particles induced greater degrees of toxicity than the larger (uncoated) particles	Amato et al. [2006]
L929 mouse fibroblasts, RAW 264.7 and D3 embryonic stem cells	20-, 80-, 110-nm-diameter AgNPs, mostly spherical	0.1–100 µg/mL	24 hrs for RAW 264.7 and L929; 10 days for D3 cells	For L929 and RAW 264.7: metabolic activity highest with 20-nm AgNPs; RAW 264.7: increased ROS generation with 20-nm AgNPs; L929: compromised cell membrane integrity with all sizes	NA	Toxicity of AgNPs and silver ions dependent on particle size and cell type	Park et al. [2011c]

Cell Type	Particle Characteristics	Exposure Details		Major Outcomes	NOAEL/ LOAEL	Comments	Reference
		Concentrations/ Doses	Duration				
Cell lines: Osteoblastic MC3T3-E1, PC12, rat adrenal medulla, human cervical cancer, HeLa, CHO	10-, 50-, 100-nm-diameter AgNPs	10, 20, 40, 80, or 160 µg/mL: after 24-hr incubation, concentrations were 1,2,4, 8, and 16 µg	Additional incubation for 24, 48, or 72 hrs	Size- and dose-dependent cellular toxicity for all cell lines; ROS generation and cytotoxicity increased as size and concentration of AgNPs increased	NA	Toxicity of AgNPs dependent on particle size and cell type; effect may be related to cellular uptake processes from cell membrane to nuclear pores	Kim et al. [2012]
Dalton's lymphoma cell lines	50 nm in diameter; produced in *Bacillus licheniformis* cultures incubated in the presence of silver nitrate	Silver concentration of 500 nM was calculated for the IC_{50}	24-hr incubation	Measurement of caspase 3 in cell lysates showed marked increase in activity in comparison with controls; fragmentation of DNA indicated presence of double-strand breaks	NA	Data indicated a potential antitumor property of AgNPs and the relevance of apoptosis to this process	Sriram et al. [2010]

Cell Type	Particle Characteristics	Exposure Details		Major Outcomes	NOAEL/ LOAEL	Comments	Reference
		Concentrations/ Doses	Duration				
Bacteria/Viruses							
Four histidine-requiring strains of *Salmonella typhimurium* (TA98, TA100, TA1535, TA1537); one tryptophan-requiring strain of *Escherichia coli* (WP2uvrA)	10 nm average particle size; colloidal; absence of metabolic activation; presence of metabolic activation	0, 7.8, 15.6, 31.2, 62.5, 125, 250, 500 and 1000 µg/mL	6- and 24-hr incubation	No significant number of revertant colonies observed in any strain, regardless of metabolic activation; no significant increase in cells with polyploidy or endoreduplication, regardless of metabolic activation	NA	Absence of metabolic activation: cytotoxic effect at 15.6 µg/mL; Presence of metabolic activation: cytotoxicity induced above 31.2 µg/mL	Kim et al. [2013]
E. coli (wild-type K12 strain MG1655) with bovine serum albumin	Spherical AgNPs: 9.3 nm in diameter	AgNPs: 0.4 and 0.8 nm; $AgNO_3$: 6 and 12 nm	5–30 min	Short-term incubation of *E. coli* with AgNPs provided evidence of membrane destabilization; reduction in membrane potential; depletion of intracellular potassium and ATP	NA	Silver presented in the nanoparticle form was more efficient at deterring bacterial growth	Lok et al. [2006]

E.8 Dermal Absorption (in Vitro)

A series of experiments by Larese et al. [2009] examined the capacity of AgNPs to penetrate human skin in vitro. The researchers used Franz diffusion cells to monitor the penetration of silver through either intact or abraded previously frozen, full-thickness skin preparations. The preparation was a 0.14-weight percent suspension of PVP-coated AgNPs in ethanol, with a mean diameter of 25 ± 7.1 nm (range, 9.8–48.8 nm). The use of a PVP coat ensured structural stability of the particles and deterred aggregation. The particles were applied to the skin in a 1:10 dilution of synthetic sweat (pH, 4.5). After 24 hours, median silver concentrations of 0.46 and 2.32 nanograms per square centimeter (ng/cm^2) were obtained in the receptor fluid for intact and damaged skin, respectively. Penetration of silver proceeded in a linear fashion between 4 and 24 hours through abraded skin but leveled off after approximately 8 hours in intact skin. The absorption rates of silver through abraded skin where about fivefold higher than for intact skin. Using TEM, the authors observed silver deposition in the stratum cornea and upper layers of the epidermis.

APPENDIX F

Toxicological and Toxicokinetic Effects of Silver Nanoparticles in Experimental Animal Studies

F.1 Inhalation Exposure

F.1.1 Toxicokinetics

The absorption and distribution of AgNPs via the inhalation route were studied in 16 female F344 rats that received a single 6-hour exposure to AgNPs at a concentration of 133 µg/m^3 and subsequently were killed (four animals per time point) at 0, 1, 4, or 7 days post-exposure [Takenaka et al. 2001]. The AgNPs, as generated by a spark discharging through an argon atmosphere, were compact and spherical, with a median diameter of 17 ± 1.2 nm (GSD = 1.38) and minimal aggregation. Groups of four rats were killed on days 0, 1, 4, and 7 following exposure. Immediately after exposure, silver was detected at elevated concentrations in the lungs, nasal cavity, liver, and blood, but the concentrations declined over time. The researchers detected a total of 1.7 µg of silver in the lungs immediately after exposure had ended, by using inductively coupled plasma mass spectroscopy (ICP-MS cannot differentiate elemental from ionic silver). However, this amount dropped quickly, and only about 4% of the initial pulmonary burden was present after 7 days. Evidence that absorption of the nanoparticles had occurred came from the detection of 8.9 nanograms per gram wet weight (ng/g) silver in the blood on the first day. This was lower in subsequent analyses, as silver was distributed to secondary target tissues such as the liver, kidney, heart, and tracheobronchial lymph nodes. Absorption data for inhaled AgNPs were compared with those obtained when 150 microliters (µL) of an aqueous solution of silver nitrate was intratracheal instilled in 12 animals. Similarly, in another phase of the experiment, a 150-µL aqueous suspension of AgNPs was intratracheal instilled in seven animals. A significant amount of aggregation of the AgNPs had occurred in the latter preparation, and in contrast to the findings with monodisperse AgNPs, up to 32% of the silver from the aggregated preparation was retained in the alveolar macrophages after 4 or 7 days. The water-soluble silver was rapidly

cleared from the lungs in a manner similar to that of the monodispersed AgNPs, suggesting that both entities can be readily absorbed via the lungs and undergo systemic distribution.

F.1.2 Toxicological effects

Inhalation studies reported by Ji et al. [2007a,b], Sung et al. [2008, 2009, 2011], and Song et al. [2013] exposed Sprague-Dawley rats to AgNPs that were generated by using a small ceramic heater and an air supply to disperse defined amounts of AgNPs from an unspecified source material into the inhalation chambers. The particles were found to be composed of elemental silver, monodisperse and spherical, with diameters predominantly in the 15–20-nm range. In the acute study, five rats per sex per group received a single 4-hour exposure to 0 particles (fresh air controls); 0.94×10^6 particles/cm^3 (76 µg/m^3 silver; low concentration); 1.64×10^6 particles/cm^3 (135 µg/m^3 silver; mid concentration); or 3.08×10^6 particles/cm^3 (750 µg/m^3 silver; high concentration) [Sung et al. 2011]. Mortality, clinical signs, body weight changes, food consumption, and lung function were monitored over a 2-week period after exposure. At necropsy, weights of the major organs were compared to those of controls. Lung function parameters examined included tidal volume, minute volume, respiration rate, inspiration and expiration times, and peak inspiration and expiration flows. All animals survived exposure and the 2-week observation period, and there were no clinical signs of toxicity. Food consumption and body weights were closely similar to those of controls among the groups. Likewise, lung function tests showed no significant differences between the groups and controls. Sung et al. [2011] pointed to the difficulty of generating higher concentrations of monodisperse nanoparticles in their system. Nonetheless, the authors determined that the high concentration of 750 µg/m^3 was 7.5 times higher than the ACGIH TLV (100 µg/m^3) for silver dust and probably more than 600 times the particle surface area for silver dust, assuming a 4-µm diameter for the latter and a nanoparticle surface area of 8.69×10^9 nm^2/cm^3. However, no acute toxicological effects of AgNPs at this exposure concentration were evident in these studies.

In a 28-day inhalation study, the same researchers exposed ten 8-week-old specific-pathogen-free (SPF) Sprague-Dawley rats per sex per group 6 hours/day, 5 days/week, for 4 weeks to 0 particles (fresh air controls); 1.73×10^4 AgNPs/cm^3 (0.48 µg/m^3 silver; low concentration); 1.27 ×

10^5/cm^3 (3.48 µg/m^3 silver; mid concentration); or 1.32 × 10^6/cm^3 (61 µg/m^3 silver; high concentration), following OECD Test Guideline 412 [Ji et al. 2007b]. Respective geometric mean particle diameters (and geometric standard deviations) were 11.93 nm (0.22), 12.40 nm (0.15), and 14.77 nm (0.11); the higher diameter at the high concentration was explained as being due to agglomeration of particles. Parameters monitored included clinical signs, body weight changes, and, at term, hematology and clinical chemistry values, organ weights, tissue silver, and histopathologic effects. The body weight changes among the groups did not differ significantly from those of controls, and there were no significant organ weight changes in either males or females after 28 days of exposure to AgNPs. Although isolated fluctuations in food consumption, hematology, or clinical chemistry parameters were not considered related to treatment, Ji et al. [2007b] observed instances of cytoplasmic vacuolization in the liver of exposed animals. This response was likely due to lipid accumulation and, as a common response to hepatic injury [Eustis et al. 1990], was probably treatment related. For males there was one such case among controls and there were four cases in the low-concentration group and one each in the mid- and high-concentration groups. For females, the effects were more dose-related; there were two cases each in the control and low-concentration groups, six in the mid-concentration group, and seven in the high-concentration group. Other histopathologic effects on the liver included two cases of hepatic focal necrosis in high-concentration males and a single case among high-concentration females. No histopathologic effects of AgNPs were seen in the kidney, spleen, lungs, adrenals, heart, reproductive organs, brain, or nasal cavity. There was also a concentration-dependent increase in the concentration of silver deposited in the lungs. Likewise, silver was readily detected in the liver and brain of animals exposed at the high concentration but only marginally so in the blood, suggesting rapid clearance from the bloodstream to the tissues after inhalation.

The South Korean group also examined the potential effects of inhaled AgNPs on the respiratory mucosa of Sprague-Dawley rats [Hyun et al. 2008], as studied and reported by Ji et al. [2007b]. Ten animals per sex per group were exposed 6 hours/day, 5 days/week, for 28 days to 0 particles (fresh air controls); 1.73 × 10^4 particles/cm^3 (0.5 µg/m^3; low concentration); 1.27 × 10^5 particles/cm^3 (3.5 µg/m^3; mid concentration); or 1.32 × 10^6 particles/cm^3 (61 µg/m^3; high concentration). Histochemical staining of the respiratory mucosa showed the number and size of

neutral mucin-producing goblet cells to be increased, whereas those producing acid mucins were unchanged. No histopathologic changes were observed in the lungs or nasal cavity. Foamy alveolar macrophages were observed in rats exposed to 3.5 and 61 µg Ag/m^3. The toxicological significance of these changes was uncertain.

Sung et al. [2008, 2009] reported the toxicological effects of inhaled AgNPs from a single experiment (following OECD Test Guideline 413) in which 10 Sprague-Dawley rats per sex per group were exposed 6 hours/day, 5 days/week, for 90 days. The study was designed to identify possible adverse effects not detected in the 28-day study by Ji et al. [2007b] and Hyun et al. [2008]. AgNPs were generated and concentrations and size distributions were measured as described by Ji et al. [2007 a, b]. As reported by Sung et al. [2008], rats were exposed to 0 particles (fresh air controls); 0.7×10^6 particles/cm^3 (48.94 µg Ag/m^3); 1.4×10^6 particles/cm^3 (133.19 µg Ag/m^3); or 2.9×10^6 particles/cm^3 (514.78 µg Ag/m^3). Lung function was tested weekly on four animals per dose group, 40 minutes after the end of exposure. Respective geometric mean diameters (and geometric standard deviations) were 18.30 nm (1.10), 18.71 nm (1.78), and 18.93 nm (1.59). As a mark of pulmonary inflammation, the appearance of albumin, lactate dehydrogenase, and total protein was monitored in bronchoalveolar fluid (BAL) obtained at term. Cell counts of macrophages, polymorphonuclear cells, and lymphocytes in BAL were obtained histologically. Excised pieces of lung were examined by histopathology.

Pulmonary function was evaluated weekly in four rats per sex per group by means of a ventilated bias-flow whole-body plethysmograph to determine tidal volume, minute volume, respiratory frequency, inspiration and expiration times, and peak inspiration and expiration flow [Sung et al. 2008]. Among the lung function test results, tidal volume, minute volume, and peak inspiration flow showed dose-related deficits in response to AgNP inhalation. In addition, stained slides of lung sections indicated treatment-related increases in the incidence of mixed cell infiltrate perivascular and chronic alveolar inflammation, including alveolitis, granulomatous lesions, and alveolar wall thickening and macrophage accumulation (Table F-1). In discussing their data, Sung et al. [2008] compared the lung function deficits with those reported for subjects exposed to welding fumes, drawing the conclusion that the cumulative lung dose of AgNPs at the high dose (514.78 µg Ag/m^3) was 10–15 times less than the welding fume exposure in terms of mass dose

for a similar level of response. Therefore, it was hypothesized that surface area or particle number may be a more meaningful determinant of exposure than mass when correlated with lung function deficits and associated histopathologic changes.

Table F-1. Incidence and severity of silver nanoparticle-related histopathologic changes in the lungs of Sprague-Dawley rats

Exposure Parameters	Males				Females			
	Control	Low	Mid	High	Control	Low	Mid	High
Number (particles/cm^3) × 10^{-5}	0	6.64	14.3	28.5	0	6.64	14.3	28.5
Surface area (nm^2/cm^3) × 10^{-9}	0	1.08	2.37	6.61	0	1.08	2.37	6.61
Mass ($\mu g/m^3$)	0	48.94	133.19	514.78	0	48.94	133.19	514.78
Tissue deficits								
Accumulation (macrophage, alveolar)	3/10	5/10	5/10	8/10	7/10	4/10	4/10	6/10
Inflammation (chronic, alveolar)	2/10	3/10	2/10	7/10	3/10	2/10	0/10	8/10
Infiltration (mixed-cell perivascular)	3/10	4/10	6/10	8/10	0/10	0/10	1/10	7/10

Source: Sung et al. [2008].

In the second report, data were presented on hematology and clinical chemistry parameters, and excised pieces of the major organs and tissues were examined for histopathology changes and silver deposition [Sung et al. 2009]. There were few, if any, effects of AgNP administration during the in-life phase of the experiment, although one high-concentration male died during an ophthalmologic examination. No treatment-related effects for body weight change, food consumption or, at term, in organ weights, hematology, or clinical chemistry parameters were observed in the remaining rats. Tissue content of silver was dose-dependently increased in lung, liver, kidney, olfactory bulb, brain, and whole blood, and some histopathologic lesions were noted in the liver that appeared to be related to dose. For example, as shown in Table E-2, bile-duct hyperplasia was noted with increased incidence in higher-concentration groups. Furthermore, single-cell hepatocellular necrosis was seen in three of 10 high-concentration female rats. The

authors of the study suggested that their data were indicative of a no observed adverse effect level (NOAEL) in the region of 100 μg/m^3 that was consistent with the ACGIH TLV of 100 μg/m^3 for silver dust.

The finding of bile duct hyperplasia, in parallel with the lung function deficits plotted by Sung et al. [2008], indicated statistically significant decrements. However, hepatic effects can also be characteristic of aging rats as well as a common response to the administration of some chemicals [Eustis et al. 1990], although the findings of dose-dependent increases in lesions is most likely a result of AgNP exposure.

Table F-2. Incidence and severity of silver nanoparticle–related histopathologic changes in the livers of Sprague-Dawley rats

Exposure Parameters	Males				Females			
	Control	Low	Mid	High	Control	Low	Mid	High
Number (particles/cm^3) × 10^{-5}	0	6.64	14.3	28.5	0	6.64	14.3	28.5
Surface area (nm^2/cm^3) × 10^{-9}	0	1.08	2.37	6.61	0	1.08	2.37	6.61
Mass (μg/m^3)	0	48.94	133.19	514.78	0	48.94	133.19	514.78
Tissue deficits								
Bile duct hyperplasia	0/10	0/10	1/10	4/9	3/10	2/10	4/10	9/10
Hepatocellular necrosis (single cell)	0/10	0/10	0/10	0/9	0/10	0/10	0/10	3/10

Source: Sung et al. [2009].

Lee et al. [2010] screened for differentially expressed genes in the brains of C57Bl/6 mice exposed to AgNPs via inhalation. The nanoparticles were produced by the same procedure described in the first paragraph of this section and had characteristics similar to those used by other researchers [Sung et al. 2011, 2009, 2008; Hyun et al. 2008; Ji et al. 2007a, b]. Two groups of seven male mice were exposed to silver nanoparticles (1.91 × 10^7 particles/cm^3; geometric mean diameter, 22.18 ± 1.72 nm) 6 hours/day, 5 days/week, for 2 weeks. One of the exposure groups was observed for a 2-week recovery period before being killed for necropsy. Two other

groups of seven mice served as untreated and sham-exposed controls. When total ribonucleic acid (RNA) from the cerebrum and cerebellum was analyzed by gene microarray, the expression of 468 and 952 genes, respectively, showed some degree of response to AgNP exposure, including several associated with motor neuron disorders, neurodegenerative disease, and immune cell function. The use of real-time quantitative reverse-transcription polymerase chain reaction (RT-PCR) to analyze the expression of selected genes in whole blood identified five genes that were downregulated in response to AgNP exposure. Expression of three of the five remained suppressed throughout the 2-week recovery period, but expression of the other two returned to control levels during the recovery phase. Lee et al. [2010] considered these genes to have potential as biomarkers for recent exposure to AgNPs.

The capacity of AgNPs to bring about toxicological changes in the lung as a result of inhalation was investigated in C57Bl/6 mice by Stebounova et al. [2011]. Twenty-six male C57Bl/6 mice underwent whole-body exposure to 3300 µg/m^3 AgNPs 4 hours/day, 5 days/week, for 2 weeks. Along with 13 sham-exposed controls, equal numbers of mice were necropsied within 1 hour or 3 weeks after exposure to determine BAL composition (5 per group), lung histopathology (3 per group), and silver deposition to the major organs (5 per group). The AgNPs were a commercial product with a stated particle size of 10 nm. The PVP-coated particles were ultrasonicated in water, nebulized to an aerosol, and then dried at 110°C prior to introduction into the exposure chamber. The AgNPs showed a bimodal particle size distribution, with peak maxima at 5 nm (85%–90% of the particle count) and 22 nm (<15%). However, in use, the aerosolized nanoparticles showed a degree of aggregation (with a geometric mean diameter of 79 nm). Stebounova et al. [2011] reported a median of 31 µg silver per gram (g) dry weight in the lungs of mice necropsied immediately after exposure. Those necropsied after a 3-week recovery period had a median silver content of 10 µg/g; two of the five mice had none detected. Silver was also detected in the BAL of exposed animals, with mean concentrations of 13.9 µg/L in animals necropsied at cessation of exposure and 1.7 µg/L in those necropsied 3 weeks post-exposure. However, the silver content in the heart, liver, and brain was below the detection limit. In examining the cell content and presence of biomarkers in BAL from silver-exposed mice, the authors reported that the numbers of macrophages and neutrophils were approximately double those in the BAL of controls, although no biologic significance was assigned to this change.

Furthermore, there were no treatment-related changes in total protein levels or lactate dehydrogenase (LDH) activity, and most cytokines assayed were below their limits of detection. Lung histopathology yielded unremarkable findings, allowing Stebounova et al. [2011] to conclude that overall, C57Bl/6 mice showed minimal pulmonary inflammation or cytotoxicity when exposed to AgNPs under the prevailing exposure conditions.

Kim et al. [2011a] reported on the evaluation of genotoxic potential of AgNPs that were generated as described by Ji et al. [2007a] and Sung et al. [2008]. Male and female Sprague-Dawley rats were exposed by inhalation for 90 days according to OECD Test Guideline 413. Rats were exposed to AgNPs (18 nm in diameter) at concentrations of 0.7×10^6 particles/cm^3 (low dose), 1.4×10^6 particles/cm^3 (middle dose), and 2.9×10^6 particles/cm^3 (high dose) for 6 hours per day and then killed 24 hours after the last administration. The femurs were removed and bone marrow was collected and evaluated for micronucleus induction according to OECD Test Guideline 474. The in vivo micronucleus test was used for detection of cytogenetic damage. Although a dose-related increase was found in the number of micronucleated polychromatic erythrocytes (MNPCEs) in the male rats, no significant treatment-related increase in MNPCEs was found in the male and female rats in comparison with the negative controls. These findings were consistent with those reported by Kim et al. [2008], in which no genotoxicity (per in vivo micronucleus test) was found in rats following the oral administration of AgNPs for 28 days.

Song et al. [2013] reported the lung effects in male and female Sprague-Dawley rats (17 males and 12 females per exposure group) following 12-week inhalation exposure to AgNPs (14–15 nm in diameter). Exposure concentrations were 49 µg/m^3 (0.66×10^6 particles/cm^3; low dose); 117 µg/m^3 (1.41×10^6 particles/cm^3; middle dose); or 381 µg/m^3 (3.24×10^6 particles/cm^3; high dose) for 6 hours per day. Lung function was measured every week during the exposure period and after cessation of exposure. Animals were killed after the 12-week exposure period and at 4 and 12 weeks after the exposure cessation. Lungs were analyzed for silver concentration with use of NIOSH Analytical Method 7300. Song et al. [2013] noted that histopathologic examination of rat lung tissue showed “a significant increase in the incidence of mixed cell infiltrate, perivascular and chronic alveolar inflammation, including alveolaritis, granulomatous lesions, and alveolar wall thickening and alveolar macrophage accumulation in both the male and female rats.” These

effects were observed in the middle- and high-dose groups of male rats and in the high-dose group of female rats, at the end of the 12-week exposure. Gradual clearance of AgNPs and decreased inflammation of the lungs were observed in female rats but not in the high-dose males during the 12-week recovery period. The findings suggest a possible NOAEL of 49 μg/m^3 (low dose) and a lowest observed adverse effect level (LOAEL) of 117 μg/m^3 (middle dose), although the authors suggested that the effects at the middle dose could be considered a NOAEL on the basis of similar effects (minimal accumulation of macrophages and inflammation in the alveoli) to those observed in the control group of the study by Sung et al. [2009]. Some of the lung effects noted by Song et al. [2013] were reported to persist at the end of the12-week exposure period, and male rats were observed to be more susceptible than the females to the lung effects of AgNP exposure. Lung function decreases (including tidal volume, minute volume, and peak expiratory flow) and lung inflammation were observed in male rats and persisted in the high-dose group at 12 weeks post-exposure. In female rats, no decrease in lung function was observed, and the lung inflammation showed gradual recovery after cessation of exposure [Song et al. 2013]. A dose-dependent statistically significant increase in silver concentration was observed in all tissues from the male and female rat groups exposed to AgNPs for 12 weeks, except for the female brain. Silver accumulation was still observed in some tissues at 4 weeks after the end of exposure (including the liver, kidneys, spleen, and blood, and in the ovaries in female rats). Silver concentrations remained significantly increased (in comparison with the unexposed control rats) in the liver and spleen at 12-weeks post-exposure. The silver concentrations in the kidneys also showed a gender difference, with the female kidneys containing five times more accumulated silver than the male kidneys. No histopathologic effects of silver were observed in any organs other than the lungs [Song et al. 2013].

In a follow-up study, Dong et al. [2013] investigated the gender-dependent effect of AgNPs on the kidney gene level, based on toxicogenomic studies of kidneys from rats exposed to AgNPs via inhalation for 12 weeks. The exposure conditions were the same as those employed by Song et al. [2013], and the study included both male and female SPF Sprague-Dawley rats, divided into four groups. The male groups (n = 17) consisted of 5 rats for 12-week exposure, 4 for 4-week recovery, 4 for 12-week recovery, and 4 for micronucleus testing after 12-week exposure. The female groups (n = 13) consisted of 5 rats for 12-week exposure, 4 for 4-week recovery, and 4 for

12-week recovery. The air-control exposure group included four male and female rats. Exposure for the low-dose group was a target dose of 0.6×10^6 particles/cm^3 (1.0×10^9 nm^2/cm^2, 48.76 μg/m^3); for the medium-dose group, a target dose of 1.4×10^6 particles/cm^3 (2.5×10^9 nm^2/cm^2, 117.14 μg/m^3); and for the high-dose group, a target dose of 3.0×10^6 particles/cm^3 (5.0×10^9 nm^2/cm^2, 381.43 μg/m^3). AgNPs were spherical, with diameters <47 nm (range, 4–47 nm; GSD, 1.71). After a 12-week exposure, silver concentrations in the kidneys confirmed a gender difference: in the low- and medium-dose groups there was a twofold higher silver concentration in female versus male kidneys, and a fourfold higher silver concentration in the high-dose female kidneys was consistent with results previously reported [Kim et al. 2008; Sung et al. 2009; Song et al. 2013]. These gender differences have been suggested to be related to metabolism and hormonal regulation, because the kidneys are a target organ for several hormones such as thyroid hormones and testosterone [Kim et al. 2009a]. Gene expression changes were evaluated in the study by means of a deoxyribonucleic acid (DNA) microarray of the kidneys for the low- and high-dose groups of male and female rats. The genes that were upregulated or downregulated by more than 1.3-fold ($P < 0.05$) were regarded as significant. As a result, 104 genes were found to have been upregulated or downregulated by more than 1.3-fold in male rats. Among the 104 genes changed by exposure, 24 genes were involved in the KEGG pathway and related to 49 biologic pathways. In the female kidneys, 72 genes were found to have been upregulated or downregulated by more than 1.3-fold. Among the 72 genes changed by exposure to either the low or high dose, 21 genes were involved in the KEGG pathway and related to 33 biologic pathways. The gender gene profiling in the study showed a predominant expression of metabolic enzyme-related genes in the male rat kidneys, versus a predominant expression of extracellular signaling-related genes in the female rat kidneys. However, no significant gene alterations were observed in the redox system, inflammation, cell cycle, and apoptosis-related genes.

Roberts et al. [2013] reported on the results of an inhalation study with rats exposed to nanoscale silver to assess pulmonary and cardiovascular responses from acute exposure. Two sources of AgNPs were used in the study; the first was a commercial antimicrobial product that contained 20 mg/L total silver (75% colloidal silver and 25% silver ions), and the other was a synthesized AgNP sample from the National Institute of Standards and Technology (NIST), reported to be 1,000 mg/L stock silver in deionized water (100% colloidal silver). Male Sprague-Dawley rats were

exposed by inhalation for 5 hours to a low concentration (100 µg/g/m^3) of the commercial antimicrobial product (20 mg/L total silver; ~33 nm mean aerodynamic diameter [MAD]) or to 1000 µg/m^3 in a suspension from the NIST sample (200 mg/L total silver; ~39 nm MAD). Estimated lung burdens determined from deposition models were 0 (control aerosol), 1.4 µg Ag/rat (low dose), and 14 µg Ag/rat (high dose). The low dose was selected to be equivalent to the TLV set by the ACGIH for particulate silver (100 µg/m^3). Two sets of exposures with paired controls were conducted for each dose. For each exposure set and each dose, 12 rats were exposed to air (n = 6 for day 1 and n = 6 for day 7) and 12 rats were exposed to AgNPs (n = 6 for day 1 and n = 6 for day 7). Rats from one set of exposures were killed on days 1 and 7 for evaluation of pulmonary response (inflammation, cell toxicity, alveolar air/blood barrier damage, macrophage activity, blood cell differentials) and for microvascular studies (responsiveness of tail artery to vasoconstrictor or vasodilatory agents, heart rate and blood pressure in response to isoproterenol or norepinephrine, respectively). Rats from the second set of exposures were killed on days 1 and 7 following measures for hemodynamic response. No significant changes in pulmonary or cardiovascular parameters were observed for either the commercial or NIST samples at days 1 and 7 post-exposure, although slight cardiovascular changes were observed in the 1.4-µg exposure group, possibly because of the higher fraction of ionic silver in the commercial product than in the NIST sample.

F.2 Oral Exposure

F.2.1 Toxicokinetics

The absorption and distribution of AgNPs via the oral route was studied by Loeschner et al. [2011] in groups of seven or nine female Wistar rats. The AgNPs were made by reducing silver nitrate with hydrazine in the presence of polyvinylpyrrolidone (PVP). The resulting nanoparticles were sedimented by centrifugation and dialyzed against deionized water. Size analysis showed the existence of two populations. The first, comprising about 90% of the material, was spherical, with a mean diameter of 14 ± 2 nm. Although the second population was larger (with a mean diameter of 50 ± 9 nm), these particles were also shown to be distinct nanoparticles rather than agglomerates.

Female Wistar rats (*n* = 9) received 12.6 milligrams per kilogram body weight per day (mg/kg-day) silver for 28 days via twice-daily gavage with the AgNP suspension, while seven rats underwent similar gavage with 9 mg/kg-day silver from an 11.5-mg/mL aqueous solution of silver acetate. Nine animals underwent gavage with an 11.5-mg/mL aqueous solution of PVP as vehicle controls. During the third week of the study, rats were kept for 24 hours in metabolic cages to obtain samples of urine and feces. At term, samples of blood, brain, stomach, liver, kidney, lung, and muscle were taken for silver analysis (by ICP-MS), histopathology, scanning electron microscopy (SEM), and TEM characterization, as well as auto-metallography (AMG) and EDS.

A substantial proportion of the oral load of silver appeared in the feces of animals exposed to AgNPs (63 ± 23%) and the silver acetate solution (49 ± 21%), indicating some absorption of silver in the stomach, small intestine, liver, kidney, muscle, and lungs. However, Loeschner et al. [2011] were unable to assess the contribution of hepatobiliary recirculation to these values. A greater proportion of the oral load of silver acetate was absorbed than of AgNPs, although the use of AMG to locate silver within target tissues did not reveal significant differences in the disposition of the element between the two administered forms. For example, silver was located in the lamina propria at the tips of the villae in the ileum but not in the epithelial cytoplasm. The use of EDS confirmed that granules in the lysosomes of macrophages consisted of silver, and additional signals identified as selenium and sulfur were also detected. In the liver there was intense staining of the Kupffer cells and around the central veins and portal tracts. In both cases, staining the kidney for silver located it in the glomeruli and proximal tubules. The authors concluded that although silver concentrations in target organs were generally lower after administration of silver nanoparticles than with water-soluble forms of the element, there were few if any differences in the distribution pattern of silver from either source. Given the similarities in disposition within the tissues, Loeschner et al. [2011] were unable to determine whether AgNPs were absorbed as an entity or whether they had dissolved in the gastrointestinal tract, followed by re-deposition in the tissues.

An experiment by Park et al. [2011a] determined the bioavailability and toxicokinetics of citrate-coated AgNPs in male Sprague-Dawley rats. As obtained from a commercial vendor, the particles were 7.9 ± 0.95 nm in diameter and coated with citrate; they were employed by the researchers

from a 20% (w/v) aqueous solution. Other physical and chemical data included a mean particle volume of 1.9×10^3 nm^3, a mean surface area of 7.53×10^2 nm^2/particle, and a mean particle mass of 2×10^{-17} g. Animals received AgNPs at concentrations of 1 or 10 milligrams per kilogram body weight (mg/kg) orally or intravenously. After treatment, blood samples were taken at 10 minutes and then at 1, 2, 4, 8, 24, 48, and 96 hours. Feces and urine samples were collected for 24 hours after treatment, and excised pieces of liver, lung, and kidney were obtained at 24 and 96 hours post-dosing for silver analysis by ICP-MS.

With regard to absorption, a comparison of the ratio of the plasma areas under the curves for oral versus intravenous administration gave measures of the bioavailability for oral exposure to this species of nanoparticles. Values of 1.2% to 4.2% of the oral load were obtained, depending on the size of the applied dose. For distribution, no AgNPs were detected in lung or kidney after oral administration. However, there was a slight elevation of silver content in the liver of animals orally exposed to 10 mg/kg. In fact, most of the orally applied AgNPs were recovered in the feces, suggesting that only a small proportion of the load had been absorbed. However, it is unclear how much of the fecal recovery of silver had been recycled through the hepatobiliary circulation after absorption. The fact that some silver was released to the feces after intravenous injection suggests that AgNPs could be voided after passage through the bile duct. Park et al. [2011a] speculated that gastrointestinal absorption of AgNPs might be low because of the citrated coat. It was thought that the presence of this hydrophilic center might render gastrointestinal absorption more difficult. However, the portion of the load that was absorbed was predominantly sequestered in the liver.

Although the citrate-coated AgNPs employed by Park et al. [2011a] appeared not to be readily absorbed via the oral route and showed no signs of tissue deposition other than in the liver, an earlier experiment by Kim et al. [2009a] detected silver deposition in the kidney, urinary bladder, and adrenal gland of F344 rats after oral administration of a proprietary preparation of 60 nm AgNPs dispersed in 0.5% carboxymethyl cellulose (CMC). The authors provided little physical and chemical information about the nanoparticles employed but stated that the preparation was at least 99.98% pure. As determined by specific staining of thin sections of excised tissue pieces, it

appeared that silver deposition in these tissues was much more prevalent in female rather than male F344 rats. There was no obvious explanation for this disparity.

Of relevance to absorption as well as the toxicological impacts of silver nanoparticles, Park et al. [2010b] orally administered repeated doses of 1 mg/kg AgNPs to ICR mice daily for 14 days. The AgNPs were initially suspended in tetrahydrofuran (THF) with sonication. Subsequently, the solvent was allowed to evaporate and was replaced with the same volume of de-ionized water. A critical feature of the experiment was the use of batches of AgNPs that had been screened by size. Thus, groups of five mice were orally administered AgNPs of 22, 42, or 71 nm, or silver particles that averaged 323 nm in diameter. The distribution of silver, the clinical chemistry fluctuations, the histopathologic findings, and the detection and measurement of cytokines were then described in relation to particle size. A critical finding was that silver from the smaller nanoparticles (up to and including 71 nm) was detected in brain, lung, liver, kidney, and brain, whereas the larger AgNPs (323 nm) were not detected in these tissues. Another response that was observed after administration of AgNPs, but not the larger silver microparticles, was increased serum concentrations of transforming growth factor-beta (TGF-β). Some differences in the subpopulations of whole-blood lymphocytes were also reported with varying particle size, but the data were less robust. However, the findings were consistent with the concept that small AgNPs are more active in exerting toxicological responses because of their expedient transport to susceptible sites.

A subacute oral AgNP exposure study with Sprague-Dawley rats was reported by Lee et al. [2013a], who focused on the clearance kinetics of tissue-accumulated silver. Rats were assigned to three groups, with 20 rats per group: control (no exposure), low dose (100 mg/kg body weight), and high dose (500 mg/kg body weight), and exposed to two different sizes of citrate-coated AgNPs (average diameter, 10 and 25 nm) over 28 days. Rats were observed during recovery for 4 months to identify the clearance of the tissue-accumulated silver. Regardless of the AgNP size, the silver content in most tissues gradually decreased during the 4-month recovery period. The exceptions were the silver concentrations in the brain and testes, which did not clear after the 4-month period, indicating an obstruction to the transporting of accumulated silver out of these tissues. Although the clearance half-times differed according to dose and gender, the tissues with

no biologic barrier, such as the liver, kidneys, and spleen, showed a similar clearance trend. The silver concentration clearance was in this order:

blood > liver = kidneys > spleen > ovaries > testes = brain.

The different AgNP sizes used in the study had minimal effect on adsorption, distribution, metabolism, and excretion, although the size difference was relatively narrow. The authors suggested that these findings support the hypothesis that silver toxicity originates mainly from silver ions, and in this study it was generated from the surface of the AgNPs. The findings also indicate that coated AgNPs and size differences may have minimal effect on adsorption, distribution, metabolism, and excretion.

F.2.1 Toxicological effects

In a 28-day study by Kim et al. [2008] of the toxicological impacts of oral exposure to AgNPs, 4-week-old male and female SPF Sprague-Dawley rats (10 per dose group) underwent gavage with AGNPs (average diameter, 60 nm; range, 53–71 nm) in an aqueous solution of 0.5% carboxymethyl cellulose (CMC) as the vehicle. The authors provided little physical and chemical information about the nanoparticles employed but stated that the preparation was at least 99.98% pure. The experiment followed OECD Test Guideline 407, using doses of silver at 0, 30, 300, or 1,000 mg/kg that were given for 28 days. At the conclusion of the dosing phase, animals were unfed for 24 hours and then anesthetized to facilitate the withdrawal of blood for measuring hematologic and clinical chemistry parameters. Major organs and tissues were excised, weighed, and processed for silver determination and histopathologic examination. The rat bone marrow micronucleus (MN) test was carried out according to OECD Test Guideline 474. Clinical signs were unremarkable during the in-life phase of the experiment, and no compound-related changes in body weight gain or food consumption were observed. At term, there were no dose-dependent changes in organ weights, hematologic parameters, or bone marrow cytotoxicity. However, there were treatment-related increases in serum cholesterol concentration and AP activity that, at the highest dose, were significantly different from levels in controls (Table F-3).

Table F-3. Serum cholesterol concentration and alkaline phosphatase activity in Sprague-Dawley rats that underwent gavage with AgNPs for 28 days

Dose Group (mg/kg)	Serum Cholesterol Concentration (mg/dL)		Alkaline Phosphatase Activity (IU/L)	
	Males	Females	Males	Females
0	69.0 ± 8.2	89.6 ± 9.1	427.2 ± 70.6	367.6 ± 125.7
30	73.1 ± 16	85.6 ± 12.2	475.4 ± 98.5	335.4 ± 79.0
300	82.1 ± 21.7	102.9 ± 17.7†	613.7 ± 128.6†	403.3 ± 75.9
1,000	87.5 ± 13.1*	117.5 ± 14.1†	837.7 ± 221.5†	499.0 ± 107.3†

*$P < 0.05$; †$P < 0.01$ versus controls, as calculated by the authors.

IU/L = International units per liter.

Source: Kim et al. [2008].

As tabulated by the authors, dose-related increases in silver content were noted in the blood and tissues such as testis, kidney, liver, brain, lung, and stomach, with a twofold higher accumulation in the kidneys of female rats versus males. Though difficult to explain mechanistically, this difference was consistent with that observed in F344 rats by Kim et al. [2009a]. Histopathologic examination of the liver showed an increased incidence of bile duct hyperplasia in AgNP-receiving rats. Other hepatic responses included infiltration of inflammatory cells in the hepatic lobe, portal tract, and dilated central veins. These changes are consistent with the clinical chemistry data, pointing collectively to a possible silver-related perturbation of the metabolism and structural architecture of the liver.

In a second oral study, scientists from the same research group carried out an exposure regimen identical to that used by Kim et al. [2008] but with the primary focus on silver deposition and changes to the structure of the ileum, colon, and rectum [Jeong et al. 2010]. The AgNPs were about 60 nm in diameter on average and were dispersed in an aqueous solution of 0.5% CMC at doses of 0 (vehicle control), 30, 300, or 1,000 mg/kg-day for 28 consecutive days. The ileum, colon, and rectum were assessed for general histologic structure and amounts of mucins in the mucosa. Specific histochemical staining procedures were used to detect and distinguish between mucins, and the intensity of staining was subjectively scored to assess the amounts of mucins. In

addition to the use of hematoxylin/eosin to stain mounted sections of these tissues, periodic acid-Schiff stain was used to detect neutral mucins, Alcian blue was used for acidic mucins, and high-iron diamine plus Alamar Blue (AB) was used to distinguish sulfated from nonsulfated mucins. There was a dose-dependent accumulation of AgNPs in the lamina propria of the small and large intestine, with higher numbers of goblet cells that had released their mucus, as compared to the number in controls. Given the detection of fluctuating amounts of differentially stained mucins among the groups, the researchers suggested that AgNPs might induce the discharge of mucus granules with abnormal compositions.

In addition to their experimental administration of differently sized AgNPs to ICR mice, as described in F.2, Park et al. [2010a] undertook a 28-day gavage study in which three mice per sex per group underwent gavage with 0 (vehicle control), 250, 500, or 1,000 μg/kg AgNPs (average particle diameter, 42 nm) dispersed in an aqueous medium. Major organs and tissues were excised at term for silver analysis and histopathologic examination. Blood samples were measured for clinical chemistry parameters and the presence of cytokines. Although there were no histopathologic changes in the livers or small intestines of the treated groups, some liver-related clinical chemistry parameters changed in relation to dose, including the activities of AP and AST in high-dose mice (both sexes). Additionally, the activity of ALT was increased in high-dose females but not males. The only organ or tissue where histopathologic changes were observed was the kidney, where signs of slight cell infiltration were noted in the cortex of high-dose mice of either sex. Changes in the levels of cytokines and immunoglobulin (Ig)-E were also noted in high-dose mice, in comparison with the control group. These differences are listed in Table F-4.

The authors noted that their doses were far lower than those that induced histopathologic responses in the liver of Sprague-Dawley rats after oral exposure [Kim et al. 2008]. Therefore, they concluded that doses of AgNPs at these low concentrations can induce inflammatory responses by repeated oral administration.

In a follow-up study to Park et al. [2010a], Kim et al. [2010a] treated 10 F344 rats per sex per group by gavage with AgNPs (average diameter, 56 nm; range, 25–125 nm) for 13 weeks at

silver doses of 0, 30, 125, or 500 mg/kg-day. The monodisperse and nonaggregated AgNPs were dispersed in an aqueous solution of 0.5% CMC that also constituted the vehicle control. As before, clinical signs, body weights and food consumption were monitored in the in-life phase of the experiment. At term, blood was withdrawn to measure hematologic and clinical chemistry parameters.

Table F-4. Levels of cytokines in the serum of high-dose and control mice as a result of oral administration of AgNPs to ICR mice for 28 days

Parameter	Controls (*n* = 3)	High-dose group (*n* =3)
Pro-inflammatory cytokines (pg/mL)		
Interleukin (IL)-1	ND	8.8 ± 0.7†
Tumor necrosis factor (TNF)-α	1.21	3.41 ± 0.06
IL-6	1.44	13.75 ± 0.57†
Thyroid helper (Th)1–type cytokines (pg/mL)		
IL-12	35.5	76.86 ± 5.2†
Interferon (IFN)-γ	ND	0.52 ± 0.04
Th-2-type cytokines (pg/mL)		
IL-4	ND	2.7 ± 0.07‡
IL-5	ND	1.34 ± 0.01
IL-10	ND	29.02 ± 1.7†
TGF-β (pg/mL)	ND	6.73 ± 0.52†
Ig E (ng/mL)	3.28	6.04 ± 0.74‡

ND = not detected.

†$P < 0.01$; ‡$P < 0.05$.

Source: Park et al. [2010a].

Organ weights were recorded, and excised pieces of the major tissues and organs were processed for histopathologic examination and measurement of silver content.

Most major organs and tissues showed a dose-dependent increase in silver content. However, as observed in other studies of AgNPs in experimental animals [Kim et al. 2009a, 2008], there was an increased deposition of silver in female kidneys versus males' at equivalent doses. The authors of the study did not mention whether any of the exposed animals showed clinical signs of toxicity, but there were no significant changes in food consumption and water intake among the groups. Likewise, there were no dose-related changes in body weights of female rats, although high-dose males showed less body weight gain than controls after 4, 5, and 7 weeks of exposure. Body weight gain was also less in mid-dose males than in controls after 10 weeks. At term, there were few if any changes in organ weights associated with exposure to AgNPs. However, high-dose males showed an increase in the weight of the left testis and low- and mid-dose females showed decreases in weight of the right kidney. In a manner similar to the 28-day oral study in Sprague-Dawley rats [Kim et al. 2008], the most clear-cut treatment-related changes in clinical chemistry parameters were increases in AP activity in high-dose females (versus controls) that achieved statistical significance, as well as statistically significant increases in serum cholesterol concentration in high-dose rats of both sexes. Perhaps the most noteworthy toxicological responses to AgNPs in this study were histopathologic changes to the liver that showed a dose-related trend. Specifically, there were increased incidences in minimal to mild bile duct hyperplasia in both sexes of F344 rats. The proportions of males affected were 4/10 (controls), 7/10 (low dose), 9/10 (mid dose), and 6/10 (high dose); the respective proportions of affected females were 3/10, 7/10, 8/10, and 7/10. These responses are similar to those in Sprague-Dawley rats described by Kim et al. [2008] following their 28-day oral exposure study and by Sung et al. [2009] following their 90-day inhalation study. However, related changes in such clinical chemistry parameters as serum cholesterol concentration or AP activity were not observed in the latter study. In summarizing their data, Kim et al. [2010a] concluded that a LOAEL of 125 mg/kg, with a NOAEL of 30 mg/kg, would be appropriate from their data. However, since the incidences of bile duct hyperplasia in the low-dose groups were elevated in comparison with controls and were clearly part of a dose-related trend, the point of departure for these responses could be lower than 30 mg/kg.

In a study to examine the toxicokinetics and tissue distribution of two types of AgNPs, $AgNO_3$ (soluble silver ion-Ag^+), and two negative controls, five groups of Sprague-Dawley rats (five per

group) were exposed by gavage daily for 28 days to <20-nm non-coated or <15-nm PVP-coated AgNPs and to $AgNO_3$ [van der Zande et al. 2012]. All groups of rats were followed for 8 weeks. Dissection was performed on day 29 and at 1 week and 8 weeks post-exposure. Silver was present in all examined organs (liver, spleen, kidney, testis, lungs, brain, heart), and the highest levels in all silver treatment groups were in the liver and spleen. Silver concentrations in the organs were highly correlated to the amount of Ag^+ in the silver nanoparticle suspension, indicating that mainly Ag^+ (and to a lesser extent, AgNPs) passed the intestines in the AgNP-exposed rats. In all groups, silver was cleared from most organs at 8 weeks post-exposure, except for the brain and testis. By means of single-particle ICP-MS, AgNPs were detected in the AgNP-exposed rats but also in $AgNO_3$-exposed rats, demonstrating the in vivo formation (or precipitation) of nanoparticles from Ag^+ that were probably composed of silver salts. Biochemical markers and antibody levels in blood, lymphocyte proliferation and cytokine release, and NK-cell activity did not reveal hepatotoxicity or immunotoxicity from the silver exposure. Results of the study suggest that oral exposure to AgNPs appears to be similar to exposure to silver salts. The authors noted that the consequences of in vivo formation of AgNPs and the long retention of silver in the brain and testis warrant further assessment of the potential health risk.

Park [2013] also investigated toxicokinetic differences and toxicities of AgNPs and silver ions in rats after a single oral administration of 2 mg/kg (low dose) or 20 mg/kg (high dose). Male Sprague-Dawley rats (n = 5) were given a dose of either AgNPs (diameter, ~7.9 nm) or silver ions (Ag^+). The AUC_{24hr} of Ag^+ was 3.81 ± 0.57 µg/d/mL when rats were treated with a dose of 20 mg/kg, whereas that of AgNP was 1.58 ± 0.25 µg/d/mL. Blood levels, tissue distributions, and excretion of silver were measured up to 24 hours after oral administration. Tissue distribution of silver in liver, kidneys, and lungs was higher when Ag+ was administered than when AgNPs were administered. Silver concentrations in blood of rats treated with AgNPs were lower than those of rats treated with Ag^+ at the same dose. Blood silver concentrations in rats treated with 20 mg/kg AgNPs were also found to be lower than those of rats administered 2 mg/kg Ag^+. Decreased red blood cell counts, hematocrit levels, and hemoglobin levels were found in Ag^+-treated groups, whereas increased platelet counts and mean platelet volume were noted in the AgNP-treated rats. The concentrations of silver in both the lung and liver were lower in rats treated with AgNPs than in rats treated with Ag^+, and the highest concentration of silver was found in the liver of rats

treated with Ag^+ (20-mg/kg dose). Orally administered AgNPs were not absorbed in the gastrointestinal tract but excreted via feces; however, excretion of silver through feces was negligible for rats treated with the same dose of Ag^+, a finding indicating that bioavailability of Ag^+ may be greater than with AgNPs.

In a survey of the acute toxicity of AgNPs, Maneewattanapinyo et al. [2011] attempted to determine a median lethal dose (LD_{50}) for AgNPs in ICR mice. The AgNPs were produced by reducing a silver nitrate solution with sodium borohydride in the presence of soluble starch as a stabilizer. The particles were stated to be of high purity (99.96% silver), spherical, and with a narrow size range of 10–20 nm. Additionally, the content of free silver ions was very low (<0.04%). There were no deaths among mice observed for 14 days after a dose of 5,000 mg/kg, and there were no clinical signs of toxicity, reduced weight gain, hematologic or clinical chemistry changes, or gross and histopathologic findings. The oral LD_{50} in ICR mice was thus designated as >5,000 mg/kg.

Subacute toxicity of 14-nm AgNPs stabilized with PVP and ionic silver in the form of silver acetate was investigated in 4-week-old male (6 per dose) and female (10 per dose) Wistar Hannover Galas rats for 28 days [Hadrup et al. 2012a]. Animals received by gavage a vehicle control and AgNP doses of 2.25 or 9 mg/kg BW/day or silver acetate doses of 9 mg silver/kg BW/day for 28 days. Clinical, hematologic, and biochemical parameters, organ weights, and macroscopic and microscopic pathologic changes were evaluated. No increase in AP or cholesterol was found for AgNPs at doses of up to 9 mg/kg/day. Also, no observable effects were noted on the microbiologic status of the rats' gastrointestinal tract caused by ingesting AgNPs. However, effects were observed for silver acetate (ionic form) at a dose of 14 mg/kg/day, including an increase in AP, decrease in plasma urea, and decrease in thymus weights. These results were in contrast to those for Kim et al. [2008, 2010] in studies in which a NOAEL of 30 mg Ag/kg (lowest dose tested) was found in Sprague-Dawley rats when exposed by gavage for 28 and 90 days to 60-nm-diameter AgNPs.

Hadrup et al. [2012b] also compared the neurotoxic effects, in vivo and in vitro, of PVP-stabilized AgNPs (average diameter, 14 nm) and silver acetate. Following 28 days of oral administration,

AgNP (4.5 and 9 mg/kg/day) and silver acetate (9 mg/kg/day) significantly increased the concentration of dopamine in the brains of Wistar female rats, whereas the brain concentration of 5-hydroxytryptamine (5-HT) was increased only by AgNP at a dose of 9 mg/kg/day. However, in the 14-day range-finding study, the brain dopamine concentration decreased in rats treated with AgNP at doses of 2.25 and 4.5 mg/kg/day. Three solutions consisting of (1) AgNP, (2) an ionic silver solution obtained by filtering a nanosilver suspension, and (3) silver acetate were found in neuronal-like PC12 cells in vitro. AgNPs were not observed to cause necrosis. However, cell viability was decreased and apoptosis (involving both the mitochondrial and the death receptor pathways) was found for all three solutions, with silver acetate being most potent. The findings suggest that the ionic silver and 14-nm AgNP preparations have similar neurotoxic effects, possibly due to the release of ionic silver from the surface of AgNPs.

Pre-pubertal male Wistar rats (n = 30) were orally treated with 15 or 30 µg/kg/day AgNPs (~86 nm in diameter) from postnatal day 23 to postnatal day 58 (35 days at a total dose of 131–263 µg Ag/rat) and killed on postnatal day 102 to evaluate the effects on sexual behavior and reproduction [Mathias et al. 2014]. The acrosome integrity, plasma membrane integrity, mitochondrial activity, and morphologic alterations of the sperm were analyzed. Sexual partner preference, sexual behavior, and serum concentrations of follicle stimulating hormone (FSH), luteinizing hormone (LH), testosterone, and estradiol were also recorded. No measurements of blood silver were made. Exposure to AgNPs was found to reduce the acrosome and plasma membrane integrities, reduce mitochondrial activity ($P < 0.05$), and increase the abnormalities of the sperm (<0.01) in both the 15- and 30-µg/kg groups versus controls. AgNP exposure also delayed the onset of puberty, although no changes in body growth were observed in either treatment group. The animals did not show changes in sexual behavior or serum hormone concentrations. The serum concentrations of FSH, LH, testosterone, and estradiol were not significantly different between the experimental groups. Because the hormone profiles of testosterone, estradiol, FSH, and LH were not altered by AgNP treatment, the investigators suggested that the defective sperm function and morphology observed in this study may have resulted from defective spermatogenesis due to direct effects of AgNPs on spermatic cells. Similar findings of increased sperm morphologic abnormalities were observed by Gromadzka-Ostrowska et al. [2012] following a single intravenous dosing of AgNPs in rats.

In a second oral study, scientists from the same research group [Sleiman et al. 2013] carried out a similar exposure regimen with male Wistar rats (*n* = 30) exposed to AgNPs (~86 nm) during the pre-pubertal period and killed on postnatal days 53 and 90. Animals were treated orally with either 15 µg/kg BW or 50 µg/kg BW, from postnatal day 23 until postnatal day 53. Growth was assessed by daily weighing. The progress of puberty in the rats was measured by preputial separation, while spermatogenesis was assayed by measuring the sperm count in testes and epididymis and examining the morphologic and morphometric characteristics of seminiferous epithelium by stereo-logic analysis. In addition, testosterone and estradiol levels were assayed by radioimmunoassay. The weight of animals during postnatal days 34 to 53 was lower in the 50-µg/kg treatment group than in the control group and the 15-µg/kg treatment group; however, at 90 days postnatal, the growth among groups was not markedly different. A numerical reduction in total and daily sperm production was observed in the 50-µg/kg AgNP group on postnatal day 53. On postnatal day 90, both treatment groups had significantly lower total and daily sperm production ($P < 0.05$) in comparison with the control group. Decreased sperm reserves in the epididymis and diminished sperm transit time were also observed on postnatal day 53. However, no alterations of testosterone and estradiol serum concentrations were found on postnatal days 53 and 90. On postnatal days 53 and 90, discontinuity and disorganization of seminiferous epithelium, cellular debris in the lumen, and sloughing of the germinal cells from the epithelium into the tubular lumen were found. The presence of cellular debris and germinal epithelial cells in the tubular lumen and vesicles was suggested as being a possible impairment to the spermatogenesis process.

F.3 Exposure via Other Routes

F.3.1 Dermal

Wahlberg [1965] reported on a series of percutaneous studies with guinea pigs in which they used various metal compounds to evaluate the rate of absorption. The rate of absorption for silver nitrate (2 mL applied to skin and observed 3 weeks post-exposure) was found to be small (<1% per 5-hour period) compared to the rate of absorption of the other metals. The rates of dermal

absorption were compared to the toxicity of silver nitrate and the other metals following intraperitoneal administration at a dose of 2 mL. The relative toxicity (mortality) observed for the various metals following intraperitoneal administration was comparable to the rate of dermal absorption found with guinea pigs; the lowest mortality rate was among guinea pigs exposed to silver.

Two recently published studies examined the dermal toxicity of AgNPs in female weanling pigs [Samberg et al. 2010] and guinea pigs [Korani et al. 2011]. In the study by Samberg et al. [2010], female pigs were topically exposed to washed and unwashed AgNPs (average diameters of 20 and 50 nm) that were suspended in deionized water solutions of 0.34, 3.4, or 34 µg/mL over a 14-day period. The site of application was then examined for irritation on the basis of the Draize scoring system, and excised pieces of skin were examined by light and electron microscopy. Other than a general graying of the skin, there were no direct signs of topical irritation, although some indications of focal inflammation and edema were seen when the skin was viewed under light microscopy. For example, the authors noted the occurrence of epidermal hyperplasia with an extension of rete pegs into the dermis. However, the AgNPs themselves appeared to be limited to the superficial layers of the stratum cornea. These findings were consistent with those reported by Kim et al. [2013], who evaluated the irritation potential of AgNPs (10 nm average particle size) in New Zealand White rabbits and SPF guinea pigs. During the study with rabbits, no significant clinical signs or deaths were observed. In the initial test, no signs of irritation to the cornea, iris, or conjunctiva were observed 1, 24, 48, and 72 hours after removal of the test substance. When AgNPs were applied to the skin of SPF guinea pigs in accordance with OECD Test Guideline 406, none of the tested animals showed any significant body weight change, abnormal clinical signs, or death during the experimental period. However, these findings contrasted with those reported by Korani et al. [2011], in which an array of changes to the skin of Hartley guinea pigs were observed following dermal application of aqueous solutions of colloidal AgNPs (<100-nm diameters) at concentrations of 100 and 1,000 µg/mL in an acute study (6 animals/dose) using OECD Test Guideline 402 and three concentrations of 100, 1,000, and 10,000 µg/mL (6 animals/dose) in a subchronic study. In the acute study, 10% of the body surface was exposed and examined 1, 24, 48, and 72 hours post-exposure for presence of edema, erythema, or any type of dermal change. Observations continued for 14 days. In the subchronic study, a shaved

skin area of 5 cm × 5 cm was applied 5 days/week with 100, 1000, or 10,000 µg/mL AgNPs for 13 weeks; skin of the positive controls was rubbed with 100 µg/mL of $AgNO_3$. Korani et al. [2011] described an array of changes to the skin as a result of either dosing regimen, with increasing severity in such responses as epidermal thickness, inflammation, presence of round and clear cells, and reduced papillary in relation to dose and exposure duration. Similar skin inflammatory responses were recorded in all treatment groups in the subchronic study. Increased incidence of histopathologic responses in the liver and spleen were also reported for the subchronic study, with signs of necrosis at the highest dose. The results indicate that dermal contact with AgNPs causes slight histopathologic abnormalities of the skin, liver, and spleen of animals that can occur at dermal concentrations >0.1 mg/kg (>100 µg).

Ling et al. [2012] reported on the potential dermal exposure risk to workers for nanoscale zinc oxide powder, multiwall carbon nanotubes, and nanoscale silver (Ag-colloid, Ag-liquid) so that appropriate risk management practices could be incorporated in the workplace to protect workers. The assessment of workers' risk of exposure to nanoscale silver focused on the potential for dermal absorption of silver during the handling of nanoscale silver-colloid (average diameter, 9.87 nm) and silver-liquid (average diameter, 13.04 nm). Based on criteria by OECD [2004], WHO [2010], and EPA [2004], two skin exposure techniques were used (transdermal Franz diffusion cell drive and tape stripping) to evaluate dermal absorption of nanoscale silver. Excised porcine skin was used as a model for human skin in the transdermal Franz diffusion cell test. Nanoscale silver-colloid and silver-liquid samples flowed with specific rates through a portion of the skin for 18 hours. The sampled porcine skin and remaining fluids were analyzed for silver with use of flame atomic absorption spectrometry (FAAS); silver concentrations from the remaining skin and fluids were then added and compared with the original amounts. For the tape stripping technique, nanoscale silver-colloid and silver-liquid at concentrations of 20 µg/mL and 300 µg/mL, respectively, were applied evenly on human skin for 2 hours. After this, tapes with areas of 5 cm^2 were patched on the human skins and subjected to pressure, followed by immediate tape stripping. Stripping was repeated 5 times, with each taking up 6 to 8 layers of the stratum cornea, yielding about 30 to 40 cell layers of the stratum cornea being removed. The stripping tapes were analyzed by using inductively coupled plasma mass spectrometry (ICP/MS) to quantify silver contents. Results of the tape stripping analysis showed that the distribution of nanoscale silver

colloid and silver liquid was predominantly on the first and second stripping's of the stratum cornea. This occurred at both the 20-µg/mL and 300-µg/mL concentrations, indicating a low rate of skin penetration over a short period of exposure. In addition, the experiments showed that organic modifiers affected the infiltration of nanoscale silver. When a less polar solvent such as isopropyl alcohol was used, the penetration rate was higher than for other polar solvents.

Although the dermal toxicity data from studies of animals and studies using porcine skin are limited, they suggest that AgNPs are capable of penetrating the skin epidermis [Larese et al. 2009; Ling et al. 2012], induce some systemic toxicity [Korani et al. 2011], and can cause topical irritation at the site of contact [Samberg et al. 2010; Korani et al. 2011].

F.3.2 Intratracheal instillation or pharyngeal aspiration

F.3.2.1 Silver nanoparticles

Intratracheal instillation has been employed to study the in vivo responses to AgNPs in the lungs of experimental animals. For example, Park et al. [2011b] administered AgNPs at doses up to 500 µg/kg (single instillation) to ICR mice and examined the resulting inflammation by measuring the concentration of cytokines in BAL and in the blood. The commercially supplied AgNPs were originally suspended in THF with sonication. After all of the solvent had been allowed to evaporate, the particles were reconstituted in phosphate-buffered saline (PBS). A histopathologic analysis was also carried out on excised pieces of lung, and changes in gene expression were assessed by using a microarray method. The AgNPs were dispersed in an aqueous medium, and there was evidence of aggregation in that the average diameter of particles was 243.8 nm. A considerable number of dose-related changes were evident in the cytokine composition of BAL and blood as a result of exposure to AgNPs. In BAL, the most dramatic increases in cytokine levels were manifest in IL-1, IL-6, IL-10, and TGF-β. These agents appeared to reach a maximum concentration 28 days after exposure. In the blood, concentrations of IL-6, IL-12, IFN-γ, and IL-10 showed significant increases on the day after instillation. Histopathologic analysis indicated inflammatory responses, such as infiltration of alveolar macrophages, in lung tissue on day 1 but not on days 14 and 28. The responses were characterized by the presence of cell debris, dead

neutrophils, and foreign bodies. A substantial number of changes in gene expression resulted from intratracheal instillation of AgNPs, with 261 genes being upregulated and 103 genes downregulated. Changes in the functionality of induced genes appeared to be related to tissue damage.

Intratracheal instillation of AgNPs in male Sprague-Dawley rats was also observed to cause an increase in the cellular and protein content of BAL fluid [Roberts et al. 2012]. Rats were exposed to AgNPs (20 nm in diameter) with a 0.3%-by-weight coating of PVP. Dispersion of AgNPs in a physiologic medium caused some degree of aggregation, as indicated by the average particle size of 180 nm. AgNPs were administered weekly for 8 weeks at 0, 9.35, or 112 µg, with subsequent termination and evaluation after 7, 28, or 84 days. The high dose of AgNPs was observed to induce acute pulmonary injury and inflammation that appeared to resolve over time.

F.3.2.2 Silver nanowires

Kenyon et al. [2012] studied the lung toxicity of silver nanowires (AgNWs) of varying lengths in male Sprague-Dawley rats (by intratracheal instillation of long [20 µm] or short [4 µm] AgNWs, about 50 nm in diameter). Rats were administered AgNW doses of 10, 50, 125, or 500 µg, alpha-quartz (positive control) at 500 µg, or dispersion medium (vehicle control). Both wire samples caused a dose-dependent increase in lung injury (lactate dehydrogenase activity and albumin content in lavage fluid) and inflammation (increased lung neutrophils and phagocyte oxidant production). Neither the short nor the long wires at the 10-µg dose had any effect on lung toxicity. The longer wires caused slightly more lung injury immediately following exposure, whereas the shorter wires induced greater toxicity over the time course. The authors suggested this finding may be due to greater wire number and surface area in the short wire sample when samples were compared on an equivalent mass basis.

Schinwald et al. [2012] studied the role of length of silver nanowires (AgNWs) on the acute lung responses in mice (C57BL/6, female, 9 weeks old). Mice (five per group) were exposed by pharyngeal aspiration to AgNWs of different lengths (3, 5, 10, or 14 µm) or to short or long fibers of amosite (SFA or LFA). The doses were selected to equalize the number of fibers per mouse,

which resulted in mass doses of 10.7, 10.7, 17.9, 35.7, and 50 µg/mouse for SFA, AgNW3, AgNW5, AgNW10, AgNW14, and LFA, respectively. The 50-µg dose was selected from an initial dose-response series as one that resulted in a persistent inflammatory response with AgNW14 and LFA. The acute inflammation response was evaluated 24 hours after aspiration exposure. A length-dependent trend in the pulmonary inflammatory response was observed for the AgNWs, yet only the mice exposed to the longest (14 µm) AgNW showed a statistically significant increase in the granulocytes in BAL fluid. A nonlinear relationship was observed between exposure to AgNW by length and inflammation response, which suggested a length threshold based on a "discernible step-increase in granulocyte recruitment at a length between 10 and 14 µm" [Schinwald et al. 2012]. Frustrated phagocytosis (defined as incomplete uptake of fibers by cells) was observed in mice exposed to AgNW14 or LFA. Histopathology performed 24 hours after aspiration showed minor granulomas and lymphocyte infiltrates in mice exposed to AgNW5 or AgNW10. More extensive granuloma and lymphocyte infiltrates were observed in mice exposed to AgNW14 and LFA, which was consistent with the BAL inflammation findings. Although the AgNW14 produced more granulomatous areas compared to shorter fibers, that response was still relatively minor compared to the “extensive interstitial thickening and remodeling of the alveolar spaces after LFA treatment” [Schinwald et al. 2012]. The author’s note that their results need to be confirmed in long-term inhalation studies using a range of different nanofibers at plausible exposure concentrations, before these thresholds for risk assessment can be used.

F.3.3 Subcutaneous, intravenous, or intraperitoneal injection

F.3.3.1 Kinetics following subcutaneous injection

Tang et al. [2008] investigated the potential of AgNPs (50–100 nm in diameter) and silver microparticles (2–20 µm in diameter) to cross the blood–brain barrier. Wistar rats (90 females) were given a subcutaneous injection of either AgNPs or silver microparticles, and five rats from each group were killed at weeks 2, 4, 8, 12, 18, and 24 to obtain brain tissue to measure silver concentrations. Silver concentrations were higher for the AgNP group than for the silver microparticle and control groups and reached statistical significance at 4 weeks ($P < 0.05$). In the

AgNP group silver concentrations reached a peak of 0.41 µg ± 0.16 µg at week 12 and did not change significantly by week 24. No significant difference in silver concentrations between the silver microparticle group and control group was detected ($P > 0.05$). It could not be determined whether the silver concentrations in the brain were a result of AgNPs or Ag^+. However, in ultrastructural analysis, AgNPs were detected in vascular endothelial cells from the abnormal blood–brain barrier, which could have resulted from transcytosis of the endothelial cells of the brain–blood capillary. No abnormal substance was detected in the brains of rats from the control group and the silver microparticle group. However, many pyknotic, necrotic neurons were detected in the brain of the AgNP exposure group between 2 and 24 weeks.

Tang et al. [2009] also studied the distribution of AgNPs over a 24-month period after the subcutaneous injection of elemental AgNPs or silver microparticles in female Wistar rats at a single dose of 62.8 mg/kg. The preparation of nanoparticles (5 mg/mL in physiologic medium) was reported to be 50–100 nm in diameter, mostly spherical, and with a low degree of aggregation. The tissue and subcellular distribution of silver associated with this preparation was compared with that of a preparation of silver microparticles. These were said to be of various shapes and sizes, ranging from 2 to 20 µm. Although most of the silver from both nanoparticles and microparticles accumulated at the site of administration, ICP-MS showed that about 0.15% of the nanoparticle load reached the bloodstream and was distributed to remote sites, including kidney, liver, spleen, brain, and lung. By contrast, silver microparticles did not pass to the general circulation to any great extent (no more than 0.02% of the injected load), and their distribution to the tissues was therefore markedly less than that of AgNPs. However, fecal excretion of silver from silver microparticles was greater than that from nanoparticles during early follow-up (2 weeks after injection). This pattern was reversed on later sampling dates (up to 24 weeks). For AgNPs, histopathologic examination of these target organs by TEM and EDS revealed localization of internalized silver. This showed silver-containing electron-dense droplets (as opposed to dissolute silver ions) in the renal tubular epithelial cells, at the margin of the renal capsule, and in hepatocytes, hepatic sinusoidal and perisinusoidal spaces, lymphocytes in the splenic cord, cerebral neurons, vascular endothelial cells of the blood-brain barrier, and alveolar epithelial cells.

F.3.3.2 Kinetics following intravenous injection

Corroborative evidence of the distribution of internalized AgNPs to the liver has come from studies in which the deposition of intravenously injected ^{125}iodine-labeled AgNPs was monitored by single-photon emission computerized tomography (SPECT) imaging in Balb/c mice and Fischer CDF rats [Chrastina and Schnitzer 2010]. The PVP-coated AgNPs were spherical and largely monodispersed, with an average diameter of 12 nm. In addition to the SPECT imaging, the major organs were excised from the animals at term and counted for radioactivity. SPECT imaging gave a strong signal in the abdominal area that was thought to be associated with the liver and spleen. Less-intense signals were associated with the lung and bone. The level of activity in the blood after 24 hours was comparatively low, suggesting translocation from the blood via the mononuclear phagocyte system.

In a study to assess the distribution and excretion of silver, Klaassen [1979] intravenously administered silver nitrate in the femoral vein of rats (0.01, 0.03, 0.1, or 0.3 mg/kg Ag/kg), rabbits (0.1 mg/kg Ag/kg), and dogs (0.1 mg/kg Ag/kg). Within 4 days post administration of silver to rats dosed at 0.1 mg/kg Ag/kg, 70% of the silver was excreted in the feces and <1% into the urine. The disappearance of silver from the plasma and its excretion into the bile were measured for 2 hours after the intravenous administration of 0.01, 0.03, 0.1, and 0.3 mg/kg of silver to rats. The concentration of silver in the bile was 16–20 times higher than that in the plasma. For the two lower doses, the overall plasma-to-bile gradient was due almost equally to the plasma-to-bile gradient and the liver-to-bile gradient, whereas for the doses at the two higher concentrations of silver the liver-to-bile gradient became more important. Marked species variation in the biliary excretion of silver was observed. Rabbits and dogs excreted silver at rates about 1/10 and 1/100, respectively, of that observed in the rat. Although it is difficult to determine the excretion rate of silver in the bile of humans, the results indicate that biliary excretion is an important route for the elimination of silver.

Lee et al. [2013c] also found the serum kinetics, tissue distribution, and excretion of citrate-coated AgNPs in rabbits to be similar to those found by Klaassen [1979] following intravenous injection. Citrate-coated AgNPs (~7.9-nm diameter) were intravenously injected into the ear vein of four

SPF New Zealand white male rabbits at doses of 0.5 mg/kg and 5 mg/kg, based on dose selection following the Organization for Economic Cooperation and Development (OECD) test guideline 417. Blood was sampled from the vein of the collateral ear before and after treatment, at 5, 10, and 30 minutes; at 1, 2, 6, and 12 hours; at the end of days 1 through 7; and at days 14, 21, and 28. Blood samples were also collected from the non-treated control group, at 1, 7, and 28 days. The concentration of AgNPs in the serum was at its highest 5 minutes following treatment, and 90% of the AgNPs were eliminated from the serum at 28 days. Tissue distribution of AgNPs was determined in the liver, lung, kidney, brain, spleen, testis, and thymus, revealing that the liver, spleen, and kidney were the main target organs. This finding was consistent with findings in other studies [Lankveld et al. 2010; Loeschner et al. 2011; Park et al. 2011]. Although the accumulated level of silver in the 5-mg/kg-dose group was higher than that in the 0.5-mg/kg-dose group, tissue accumulations of AgNPs observed in the high-dose group were not always 10-fold higher than in the low-dose group. The excretion of AgNPs through urine, in comparison with feces, was very low during the entire experimental period; more than 90% of AgNPs was still present in the body in the high-dose group at day 7, and 85% still remained in the low-dose group over the same period. Pigmentation in the liver was the main finding of histopathology at 7 and 28 days, whereas no pigmentation was observed in the non-treated control rabbits. Inflammatory cell infiltration was significantly increased in the liver, lung, and kidneys of the AgNP-treated rabbits. However, there were no significant histologic findings in the brain and thymus.

Dziendzikowska et al. [2012] evaluated the time-dependent biodistribution and excretion of silver by administering intravenously 20- and 200-nm AgNPs to male Wistar rats at a dose of 5 mg/kg body weight (bw) (2 exposure and 1 control group of 23 rats each). The study was designed to (1) analyze the effect of AgNP size on rat tissue distribution at different time points, (2) determine the accumulation of AgNPs in target organs, (3) analyze the intracellular distribution of AgNPs, and (4) examine the excretion of AgNPs by urine and feces. Biologic material was collected at 24 hours and at 7 and 28 days after injection and analyzed by ICP-MS and TEM. AgNPs were found to translocate from the blood to the main organs (lungs, liver, spleen, kidneys, and brain), and the highest concentration of silver was in rats treated with 20-nm AgNPs, in comparison with 200-nm AgNPs. The highest concentration of silver was found in the liver after 24 hours, indicating that the liver may be the first line of defense as a consequence of intravenous administration and/or

because of the activation of metal-lothioneins, involved in detoxication of heavy metals such as silver [Wijnhoven et al. 2009]. In addition, the high silver deposition in the liver (8 µg/g wet weight) may have been associated with effective filtration and the presence of specific subpopulations of mononuclear phagocytic cells that can be involved in the sequestration of nanoscale particles. The concentration of silver in the liver decreased over time and reached the lowest concentration at 28 days post-administration. These findings possibly indicate a purification of the liver and redistribution of AgNPs to other organs or its excretion from the body in bile [Kim et al. 2010a; Park et al. 2011a]. Silver concentrations found in the lungs (that is, accumulated in alveolar macrophages) were similar to those observed in the spleen after 7 days, and the concentration of silver in the kidneys and brain increased with time and peaked at 28 days. Despite the high concentration of silver in the kidneys, the rate of silver excretion in the urine was low, which might be explained by the lack of renal glomerular filtration and tubular excretion of the kidneys if the particle size is larger than the distance of cell membranes, ranging from 5.5 to 10 nm. The size of AgNPs (20-nm particles) and their ability to accumulate in various organs were the highest. These findings are consistent with those of Lankveld et al. [2010], who showed a higher level of small (20-nm) AgNPs in the liver and a lower level in the kidneys, brain, and heart, whereas large AgNPs (80 and 100 nm) were concentrated mainly in the spleen and (in smaller amounts) in the liver and lungs. Repeated administration of AgNPs resulted in accumulation of silver in the liver, lung, and spleen, indicating a possible mechanism responsible for the distribution of different-sized nanoscale particles. These findings were consistent with those suggested by Li and Huang [2008], who found that particles smaller than the pores of liver fenestrae (about 100 nm) are captured more efficiently by the liver, whereas larger particles are absorbed with greater affinity in the spleen.

The distribution and biokinetics of AgNPs were also evaluated by Xue et al. [2012] following intravenous administration of AgNPs in the tail vein of ICR mice. Mice (three exposure groups and a control group, with six male and female mice per group) were exposed to doses of AgNPs at 7.5, 30, or 120 mg/kg. Average primary particle size of purchased AgNPs, as determined by TEM, was 21.8 nm (10–30 nm), but agglomeration of particles (up to 117-nm diameter) was observed to occur at the time of intravenous administration. Toxic effects were assessed via general behavior, serum biochemical parameters, and histopathologic observation of the mice.

Biokinetics and tissue distribution of AgNPs were evaluated at a dose of 120 mg/kg. Silver analysis using ICP-MS was used to quantify silver concentrations in blood and tissue samples at predetermined time intervals. After 2 weeks, AgNPs exerted no obvious acute toxicity in the mice; however, inflammatory reactions in lung and liver cells were induced in mice treated at the 120-mg/kg dose level. The distribution of silver was observed in all major organs, with the highest levels found in the spleen and liver, followed by the lungs and kidneys. Silver was retained in the spleen for the entire experiment, whereas the 120-µg/g silver concentration found in the liver slowly decreased over 14 days. In the lungs, silver concentrations decreased from days 1 through 7 but increased slightly from days 7 through 14. The elimination half-lives and clearance of AgNPs were 15.6 hours and 1.0 ml/hr for male mice, and 29.9 hours and 0.8 ml/hr for female mice. A gender-related difference in the biokinetic profiles of blood, as well as the distribution of silver to the lungs and kidneys, was observed, with significantly higher levels of silver found in the female mice than in male mice at 14 days post-injection. This gender difference in organ-specific silver concentration is consistent with findings reported by Kim et al. [2008] and Sung et al. [2008] in rats exposed to AgNPs. Mild histopathologic changes were also found in the lungs and liver of mice in the 120-mg/kg exposure group [Xu et al. 2012]. These findings are similar to those previously reported by Kim et al. [2008], in which liver damage was found in Sprague-Dawley rats exposed by oral administration to 300 mg AgNPs.

F.3.3.3 Toxicological effects following intravenous or intraperitoneal injection

A series of experiments by Sharma et al. [2010] in Sprague-Dawley rats examined the capacity of aqueous dispersions of manufactured AgNPs (50–60 nm in diameter) to disrupt the blood-brain barrier. Silver nanoparticles were administered intravenously (30 mg/kg), intraperitoneal (50 mg/kg), or as a cortical superfusion (20 µg/10 µL) in a 0.7% sodium chloride solution containing 0.05% Tween 80. The authors measured the permeability of the blood-brain barrier to a sterile solution of Evans blue albumin or a ^{131}iodine tracer given intravenously and assessed the potential for edema formation in the brain by measuring tissue water content. AgNPs altered the blood-brain barrier to Evans blue albumin and radioiodine when administered intravenously or as a cortical superfusion but not by intraperitoneal administration. The leakage of Evans blue albumin was evident on the ventral surface of the brain and in the proximal frontal cortex. Cortical

superfusion with nanoparticles gave moderate opening of the blood-brain barrier to protein tracers, with leakage of Evans blue albumin as well. A significant increase in brain water content was seen after administration of AgNPs intravenously or by cortical superfusion. As before, intraperitoneal administration was ineffective. In discussing their results, Sharma et al. [2010] stated that the increase in brain water content in areas where leakage of Evans blue albumin was observed was consistent with the capacity of systemically applied AgNPs to bring about edema formation and subsequent brain damage. A possible result of these changes could be AgNP-induced brain dysfunction, thereby raising the possibility of an association between acute exposure to AgNPs and neurodegenerative changes.

Although the intraperitoneal injection of AgNPs was ineffective in bringing about changes to the blood-brain barrier in Sprague-Dawley rats [Sharma et al. 2010], a study by Rahman et al. [2009] showed this route of application to be useful in bringing about changes in gene expression to regions of the brain in male C57BL/6N mice. They were intraperitoneal injected with 100, 500, or 1,000 mg/kg of 25-nm-diameter AgNPs and then killed after 24 hours. Total RNA was extracted from the caudate nucleus, frontal cortex, and hippocampus and analyzed by means of RT-PCR. Differential alterations in gene expression implicated AgNP-induced changes in apoptosis and free-radical-induced oxidative stress.

Sriram et al. [2010] studied the antitumor activity of AgNPs in a Dalton's lymphoma ascites tumor model, using both in vivo and in vitro experimental protocols. In the in vivo phase of the study, AgNPs were intraperitoneal injected into tumor-bearing Swiss albino mice (females), and their survival times and tumor volumes were compared to those of untreated mice. The researchers used a novel approach to AgNPs synthesis in which a culture of *Bacillus licheniformis* was incubated in the presence of silver nitrate for 24 hours; subsequent ultrasonication and filtration of cell debris yielded a suspension of AgNPs, which were then harvested by centrifugation. TEM analysis indicated that the endotoxin-free particles were mostly spherical and largely free from aggregation, with an average diameter of 50 nm. Key data emerging from the in vivo phase of the study was the reduction in survival time to 18 ± 1 days, compared with a stated duration of 50 ± 2 days in non-tumor-bearing controls. Animals that had been intraperitoneal injected daily with 500-nm AgNPs for 15 days survived for 32 ± 3 days and showed a marked reduction in tumor volume.

Associated with the increased survival time and lower tumor volume in AgNP-treated mice was a decline in the elevated white blood cell and platelet counts that were seen in untreated ascites-bearing mice. Other hematologic parameters remained within the normal range for all groups. In discussing their data, Sriram et al. [2010] mentioned that an important characteristic of anticancer agents would be the capacity to induce apoptosis, which, as their in vitro experiments and many other research reports have shown, is a consistent response to AgNP exposure.

Gromadzka-Ostrowska et al. [2012] described the results of a study in which male Wistar rats (four groups, 24/group) were intravenously injected (tail vein) with AgNPs to assess the effects on spermatogenesis and seminiferous tubule morphology. The described experimental study featured changes to the applied concentration and dimensions of the AgNPs. Thus, animals received either 5 or 10 mg/kg AgNPs that were roughly 20 nm in diameter, 5 mg/kg of AgNPs that measured 200 nm, or 0.9% NaCl for the control group. Rats were killed at 24 hours, 7 days, or 4 weeks after treatment. Additionally, sperm counts were taken and germ cells assessed for DNA damage by means of the comet assay. Silver nanoparticles at different doses and particle sizes appeared to be associated with increased comet tail moments after different durations. The frequency of abnormal spermatozoa in epididymal semen from experimental groups was not significantly different, as compared with the NaCl group at the given time points. However, in all treated groups, the number of abnormal spermatozoa found 1 or 4 weeks after treatment was higher ($P < 0.05$). The comet assay showed that DNA damage (% DNA in tail) in the germ cells was significantly increased at 24 hours in the 5- and 10-mg/kg (20-nm Ag) groups ($P \leq 0.05$) but declined with time post-exposure. No difference in the DNA damage level was found between the control group and the 5-mg/kg group (200-nm Ag) at all post-exposure time points. The results were interpreted “as suggestive” that AgNP genotoxicity was more pronounced in mature sperm cells in the epididymis than in spermatozoa in seminiferous epithelium. Histologic examination of the testes showed change in the testes seminiferous tubule morphometry in the rats treated with 200-nm AgNPs.

Kim et al. [2009b] administered AgNPs intravenously to Sprague-Dawley rats (two per sex per group) to correlate clinical chemistry, histopathologic, and toxicogenomic responses, with the aim of identifying biomarkers for AgNP exposure. Animals were exposed to an unstated number of

injections of AgNP preparations over a 4-week period. Exposure groups included a nonexposed control group, group I (receiving 100 mg/kg silver in 50- to 90-nm particles), and group II (receiving 1 mg/kg silver in 1- to 10-nm particles). The AgNPs were dispersed in an aqueous medium containing amino acids. The only clinical chemistry changes observed were statistically significant increases in serum cholesterol concentrations in the two exposed groups and reductions in serum creatinine levels that also achieved statistical significance. Histopathology examination of major tissues and organs showed silver particle deposition in the hepatic sinusoids and Kupffer cells. These effects were associated with moderate lymphocyte aggregation, destruction of hepatocytes, and lymphocytic infiltration of the hepatic perivenular area. Though not necessarily associated with histopathologic disorders, other sites of silver deposition were the lung alveolar septum, kidney glomerulus, and spleen white pulp. The most striking hematologic finding was a marked increase in the lymphocyte/granulocyte ratio in the AgNP-exposure groups, compared to controls. Kim et al. [2009b] also observed alterations in gene expression in rats exposed to AgNPs when total RNA was extracted from the livers of control and exposed groups and used as a basis for microarray analysis. Using a threshold of 1.2 to assign genes into upregulated or downregulated categories, the researchers sorted 191 and 187 genes into these respective categories when the findings for groups I and II were considered together. Twenty genes were found to be commonly expressed in groups I and II, four of which (SLC7A13 [solute carrier family 7, member 13], PVR [poliovirus receptor], TBXAS1 [thromboxane A synthetase 1], and CKAP4 [cytoskeleton-associated protein 4]) were proposed as size-independent genomic biomarkers. Ten other genes were proposed as sentinels for the AgNP-induced histopathologic and clinical chemistry changes.

The same researchers also injected two male Sprague-Dawley rats per group with 50-nm AgNPs at doses of 0 (control), 1, or 100 mg/kg at 2- to 3-day intervals over a 4-week period, prior to performing a proteomic analysis of liver, lung, and kidney tissues [Kim et al. 2010b]. Protein extracts from liver, lung, and kidney were separated by means of two-dimensional gel electrophoresis. Protein spots selected as differentially expressed were cut from the gels, digested, and then identified with matrix-assisted laser desorption/ionization time of flight mass spectrometry (MALDI-TOF MS) and peptide mass fingerprinting. Functional analysis of the differentially expressed proteins, as related to exposure to AgNPs, demonstrated outcomes such

as apoptosis, generation of reactive oxygen species (ROS), thrombus formation, and inflammation. Differentially expressed proteins in the kidney also appeared to be associated with indicators of metabolic disorders such as diabetes.

Tiwari et al. [2011] also reported an increase in ROS levels when Wistar rats were injected intravenously through the tail vein at doses of 4, 10, 20, and 40 mg/kg AgNPs (15–40 nm in diameter) at 5-day intervals over 32 days. Histopathologic examination revealed significant changes ($P < 0.01$) in hematologic parameters (WBCs, platelets, hemoglobin, and RBCs) in the 20- and 40-mg/kg groups. In the 40-mg/kg group, statistically significant increases were also found in the liver function enzymes alanine aminotransferase (ALT), aspartate aminotransferase (AST), AP, gamma glutamyl transpeptidase, and bilirubin. AgNP deposition was reported to be found primarily in the liver and kidney of rats exposed at doses of 20 and 40 mg/kg. ROS was found to increase in all groups in a dose-related manner. The investigators suggested that the deposited AgNPs are endocytosed and interact with mitochondria to produce ROS. These increased levels of ROS (AgNP in doses >20 mg/kg) enhance H_2O_2 levels, which can cause damage in the DNA strand, chromosome aberration, and conformational changes in proteins. AgNP doses <10 mg/kg were considered to be safe for biomedical application.

Austin et al. [2012] intravenously injected pregnant CD-1 mice with AgNPs (average diameter, 50 nm; range, 30–60 nm) on gestation days (GDs) 7, 8, and 9 at dose levels of 0 (citrate buffer), 35, or 66 µg Ag/mouse (group sizes of 6–12) to evaluate the distribution of AgNPs in pregnant mice and their developing embryos. Additional groups of mice were treated with silver nitrate (dissolved in 0.25 M mannitol) at dose levels of 9 and 90 µg Ag/mouse. Group sizes were nine and three mice for the 9- and 90-µg dose levels, respectively. Mice were euthanized on GD 10, and tissue samples were collected and analyzed for silver content. A significant increase ($P < 0.05$) in AgNP content as compared to that in silver nitrate–treated animals was observed in nearly all tissues; AgNP accumulation was significantly higher in liver, spleen, lung, tail (injection site), visceral yolk sac, and endometrium; the highest levels of silver were found in the liver, spleen, and visceral yolk sac. Concentrations of silver in embryos were about 25-fold less than those seen in the placenta or visceral yolk sac, suggesting that AgNPs become sequestered in visceral yolk sac vesicles and do not reach the fetal circulation in significant amounts; no adverse

morphologic effects on the developing embryos were observed. Austin et al. [2012] proposed that pinocytosis might be responsible for AgNP uptake by the visceral yolk sac.

The teratogenicity potential of AgNPs in pregnant 3- to 4-month-old Wistar rats was investigated by Mahabady [2012]. Pregnant rats (n = 30) were randomly divided into five groups (24 pregnant rats in treatment group and six pregnant rats in saline control group). Two subgroups of six rats in one treatment group were given either 0.4 or 0.8 mg/kg nanosilver intraperitoneal on GD 8. The same doses of nanosilver were also administered to a second treatment group (two groups of six rats) on GD 9. All animals were killed on GD 20; the uterus was exteriorized and the number and location of fetuses and resorptions were noted. The mean of weight, volume, and width of fetuses' placenta decreased significantly ($P < 0.05$) in both treatment groups in comparison with the saline control group; no observed skeletal abnormalities were observed in the fetuses. No information was provided on the size of the AgNPs or whether the AgNPs were coated.

Liu et al. [2013] reported that AgNPs do not affect spatial cognition or hippocampal neurogenesis in adult male ICR mice (n = 15 per dose, n = 10 for control). Mice were administered via intraperitoneal injection non-coated AgNPs with an average diameter of 36.3 nm at doses of 0 (control), 25, or 50 mg/kg, once a day in the morning for 7 consecutive days. Another group of mice received scopolamine (3 mg/kg) as a positive control for the behavioral studies. The spatial learning and memory ability was assessed with the Morris water maze test; after the behavioral test, mice were injected with bromodeoxyuridine and killed on days 1 and 28 post-exposure, and the brains were evaluated for proliferating cells. The test results showed that AgNP exposure did not alter either reference memory or working memory in the mice, in comparison with those in the non-exposed control group. Also, in the AgNP treatment groups no differences were revealed in hippocampal progenitor proliferation or on the survival and differentiation of newly generated cells.

Lee et al. [2013b] intraperitoneal injected Sprague-Dawley rats (300–350 g/bw) with AgNPs (10–30 nm in diameter) at concentrations of 500 mg/kg to test the hypothesis that autophagy plays a role in mediating hepatotoxicity in animals. Autophagy is a homeostatic mechanism to promote cell survival by facilitating the removal of malformed or injured proteins or organelles [Lee et al.

2013b]. This study focused on the interrelationship between energy metabolism, autophagy, apoptosis, and hepatic dysfunction. All animals were killed on days 1, 4, 7, 10, or 30 post-exposure, and the concentration of silver in the liver was found to be 58–81 μg/g. Uptake of AgNPs was observed to be rapid but not proportional to the blood Ag concentration. Declination of ATP (-64% in day 1) and autophagy (determined by LC3-II protein expression and morphologic evaluation) increased and peaked on the first day. ATP content remained at a low level even though the autophagy had been activated. Apoptosis began to rise sigmoidally at days 1 and 4, peaked at day 7, and remained constant during days 7–30 post-exposure. Meanwhile, autophagy exhibited a gradual decrease from days 1 to 10, and the decrease at day 30 in comparison with the control group was statistically significant. The decline in autophagy, along with a high concentration of silver in the liver, was interpreted by the authors as causing insufficient self-protection, which contributed to the observed hepatotoxicity. An inflammatory response in the liver was observed by histopathologic evaluation on day 10 and was seen to progress to an advanced degree on day 30, when liver function was impaired.

Table F-5. Summary of in vivo toxicological studies of silver nanoparticles (AgNPs) and nanowires (AgNWs)

Species	Particle Characteristics	Exposure Details		Critical Effect(s)	NOAEL/LOAEL	Comments	Reference
		Concentration/ Dose	Duration				
Inhalation Exposure – Acute or Subacute							
Sprague-Dawley rats; 5 of each sex per group	Mostly spherical, 15–20 nm in diameter	0, 76, 135, or 750 µg/m^3	Single 4-hr exposure	Clinical signs and lung function parameters	−/−	No adverse effects observed	Sung et al. [2011]
Sprague-Dawley rats; 10 of each sex per group	Mostly spherical, diameter range 2–65 nm (median, 16 nm)	0, 0.48, 3.48, or 61 µg/m^3	6 hrs/day, 5 days/week for 4 weeks	Slight cytoplasmic vacuolization of the liver	0.48/3.48 µg/m^3	Dose-response effect in females only	Ji et al. [2007b]
Sprague-Dawley rats; 10 of each sex per group	Mostly spherical, diameter range 2–65 nm (median, 16 nm)	0, 0.48, 3.48, or 61 µg/m^3	6 hrs/day, 5 days/week for 4 weeks	Increase in number and size of the neutral mucin-producing goblet cells	0.48/3.48 µg/m^3		Hyun et al. [2008]
C57Bl/6 mice; 3×26 test animals, 13 controls	Spherical PVP-coated particles, >85% approx. 5 nm in diameter, but with 79-nm (GM) aggregates	0, 3,300 µg/m^3	4 hrs/day, 5 days/week for 2 weeks	Minimal pulmonary inflammation	3,300 µg/m^3	Single concentration tested	Stebounova et al. [2011]

Table F-5. Summary of in vivo toxicological studies of silver nanoparticles (AgNPs) and nanowires (AgNWs)

Species	Particle Characteristics	Exposure Details		Critical Effect(s)	NOAEL/LOAEL	Comments	Reference
		Concentration/ Dose	Duration				
Sprague-Dawley male rats; 12 exposed and 12 controls	Two types of mostly spherical Ag [75% colloidal and 25% silver ions with 33-nm MAD; and 100% colloidal with 39-nm MAD]	0, 100 µg/m^3 (1.4 µg Ag/rat lung) or 1000 µg/m^3 (14 µg Ag/rat lung)	Single 5-hr exposure; evaluated 1 and 7 days post-exposure	No acute toxicity in pulmonary or cardiovascular parameters	-/-	No adverse effects observed	Roberts et al. [2013]
C57BL/6 male mice (2 groups of 7)	AgNPs geometric mean diameter, 22.18 ± 1.72 nm	AgNPs (1.91×10^7 particles/cm^3)	6 hrs/day, 5 days/week for 2 weeks; one of the groups was observed for 2 weeks of recovery before necropsy	RNA analysis of cerebrum and cerebellum showed several genes associated with motor neuron disorders, neurodegenerative disease, etc.; genes from whole blood modulated in parallel to those in the brain	NA	Investigators believe that these genes could serve as biomarkers for AgNP exposure	Lee et al. [2010]

Table F-5. Summary of in vivo toxicological studies of silver nanoparticles (AgNPs) and nanowires (AgNWs)

Species	Particle Characteristics	Exposure Details		Critical Effect(s)	NOAEL/LOAEL	Comments	Reference
		Concentration/ Dose	Duration				
Fischer rats (F344/DuCrl); 12 males in each of 3 groups	15 nm and 410 nm (200-nm primary particles)	15-nm group: mass, 179 µg/m^3; particle number, 3.8 × 10^6. 410-nm group: mass, 167 µg/m^3; particle number, 2.0 × 10^4. Air-only group:	Nose-only 6 hrs per day, followed by 4 consecutive days to air only; 6 rats from each group killed 24 h after 4 days' exposure to air; remaining 6 rats killed 7 days after air exposure	No lung lesions observed; acute pulmonary inflammation response to 15-nm AgNPs post-exposure after 4 days of air exposure, but effects resolved after 7 days post-exposure	NA	AgNPs observed inside lung cells at 24 h post-exposure; average particle size reduced to <5 nm, attributed to dissolution; toxicity related to lung dose and particle number/ surface area	Braakhuis et al. [2014]
Inhalation – Subchronic							
Sprague-Dawley rats; 10 of each sex per group	Mostly spherical, diameter range 2–65 nm (median, 16 nm)	0, 49, 133, or 515 µg/m^3.	6 hrs/day, 5 days/week for 90 days	Lung function deficits, alveolar inflammation, macrophage accumulation	133 (49) /515 µg/m^3	Lung function and histologic deficits at high dose	Sung et al. [2008]
Sprague-Dawley rats; 10 of each sex per group	Mostly spherical, diameter range 2–65 nm (median, 16 nm)	0, 49, 133, or 515 µg/m^3	6 hrs/day, 5 days/week for 90 days	Bile duct hyperplasia; hepatocellular necrosis	133/515 µg/m^3	Same experiment as Sung et al. [2008]	Sung et al. [2009]

Table F-5. Summary of in vivo toxicological studies of silver nanoparticles (AgNPs) and nanowires (AgNWs)

Species	Particle Characteristics	Exposure Details		Critical Effect(s)	NOAEL/LOAEL	Comments	Reference
		Concentration/ Dose	Duration				
Sprague-Dawley rats; 17 males and 12 females per group	Spherical, non-agglomerated; diameter range 4–45 nm (median, 14–15 nm)	0, 49, 117, or 381 μg/m^3	6 hrs/day, 5 days/week for 12 weeks	Lung function decrease, persistent lung inflammation in male rats; lung inflammation with gradual recovery in female rats	117 (49) /381 (117) μg/m^3	Silver nanoparticles generated as reported previously [Ji et al. 2007a]	Song et al. [2013]
Sprague-Dawley male and female rats; 4 groups of 10	AgNPs with 18-nm diameter	0.7 × 10^6 particles/cm^3 (low dose), 1.4 × 10^6 particles/cm^3 (middle dose), 2.9 × 10^6 particles/cm^3 (high dose)	6 hrs/day for 90 days; killed 24 hrs after last treatment	Bone marrow tested for toxicity with micronucleus assay; no treatment-related genetic toxicity observed	NA		Kim et al. [2011a]
Sprague-Dawley male and female rats; 17 male and 12 female per group	Spherical AgNPs with diameters <47 nm (range, 4–47 nm)	0.6 × 10^6 particles/cm^3 (low dose), 1.4 × 10^6 particles/cm^3 (middle dose), 3.0 × 10^6 particles/cm^3 (high dose)	6 hrs/day, 5 days/week for 12 weeks; rats given micronucleus gene test at end of 12 weeks or after 4- or 12-week recovery	Genes found to be up- and down-regulated for the kidney by more than 1.3-fold (P < 0.05): 104 genes for males and 72 for females	NA	Female rats show a 2–4-fold higher Ag concentration in kidneys, possibly due to metabolism and hormonal regulation	Dong et al. [2013]

Table F-5. Summary of in vivo toxicological studies of silver nanoparticles (AgNPs) and nanowires (AgNWs)

Species	Particle Characteristics	Exposure Details		Critical Effect(s)	NOAEL/LOAEL	Comments	Reference
		Concentration/ Dose	Duration				
Oral Exposure							
Sprague-Dawley rats; 10 of each sex per group	60-nm diameter in aqueous 0.5% carboxymethyl-cellulose (CMC), shape not specified*	0, 30, 300, or 1,000 mg/kg-day by gavage	28 days	Increases in serum cholesterol and alkaline phosphatase; liver histopathology	30/300 mg/kg-day	Silver deposited in major organs and tissues	Kim et al. [2008]
Sprague-Dawley rats, 4 males per group/time point	Citrate-coated 7.9-nm diameter in an aqueous medium, shape not specified	1 or 10 mg/kg	Single exposure	Silver deposition in plasma, feces, urine, and the major tissues and organs	−/1 mg/kg	Citrate-coating of the particles may have deterred absorption	Park et al. [2011a]
ICR mice; 5 of each sex per group	22-, 42-, 71-, and 323-nm-diameter particles in an aqueous medium, shape not specified	1 mg/kg-day	14 days	Silver deposition in a wide range of tissues; increased serum concentrations of TGF-β	NA	Smaller particles were more effective	Park et al. [2010b]
ICR mice; 3 of each sex per group	42-nm diameter in an aqueous medium, shape not specified	0, 250, 500, or 1,000 µg/kg-day by gavage	28 days	Increases in serum AP, AST, ALT, and cytokines; kidney histopathology	500/1,000 µg/kg-day		Park et al. [2010a]

Table F-5. Summary of in vivo toxicological studies of silver nanoparticles (AgNPs) and nanowires (AgNWs)

Species	Particle Characteristics	Exposure Details		Critical Effect(s)	NOAEL/LOAEL	Comments	Reference
		Concentration/ Dose	Duration				
F344 rats; 5 of each sex per group	60-nm diameter in aqueous 0.5% CMC, shape not specified*	0, 30, 125, or 500 mg/kg-day by gavage	90 days	Kidney histopathology and silver deposition	ND	Heavier silver deposition was observed in females	Kim et al. [2009a]
F344 rats; 10 of each sex per group	60-nm diameter in aqueous 0.5% CMC, spherical and monodisperse	0, 30, 125, or 500 mg/kg-day by gavage	90 days	Increases in serum cholesterol and AP; liver histopathology	30/125 mg/kg-day	NOAEL and LOAEL are as specified by the study authors	Kim et al. [2010a]
Sprague-Dawley rats; 10 of each sex per group	60-nm diameter in aqueous 0.5% CMC, shape not specified*	0, 30, 300, or 1,000 mg/kg-day by gavage	28 days	Intestinal silver deposition: Goblet cell activation	ND	Data are semi-quantitative	Jeong et al. [2010]
ICR mice (up-down procedure for oral lethality)	Spherical, starch-stabilized particles of 10–20-nm diameter	5,000 mg/kg	Single dose	No lethality or signs of toxicity	ND	The oral LD_{50} was >5,000 mg/kg	Maneewattana-pinyo et al. [2011]
Sprague-Dawley rats; 5 groups of 5	< 20-nm non-coated, <15-nm PVP and $AgNO_3$ particles	Ag = 90 mg/kg bw; $AgNO_3$ = 9 mg/kg bw, by gavage	28 days	Silver deposition; silver cleared from organs except for brain and testis	ND	AgNPs similar to exposure to silver salts	Van der Zande et al. [2012]

Table F-5. Summary of in vivo toxicological studies of silver nanoparticles (AgNPs) and nanowires (AgNWs)

Species	Particle Characteristics	Exposure Details		Critical Effect(s)	NOAEL/LOAEL	Comments	Reference
		Concentration/ Dose	Duration				
Female Wistar rats; 5 groups of 6	14-nm diameter AgNPs or Ag acetate (ionic silver)	Control (PVP, 11.5 mg/mL), 2.25, 4.5, or 9 mg AgNP/kg bw/day, or 14 mg AgAc/kg bw/day	28 days	Decrease in dopamine concentration (5-HT) in brain at 14 days but increase at 28 days for AgNPs; increase in noradrenaline brain concentration at 28 days for AgAc but not AgNP	ND	Ionic silver and 14-nm AgNP have similar neurotoxic effects	Hadrup et al. [2012b]

Table F-5. Summary of in vivo toxicological studies of silver nanoparticles (AgNPs) and nanowires (AgNWs)

Species	Particle Characteristics	Exposure Details		Critical Effect(s)	NOAEL/LOAEL	Comments	Reference
		Concentration/ Dose	Duration				
Hannover Galas male rats; 3 groups of 6	14-nm AgNP (stabilized with PVP), or Ag acetate (ionic silver)	Control (PVP, 11.5 mg/mL), 4.5 mg Ag/kg bw/day once or twice daily, for total dose of 4.5 or 9 mg/kg bw	Killed on day14	No evidence of toxicological effects in AgNP-exposed groups; decreased body weights; increases in plasma alkaline phosphatase absolute and thymus weights in Ag acetate–exposed groups	ND	Some toxicity at 9 mg/kg bw/day ionic silver dose but not at an equimolar AgNP dose	Hadrup et al. [2012a]
Hannover Galas rats: 4 groups of females,11 per group; 2 groups of males, 6 per group		Control (PVP, 11.5 mg/mL) administered to 10 females and 6 males twice/day; AgNPs at 2.25 mg Ag/kg bw/day (8 females), 4.5 mg Ag/kg bw/day (8 females), or 9.0 mg Ag/kg bw/day (10 females and 6 males twice/day at 4.5); or 14 mg Ag acetate/kg bw/day in 11 mg/mL PVP (8 females twice/day)	Killed on day 28				

Table F-5. Summary of in vivo toxicological studies of silver nanoparticles (AgNPs) and nanowires (AgNWs)

Species	Particle Characteristics	Exposure Details		Critical Effect(s)	NOAEL/LOAEL	Comments	Reference
		Concentration/ Dose	Duration				
Sprague-Dawley rats (male and female), 3 groups of 20	Citrate-coated (avg. diameters 10 and 25 nm)	Control (0.9% citrate), 100 mg/kg bw, 500 mg/kg bw)	Subacute; exposed Once/day for 28 days; killed at 1, 2, and 4 months	AgNPs remained in brain and testes at 4 months	NA	Bio-persistence study; silver clearance concentration in blood > liver = kidneys > spleen > ovaries > testes = brain	Lee et al. [2013a]
Male Wistar rats (*n* = 30)	AgNPs (~86-nm diameter)	15 or 50 µg/kg bw	Exposed from post-natal day 23 to day 53 and killed on days 53 and 90	Reduction in total and daily sperm production observed in 50-µg/kg group at day 53; at 90 days both exposure groups had lower sperm production ($P < 0.05$)	ND	Presence of cellular debris and germinal epithelial cells in tubular lumen and vesicles suggestive of possible impairment to spermato-genesis process	Sleiman et al. [2013]

Table F-5. Summary of in vivo toxicological studies of silver nanoparticles (AgNPs) and nanowires (AgNWs)

Species	Particle Characteristics	Exposure Details		Critical Effect(s)	NOAEL/LOAEL	Comments	Reference
		Concentration/ Dose	Duration				
Male Wistar rats (*n* = 30)	AgNPs (~86-nm diameter)	15 or 30 µg/kg bw	Exposed from post-natal days 23 through 58 (35 days at a total dose of 131–263 µg Ag/rat) and killed on postnatal day 102	Reduction in acrosome and plasma membrane integrities, reduced mitochondrial activity, and abnormalities of sperm in both dose groups; no change in sexual behavior or serum hormone	ND	Possible direct effect of AgNPs on spermatic cells	Mathias et al. [2014]
Male Sprague-Dawley rats (*n* = 5)	AgNPs (~7.9-nm diameter)	2 mg/kg or 20 mg/kg	Up to 24 hrs	Silver concentrations in blood, liver, and lungs higher with Ag^+ than with AgNPs at all doses	NA	Bioavailability of Ag^+ appears to be greater than with AgNPs	Park [2013]

Table F-5. Summary of in vivo toxicological studies of silver nanoparticles (AgNPs) and nanowires (AgNWs)

Species	Particle Characteristics	Exposure Details		Critical Effect(s)	NOAEL/LOAEL	Comments	Reference
		Concentration/ Dose	Duration				
Dermal Exposure							
Pigs; strain, sex, and number not stated	Spherical, 20- and 50-nm washed and unwashed particles	Up to 34 µg/mL applied to the shaved dorsal surface	14 days	No observed erythema or edema; slight epidermal hyperplasia was seen microscopically	ND		Samberg et al. [2010]
Male Hartley guinea pigs; 6 per group F	<100-nm particles of various shapes and degrees of aggregation	0,100, or 1000 µg/mL	Single acute exposure with a 14-day observation period	No lethality: some histopathologic changes to skin	−/100 µg/mL		Korani et al. [2011]
Male Hartley guinea pigs; 6 per group	<100-nm particles of various shapes and degrees of aggregation	0, 100, 1000, or 10,000 µg/mL	Subchronic; once daily, 5 days/week for 13 weeks	Skin perturbation; liver and spleen histopathology	−/100 µg/mL		Korani et al. [2011]

Table F-5. Summary of in vivo toxicological studies of silver nanoparticles (AgNPs) and nanowires (AgNWs)

Species	Particle Characteristics	Exposure Details		Critical Effect(s)	NOAEL/LOAEL	Comments	Reference
		Concentration/ Dose	Duration				
Intratracheal Instillation and Pharyngeal Aspiration							
Sprague-Dawley rats; number and sex not stated	20-nm PVP-coated particles that aggregated in a physiologic medium	0, 9.35, or 112 µg/mL	IT instillation once weekly for 8 weeks, with various recovery periods up to 84 days	Albumin, LDH, neutrophils, and lymphocytes increased in BAL in comparison with controls	9.35/112µg	Pulmonary injury and inflammation resolved with time	Roberts et al. [2012]
Male ICR mice (*n* = 48); 12 per group	AgNP at 243.8-nm average diameter	0, 125, 250, and 500 µg/kg	Single IT instillation; histopathologic analysis at different time points from treatment (1, 7, 14, and 28 days)	Dose-related change in cytokine composition of BAL and blood, with maximum concentration found at 28 days; changes in gene expression; marked inflammatory response from day 1 to 28	NA	Changes in functionality of induced genes appears to be related to tissue damage	Park et al. [2011b]

Table F-5. Summary of in vivo toxicological studies of silver nanoparticles (AgNPs) and nanowires (AgNWs)

Species	Particle Characteristics	Exposure Details		Critical Effect(s)	NOAEL/LOAEL	Comments	Reference
		Concentration/ Dose	Duration				
Male Sprague-Dawley rats	Ag nanowires approx. 50-nm diameter; lengths 4 or 20 µm	10, 50, 125, or 500 µg; alpha-quartz positive control at 500 µg or dispersion medium vehicle control	Single IT instillation	Both samples showed dose-dependent lung injury and inflammation	NA	Shorter wires' greater toxicity over time possibly due to more wires/surface area per equivalent mass dose	Kenyon et al. [2012]
Female C57BL/6 mice; 5 per exposure group	Ag nanowires with lengths of 3, 5, 10, or 14 µm	Doses set to equalize number of wires/mouse: 10.7, 10.7, 17.9, 35.7, and 50	Single pharyngeal aspiration; acute inflammation response evaluated 24 hrs post-exposure	Nanowire length-dependent trend in pulmonary inflammation; statistically significant increase in granulocytes in BAL only with 14-µm Ag wires	NA	Suggested Ag nanowire threshold between 10- and 14-µm lengths	Schinwald et al. [2012]

Table F-5. Summary of in vivo toxicological studies of silver nanoparticles (AgNPs) and nanowires (AgNWs)

Species	Particle Characteristics	Exposure Details		Critical Effect(s)	NOAEL/LOAEL	Comments	Reference
		Concentration/ Dose	Duration				
Intravenous Administration							
Male Wistar rats; 4 groups of 24	20- or 200-nm, almost spherical, agglomerated in solution	0, 5, or 10 mg/kg for the 20-nm particles, 0 and 5 mg/kg for the 200-nm particles	Single exposure (tail vein) with various recovery periods up to 4 weeks	Reduced sperm count, increased comet tail moments in germ cells	−/5 mg/kg		Gromadzka-Ostrowska et al. [2012]
Sprague-Dawley rats; sex not stated; 5–8 per group	50–60-nm particles in 0.7% NaCl containing 0.05% Tween 80, shape not specified	30 mg/kg	Single exposure	Leakage of Evans blue dye into the brain, brain edema	−/30 mg/kg		Sharma et al. [2010]
Sprague-Dawley rats; 2 of each sex per group	Spherical 50–90 nm or 1–10 nm in diameter, but with aggregation in aqueous medium	100 mg/kg for the larger species, 1 mg/kg for the smaller	One injection in tail vein 3 days/week for 4 weeks	Silver deposition, changes to the lymphocyte/ granulocyte ratio, changes in gene expression	NA	Dosing regimen insufficiently described	Kim et al. [2009b]

Table F-5. Summary of in vivo toxicological studies of silver nanoparticles (AgNPs) and nanowires (AgNWs)

Species	Particle Characteristics	Exposure Details		Critical Effect(s)	NOAEL/LOAEL	Comments	Reference
		Concentration/ Dose	Duration				
Sprague-Dawley rats; 2 males per group	Spherical 50-nm-diameter particles in an aqueous medium; some larger particles (up to 100 nm in length) were rod-shaped	0, 1, or 100 mg/kg	One injection in tail vein every 2–3 days for 4 weeks	Proteomic analysis of liver, kidney, and lung	NA	Functional analysis of proteomic changes implicated ROS formation and apoptosis in relation to silver nanoparticles treatment	Kim et al. [2010b]
Wistar rats; 4 dose groups and a control group; male and female rats; *n* per group not stated	Spherical 15–40-nm-diameter particles dispersed in ethylene glycol	4, 10, 20, or 40 mg/kg; phosphate buffer saline as control substance	One injection in tail vein at 5-day intervals over 32 days	Hematologic changes in WBC, platelet counts, hemoglobin, and RBC in 20- and 40-mg/kg groups; increase in liver function enzymes, ALT, AST, AP, GGTP in 40-mg/kg group	NOAEL at 10 mg/kg	ROS increased in all groups in a dose-related manner	Tiwari et al. [2011]

Table F-5. Summary of in vivo toxicological studies of silver nanoparticles (AgNPs) and nanowires (AgNWs)

Species	Particle Characteristics	Exposure Details		Critical Effect(s)	NOAEL/LOAEL	Comments	Reference
		Concentration/ Dose	Duration				
CD-1 pregnant mice; groups of 6 to 12	Spherical 50-nm-diameter particles of $AgNO_3$	Doses of 0 (*n* = 11), 35 (*n* = 12), 66 (*n* = 6) µg AgNPs on the 7th, 8th, and 9th day of gestation; doses of 9 (*n* = 9) and 90 (*n* = 3) µg $AgNO_3$ on same days of gestation	One injection of each dose on the 7th, 8th, and 9th day of gestation; killed 24 hrs after 3rd injection	AgNPs identified in most maternal organs, extra-embryonic tissues, and embryos	NA		Austin et al. [2012]
Male Wistar rats; 2 exposure groups and 1 control group; 23 per group	20- and 200-nm-diameter AgNPs	Doses of 0 (control group) and 5 mg/kg (exposure groups)	One injection; killed at 24 hrs, 7 days, and 28 days	AgNPs identified in liver, lungs, spleen, kidneys, and brain; highest concentration of Ag in liver at 24 hrs	NA	Highest concentration of Ag found with 20-nm AgNPs	Dziedzikowska et al. [2012]
ICR mice; 3 exposure groups and 1 control group; 6 male and female mice per group	21.8 nm average primary AgNP (range, 10–30 nm)	Doses of 0 (control group) and 7.5, 30, or 120 mg/kg	One injection; killed 10 min to 24 hrs post-injection for biokinetics; at 7 and 14 days post-injection for histopathology	No acute effects at 14 days; Ag found in all major organs, with highest concentration in liver and spleen	NA	Highest concentration of Ag found in lungs and kidneys of female mice	Xue et al. [2012]

Table F-5. Summary of in vivo toxicological studies of silver nanoparticles (AgNPs) and nanowires (AgNWs)

Species	Particle Characteristics	Exposure Details		Critical Effect(s)	NOAEL/LOAEL	Comments	Reference
		Concentration/ Dose	Duration				
Female Balb/c mice (*n* = 4) and female Fisher CDF rats; *n* not stated	PVP-coated AgNPs were spherical with 12-nm avg. diameter	Iodine-125-labeled AgNPs Mice: 4 µCi of the ^{125}I-AgNP Rats: 20 µCi of the ^{125}I-AgNP	One injection; Ag distribution evaluated at 30 min, 4 hrs, and 24 hrs with CT-SPECT imaging of organs	Prominent uptake of AgNPs in liver and spleen; level of AgNPs in blood relatively low at 24 hrs	NA		Chrastina and Schnitzed [2010]
Sprague-Dawley male rats; New Zealand white male rabbits; male dogs; *n* not stated	Particle characterization not given	Ag nitrate mixed with ^{110}Ag given in femoral vein of rats (0.01, 0.03, 0.1, 0.3 mg/kg), rabbits (0.1 mg/kg), and dogs (0.1 mg/kg)	One injection; ^{110}Ag measured in urine and feces at 24-hr periods for 4 days	25%–45% of Ag excreted into bile during first 2 hrs; 70% excreted within 4 days; highest concentration of Ag occurred in liver at 2 hrs	NA	Ag concentration in bile 16–20 times higher than that found in plasma	Klaassen [1979]

Table F-5. Summary of in vivo toxicological studies of silver nanoparticles (AgNPs) and nanowires (AgNWs)

Species	Particle Characteristics	Exposure Details		Critical Effect(s)	NOAEL/LOAEL	Comments	Reference
		Concentration/ Dose	Duration				
SPF New Zealand white male rabbits (*n* = 4)	Citrate-coated AgNPs (~7.9-nm diameter)	Injected into ear vein at doses of 0.5 mg/kg and 5 mg/kg	One injection; blood taken for Ag analysis from other ear at post-treatment times of 5, 10, and 30 min; 1, 2, 6, and 12 hrs; days 1 through 7; and days 14, 21, and 28	Concentration of AgNP in serum at highest concentration 5 min from treatment; 90% of AgNPs eliminated from serum at 28 days; tissue distribution of AgNPs highest in liver, spleen, and kidney	ND	Pigmentation found in liver at 7 and 28 days; inflammatory cell infiltration increased in livers, lungs, and kidneys	Lee et al. [2013c]
Intraperitoneal Injection							
Male C57BL/6N mice	25-nm particles, shape not specified	0, 100, 500, or 1,000 mg/kg	Single exposure	Altered gene expression in extracted regions of the brain	ND	RT-PCR analysis used oxidative stress and antioxidant defense arrays	Rahman et al. [2009]
Female Wistar pregnant rats (*n* = 30); 4 treatment groups and 1 control group	Nanosilver, size and type not specified	4 groups given either 0.4 and 0.8 mg/kg at 8th day gestation or 0.4 and 0.8 mg/kg at 9th day gestation	Single exposure; killed at 20th day gestation	No evidence of teratogenicity; mean weights and lengths decreased in comparison with controls	NA		Mahabady [2012]

Table F-5. Summary of in vivo toxicological studies of silver nanoparticles (AgNPs) and nanowires (AgNWs)

Species	Particle Characteristics	Exposure Details		Critical Effect(s)	NOAEL/LOAEL	Comments	Reference
		Concentration/ Dose	Duration				
Female ascites tumor-bearing Swiss albino mice	Spherical 50-nm particles (biologically produced)	500 nm	Daily for 15 days	Increased survival time and reduced tumor volume	NA		Sriram et al. [2010]
Sprague-Dawley rats; sex not stated; 5 to 8 per group	50–60-nm particles in 0.7% NaCl containing 0.05% Tween 80, shape not specified	50 mg/kg	Single exposure	No evidence of blood-brain barrier permeability or brain edema	NA		Sharma et al. [2010]
Sprague-Dawley rats; sex not stated; 6 to 8 per group	10–30-nm particles dispersed in deionized water	500 mg/kg^{-1}	Single exposure	Decrease in autophagy; liver function impairment; hepatotoxicity	NA		Lee et al. [2013b]

Table F-5. Summary of in vivo toxicological studies of silver nanoparticles (AgNPs) and nanowires (AgNWs)

Species	Particle Characteristics	Exposure Details		Critical Effect(s)	NOAEL/LOAEL	Comments	Reference
		Concentration/ Dose	Duration				
Male ICR mice; control group (*n* = 10); 3 experimental groups (*n* = 15) and 1 positive control group (*n* = 10)	Generally spherical with average diameter of 36.3 nm	Control group (*n* = 10) received 0.9% normal saline; 3 experimental groups (*n* = 15) received 10, 25, or 50 mg/kg bw AgNPs; 1 positive control group (*n* = 10) received scopolamine (3 mg/kg bw)	Daily for 7 days	No evidence of an effect on altering the reference memory or working memory	NA	Exposure to AgNPs did not affect neurocognitive outcome or hippocampal neurogenesis	Liu et al. [2013]
Subcutaneous Injection							
Wistar rats; 90 females	AgNPs: 50–100-nm diameter; Ag microparticles: 2–20-µm diameter, control group	Single exposure: 62.8 mg/kg in a volume of 1 mL	Single exposures; 5 rats from each group killed at weeks 2, 4, 8, 12, 18, and 24 for analysis of Ag concentration in brain	Ag concentration higher for AgNPs than for Ag microparticles; Ag concentration peaked at 12 weeks and remained constant	NA	Could not determine whether Ag concentrations in brain were result of AgNPs or Ag+	Tang et al. [2008]

Table F-5. Summary of in vivo toxicological studies of silver nanoparticles (AgNPs) and nanowires (AgNWs)

Species	Particle Characteristics	Exposure Details		Critical Effect(s)	NOAEL/LOAEL	Comments	Reference
		Concentration/ Dose	Duration				
Wistar rats; 90 females	AgNPs: 50–100-nm diameter; Ag microparticles: 2–20-µm diameter, control group	Single exposure: 62.8 mg/kg in a volume of 1 mL	Single exposure; 5 animals from each group killed at weeks 2, 4, 8, 12, 18, and 24 for analysis of Ag concentration in brains, liver, spleen, lung, and kidney	Concentrations of AgNPs in organs significantly higher than those of Ag microparticles	NA	Ag microparticles did not pass to the general circulation (~0.02% of the injected load)	Tang et al. [2009]

CMC = carboxymethyl cellulose; GGTP = gamma glutamyl transpeptidase; GM = geometric mean; 5-HT = 5-hydroxytryptamine; MAD = mean aerodynamic diameter; NA = not applicable; ND = no data; PVP = polyvinylpyrrolidone.

*By analogy to the findings in Kim et al. [2010a], these particles are likely to have been spherical.